Miniaturization in Alestidae (Ostariophysi: Characiformes)

by

Meghan Dueck

A thesis submitted in partial fulfillment of the requirements for the degree of

Master of Science

in
Systematics and Evolution

Department of Biological Sciences
University of Alberta

Abstract

Alestidae (African tetras) is one of the most species-rich families of the order Characiformes and exhibits a pronounced diversity of body size. Two independent miniaturization events (a drastic phylogenetic decrease in body size) have been identified in Alestidae. Miniaturization is frequently accompanied by morphological novelties, structural reductions and losses, hyperossifications, and increased intraspecific variation, which can create difficulties when establishing natural classifications. Traditionally, all "small" species of Alestidae with reduced multicuspid teeth were grouped in the tribe Petersiini. This tribe has since been recognized as polyphyletic, but a limited understanding of the intrarelationships of Alestidae persists. Few osteological descriptions for small-bodied alestids are available but are needed to assess the effects of miniaturization on osteological features of these fish. I conducted morphological studies of continuous measurements and meristic characters within a sample of a small-bodied alestid, *Hemigrammopetersius barnardi* (Herre) (*n* = 161), and a petersiin with a comparatively larger body size, *Petersius conserialis* Hilgendorf (*n* = 17). Specimens of *H. barnardi*, *P. conserialis*, and juveniles of an alestid that attains a larger adult size, *Alestes dentex* (Linnaeus), were cleared and counterstained for bone and cartilage for comparative osteological analyses and to identify potential convergent features resulting from a decrease in body size. Measurements in the examined sample of *H. barnardi* was normally distributed; all specimens had a relatively small body size (19.2 – 34.9 mm standard length) compared with the reported maximum standard length of 70 mm for *H. barnardi*. Potential sexual dimorphism was identified in the anal fin of cleared and stained specimens of *H.*

barnardi, supporting previous observations in the literature. I compared osteological descriptions for *H. barnardi* and *P. conserialis*, which represent some of the few osteological descriptions for small-bodied characiforms and will serve as a foundation for future comparisons. I describe a size series for *P. conserialis* that addresses previous discrepancies in the literature regarding the presence or absence of a parietal fontanelle and reports the presence of a parietal fontanelle in all examined specimens. I document negative allometric growth between standard length and the length and width of the parietal fontanelle. Finally, I compared specimens of *H. barnardi* and *P. conserialis* to juvenile specimens of *A. dentex*. This allowed the identification of features that are convergent due to a decrease in body size. I found that certain bones, including the supraorbital and postcleithrum 3, are absent in *H. barnardi* but are present in *A. dentex* and *P. conserialis*. In addition, I found reductions to the lateral line system, such as the loss of the anterodorsal branch of the circumorbital sensory canal on the dermosphenotic and an incomplete lateral line, in *H. barnardi* in comparison with other examined species. These features arise towards the end of development and have been reported as lost or reduced in other small and miniature characiforms. Caution should be used when including features that are susceptible to developmental truncation for phylogenetic analyses as they are likely to independently occur with body size decreases and may not be indicative of close phylogenetic relationships.

Acknowledgements

I am forever indebted to the many individuals who have substantially contributed to my thesis work and continual development as a scientist. I would not be where I am today without their commitment and passion.

1. I wish to express my deepest gratitude to my supervisor, Dr. Alison Murray, for her expertise, encouragement, and countless revisions. It was an honor to work with Dr. Murray, her commitment to her students and their learning has tremendously enriched my experience as a graduate student and I will be forever grateful.
2. A huge thank you to Dr. Heather Proctor for her invaluable feedback throughout the project and for being on my supervisory committee.
3. I would like to pay my special regards to John Acorn, for taking the time to read my thesis as the arm's length examiner.
4. Thank you to additional faculty and staff from the Department of Biological Sciences at the University of Alberta. They made the entire process of my masters exceptionally easier by assisting with mind-boggling administrative requirements to providing thought-provoking conversations and advise on select skills. I would like to extend my gratitude to Dr. Aaron LeBlanc, Dr. Audrey Reid, Dr. Braden Barr, Dr. Corwin Sullivan, Mark Wolansky, Dr. Michael Caldwell, Dr. Robert Holmes, and Shelley Scott.
5. I am grateful to the Department of Biological Sciences and the Government of Alberta for providing funding that enabled this project.
6. A huge thank you to Emily Drystek, who set aside her valuable time to provide advice on resume-writing, interview tips, and general skills to help succeed outside academics.
7. My deepest gratitude to past and present fellow graduate students: Aaron Dyer, Annie McIntosh, Curtis Dinn, Emily Upham-Mills, Dr. Gregory Funston, Dr. Ilaria Paparella, Jasdeep Kaur, Katherine Bramble, Luthfur Rahman, Mark Powers, Matthew Rhodes, Oksana Vernygora, Rebekah Vice, Samantha Hamilton, Sinjini Sinha, Sydney Mohr, and Yan-yin Wong.

8. I am thoroughly grateful to those who have supported my previous research endeavors, encouraged my research interests, and continually check in on me and offer help in any possible way. I would specifically like to thank Dr. Bernadette Quémerais, Dr. Binal Gandhi, Eduardo Reyes-Serratos, Dr. Mrinal Das, Dr. Paige Lacy, Samineh Kamravaei, Dr. Sindhu Nair, and Dr. Vivek Gandhi.

Finally, words will never express how exceptionally grateful I am for the extensive patience, understanding, and support of my family and friends. Specifically, my parents (Irv and Denise Dueck), sibling and roomie (Jessica Dueck), best friends (Nicole Roshko and Jenna LaBerge), and boyfriend and icecream-provider (Gavin Bradley). If it wasn't for them, I would have shed a lot more tears.

Table of Contents

List of Tables

List of Figures

List of Abbreviations

aa	Anguloarticular
ach	Anterior ceratohyal
ao	Antorbital
ap1	Anal pterygiophore 1
aps	Anal pterygiophores
ar	Anal rays
bb1-3	Basibranchials 1-3
bh	Basihyal
boc	Basiooccipital
brst	Branchiostegal rays
c	Claustrum
cb1-5	Ceratobranchials 1-5
cl	Cleithrum
cm	Coronomeckelian
CMN F	Canadian Museum of Fish Collection, Ottawa, Canada
cor	Coracoid
dent	Dentary
dhh	Dorsal hypohyal
dsph	Dermosphenotic
eb1-5	Epibranchials 1-5
ect	Ectopterygoid
end	Endopterygoid
ep1-3	Epurals 1-3
epi	Epioccipital
es	Extrascapula
exo	Exoccipital
fr	Frontal

hb1-2	Hypobranchials 1-2
HL	Head length
hy1-6	Hypurals 1-6
hyo	Hyomandibula
icl	Intercalarium
ih	Interhyal
io1-5	Infraorbitals 1-5
iop	Interopercular
is	Inner symphyseal tooth
isc	Ischiac process of the pelvic girdle
leth	Lateral ethmoid
lgc	Lagenar capsule
max	Maxilla
mcor	Mesocoracoid
met	Metapterygoid
meth	Mesethmoid
na	Nasal
nc	Neural crest
op	Opercle
osph	Orbitosphenoid
pa	Parietal
pal	Palatine
pb1-4	Pharyngobranchials 1-4
PCA	Principal component analysis
pch	Posterior ceratohyal
pcl1-3	Postcleithra 1-3
phyp	Parhypural
pmx	Premaxilla
pop	Preopercle

ppr	Pubic process of the pelvic girdle
pro	Prootic
psph	Parasphenoid
pto	Pterotic
ptsph	Pterosphenoid
ptt	Posttemporal
pu1-2	Preural centra 1-2
qu	Quadrate
ra	Retroarticular
s	Scaphium
sca	Scapula
scl	Supracleithrum
SL	Standard length
so	Supraorbital
soc	Subopercle
sph	Sphenotic
sym	Symplectic
tc	Tooth crypt
TL	Total length
tr	Tripus
u1	Ural centrum 1
un	Uroneural
us	Urostyle
USNM	U. S. National Museum Smithsonian Institution
v1-9	Vertebrae 1-9
vhh	Ventral hypohyal
vo	Vomer

Chapter 1: Introduction

1.1 General Introduction

The superorder Ostariophysi accounts for 75% of freshwater fishes and consists of two series: (i) Anotophysi (with the single order Gonorhynchiformes) and (ii) Otophysi (with four orders: Gymnotiformes, Siluriformes, Cypriniformes, and Characiformes) (Rosen & Greenwood, 1970; Nelson *et al.*, 2016; Chakrabarty *et al.*, 2017). Series Otophysi is characterized by the Weberian apparatus, a modification to the swim bladder and anterior four or five vertebrae (Rosen & Greenwood, 1970; Nelson *et al.*, 2016). The Weberian apparatus amplifies sound waves to enhance hearing and the evolutionary success of otophysans has been attributed to it (Chardon & Vandewalle, 1997; Braun & Grande, 2008). Tremendous diversity is found throughout Otophysi, including familiar fishes such as catfishes, carps, electric eels, and piranhas (van der Laan *et al.*, 2020).

Exceptional diversity is evident throughout Characiformes – tetras, piranhas, and relatives – with over 2000 species (Fricke *et al.*, 2020), the vast majority of which are in the Neotropics (~1800 spp. in 20 families) with the remainder in Africa (~200 spp. in 4 families) (Oliveira *et al.*, 2011). Characiforms include many popular aquarium, food, and game fishes (Orti & Vari, 1997; Nelson *et al.*, 2016). Some of the exceptional diversity documented within characiforms includes their diet (piscivory, zooplanktivory, lepidophagy, detritivory, and herbivory), habitat (surface, benthic, and midwater), body shape (from deep-bodied and laterally compressed such as piranhas, to long and slender such as pencilfish), and body size (Helfman *et al.*, 2009). The pronounced variation in body size reported throughout characiforms is remarkable, ranging from tiny species less than 26 mm standard length (SL) to the large tigerfishes in Africa that exceed 1000 mm SL (Hubert *et al.*, 2005; Helfman *et al.*, 2009). Within the Characiformes, the family Alestidae exhibits the entire size range: the smallest species, *Lepidarchus adonis* Roberts has a maximum standard length (SL) of 21 mm, while the largest species *Hydrocynus goliath* Boulenger has a maximum of 1300 mm SL (Hubert *et al.*, 2005).

1.2 Alestidae

Alestidae is the largest of the four African characiform families with over 100 valid species (Oliveira *et al.*, 2011; Fricke *et al.*, 2020) and is one of the most species-rich of all characiform families (Fricke *et al.*, 2020). Alestid fishes are found only in Africa, with most in lowland rivers in Sub-Saharan Africa (Roberts, 1975; Zanata & Vari, 2005; Arroyave & Stiassny, 2011).

Members of the Alestidae were previously grouped with Characidae, their Neotropical counterparts (Greenwood *et al.*, 1966). Gery (1977, p. 18) proposed Alestidae as a separate family to include all the African members once placed in Characidae based on features that differed between Alestidae and the South American members of Characidae: members of Alestidae lack a rhinosphenoid, have a bony tube on the orbitosphenoid and lateral ethmoid that encloses the olfactory nerve, and a decurved lateral line. Gery (1977) did not conduct any analyses to test the monophyly of Alestidae. Likewise, Buckup (1998) did not test the monophyly of Alestidae but did establish that Characidae would be a polyphyletic group if it included the African genera. Orti and Meyer (1997) were the first to provide evidence for a monophyletic Alestidae using molecular data but they only included three alestids in their analysis. Since then multiple studies have provided support for a monophyletic Alestidae (Murray & Stewart, 2002; Calcagnotto *et al.*, 2005; Hubert *et al.*, 2005; Zanata & Vari, 2005; Arroyave & Stiassny, 2011).

Murray and Stewart (2002) conducted the first cladistic analysis of Alestidae using morphological features. They focused on two genera, *Alestes* and *Brycinus*, including only a handful of other genera (i.e., *Bryconaethiops, Hydrocynus, Nanopetersius, Petersius,* and *Rhabdalestes*), and identified 11 synapomorphies for the family: (i) a tubular posterior premaxilla, (ii) presence of a premaxillary pedicle, (iii) presence of a ventral flange on the maxilla, (iv) presence of a ventral depression of the parasphenoid, (v) presence of a lateral expansion on the anterior portion of the vomer, (vi) presence of an orbitosphenoid tube, (vii) a ridge along the preopercular with all the preopercular sensory canal pores opening ventrally, (viii) presence of a third posttemporal fossa in the epioccipital, (ix) presence of bony stays on the caudal fin, (x) three epurals, and (xi) sexual dimorphism of the caudal fin.

Zanata and Vari's (2005) study conducted a few years later included a more comprehensive coverage of Alestidae by including 19 genera. They did not concur with any of the synapomorphies identified by Murray and Stewart (2002) and disputed their characters as being the same feature (e.g., the form of the posterior end of the premaxilla and the presence of the premaxillary pedicle), incorrectly coded (e.g., the ventral depression of the parasphenoid in *Hydrocynus*), or they chose to not use the character in their analysis (e.g., the presence of a ventral flange on the maxilla) (Zanata & Vari, 2005). They did, however, propose six alternative synapomorphies: (i) contralateral premaxillae with medial interdigitations, (ii) two functional rows of teeth on the premaxilla, (iii) area of contact of ectopterygoid with palatine narrow, (iv) no ligamentous attachment of ectopterygoid to neurocranium, (v) four branchiostegal rays, and (vi) no ossification associated with first dorsal-fin proximal radial (Zanata & Vari, 2005). They also suggested an additional eight “ambiguous” synapomorphies (Zanata & Vari, 2005, p. 93). However, Zanata and Vari's (2005) analysis proposed *Chalceus*, a South American characiform, as the sister-group to Alestidae and proposed a trans-Atlantic family. This has since been considered to be the result of poor outgroup taxon sampling and the relationship between African Alestidae and *Chalceus* has not been supported by any molecular phylogenies (Calcagnotto *et al.*, 2005; Hubert *et al.*, 2005; Arroyave & Stiassny, 2011). Overall, researchers agree that Alestidae is monophyletic but incongruent topologies due to taxon selection and data type have resulted in unclear intrarelationships.

Previous attempts at creating suprageneric groups within Alestidae have resulted in artificial classification schemes. Roberts (1969) proposed two subfamilies within Alestidae: (i) Hydrocyninae (containing *Hydrocynus*) and (ii) Alestinae (the remaining genera). Alestinae was further divided into two tribes, Alestini and Petersiini, based on dental characteristics and body size (Poll, 1967; Roberts, 1969; Gery, 1977, 1995). Petersiini includes all small-bodied alestid genera with the lack of a “shoulder” on the multicuspid teeth (i.e., *Alestopeterius, Arnoldichthyes, Bathyaethiops, Brachypetersius, Clupeocharax, Duboisialestes, Hemigrammopetersius, Ladigesia, Lepidarchus, Micralestes, Nannopetersius, Petersius, Phenacogrammus, Rhabdalestes, Tricuspidalestes, Virilia*) (Gery, 1995). The subfamilial and tribal classification systems are now widely recognized as artificial due to many overlapping features that vary between and within species (Stiassny & Schaefer, 2005) and because both classification schemes are polyphyletic (Murray & Stewart, 2002; Calcagnotto *et al.*, 2005; Hubert *et al.*, 2005; Arroyave & Stiassny, 2011). Previous work on Alestidae has led to unresolved relationships and a stronger understanding of variation present within species and the establishment of reliable features for determining a natural classification is still lacking.

The size disparity in Alestidae may contribute to the difficulties in determining a natural classification. At least two independent miniaturization events have been hypothesized in Alestidae (Hubert *et al.*, 2005; Zanata & Vari, 2005). Absent and reduced morphological features commonly reported in small fishes may occur convergently, creating problems for establishing natural classifications. A strong foundation of how small body sizes in Alestidae influences morphology will help determine reliable features for assessing evolutionary relationships.

1.3 Miniaturization in Fish

Miniaturization is a phylogenetic decrease in body size that, in addition to change in size, can result in alterations to physiology, behavior, or other aspects of morphology (Hanken & Wake, 1993). It is a common phenomenon reported throughout most vertebrate lineages (e.g., Hanken, 1983; Yeh, 2002; Masters *et al.*, 2014) and is frequently found in teleosts (e.g., Ruber *et al.*, 2007; De Santana & Crampton, 2011; da Graca *et al.*, 2019). Morphological novelties, reduced structural features, hyperossification, and increased intraspecific variation frequently accompany body size decreases (Weitzman & Vari, 1988; Hanken & Wake, 1993; Frobisch & Schoch, 2009). Researchers have attempted to establish criteria for defining miniature and small body sizes. Purvis and Harvey (1996) proposed that when no obvious dichotomy in a size distribution is present, then the smallest quarter of species may be considered miniatures. Specifically in relation to body sizes in fish, Lindsey (1966) and Miller (1994) suggested that fish less than 100 mm total length (TL) as adults have a 'small' body size in relation to the distribution of body size among all fishes. Castro (1999) considered 'small' fishes as those with a SL less than 150 mm. The definition for miniature provided by Weitzman and Vari (1988) has persisted and is used today. They defined 'miniature' fish as a species that does not exceed 26 mm SL or reaches sexual maturity before 20 mm SL, along with the presence of lost and reduced morphological features (Weitzman & Vari, 1988). Two types of miniature fish have been identified based on the appearance of adults: (i) proportional dwarfs, which resemble smaller versions of the adults of larger-bodied fish (Gould, 1977), and (ii) developmentally truncated fish, which at adulthood resemble juveniles of larger-bodied relatives (Britz & Conway, 2009, 2016).

Three species of Alestidae are miniature fish according to Weitzman and Vari's (1988) definition. Miniature alestids are considered proportional dwarfs due to the presence of only a few developmentally truncated features in comparison to severely truncated miniatures (e.g., *Schindleria* from Johnson and Brothers (1993) and *Paedocypris* from Britz and Conway (2009)). Conway and Moritz (2006) listed miniature African fishes, including only one miniature alestid, *Lepidarchus adonis*. They strictly employed Weitzman and Vari's (1988) first criterion of miniatures – a SL less than 26 mm – and, consequently, did not include *Micralestes pabrensis* (Roman), previously classified within the genus *Virilia*, an alestid that reaches a maximum of 52 mm SL (Paugy, 1990a) but matures before 20 mm SL (Zanata & Vari, 2005; Conway & Moritz, 2006). One new miniature alestid has been described since Conway and Moritz's (2006) review, *Bathyaethiops baka* Moritz and Schliewan. However, numerous alestids have a small body size and with phylogenetic hypotheses suggesting at least two independent miniaturization events in Alestidae (Hubert *et al.*, 2005; Zanata & Vari, 2005) and a gradual increase in morphological losses and reductions with decreasing body size in a phylogenetic context (Zanata & Vari, 2005) convergences may have developed.

In this thesis, I do not examine any true miniatures according to Weitzman and Vari's (1988) definition, but instead assess the small-bodied alestid, *Hemigrammopetersius barnardi* (Herre), which has some morphological features that have been reduced or lost. Overall, the literature varies in the use of terminology for 'small', 'miniature', and 'dwarf' fishes; therefore, for the purposes of this thesis, a 'small' fish, will be considered a fish less than 150 mm SL according to Castro's (1999) definition and a 'miniature' fish will be considered a fish less than 26 mm SL or that reaches sexual maturity by 20 mm SL according to Weitzman and Vari's (1988) definition. A summary of definitions for 'small' fishes (along with those used in this thesis) is provided in Appendix A.

1.4 Thesis Objectives

I will thoroughly examine the osteology of three alestids, (i) *H. barnardi*, (ii) *Petersius conserialis* Hilgendorf, and (iii) *Alestes dentex* (Linnaeus). *Hemigrammopetersius barnardi* is a small-bodied alestid that reaches a maximum of 70 mm SL (Eccles, 1992). *Petersius conserialis*, a member of the small-bodied group Petersiini, attains a larger body size in comparison to other petersiins with a maximum of 145 mm TL (Poll, 1967). Finally, the morphology of small, presumed juvenile, specimens of *A. dentex*, an alestid that attains a much larger size as an adult (maximum of 550 mm TL (Paugy, 1990b)), will be assessed.

Previous work on the osteology in Alestidae has focused mostly on larger species (e.g., Brewster, 1986; Murray, 2004). Few osteological descriptions of small-bodied and miniature characiforms exist and are needed for future osteological comparisons with other small and miniature taxa (Pastana *et al.*, 2017). The osteological descriptions of the small alestids provided in this thesis will establish a foundation for future comparisons and help identify morphological changes that potentially accompany decreasing body size in a phylogenetic context.

Therefore, my first objective is to describe the osteology and evaluate intraspecific variation in a sample of specimens of *H. barnardi* (*n* = 161). My second objective is to assess a size series of an alestid species that has remained an enigma since being described in 1894, *P. conserialis*. Limited specimen availability has resulted in limited knowledge on the osteology of *P. conserialis*, particularly their cranial anatomy, which I will attempt to clarify here. The final objective is to compare the osteology of *H. barnardi*, *P. conserialis,* and comparably sized, juveniles of an alestid that attains a much larger adult size, *A. dentex*, to identify potential convergent features resulting from a decrease in body size that are not indicative of evolutionary relationships. My thesis will establish a better understanding of small body sizes in Alestidae and the accompanying morphologies. This work will have broader implications for assessing features in miniature and small fish that may independently evolve as a result of small-body size.

1.5 References

Arroyave, J., & Stiassny, M. L. J. (2011). Phylogenetic relationships and the temporal context for the diversification of African characins of the family Alestidae (Ostariophysi: Characiformes): Evidence from DNA sequence data. *Molecular Phylogenetics and Evolution, 60*(3), 385-397.

Braun, C. B., & Grande, T. (2008). Evolution of peripheral mechanisms for the enhancement of sound reception. In J. F. Webb, R. R. Fay, & A. N. Popper (Eds.), *Fish Bioacoustics* (pp. 99-144). New York: Springer.

Brewster, B. (1986). A review of the genus *Hydrocynus* Cuvier 1819 (Teleostei: Characiformes). *Bulletin of the British Museum of Natural History (Zoology), 50*(3), 163-206.

Britz, R., & Conway, K. W. (2009). Osteology of *Paedocypris*, a miniature and highly developmentally truncated fish (Teleostei: Ostariophysi: Cyprinidae). *Journal of Morphology, 270*(4), 389-412.

Britz, R., & Conway, K. W. (2016). *Danionella dracula*, an escape from the cypriniform bauplan via developmental truncation? *Journal of Morphology, 277*(2), 147-166.

Buckup, P. A. (1998). Relationships of the Characidiinae and phylogeny of characiform fishes (Teleostei: Ostariophysi). In L. R. Malabarba, R. E. Reis, R. P. Vari, Z. M. S. Lucena, & C. A. S. Lucena (Eds.), *Phylogeny and Classification of Neotropical Fishes* (pp. 123-144). Porto Alegre, Brasil: EDIPUCRS.

Calcagnotto, D., Schaefer, S. A., & DeSalle, R. (2005). Relationships among characiform fishes inferred from analysis of nuclear and mitochondrial gene sequences. *Molecular Phylogenetics and Evolution, 36*(1), 135-153.

Castro, R. M. C. (1999). Evolucao da ictiofauna de riachos Sul-Americanos: Padroes gerais e possiveis processos causais. In R. Mazzoni & P. R. Peres-Neto (Eds.), *Ecologia de Peixes de Riachos* (Vol. 6, pp. 139-155). Rio de Janeiro, Brazil.

Chakrabarty, P., Faircloth, B. C., Alda, F., Ludt, W. B., McMahan, C. D., Near, T. J., Dornburg, A., Albert, J. S., Arroyave, J., Stiassny, M. L. J., Sorenson, L., & Alfaro, M. E. (2017). Phylogenomic systematics of ostariophysan fishes: ultraconserved elements support the surprising non-monophyly of Characiformes. *Systematic Biology, 66*(6), 881-895.

Chardon, M., & Vandewalle, P. (1997). Evolutionary trends and possible origin of the Weberian apparatus. *Netherlands Journal of Zoology, 47*(4), 383-403.

Conway, K. W., & Moritz, T. (2006). *Barboides britzi*, a new species of miniature cyprinid from Benin (Ostariophysi: Cyprinidae), with a neotype designation for *Barboides gracilis*. *Ichthyological Exploration of Freshwaters, 17*(1), 73-84.

da Graca, W. J., Ota, R. R., & Domingues, W. M. (2019). A new species of miniature *Characidium* (Characiformes: Crenuchidae) from the upper Rio Paraguay basin, Mato Grosso state, Brazil. *Journal of Fish Biology, 95*(6), 1480-1485.

De Santana, C. D., & Crampton, W. G. R. (2011). Phylogenetic interrelationships, taxonomy, and reductive evolution in the Neotropical electric fish genus *Hypopygus* (Teleostei, Ostariophysi, Gymnotiformes). *Zoological Journal of the Linnaean Society, 163*(4), 1096-1156.

Eccles, D. H. (1992). *FAO species identification sheets for fishery purposes. Field guide to the freshwater fishes of Tanzania. Prepared and published with the support of the United Nations Development Programme (project URT/87/016).* Rome: FAO.

Fricke, R., Eschmeyer, W. N., & Fong, J. D. (2020). Species by family/subfamily. Retrieved from http://researcharchive.calacademy.org/research/ichthyology/catalog/SpeciesByFamily.asp

Frobisch, N. B., & Schoch, R. R. (2009). Testing the impact of miniaturization on phylogeny: Paleozoic dissorophoid amphibians. *Systematic Biology, 58*(3), 312-327.

Gery, J. (1977). *Characoids of the World*. USA: T.F.H. Publications, Inc. Ltd.

Gery, J. (1995). Description of new or poorly known Alestinae (Teleostei: Characiformes: Alestidae) from Africa, with a note on the generic concept in the Alestinae. *Journal of Ichthyology and Aquatic Biology, 1*(4), 37-64.

Gould, S. J. (1977). *Ontogeny and Phylogeny*. Cambridge, Massachusetts: Belknap Press.

Greenwood, P. H., Rosen, D. E., Weitzman, S. H., & Myers, G. S. (1966). Phyletic studies of teleostean fishes with a provisional classification of living forms. *Bulletin of the American Museum of Natural History, 131*(4), 339-455.

Hanken, J. (1983). Miniaturization and its effects on cranial morphology in plethodontid salamanders, genus *Thorius* (Amphibia, Plethodontidae). 2. The fate of the brain and sense-organs and their role in skull morphogenesis and evolution. *Journal of Morphology, 177*(3), 255-268.

Hanken, J., & Wake, D. B. (1993). Miniaturization of body-size - organismal consequences and evolutionary significance. *Annual Review of Ecology and Systematics, 24*, 501-519.

Helfman, G. S., Collette, B. B., Facey, D. E., & Bowen, B. W. (2009). *The Diversity of Fishes: Biology, Evolution, and Ecology*. Chichester, West Sussex: Wiley-Blackwell: John Wiley & Sons LTD.

Hubert, N., Bonillo, C., & Paugy, D. (2005). Early divergence among the Alestidae (Teleostei, Ostariophyses, Characiformes): Mitochondrial evidences and congruence with morphological data. *Animal Biology and Pathology, 328*(5), 477-491.

Johnson, G. D., & Brothers, E. B. (1993). *Schindleria*: A paedomorphic goby (Teleostei: Gobioidei). *Bulletin of Marine Science, 52*(1), 441-471.

Lindsey, C. C. (1966). Body sizes of poikilotherm vertebrates at different latitudes. *Evolution, 20*(4), 456-465.

Masters, J. C., Genin, F., Silvestro, D., Lister, A. M., & DelPero, M. (2014). The red island and the seven dwarfs: body size reduction in Cheirogaleidae. *Journal of Biogeography, 41*(10), 1833-1847.

Miller, P. J. (1994). *Miniature Vertebrates: The Implications of Small Body Size*. Oxford: Clarendon press.

Murray, A. M. (2004). Osteology and morphology of the characiform fish *Alestes stuhlmannii* Pfeffer, 1896 (Alestidae) from the Rufiji River basin, East Africa. *Journal of Fish Biology, 65*(5), 1412-1430.

Murray, A. M., & Stewart, K. M. (2002). Phylogenetic relationships of the African genera *Alestes* and *Brycinus* (Teleostei, Characiformes, Alestidae). *Canadian Journal of Zoology-Revue Canadienne De Zoologie, 80*(11), 1887-1899.

Nelson, J. S., Grande, T., & Wilson, M. V. H. (2016). *Fishes of the World* (Fifth edition ed.). Hoboken, New Jersey: John Wiley & Sons.

Oliveira, C., Avelino, G. S., Abe, K. T., Mariguela, T. C., Benine, R. C., Orti, G., Vari, R. P., & Correa e Castro, R. M. (2011). Phylogenetic relationships within the speciose family Characidae (Teleostei: Ostariophysi: Characiformes) based on multilocus analysis and extensive ingroup sampling. *BMC Evolutionary Biology, 11*(275), 1-25.

Orti, G., & Meyer, A. (1997). The radiation of characiform fishes and the limits of resolution of mitochondrial ribosomal DNA sequences. *Systematic Biology, 46*(1), 75-100.

Orti, G., & Vari, R. P. (1997). Characiformes. Tetras, piranhas, hatchetfishes, headstanders, pencilfishes, and their relatives. *The Tree of Life Web Project*. Retrieved from http://tolweb.org/Characiformes/15062/1997.01.27

Pastana, M. N. L., Dagosta, F. C. P., & Esguicero, A. L. H. (2017). A new sexually dichromatic miniature *Hyphessobrycon* (Teleostei: Characiformes: Characidae) from the Rio Formiga, upper Rio Juruena basin, Mato Grosso, Brazil, with a review of sexual dichromatism in Characiformes. *Journal of Fish Biology, 91*(5), 1301-1318.

Paugy, D. (1990a). Characidae. In C. Leveque, D. Paugy, & G. G. Teugels (Eds.), *Faune des poissons d'eaux douces et saumatres de l'Afrique de l'Ouest* (Vol. 28, pp. 195 - 236). Musee Royal de l'Afrique Centrale, Tervuren et O.R.S.T.O.M., Paris: Tome I. Coll. Faune Tropicale n.

Paugy, D. (1990b). Note a propos des Petersiini (Teleostei: Characidae) d'Afrique occidentale. *Ichthyological Exploration of Freshwaters, 1*(1), 75-84.

Poll, M. (1967). Revision des Characidae nains Africains. *Annales du Musee Royal de l'Afrique Centrale Tervurum serie in-8 Sciences Zoologiques, 162*, 1-158.

Purvis, A., & Harvey, P. H. (1996). Miniature mammals: life-history strategies and macroevolution. In P. J. Miller (Eds.), *Miniature Vertebrates: The Implications of Small Body Size*. Oxford: Clarendon Press.

Roberts, T. R. (1969). Osteology and relationships of characoid fishes, particularly the genera *Hepsetus*, *Salminus*, *Hoplias*, *Ctenolucius*, and *Acestrorhynchus*. *Proceedings of the California Academy of Sciences, 36*(15), 391-500.

Roberts, T. R. (1975). Geographical distribution of African freshwater fishes. *Zoological Journal of the Linnean Society, 57*(4), 249-319.

Rosen, D. E., & Greenwood, P. H. (1970). Origin of the Weberian Apparatus and the relationships of the Ostariophysan and Gonorynchiform fishes. *American Museum Novitates, 2428*, 1-26.

Ruber, L., Kottelat, M., Tan, H. H., Ng, P. K. L., & Britz, R. (2007). Evolution of miniaturization and the phylogenetic position of *Paedocypris*, comprising the world's smallest vertebrate. *BMC Evolutionary Biology, 7*(1), 1-10.

Stiassny, M. L. J., & Schaefer, S. A. (2005). *Rhabdalestes aeratis*, new species (Characiformes: Alestidae): first occurrence of the genus from the Middle Congo River basin. *Ichthyological Exploration of Freshwaters, 16*(3), 271-278.

van der Laan, R., Fricke, R., & Eschmeyer, W. N. (Eds) (2020) Classification. Retrieved from http://www.calacademy.org/scientists/catalog-of-fishes-classification/

Weitzman, S. H., & Vari, R. P. (1988). Miniaturization in South American freshwater fishes; An overview and discussion. *Proceedings of the Biological Society of Washington, 101*(2), 444-465.

Yeh, J. (2002). The effect of miniaturized body size on skeletal morphology in frogs. *Evolution, 56*(3), 628-641.

Zanata, A. M., & Vari, R. P. (2005). The family Alestidae (Ostariophysi, Characiformes): a phylogenetic analysis of a trans-Atlantic clade. *Zoological Journal of the Linnaean Society, 145*(1), 1-144.

Chapter 2: Variation in the small African fish *Hemigrammopetersius barnardi* (Characiformes: Alestidae)

2.1 Introduction

Decrease in body size over evolutionary time, a commonly reported phenomenon in vertebrates (Hanken & Wake, 1993), may be accompanied by morphological novelties, reduced structural features, hyperossification, and increased intraspecific variation (Weitzman & Vari, 1988; Hanken & Wake, 1993; Yeh, 2002; Conway & Moritz, 2006). Many freshwater fishes have convergently evolved a decreased body size (e.g., Ruber *et al.*, 2007; De Santana & Crampton, 2011; Steele & Lopez-Fernandez, 2014); this includes members of Characiformes (tetras, piranhas, and relatives) (Weitzman & Vari, 1988; Zanata & Vari, 2005).

Alestidae is the largest of four African characiform families (Nelson, 2006; Oliveira *et al.*, 2011), with 119 species (Fricke *et al.*, 2019) that display pronounced body size variation: the smallest species, *Lepidarchus adonis* Roberts*,* reaches 21 mm standard length (SL), in comparison to the largest species, *Hydrocynus goliath* Boulenger*,* which reaches 1300 mm SL (Hubert *et al.*, 2005). The size difference is even more striking in a phylogenetic context, with size increases and decreases evolving independently (Hubert *et al.*, 2005; Zanata & Vari, 2005). Independent miniaturization events have created confusion in understanding evolutionary relationships within Alestidae.

Currently, relationships among members of Alestidae are poorly understood, with the previous classification into tribes based on dentition and body size being recognized as polyphyletic (e.g., Murray & Stewart, 2002; Zanata & Vari, 2005; Arroyave & Stiassny, 2011). While attempts have been made to resolve intrafamilial relationships, poor availability of specimens has prevented researchers from determining an overall resolution for alestid phylogeny (Hubert *et al.*, 2005; Zanata & Vari, 2005). Contributing to the problem is a lack of information on intraspecific variation, which may impact estimations of phylogenetic relationships based on morphology.

Intraspecific variation is reported in Alestidae (Nzeyimana & Amiet, 1992; Gery, 1995). An improved understanding of intraspecific variation within small alestid species may help resolve morphological phylogenies. In addition to minimal knowledge on the impacts of intraspecific variation in small alestids, accounts of sexual dimorphism in Alestidae are limited.

Sexual dimorphism is commonly reported in Characidae (the New World counterpart of Alestidae) including dichromatism (Pastana *et al.*, 2017) and differences in fin morphology between males and females (Schönhofen Longoni *et al.*, 2018). Previous studies have reported sexual dimorphism in the anal and caudal fins of alestids (e.g., Brewster, 1986; Murray & Stewart, 2002; Zanata & Vari, 2005); however no study has focused on evaluating sexual dimorphism. A more extensive review of sexual dimorphism in alestids, particularly smaller taxa, is required and may be beneficial in identifying evolutionary relationships.

The morphology of moderate to large alestid fishes has been examined (e.g., Brewster, 1986; Murray, 2004; Lunkayilakio & Vreven, 2008) but limited osteological descriptions for smaller characiform taxa exist (Pastana *et al.*, 2017). Species with a decreased body size may convergently develop similar features causing complications for generating phylogenetic hypotheses. An extensive review of the morphology and intraspecific variation within small species of Alestidae will help evaluate useful features for determining evolutionary relationships.

Previous phylogenetic hypotheses about intrafamilial relationships among alestids revealed that current classifications do not follow evolutionary relationships (e.g., Murray & Stewart, 2002; Calcagnotto *et al.*, 2005; Hubert *et al.*, 2005). Zanata and Vari (2005) conducted the most extensive review to date of alestid morphology and concurred with past research that the current classification does not reflect evolutionary relationships, but they refrained from proposing taxonomic changes due to limited specimen availability for their study. An increase in research assessing morphology and variation in alestids is necessary. In this chapter, I assess intraspecific morphological variation in a sample of a small alestid fish, *Hemigrammopetersius barnardi* (Herre) (*n* = 161), to provide a thorough description of its osteology and morphology.

Hemigrammopetersius barnardi is a small fish (largest reported SL = 70 mm (Eccles, 1992)) with an anteroventral keel and superior mouth, adaptations for swimming and feeding near the water's surface (Gery, 1977, 1995). It inhabits shallow waters in southern Africa (Eccles, 1992; Konings *et al.,* 2018). It was originally described as *Petersius barnardi* Herre, 1936 (holotype = 34 mm SL; *n* = 84 paratypes) after ichthyologist Dr. K. H. Barnard (Herre, 1936). Prior to the description of *P. barnardi*, Pellegrin (1928) had erected the genus *Hemigrammopetersius* for all species of *Petersius* with an incomplete lateral line and an absence of inner dentary symphyseal teeth. Because of the incomplete lateral line in *Petersius barnardi*, Poll (1945) later proposed it should be renamed *Hemigrammopetersius barnardi* (Herre, 1936). Despite debate regarding the use of features that have been noted to vary within species to justify a new generic type, such as extent of the lateral line or inner mandibular teeth (Myers, 1929; Gery, 1977; Paugy, 1990), the genus *Hemigrammopetersius* remains valid with two species according to Fricke *et al.* (2019): *H. pulcher* (Boulenger, 1909), the generic type, and *H. barnardi*.

Morphological studies and osteological descriptions of small alestids are necessary to address intraspecific variation and to compare with larger alestids to determine features that might reliably reflect phylogenetic history within Alestidae. Therefore, the aim of this study is to assess morphological variation within a sample (*n* = 161) of *H. barnardi* using measurements and osteological descriptions, while also reviewing sexual dimorphism in *H. barnardi*.

2.2 Materials and Methods

2.2.1 Materials

The examined specimens of *Hemigrammopetersius barnardi* are catalogued in the Canadian Museum of Nature Fish Collection, Ottawa, Canada (catalogue number CMN F 81-0188). I examined a total of 157 alcohol preserved specimens and four specimens previously double stained with alcian blue for cartilage, and alizarin red S for bone, and then cleared with trypsin. Specimens were collected by G. M. Bernacsek and A. J. Hopson in 1979 from the Rufiji River basin at the west end of Lake Ruwe, Tanzania, 1 km east of Mkongo. G. M. Bernacsek originally identified specimens in 1981. I confirmed specimen identification for this project based on the incomplete lateral line, superior mouth, and keeled anteroventral region.

2.2.2 Measurements

Measurements and counts for specimens were collected according to Lunkayilakio and Vreven (2008) (*n* = 63–158 depending on measurement). Transverse scale counts were counted from the dorsal fin origin. Measurements were made using a Nikon SMZ1000 stereomicroscope using a WD 123 Nikon Plan Apo 0.5x lens and a C-W 10xB/22 eyepiece reticle. Radiographs for vertebral counts were collected using a Bruker micro CT Skyscan 1172 (no filter, 50 kV, and 201 µA). Vertebrae were counted according to Brewster (1986) with the exception of transitional vertebral counts, which were difficult to reliably determine from radiographs. A summary of all measurements and meristics is available in Appendix B.

I assessed four specimens that were previously cleared and counterstained according to Taylor and Van Dyke's (1985) procedure to examine skeletal features. Comparative photographs for osteological drawings were taken with a Zeiss Stereo Discovery.V8 stereomicroscope with a Carl Zeiss 44403 6-9000 eyepiece (8x) and a variety of lenses (Zeiss Achromat S 0.3x FWD 236 mm, Zeiss Plan Apo S 0.63x FWD 81 mm, and Zeiss Plan Apo S 1.0x FWD 60 mm), with NIS-Elements F package 2.20, version 5.03. I processed the figures using Adobe Photoshop CS6. Osteological terminology follows Murray (2004), with the exception of endopterygoid for mesopterygoid from Brewster (1986) and pubic processes from Prokofiev (2001).

I completed all statistical analyses using R version 3.5.2 (R Core Team, 2017). To test the distribution of the studied specimens, I calculated the skewness, kurtosis and Shapiro-Wilk test value using the package e1071 (Meyer *et al.,* 2019). Histograms and scatterplots were completed for all measurements and meristics (Appendix C). To determine allometric or isometric growth, all measurements were changed to the logarithmic form and the slopes were calculated. I created a principal component analysis (PCA) using FactoMineR (Le *et al.*, 2008), factoextra (Kassambar & Mundt, 2017), and corrplot (Wei & Simko, 2017) packages to check for correlations among characters. An exploratory PCA was conducted using all measurement and meristic data (Appendix C) and I conducted final PCA only using the measurements that had a strong representation (a high $\cos^2$ value in dimensions 1 and 2) in the previous analyses or were highly correlated ($r > 0.70$) in the scatterplots. All measurements used for PCA were standardized by SL.

2.3 Results

2.3.1 General Body Form and External Characteristics

Hemigrammopetersius barnardi has a fusiform body, superior mouth, and keeled anteroventral region (Fig. 2.1). The eyes occupy a large portion of the head (31-49% HL, mean 39% HL; Tab. 2.1). The dorsal fin insertion is posterior on the body (49-61% SL, mean = 56% SL, Tab. 2.1), posterior to the level of the pelvic-fin insertion and anterior to the level of the anal-fin insertion. The adipose fin inserts at the level of the last anal-fin ray insertion. It has a small base and is oblong. Almost all specimens from the studied sample have an adipose fin, with the exception of two (specimens' 23 and 159), in which the adipose fin is absent. The pectoral fins insert posteroventral to the operculum. The pelvic fins insert ventrally, posterior to the distal tips of the pectoral-fin rays and do not reach the origin of the anal fin. The anal-fin base is about twice the dorsal-fin base (130-340% dorsal-fin base, mean = 220% dorsal-fin base). The caudal fin is forked. Definitions for all completed measurements are available in Appendix B

Preserved specimens are a light orange in colour with a dark stripe down the midline that originates anterior to the level of the dorsal fin insertion and extends onto the caudal peduncle. Fins are a translucent gray. All specimens I examined were previously preserved; thus, life coloration was not observed. Herre (1936) described living specimens as being olive brown, with a dusky red iridescence dorsally and a pale silver iridescence ventrally. According to Poll (1967) the lateral black stripe on the flank is silvered and a black band is present along the base of the anal fin. The fins are gray in living specimens (Poll, 1967).

Cycloid scales cover the body beginning just behind the operculum and extend onto the caudal peduncle. An incomplete lateral line begins on the first scale posterior to the operculum and drops ventrally on scales 2 or 3 (Tab. 2.2; Fig. 2.2). The lateral line ends posterior to the distal tips of the pectoral-fin rays and is 8-12 scales long. Measurements and meristics are summarized in Tables 1 and 2, respectively.

2.3.2 Intraspecific Variation in External Measurements

For most of the measurements, the assessed specimens have a normal distribution; however, some measurements demonstrate a right-skewed distribution resulting from some larger specimens (Fig. 2.3 and Appendix C summarizes the distribution). All of the length and depth measurements are positively correlated and have a slope of approximately 1.0, for example head length and eye diameter (Fig 2.4). No strong correlations (> 0.70) were found in relation to standard length and some meristics (gill rakers and total vertebrae). The distributions and correlations with SL for all measurements recorded are in Appendix C.

The exploratory PCA included all variables and explained less than 30% of the variance in the first two dimensions. The first principal component (dimension) showed a correlation between length measurements (e.g., prepectoral distance, head length), with the second principal component largely influenced by body depth. Measurements that had a high representation in the initial PCA or were highly correlated (> 0.70) were used for an additional PCA. When using select variables, the first two dimensions covered approximately 36% of the variance, a slight increase in comparison with the exploratory PCA (Fig. 2.5). This analysis also showed a correlation between length measurements for the first dimension with the second dimension represented by body depth.

2.3.3 Skull

The mesethmoid has a distinct anteromedial point in dorsal view and well-developed lateral projections just posterior to it (Fig. 2.6a) The posterior portion of the mesethmoid has three pointed projections, with a substantially longer middle point that separates the left and right frontals. The nasals are small and oval, bearing a sensory canal on the lateral portion of the bone.

The lateral ethmoids have a ventral point and a rounded edge along the posterior portion of the bone (Fig. 2.6b & c). The vomer has a straight anterior edge in ventral view. The posteroventral portion of the vomer is rounded.

A large portion of the dorsal skull roof consists of the frontals, which widen slightly posteriorly. The supraorbital sensory canal extends from the anterior to posterior of the frontals, with two anterior openings (one along the middle of each frontal and the second branching towards the suture between the two frontals), another opening at the level of the epiphyseal bar and two posterior openings that open towards the parietals and pterotics. A large fontanelle separates most of the left and right frontals, originating anterior to the epiphyseal bar and extending posteriorly behind the bar. This same fontanelle completely separates the left and right parietals and forms a notch in the anterior edge of the supraoccipital. The parietals narrow laterally. The parietal branch of the supraorbital canal continues across the parietals; the supratemporal sensory canal runs close to the posterior edge of the parietals.

The sphenotic has a lateral ventral projection at the back of the orbit. In ventral view the sphenotic has a rounded posterior edge. The pterotic has two posterior projections: the lateral projection is more prominent, with the medial projection less pronounced. In lateral view, the pterotics are narrow anteriorly and widen posteriorly. Each prootic roughly forms a rectangle with rounded corners and an anterior ridge in ventral view. They are oval shaped in lateral view and are relatively large.

The parasphenoid is bifurcated anteriorly where it contacts the vomer and bends downwards to the ventral portion of the orbit. There are two lateral wings at the posterior portion of the orbit where the parasphenoid contacts the prootics and the posterior end is also bifurcated. The orbitosphenoid and pterosphenoid are roughly rectangular in ventral view. The orbitosphenoid is visible on either side of the parasphenoid in ventral view. The anterior edge of the orbitosphenoid comes to a point, with straight lateral and posterior edges in ventral view forming a rectangle. The pterosphenoids appear rhomboid in shape with rounded corners. As for all other species of Alestidae, the rhinosphenoid is absent, which differentiates this family from the Characidae, which have this bone (Gery, 1977).

The supraoccipital has a posterior projection along the dorsal edge. The epioccipitals are large ovoid bones that surround the third post-temporal fenestra in posterior view. The exoccipitals have a slight slope along their dorsal edge and are rounded posteroventrally, where they form a large lagenar capsule with the basioccipital, commonly reported in characiforms (Fink & Fink, 1981; Brewster, 1986; Murray, 2004).

2.3.4 Jaws and Teeth

The premaxilla has a pointed ascending process and a premaxillary pedicle (Roberts, 1969), which is observed in most alestids (Murray & Stewart, 2002). The premaxillary pedicle is present as an elongate ledge on the posteroventral portion of the premaxilla where it tapers posteriorly (Fig. 2.7). The premaxillae have no interdigitating suture. Multicuspid teeth (three or more cusps) are present on the premaxillae and dentaries, with replacement teeth present in a tooth crypt (Fig. 2.8).

The anterior portion of the maxilla is narrow. The posterior portion of the maxilla widens into an oval. The maxillae are edentulous.

The dentaries have an interdigitating suture where they meet one another in the symphysis. The posterior part of the dentary is convex and the anteroventral part is upturned. The mandibular sensory canal continues onto the anguloarticular from the preopercular and extends across the lateral surface of the dentary, branching anteriorly towards the dentition. Dorsal to the mandibular sensory canal is Meckel’s cartilage, present as a long, narrow cylinder. The dentary has four teeth that substantially decrease in size posteriorly. There is no inner dentary tooth as found in larger alestids (Murray, 2004; Zanata & Vari, 2005).

The anguloarticular has a rounded dorsal expansion. The anterior portion of the anguloarticular has a rhomboid shape with the mandibular sensory canal continuing across the ventral surface. The retroarticular is a small oval-shaped bone at the posteroventral corner of the dentary. The coronomeckelian, a small oblong bone, is visible in medial view in the center of the dentary above Meckel’s cartilage.

2.3.5 Opercular Bones

The two limbs of the preopercle form a right angle with the sensory canal running along both limbs (Fig. 2.9). The sensory canal opens to the surface ventrally via pores on the horizontal arm of the preopercle. The interopercle is narrow anteriorly and wide posteriorly; it is positioned such that it extends past the posterior edge of the preopercle and just overlaps the anterior edge of the subopercle and opercle. The subopercle is a slender bone that runs the length of the posteroventral edge of the opercle. The opercle has a straight anterior edge and convex posterior edge; this creates the shape of a half circle. The opercle bears a medial facet on the anterodorsal edge for the hyomandibula.

2.3.6 Suspensorium

The palatine is narrow posteriorly and widens into a bulb anteriorly and the ectopterygoid is a narrow, slightly curved bone. The endopterygoid is wide in lateral view, and slopes medially along the dorsal portion of the bone. The metapterygoid has a posterior expansion and narrows to a rod anteriorly. As reported in other alestids, the two limbs of the quadrate form a posterior-facing 90° angle (Murray, 2004). The upper limb creates a fan shape, whereas the ventral limb is long and slim (Fig. 2.10). The symplectic is an elongate bone with a slight upward curve. The hyomandibula narrows ventrally and widens dorsally, curving laterally on the anterior portion of the bone.

2.3.7 Infraorbital Bones

The infraorbital series consists of seven bones, the antorbital, lacrimal (infraorbital 1), infraorbitals 2 through 5 and the dermosphenotic (infraorbital 6), with no supraorbital present. Instead, the lateral edge of the frontal completes the dorsal margin of the orbit.

The antorbital is a small bone forming the anterior edge of the orbit and posterodorsally fits into a notch in the dorsal portion of the first infraorbital (Fig. 2.11). The circumorbital sensory canal is present on all infraorbitals except the antorbital with an opening at either end of the canal on each bone. However, unlike other alestids that have a tripartite laterosensory canal on their dermosphenotic (Murray & Stewart, 2002; Murray, 2004; Zanata & Vari, 2005), *H. barnardi* has a single canal on the dermosphenotic.

2.3.8 Branchial Arches and Pharyngeal Region

The basihyal is long and narrow with a cartilaginous anterior tip (Fig. 2.12a). The first two basibranchials are also long and narrow with cartilaginous tips. The third basibranchial is ossified and narrower anteriorly, compared to the posterior end that is cartilaginous and wide. The hypobranchials are rectangular with cartilaginous tips. The first four ceratobranchials are long slender rods that become progressively shorter posteriorly through the series. The fifth ceratobranchial expands anteriorly to form a medial plate bearing small conical teeth on the dorsal surface.

The upper pharyngeal series consists of five epibranchials; the first three are long, rod-like bones, with the third having a projection towards the pharyngobranchials (Fig. 2.12b) and the fourth and fifth epibranchials are small, rectangular elements. The epibranchials are capped with cartilage. The four pharyngobranchials are small bones with cartilaginous tips. They connect medially to the epibranchials.

The ceratohyals articulate with the basihyal and the first basibranchial via the hypohyals. The dorsal and ventral hypohyals are curved, with the dorsal hypohyals arching ventrally and the ventral hypohyals arching dorsally, leaving an opening between them (Fig. 2.12c). The anterior ceratohyal is narrow anteriorly and widens posteriorly with a raised edge on the posterodorsal portion. The posterior ceratohyal is rectangular with the dorsal portion of the bone continuing the raised ledge from the anterior ceratohyal. The interhyal is a small triangle with rounded tips.

There are four branchiostegal rays. They are long, curved rods with the first branchiostegal ray shorter than branchiostegal rays 2-4. The first three branchiostegal rays contact the anterior ceratohyal and the fourth branchiostegal ray contacts the posterior ceratohyal.

The urohyal is narrow anteriorly with a rounded bulbous anterior end (Fig. 2.12d). Posteriorly, the urohyal expands forming a triangle in ventral view and has a median dorsal projection that forms a triangle in lateral view.

2.3.9 Paired Fins and Girdles

The extrascapular is oval with the supratemporal sensory canal running the length of it (Fig. 2.13a). The posttemporal has a narrow dorsal projection and widens into an oval ventrally. The supracleithrum is elongate. The supratemporal sensory canal crosses the posteroventral corner of the posttemporal from the extrascapular and runs the length of the supracleithrum. There are two small oval postcleithra, with the second slightly larger than the first. The first postcleithrum is positioned at the posteroventral base of the supracleithrum and the second postcleithrum is positioned medial to the posterior-most part of the cleithrum.

The cleithrum extends dorsally with a narrow arm and widens posteroventrally with a horizontal expansion. The scapula is a wide fan shape dorsally and narrows ventrally (Fig. 2.13b). The mesocoracoid is a long narrow bone that widens slightly ventrally where it contacts the coracoid. The coracoid has two wide expansions and forms approximately a 90° angle. The anterior edge is straight, with a convex posterior edge and slightly concave ventral edge. There is one unbranched and eight or nine branched pectoral fin rays.

The pelvic girdle is narrow anteriorly and widens posteriorly where the fin rays articulate. The ischiac processes on the posterior pelvic girdles directly contact each other (Fig. 2.14). The pubic processes of the pelvic girdle expand slightly laterally. The pelvic fins contain one unbranched and seven or eight branched fin rays, along with a lateral pelvic splint.

2.3.10 Weberian Apparatus and Vertebral Column

The Weberian apparatus, a modification to the first four vertebrae in Characiformes and four to five vertebrae in other ostariophysan fishes, enhances hearing. In *H. barnardi*, the neural complex has a lateral ledge and widens posteriorly over vertebrae 3 and 4 (Fig. 2.15). The tripus, a fan-shaped bone, is lateral to vertebrae 2 to 4, with the transverse processes of vertebrae 2 and 4 overlapping it. The transverse process of vertebra 3 extends anteriorly, overlapping the intercalarium and scaphium. The intercalarium is a long bone that gently curves anterodorsally. The scaphium is ovoid and is overlain by a smaller oval bone, the claustrum.

The vertebral column consists of 34-36 centra, with 15-17 abdominal centra and 18-20 caudal centra (Tab. 2.2). In cleared and stained specimens (n = 4), there are two transitional centra according to Brewster's (1986) definition (available in Appendix B), which were difficult to determine on radiographs and therefore are included in the counts of abdominal centra here. Ribs are expanded dorsally with a flange where they attach to the centra.

Intermuscular bones are present in pairs above and below the centra. The epineurals begin at centrum 9 or 10 and continue to preural 5. Whereas the epiplurals are only associated with the haemal spines and end by preural 5.

2.3.11 Dorsal and Anal Fins and Supports

The dorsal fin has two unbranched fin rays and eight to nine branched rays (Tab. 2.2). The first unbranched dorsal-fin ray is approximately half the length of the second unbranched fin ray, which is the longest. The remaining branched fin rays progressively decrease in size. The dorsal fin is falcate in shape.

The anal fin is large and falcate. It is positioned posteriorly on the body (preanal length is 63-73% SL, mean = 68% SL). The anal fin has three unbranched rays and 15 to 18 branched rays. The first unbranched ray of the anal fin is small and just visible in unstained specimens, with the remaining two unbranched rays substantially longer. The first anterior branched anal-fin ray is the longest with the remaining 14 to 17 branched fin rays decreasing in size. Sexual dimorphism may exist in the anal fin, as noted by Zanata and Vari (2005) and discussed here in Section 2.5.0.

2.3.12 Caudal Fin and Skeleton

The forked caudal fin is about a quarter of the total length (TL) (18-29% TL, mean = 24% TL). In the caudal skeleton, the urostyle extends into a posterodorsal point originating from a wide base on the anterior edge of the fused first ural and preural centrum (Fig. 2.16). The neural and haemal spines on preural centrum 2 have anterior flanges, while the neural spine on preural centrum 3 has a posterior flange. The three epurals are approximately the same size.

There are six hypurals. The first is the largest with a triangular shape and the second hypural is long and narrow directly dorsal to the first hypural. There is a space (diastema) between the first two hypurals and the remaining four. Hypurals 3-6 are rectangular or sub-triangular, with hypural 3 being the longest and the remainder progressively decreasing in size. The parhypural has an anterior flange proximally. The posterior ends of the urostyle, hypurals and parhypural remain cartilaginous.

2.4 Sexual Dimorphism

The neural spines of preural centra were previously reported to be sexually dimorphic in alestids, with males having a longer neural spine on the second preural centrum compared to females (Brewster, 1986; Murray & Stewart, 2002). Zanata and Vari (2005), however, reported variation in the length of neural spines of preural centra that does not correspond to sex. In the specimens examined here, the neural spines on the preural centra of *Hemigrammopetersius barnardi* were found to vary depending on the size of the specimen (n = 4), suggesting this variation may be related to size and is not sexually dimorphic.

In contrast, the anterior anal pterygiophores and fin rays of *H. barnardi* seem to be sexually dimorphic. Zanata and Vari (2005) identified males as having branched anterior anal-fin rays with thicker bases and a posterior projection. Recent descriptions of new alestid species also note sexual dimorphism of the anal fin, both structurally and in coloration (Stiassny & Mamonekene, 2007; Mamonekene & Stiassny, 2012). While a thickening of the anterior anal-fin rays is observed in one of the cleared and stained specimens here (Fig. 2.17a), the other three, presumably female, do not exhibit these features (Fig. 2.17b). For the specimens examined in this study there was no method available to confirm the sex of the cleared and stained individuals (*n* = 4) and any observations about dimorphism of the caudal and anal fin should be further investigated for confirmation.

2.5 Discussion

2.5.1 Intraspecific Variation

A variety of factors are responsible for intraspecific variation of morphological features commonly reported in fishes (Barlow, 1961; Lazzarotto *et al.*, 2017). A number of freshwater fishes are noted to exhibit individual phenotypic plasticity in their morphology based on their environment (Lazzarotto *et al.*, 2017). A few studies have focused on intraspecific variation in Alestidae (e.g., Nzeyimana and Amiet, 1992 and Murray, 2004). Here, I assess the intraspecific variation within a sample (*n* = 161) of *Hemigrammopetersius barnardi.*

Most size-related measurements of *H. barnardi* are normally distributed for this sample, with some demonstrating right-skewed distribution and demonstrate isometric growth (represented by a slope of approximately 1.0) (Appendix C). Overall, the size-measurements are comparable with those previously reported in the literature. I recorded a range of 22.7 to 44.5 mm TL for specimens of *H. barnardi*, whereas Morioka and Matsumoto (2002) recorded a range of 20.15 mm to 52.20 mm TL (*n* = 73) for specimens of *H. barnardi*. Poll (1967) examined four paratypes of *H. barnardi* and reported a maximum TL of 38 mm. All of these TL values are less than the reported maximum SL of 70 mm, which is published in a field guide of Tanzanian freshwater fishes and does not specify if measurements were recorded specifically for the guide or if they are from other sources (Eccles, 1992).

Poll (1967) provided other meristics, which are compared to those reported here in Table 2.3. Meristics reported by Poll (1967) and here fall within the same range. No strong correlations ('strong' defined as $r > 0.70$) were found between standard length and meristics. This was expected as fish generally do not increase the number of scales or fin rays with growth; however, Murray (2004) reported an increase in gill rakers with growth in specimens of *Alestes stuhlmanni* Pfeffer. An increase in gill rakers associated with growth and environmental factors has been reported in multiple fish species (e.g., *Sardinops caeruleus* in Villalobos & Rodriguez-Sanchez, 2002; and *Leedsichthys* sp. and *Asthenocormus* sp. in Liston, 2013). A positive correlation in relation to length and the number of gill rakers was not found here for specimens of *H. barnardi*.

The studied sample has a normal to slightly right-skewed distribution, suggesting that the fish assessed here were on average smaller with a select few reaching larger body sizes. Many of the length measurements were strongly positively correlated with each other ($r > 0.70$). As a result, the first principal component was strongly influenced by length data. The first two principal components explained less than 40% of the variance, with the first component correlated with length measurements and the second component correlated strongly with body depth.

Two of the examined specimens of *H. barnardi* do not have an adipose fin. As characiforms develop their adipose fin at the end of ontogeny (Pastana *et al.*, 2017), the variability of its presence may be the result of variation at the end of ontogeny due to changes in heterochronic events that are reported in small and miniature tetras (Dagosta *et al.*, 2014; Marinho, 2017). However, Murray (2004) reported one specimen in a sample ($n = 143$) of a larger alestid, *A. stuhlmanni,* to have no adipose fin. Thus, the lack of the adipose fin may not be limited to fish with reduced adult size and be the result of intraspecific variation.

2.5.2 Dentition of Alestidae

Species of Alestidae display a variety of dentitions, with evidence suggesting that unicuspid teeth are the result of simplification due to small body sizes or are secondarily simplified from a multicuspid dentition in larger specimens (Roberts, 1966; Poll, 1967; Brewster, 1986). Brewster (1986) proposed that the conical dentition in specimens of *Hydrocynus* was a secondary simplification. Further, Murray (2004) documented changes in the premaxillary and outer dentary teeth throughout growth in *A. stuhlmanni* from unicuspid to multicuspid, accompanied by labio-lingual thickening throughout growth. Hence, the simplified or unicuspid teeth observed in dwarf alestids (Gery, 1995) may be the result of small body size and not indicative of phylogenetic relationships.

Hemigrammopetersius barnardi has multicuspid dentition. Fewer cusps are present in specimens of *Hemigrammopetersius* compared to other small alestid species according to Poll (1967). Specimens of *H. barnardi* do not have an inner dentary symphyseal tooth (Zanata & Vari, 2005). This is in agreement with Poll's (1967) study on dwarf alestids where he noted that some genera lack the inner dentary symphyseal tooth (*Petersius, Arnoldichthys, Rhabdalestes, Alestopetersius, Clupeopetersius,* and *Lepidarchus)*.

2.5.3 Osteological Comparison of a Small Alestid to a Previously Described Alestid with a Larger Body Size

The comparison to other studies on the osteology of species of Alestidae will allow for initial identifications of potential homoplastic reductions and losses. Murray (2004) conducted a comprehensive assessment on a sample (*n* = 143) of a larger alestid, *A. stuhlmanni*, which is compared to the osteology described here.

Alestes stuhlmanni has a complete circumorbital series, compared with *H. barnardi*, which lacks the supraorbital. According to Zanata and Vari's (2005) phylogenetic hypothesis, the loss of the supraorbital is a homoplastic trait within Alestidae. Specifically, they identified two clades with this loss in their most parsimonious analysis: (i) *Ladigesia* and *Lepidarchus*, and (ii) *Hemigrammopetersius, Micralestes, Rhabdalestes,* and *Virilia* (Zanata & Vari, 2005). Azevedo (2010) associated the absence of the supraorbital with reduced body size in other characiforms. Further, *A. stuhlmanni* has a tripartite canal on the dermosphenotic, whereas *H. barnardi* has a single continuation of the circumorbital canal on the dermosphenotic. These features suggest a simplification of the circumorbital series in specimens of *H. barnardi*.

Specimens of *H. barnardi* have a simplified osteology with many of the bones being oval in shape, having rounded edges and lacking processes, in comparison with a larger fish, such as *A. stuhlmanni*, which has substantially more processes and projections (Murray, 2004). For example, the two posterior projections of the pterotics are substantially larger in specimens of *A. stuhlmanni,* extending just past the posterior edge of the basioccipital (Murray, 2004, Fig. 2), whereas in specimens of *H. barnardi* they only extend just past the anterior edge of the basioccipital.

Other examples of simplifications in the osteology of *H. barnardi* compared to *A. stuhlmanni* are found in the postcranial skeleton. The pectoral and pelvic girdles demonstrate reduced projections and processes in comparison to *A. stuhlmanni*. While specimens of *A. stuhlmanni* have a large, narrow anterior projection on the posttemporal and smaller projections on the anterior edge of the extrascapular (Murray, 2004), those same bones in specimens of *H. barnardi* have rounded, smoother edges and a smaller anterior projection on the posttemporal.

In addition to a simplification of the osteology of *H. barnardi* in comparison to the larger *A. stuhlmanni*, specimens of *H. barnardi* exhibit an increased amount of cartilage and lack of ossification of elements. This is particularly evident in the pharyngeal region. *Hemigrammopetersius barnardi* retains cartilage on the ends of most of the hypobranchials, ceratobranchials, epibranchials and pharyngobranchials, in addition to a large portion of the basihyal and basibranchials being cartilage. Further, the ceratohyals and hypohyals are connected with cartilage. While *A. stuhlmanni* also has cartilage present in the pharyngeal region, it is to a much lesser extent, with only basibranchial 4, the anterior portion of the basihyal, and the tips of the pharyngobranchials and epibranchials having cartilage (Murray, 2004). The simplification or loss of some bones and decrease in ossification may be due to the small body size exhibited by specimens of *H. barnardi*.

2.5.4 Conclusion

Many lineages of teleosts have independently evolved smaller body sizes relative to ancestral states figures are all too blurry and too small. Increase size and clarity. (Steele & Lopez-Fernandez, 2014). Possibly due to the diverse conditions present in freshwater environments, such as small streams (Castro, 1999; Knouft & Page, 2003), smaller-bodied organisms are common as they can efficiently use fewer resources (Peters, 1992) and lower the amount of competition (Douglas, 1987). Alestid fishes are found in lowland rivers throughout Africa (Roberts, 1975), with small-bodied alestids in seasonal and permanent freshwater bodies such as lakes, rivers, and marshes (IUCN, 2020), which may potentially increase the evolution of small body sizes.

A decrease in body size may contribute uncertainty to phylogenetic analyses of relationships through homoplasy resulting from decreased body-size and not evolutionary relationships (Murray & Stewart, 2002; Britz & Conway, 2009). Alestidae encompasses a pronounced range of sizes, from 21 mm SL to 1300 mm SL (Hubert *et al.*, 2005), posing difficulties in generating phylogenetic hypotheses when using morphological features. Molecular data may be used to circumvent these difficulties but poses difficulties when using old preserved species where the DNA may be destroyed. Therefore, it is crucial to understand the impact of small body sizes on morphology. Pastana *et al.* (2017) drew attention to the limited osteological descriptions of miniature characiform taxa. While *H. barnardi* is not a true miniature according to Weitzman and Vari's (1988) arbitrary definition (which is that the animal does not exceed a maximum size of 26 mm SL or reach sexual maturity by 20 mm SL), it does exhibit a decrease in body size in comparison to close relatives (Zanata & Vari, 2005). Therefore, the detailed description of the osteology of *H. barnardi* presented here provides a foundation for future osteological comparisons of alestids and studies of miniaturization.

2.6 Tables

Table 2.1. Measurements and ratios for *Hemigrammopetersius barnardi*, CMN F 81-0188, from the Rufiji River basin (n = 158 unless otherwise stated).

	Range	**Mean**	**SD**
Standard length (SL mm)	19.2 – 34.9	25.0	3.6
Total length (TL mm)	22.7 – 44.5	33.0	2.8
SL:TL	0.71 – 0.95	0.76	0.03
Body depth SL^{-1}	0.24 – 0.32	0.27	0.02
Head length (HL mm) SL^{-1}	0.20 – 0.27	0.23	0.01
Head depth SL^{-1}	0.16 – 0.28	0.21	0.01
Eye diameter HL^{-1}	0.31 – 0.49	0.39	0.03
Interorbital distance HL^{-1}	0.26 – 0.43	0.34	0.03
Snout length HL^{-1}	0.17 – 0.30	0.23	0.03
Caudal peduncle depth:Caudal peduncle length	0.53 – 0.92	0.72	0.08
Preadipose length SL^{-1} (n = 156)	0.68 – 1.18	0.87	0.04
Predorsal length SL^{-1}	0.49 – 0.61	0.56	0.02
Preanal length SL^{-1}	0.63 – 0.73	0.68	0.02
Prepelvic length SL^{-1}	0.43 – 0.54	0.49	0.02
Prepectoral length SL^{-1}	0.22 – 0.28	0.25	0.01
Dorsal fin base SL^{-1}	0.07 – 0.14	0.10	0.01
Anal fin base SL^{-1}	0.16 – 0.3	0.21	0.02

Table 2.2. Meristics for *Hemigrammopetersius barnardi*, CMN F 81-0188, from the Rufiji River basin. The number of specimens that showed each count is in brackets.

Number of	**Sample Size**					
Dorsal-fin rays	157	9 (25)	10 (132)			
Anal-fin rays	158	18 (3)	19 (64)	20 (21)	21 (70)	
Abdominal vertebrae	157	15 (28)	16 (117)	17 (12)		
Caudal vertebrae	157	18 (27)	19 (108)	20 (22)		
Total vertebrae	157	34 (36)	35 (106)	36 (15)		
Lateral line scales	120	8 (10)	9 (32)	10 (36)	11 (25)	12 (17)
Transverse scales	63	7 (19)	8 (37)	9 (7)		
Gill rakers	157	9 (25)	10 (132)			

Table 2.3. Comparison of measurements from this study to Poll's (1967) study. Roman numerals refer to unbranched fin rays and Arabic numerals refer to branched fin rays.

Measurement	**Current Study**	**Poll (1967)**
Dorsal Fin Rays	II, 7 – 8	II,8
Anal Fin Rays	III, 15 – 18	II-III, 16-17
Gill Rakers	14 – 17	15 – 16
Lateral Line Scales	8 – 12	7 – 12

2.7 Figures

Figure 2.1. Photograph of a preserved specimen of *Hemigrammopetersius barnardi*. CMN F 81-0188, specimen number 66, SL = 31.1 mm. Scale bar = 5 mm.

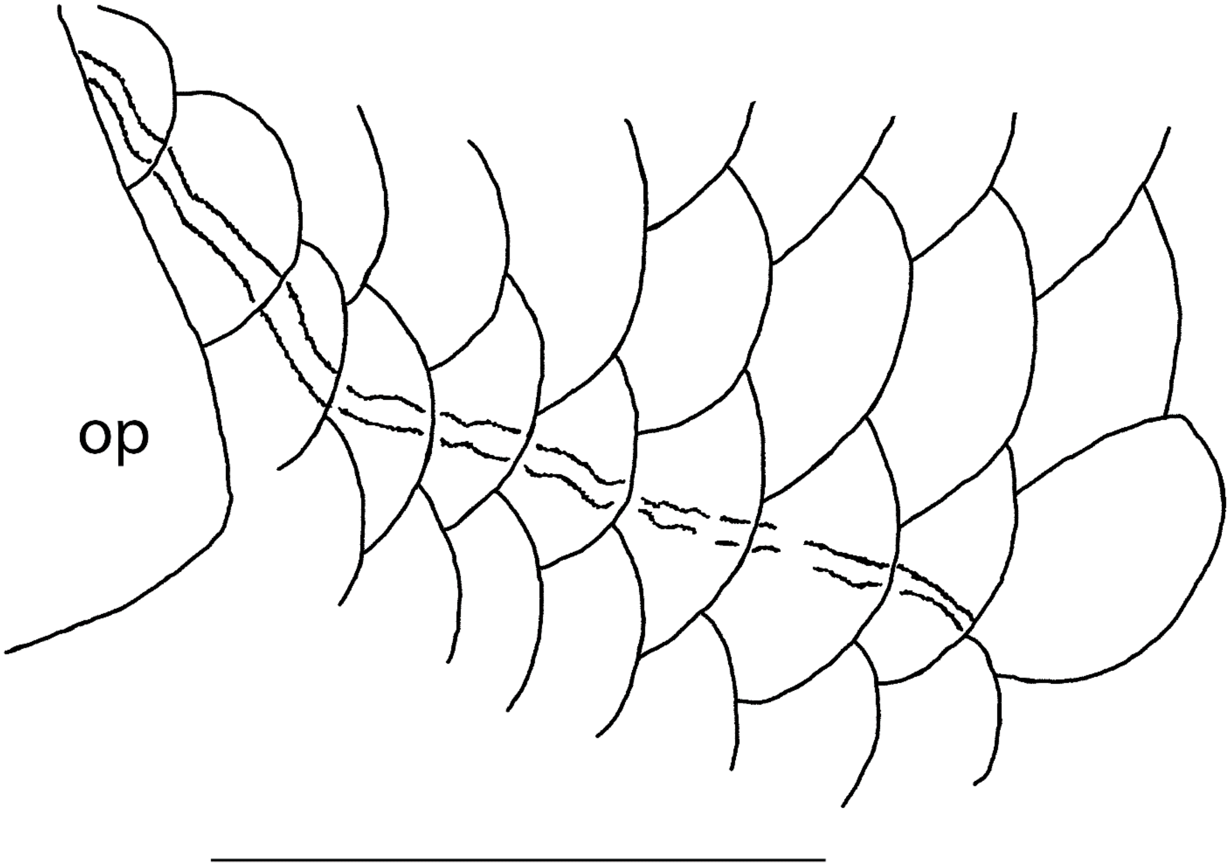

Figure 2.2. Drawing of the anterior scales of the lateral line of *Hemigrammopetersius barnardi* CMN F 81-0188, specimen number 110, SL = 29.2. Scale bar = 5 mm.

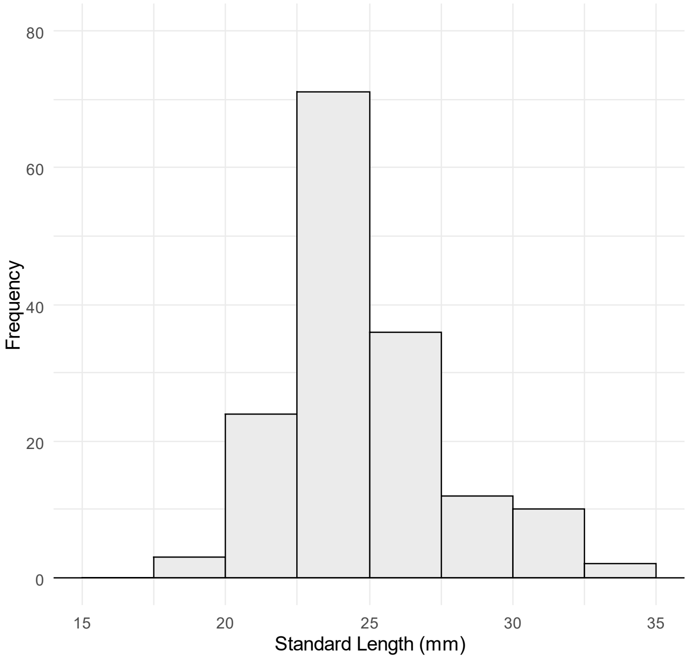

Figure 2.3. Histograms of standard length for *Hemigrammopetersius barnardi* CMN F 81-0188 (*n* = 158). All measurement data reflects a similar normal distribution as presented here.

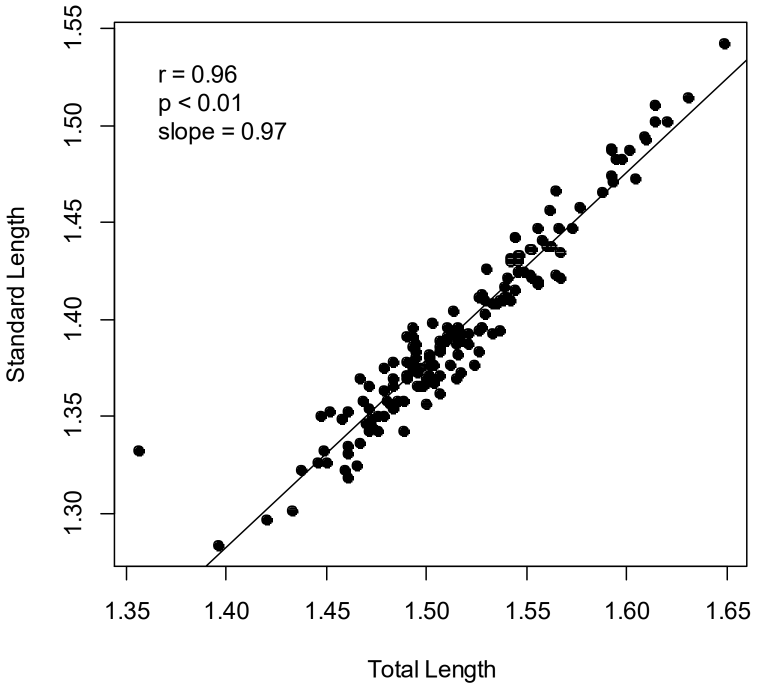

Figure 2.4. Scatterplot of standard length in relation to total length for *Hemigrammopetersius barnardi* CMN F 81-0188 (*n* = 158) using logarithmic data. Pearson correlation and slope values are in the respective top left corners. Scatterplots for remaining measurements in relation to standard length are available in Appendix C.

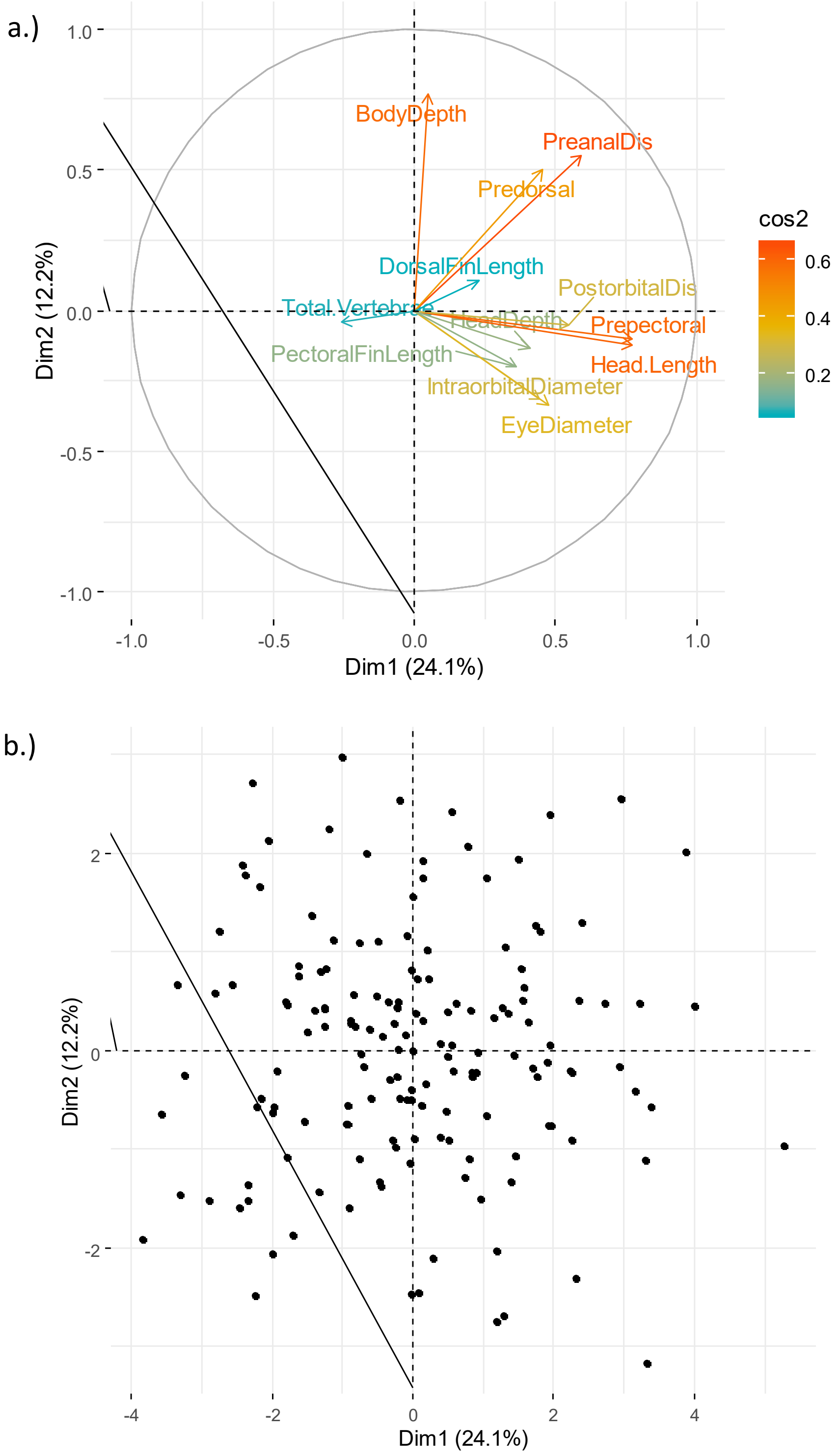

Figure 2.5. PCA of select measurements for *Hemigrammopetersius barnardi*, CMN F 81-0188, (a) a correlation circle of the representation of each variable and (b) the distribution of the individuals in the sample for dimensions 1 and 2. The first dimension represents 24.1% and the second 12.2% of the variance.

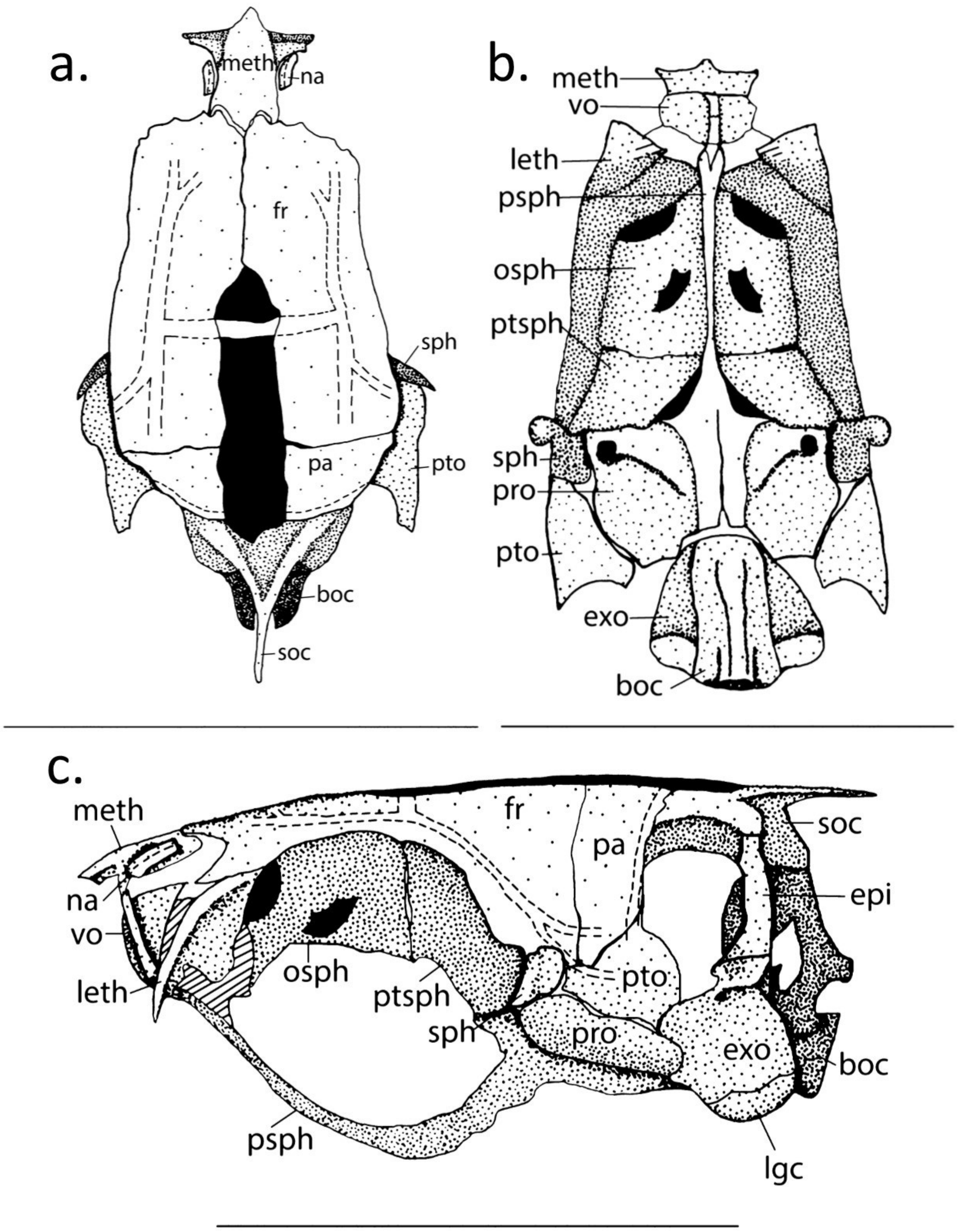

Figure 2.6. Drawing of the adult skull of *Hemigrammopetersius barnardi* CMN F 81-0188, specimen number 106, SL = 31.2 mm, (a) dorsal, (b) ventral, and (c) lateral views. Hatching represents cartilage. Scale bar = 5 mm.

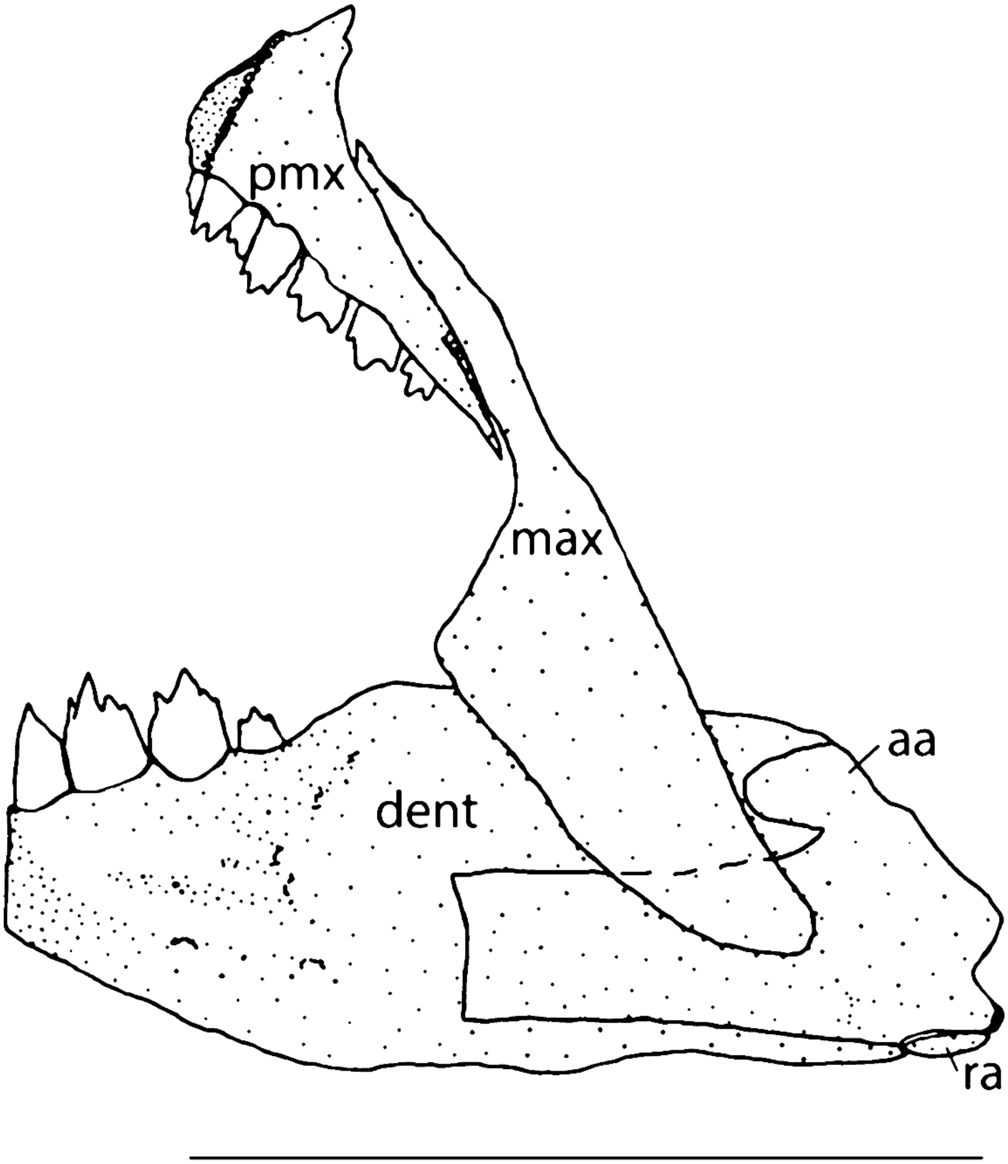

Figure 2.7. Drawing of the left jaw in lateral view of *Hemigrammopetersius barnardi* CMN F 81-0188, specimen number 106, SL = 31.2 mm. Scale bar = 1.3 mm.

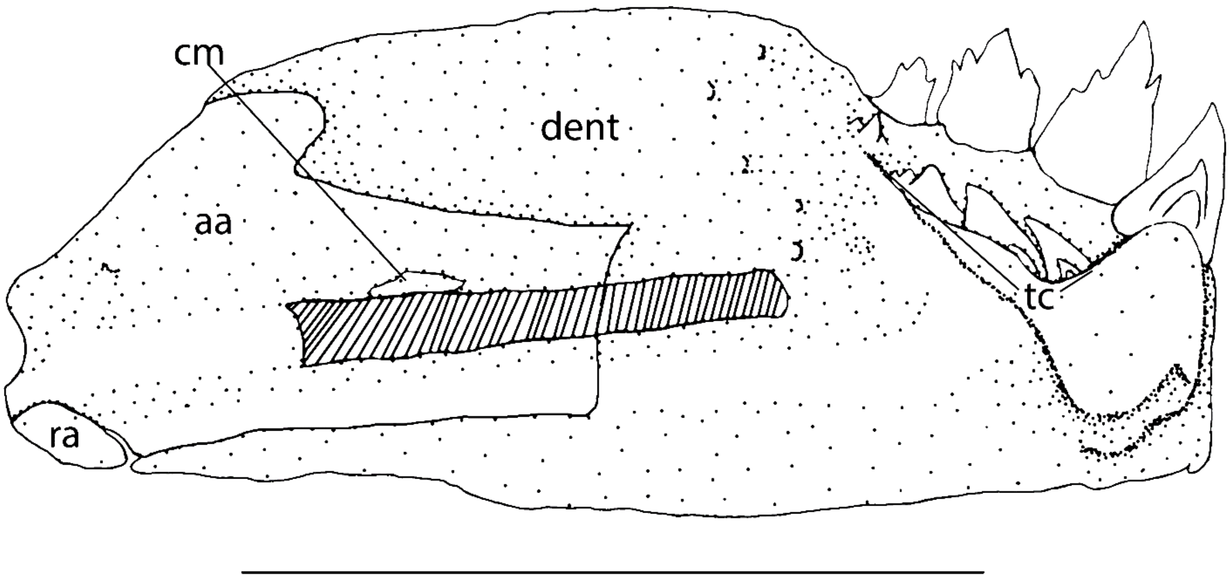

Figure 2.8. Drawing of the left dentary bone in medial view of *Hemigrammopetersius barnardi* CMN F 81-0188, specimen number 106, SL = 31.2 mm featuring the tooth crypt. Hatching represents cartilage. Scale bar = 1.3 mm.

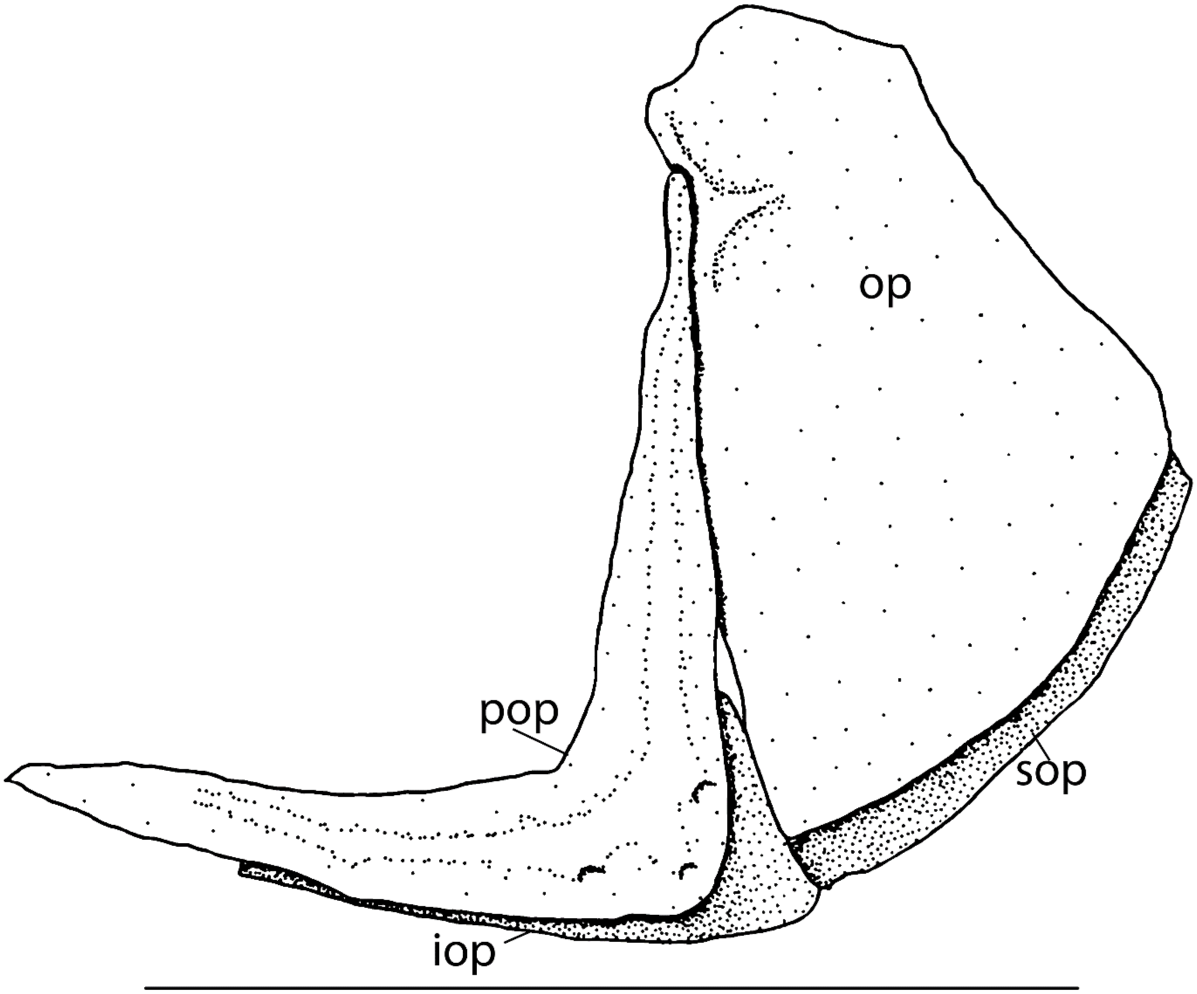

Figure 2.9. Drawing of the opercular series of *Hemigrammopetersius barnardi* CMN F 81-0188, specimen number 2, 38.6 mm SL. Scale bar = 5 mm.

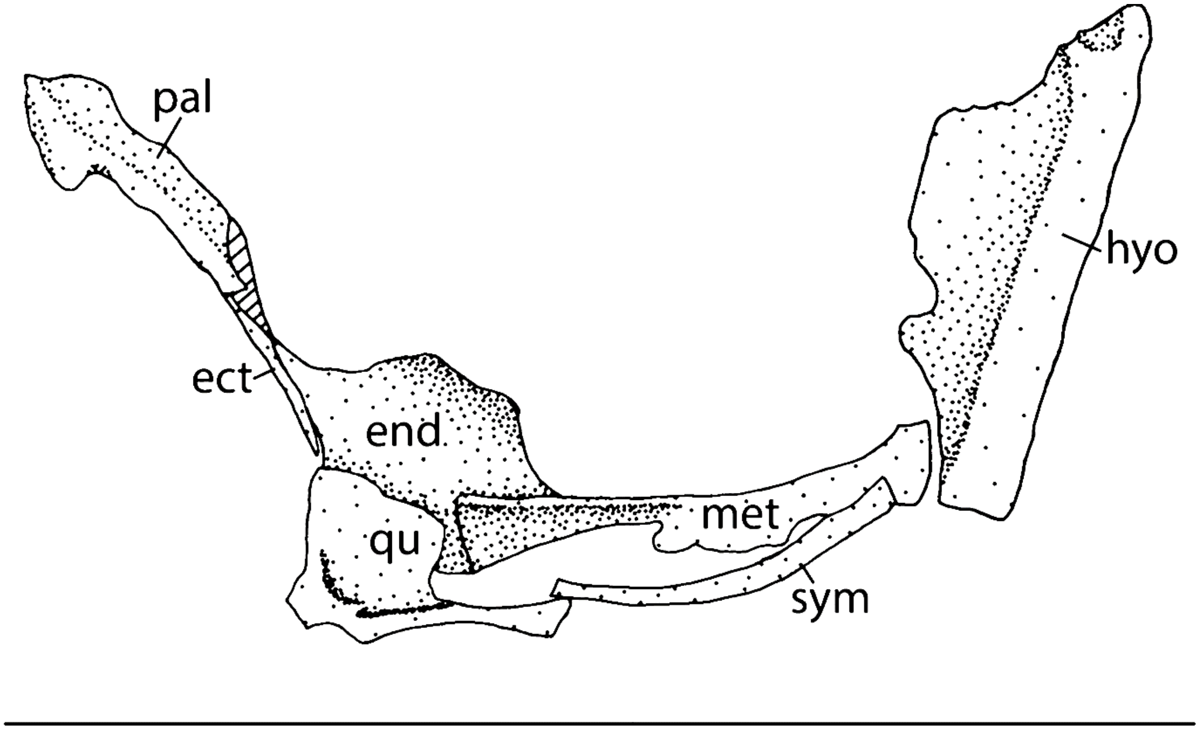

Figure 2.10. Drawing of the suspensorium of *Hemigrammopetersius barnardi* CMN F 81-0188, specimen number 106, 31.2 mm SL in lateral view. Scale bar = 5 mm.

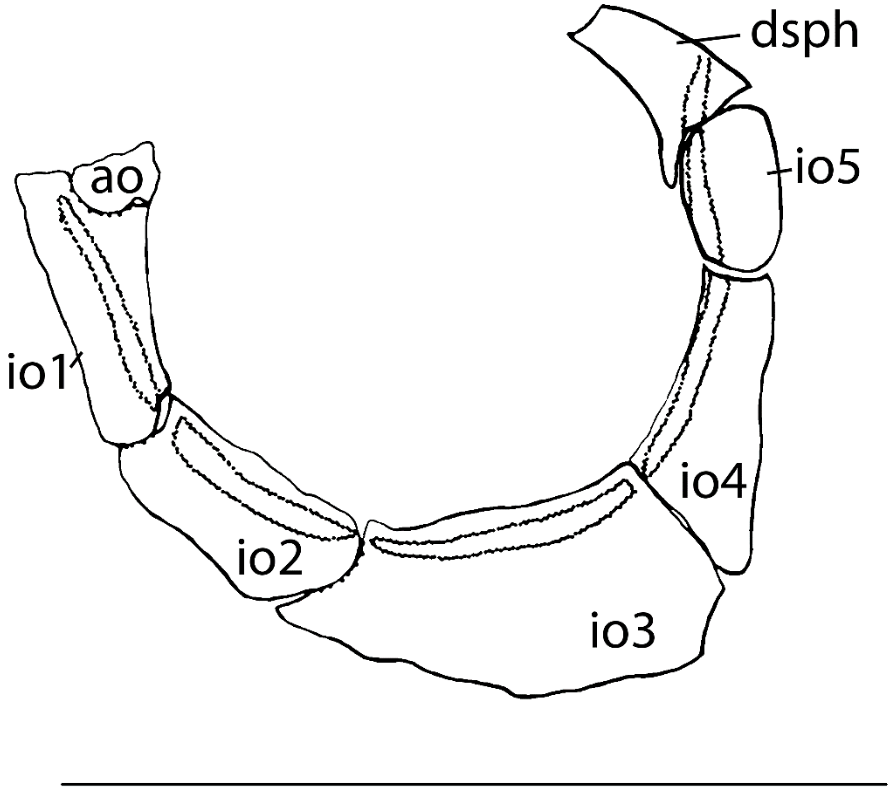

Figure 2.11. Drawing of the infraorbital series of *Hemigrammopetersius barnardi* CMN F 81-0188, specimen number 4, 32.7 mm SL. Scale bar = 5 mm.

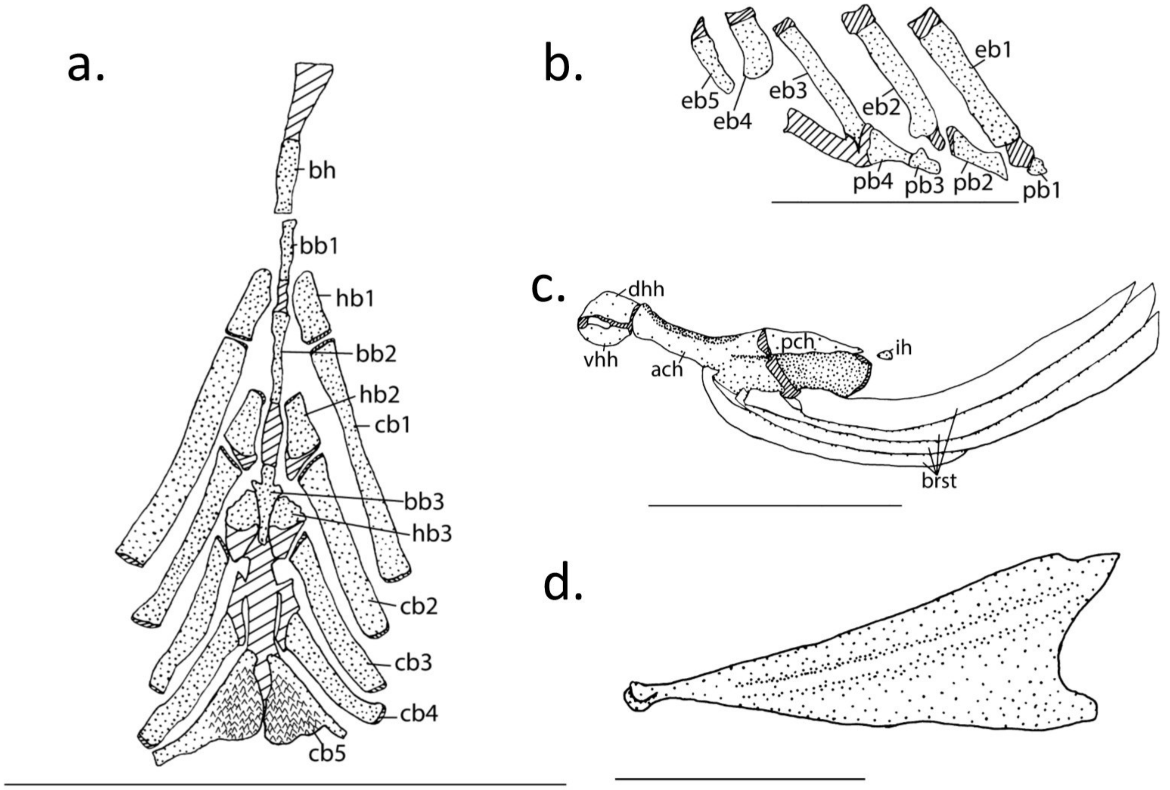

Figure 2.12. Drawing of the branchial arches and pharyngeal region of *Hemigrammopetersius barnardi* CMN F 81-0188, specimen number 106, 31.2 mm SL, (a) lower pharyngeal bones, (b) upper pharyngeal bones, (c) ceratohyal, and (d) urohyal. Hatching represents cartilage. Scale bar for a = 5 mm, scale bar for b, c and d = 1.3 mm.

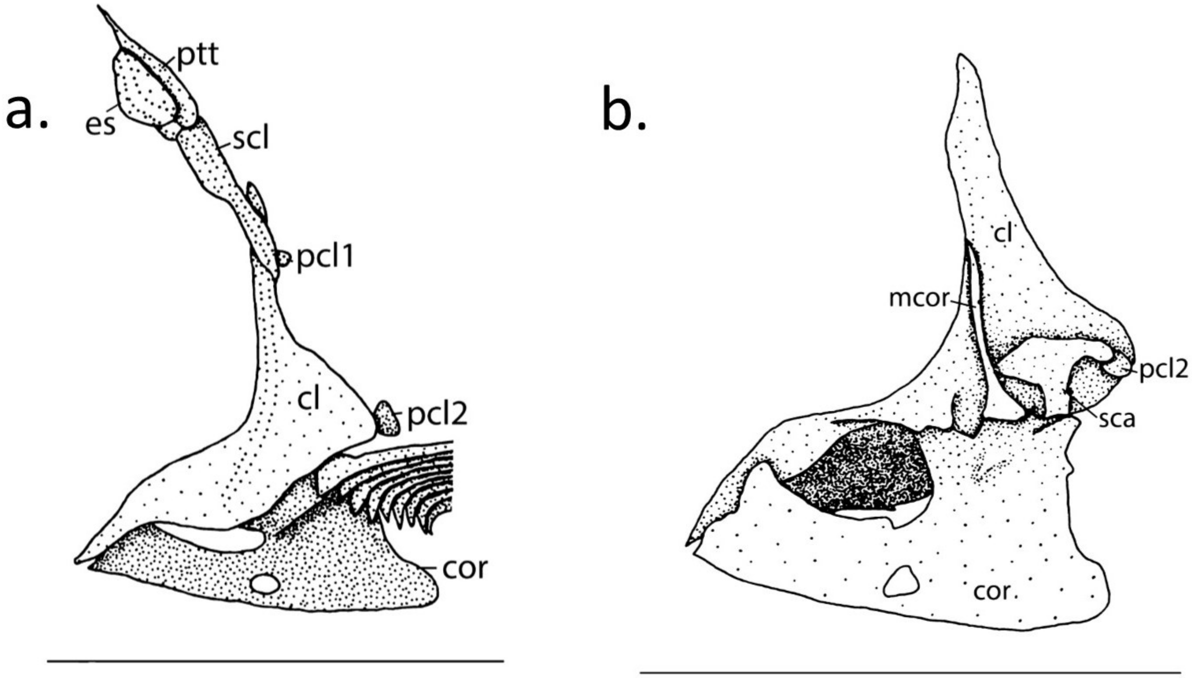

Figure 2.13. Drawing of the pectoral girdle of *Hemigrammopetersius barnardi* CMN F 81-0188, specimen number 106, 31.2 mm SL, in (a) left pectoral girdle in lateral view and (b) right pectoral girdle in medial view. Scale bar = 5 mm.

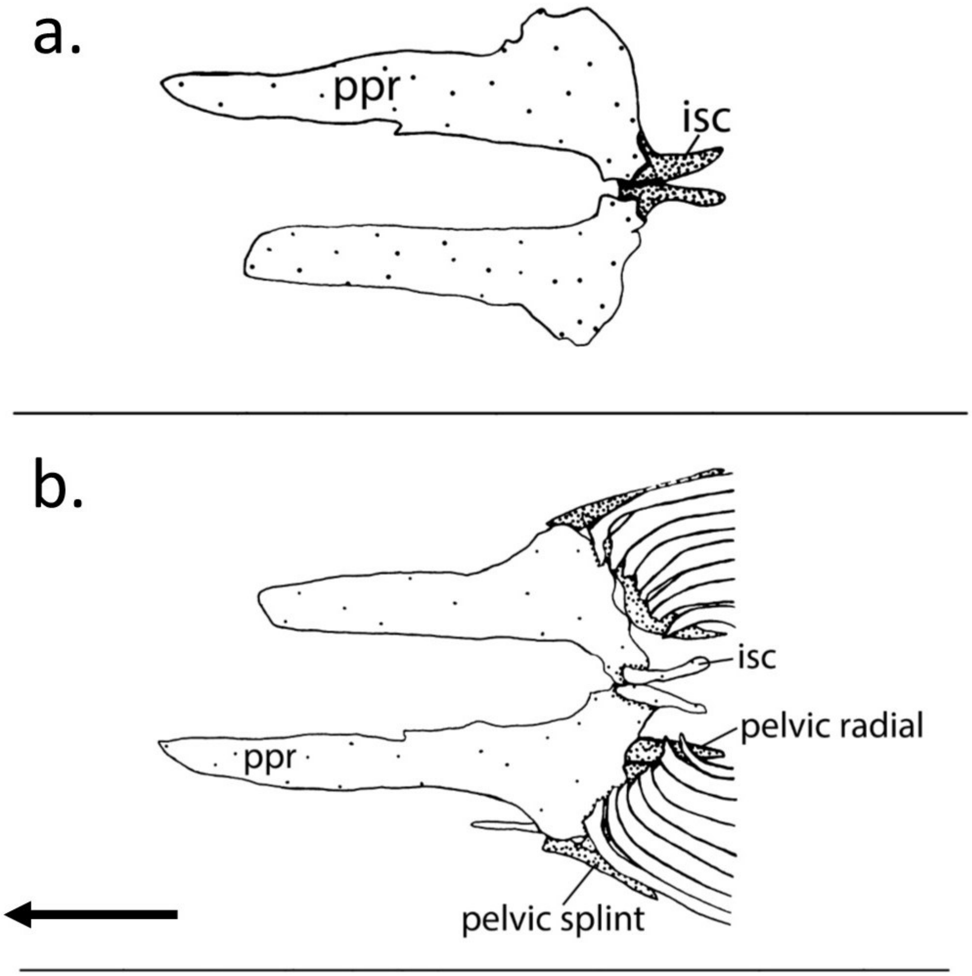

Figure 2.14. Drawing of the pelvic girdle of *Hemigrammopetersius barnardi*, CMN F 81-0188, specimen number 106, 31.2 mm SL (a) dorsal and (b) ventral view. The arrow points anteriorly. Scale bar = 5 mm.

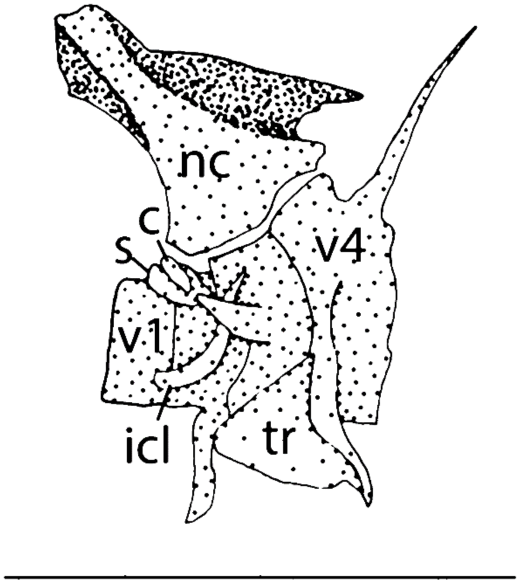

Figure 2.15. Drawing of the Weberian apparatus of *Hemigrammopetersius barnardi* CMN F 81-0188, specimen number 3, 26.2 mm SL. Scale bar = 1.3 mm.

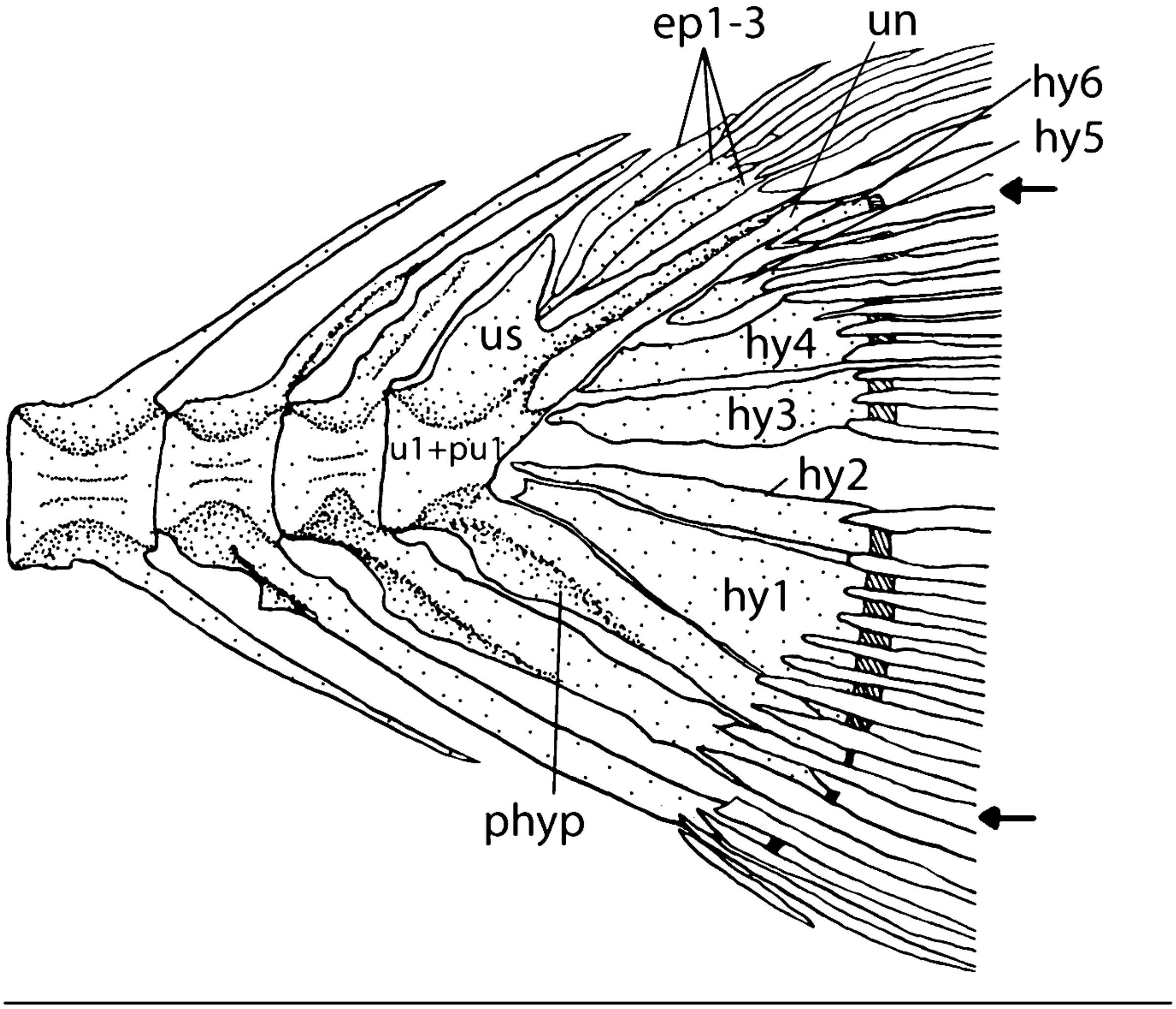

Figure 2.16. Drawing of the caudal fin of *Hemigrammopetersius barnardi* CMN F 81-0188, specimen number 4, 32.7 mm SL. Arrows indicate first (unbranched) principal fin ray. Hatching represents cartilage. Scale bar = 5 mm.

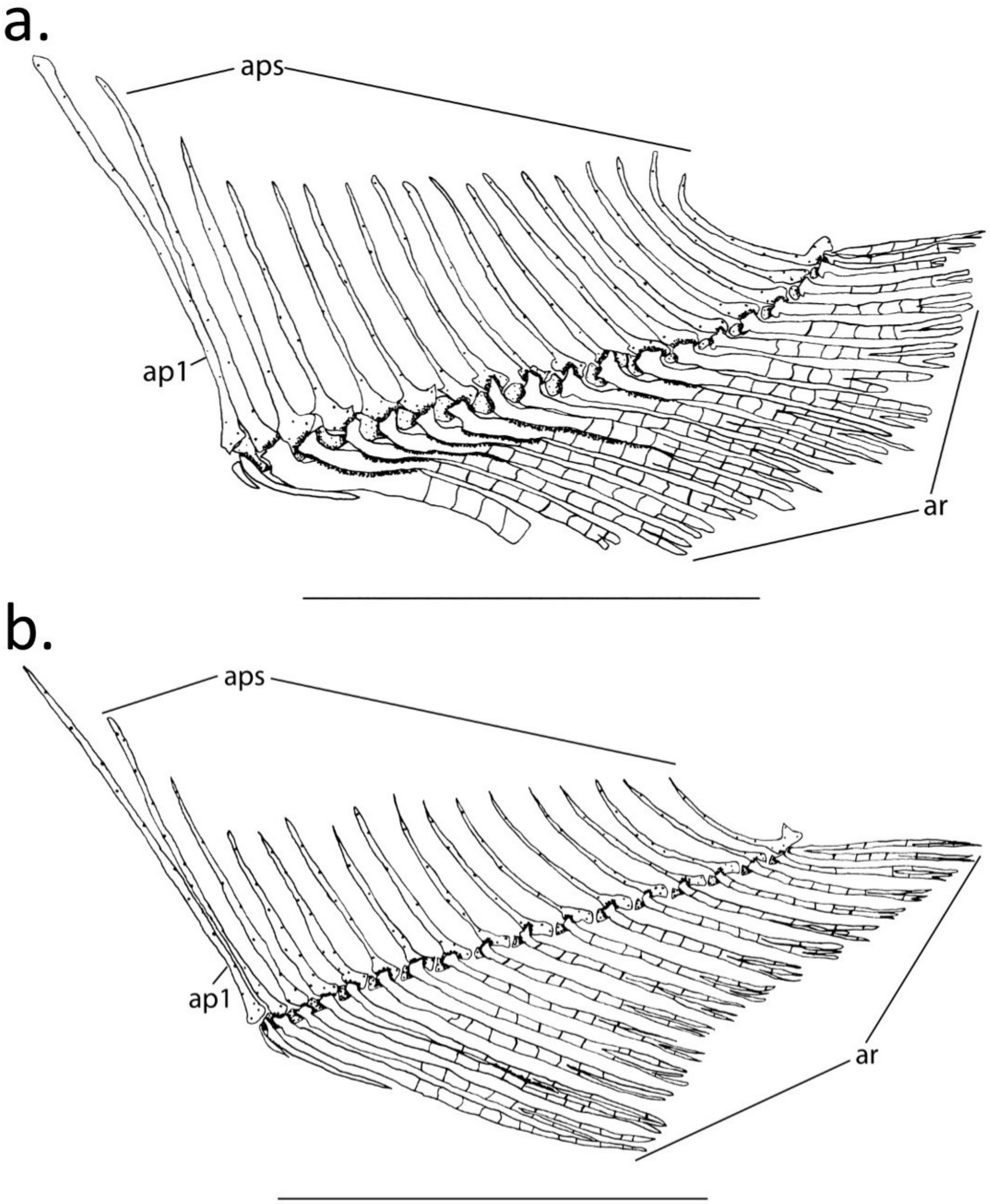

Figure 2.17. Drawing of sexual dimorphism in the anal fin of *Hemigrammopetersius barnardi* CMN F 81-0188, (a) male anal fin, specimen number 106, 31.2 mm SL, (b) female anal fin, specimen number 4, 32.7 mm SL. Scale bar = 5 mm.

2.8 References

Arroyave, J., & Stiassny, M. L. J. (2011). Phylogenetic relationships and the temporal context for the diversification of African characins of the family Alestidae (Ostariophysi: Characiformes): Evidence from DNA sequence data. *Molecular Phylogenetics and Evolution, 60*(3), 385-397.

Azevedo, M. A. (2010). Reproductive characteristics of characid fish species (Teleostei, Characiformes) and their relationship with body size and phylogeny. *Iheringia Serie Zoologia, 100*(4), 469-482.

Barlow, G. W. (1961). Causes and significance of morphological variation in fishes. *Systematic Zoology, 10*(3), 105-117.

Brewster, B. (1986). A review of the genus *Hydrocynus* Cuvier 1819 (Teleostei: Characiformes). *Bulletin of the British Museum of Natural History (Zoology), 50*(3), 163-206.

Britz, R., & Conway, K. W. (2009). Osteology of *Paedocypris*, a miniature and highly developmentally truncated fish (Teleostei: Ostariophysi: Cyprinidae). *Journal of Morphology, 270*(4), 389-412.

Calcagnotto, D., Schaefer, S. A., & DeSalle, R. (2005). Relationships among characiform fishes inferred from analysis of nuclear and mitochondrial gene sequences. *Molecular Phylogenetics and Evolution, 36*(1), 135-153.

Castro, R. M. C. (1999). Evolucao da ictiofauna de riachos Sul-Americanos: Padroes gerais e possiveis processos causais. In R. Mazzoni & P. R. Peres-Neto (Eds.), *Ecologia de Peixes de Riachos* (Vol. 6, pp. 139-155). Rio de Janeiro, Brazil.

Conway, K. W., & Moritz, T. (2006). *Barboides britzi*, a new species of miniature cyprinid from Benin (Ostariophysi: Cyprinidae), with a neotype designation for *Barboides gracilis*. *Ichthyological Exploration of Freshwaters, 17*(1), 73-84.

Dagosta, F. C. P., Marinho, M. M. F., & Camelier, P. (2014). A new species of *Hyphessobrycon* Durbin (Characiformes: Characidae) from the middle Rio Sao Francisco and upper and middle Rio Tocantins basins, Brazil, with comments on its biogeographic history. *Neotropical Ichthyology, 12*(2), 365-375.

De Santana, C. D., & Crampton, W. G. R. (2011). Phylogenetic interrelationships, taxonomy, and reductive evolution in the Neotropical electric fish genus *Hypopygus* (Teleostei, Ostariophysi, Gymnotiformes). *Zoological Journal of the Linnaean Society, 163*(4), 1096-1156.

Douglas, M. E. (1987). An ecomorphological analysis and niche packing and niche dispersion in stream fish clades. In W. J. Matthews & D. C. Heins (Eds.), *Community and evolutionary ecology of North American stream fishes* (pp. 144-149). University of Oklahoma Press: Norman.

Eccles, D. H. (1992). *FAO species identification sheets for fishery purposes. Field guide to the freshwater fishes of Tanzania. Prepared and published with the support of the United Nations Development Programme (project URT/87/016).* Rome: FAO.

Fink, S. V., & Fink, W. L. (1981). Interrelationships of the ostariophysan fishes (Teleostei). *Zoological Journal of the Linnaean Society, 72*(4), 297-353.

Fricke, R., Eschmeyer, W. N., & van der Laan, R. E. (2019). Eschmeyer's catalogue of fishes: Genera, species, references. California Academy of Sciences. Retrieved from http://researcharchive.calacademy.org/research/ichthyology/catalog/fishcatmain.asp

Gery, J. (1977). *Characoids of the World*. USA: T.F.H. Publications, Inc. Ltd.

Gery, J. (1995). Description of new or poorly known Alestinae (Teleostei: Characiformes: Alestidae) from Africa, with a note on the generic concept in the Alestinae. *Journal of Ichthyology and Aquatic Biology, 1*(4), 37-64.

Hanken, J., & Wake, D. B. (1993). Miniaturization of body-size - organismal consequences and evolutionary significance. *Annual Review of Ecology and Systematics, 24*, 501-519.

Herre, A. W. (1936). A new cyprinid genus and species and a new characin from Portuguese East Africa. *Proceedings of the Biological Society of Washington, 49*, 99-102.

Hubert, N., Bonillo, C., & Paugy, D. (2005). Early divergence among the Alestidae (Teleostei, Ostariophyses, Characiformes): Mitochondrial evidences and congruence with morphological data. *Animal Biology and Pathology, 328*(5), 477-491.

International Union for Conservation of Nature (IUCN). 2020. *The IUCN Red List of Threatened Species.* Version 2019-3. Retrieved from www.iucnredlist.org.

Kassambar, A., & Mundt, F. (2017). factoextra: Extract and visualize the results of multivariate data analyses (Version R package version 1.0.5). Retrieved from https://CRAN.R-project.org/package=factoextra

Konings, A., Bills, R., Hanssens, M., Kazembe, J., & Tweddle, D. (2018). "*Hemigrammopetersius barnardi. The IUCN red list of threatened species 2018e".* Retrieved from https://www.iucnredlist.org/species/63238/3124598

Knouft, J. H., & Page, L. M. (2003). The evolution of body size in extant groups of North American freshwater fishes: Speciation, size distributions, and Cope's rule. *American Naturalist, 161*(3), 413-421.

Lazzarotto, H., Barros, T., Louvise, J., & Caramaschi, E. P. (2017). Morphological variation among populations of H*emigrammus coeruleus* (Characiformes: Characidae) in a Negro River tributary, Brazilian Amazon. *Neotropical Ichthyology, 15*(1), 1-10.

Le, S., Josse, J., & Husson, F. (2008). FactoMineR: An R package for multivariate analysis. *Journal of Statistical Software, 15*(1), 1-18.

Liston, J. (2013). The plasticity of gill raker characteristics in suspension feeders: Implications for Pachycormiformes In Arratia, G., Schultze, H-P., & Wilson, M.V. H. (Eds). *Mesozoic Fishes 5 - Global Diversity and Evolution* (pp. 121-143). Munchen, Germany.

Lunkayilakio, S. W., & Vreven, E. (2008). *Nannopetersius mutambuei* (Characiformes: Alestidae), a new species from the Inkisi River basin, Lower-Congo. *Ichthyological Exploration of Freshwaters, 19*(4), 367-376.

Mamonekene, V., & Stiassny, M. L. J. (2012). A new *Bathyaethiops* (Characiformes: Alestidae) from the Lékoumou River (Kouilou-Niari Basin) in the Republic of Congo; First record of the genus in the Lower Guinean Ichthyofaunal Province. *Copeia, 2012*(3), 478-483.

Marinho, M. M. F. (2017). Comparative development in *Moenkhausia pittieri* and *Paracheirodon innesi* (Ostariophysi: Characiformes) with comments on heterochrony and miniaturization in the Characidae. *Journal of Fish Biology, 91*(3), 851-865.

Meyer, D., Dimitriadou, E., Hornik, K., Weingessel, A., and Leisch, F. (2019). e1071: Misc Functions of the Department of Statistics, Probability Theory Group (Formerly:E1071), TU Wien. R package version 1.7-3. https://CRAN.R-project.org/package=e1071.

Morioka, S., & Matsumoto, S. (2002). Otolith features and utility of lapillus for daily increment analysis in Malawian Characidae *Hemigrammopetersius barnardi* (Herre, 1939) (Pisces: Characidae) collected from Lake Malawi. *Aqua-Fish Technical Report 1*, 8-12.

Murray, A. M. (2004). Osteology and morphology of the characiform fish *Alestes stuhlmannii* Pfeffer, 1896 (Alestidae) from the Rufiji River basin, East Africa. *Journal of Fish Biology, 65*(5), 1412-1430.

Murray, A. M., & Stewart, K. M. (2002). Phylogenetic relationships of the African genera *Alestes* and *Brycinus* (Teleostei, Characiformes, Alestidae). *Canadian Journal of Zoology-Revue Canadienne De Zoologie, 80*(11), 1887-1899.

Myers, G. S. (1929). Cranial differences in the African characin fishes of the genera *Alestes* and *Brycinus*, with notes on the arrangement of the genera. *American Museum Novitates, 342*, 1-7.

Nelson, J. S. (2006). *Fishes of the World* (Fourth ed.). Hoboken, New Jersey: John Wiley & Sons, Inc.

Nzeyimana, F., & Amiet, J. (1992). Redescription, affinites et distribution au cameroun de *Brachypetersius altus* (Boulenger, 1899) (Characidae, Petersiini). *Cybium, 16*(1), 31-42.

Oliveira, C., Avelino, G. S., Abe, K. T., Mariguela, T. C., Benine, R. C., Orti, G., Vari, R. P., & Correa e Castro, R. M. (2011). Phylogenetic relationships within the speciose family Characidae (Teleostei: Ostariophysi: Characiformes) based on multilocus analysis and extensive ingroup sampling. *BMC Evolutionary Biology, 11*(275), 1-25.

Pastana, M. N. L., Dagosta, F. C. P., & Esguicero, A. L. H. (2017). A new sexually dichromatic miniature *Hyphessobrycon* (Teleostei: Characiformes: Characidae) from the Rio Formiga, upper Rio Juruena basin, Mato Grosso, Brazil, with a review of sexual dichromatism in Characiformes. *Journal of Fish Biology, 91*(5), 1301-1318.

Paugy, D. (1990). Note a propos des Petersiini (Teleostei: Characidae) d'Afrique occidentale. *Ichthyological Exploration of Freshwaters, 1*(1), 75-84.

Pellegrin, J. (1928). Mutanda ichthyologica: *Clupeocharax* PELLEGRIN. *Revue de Zoologie et de Botanique Africaines, 16*(1), 82.

Peters, R. H. (1992). Lessons from the size efficiency hypothesis II. The mire of complexity. *Hydrobiologia, 235/236*, 435-455.

Poll, M. (1945). Descriptions de Mormyridae et de Characidae nouveaux du Congo Belge avec une etude du genre *Stomatorhinus* et des genres de *Characidae* nains africains. *Revue de Zoologie et de Botanique Africaines, 39*(1), 37-77.

Poll, M. (1967). Revision des Characidae nains Africains. *Annales du Musee Royal de l'Afrique Centrale Tervurum serie in-8 Sciences Zoologiques, 162*, 1-158.

Prokofiev, A. M. (2001). A new genus of Neoscopelidae for *Eomyctophum gracile* Daniltshenko from the Middle Eocene of Georgia (Pisces: Osteichthyes: Myctophiformes). *Zoosystematica Rossica, 10*(1), 215 - 218.

R Core Team. (2017). R: A language and environment for statistical computing (Version 3.4.3). Vienna, Austria. Retrieved from https://www.R-project.org/

Roberts, T. R. (1966). Description and osteology of *Lepidarchus adonis*, a remarkable new characid fish from West Africa. *Standford Ichthyological Bulletin, 8*, 209-227.

Roberts, T. R. (1969). Osteology and relationships of characoid fishes, particularly the genera *Hepsetus*, *Salminus*, *Hoplias*, *Ctenolucius*, and *Acestrorhynchus*. *Proceedings of the California Academy of Sciences, 36*(15), 391-500.

Roberts, T. R. (1975). Geographical distribution of African freshwater fishes. *Zoological Journal of the Linnaean Society, 57*(4), 249-319.

Ruber, L., Kottelat, M., Tan, H. H., Ng, P. K. L., & Britz, R. (2007). Evolution of miniaturization and the phylogenetic position of *Paedocypris*, comprising the world's smallest vertebrate. *BMC Evolutionary Biology, 7*(1), 1-10.

Schönhofen Longoni, L., Giora, J., & Bernhardt Fialho, C. (2018). Development of secondary sexual characters and their relationship to ontogeny and seasonal reproductive period in *Hyphessobrycon igneus* (Ostariophysi: Characiformes). *Journal of Fish Biology, 92*(1), 131-149.

Steele, S. E., & Lopez-Fernandez, H. (2014). Body size diversity and frequency distributions of Neotropical cichlid fishes (Cichliformes: Cichlidae: Cichlinae). *Plos One, 9*(9), 1-11.

Stiassny, M. L. J., & Mamonekene, V. (2007). *Micralestes* (Characiformes, Alestidae) of the lower Congo River, with a description of a new species endemic to the lower Congo River rapids in the Democratic Republic of Congo. *Zootaxa, 1614*, 17-29.

Taylor, W. R., & Van Dyke, G. C. (1985). Revised procedure for staining and clearing small fishes and other vertebrates for bone and cartilage study. *Cybium, 9*(2), 107-119.

Villalobos, H., & Rodriguez-Sanchez, R. (2002). Pattern of increase in gill raker number of the California sardine. *Journal of Fish Biology, 60*, 256-259.

Wei, T., & Simko, V. (2017). R package "corrplot": Visualization of a Correlation Matrix (Version 0.84). Retrieved from https://github.com/taiyun/corrplot

Weitzman, S. H., & Vari, R. P. (1988). Miniaturization in South American freshwater fishes; An overview and discussion. *Proceedings of the Biological Society of Washington, 101*(2), 444-465.

Yeh, J. (2002). The effect of miniaturized body size on skeletal morphology in frogs. *Evolution, 56*(3), 628-641.

Zanata, A. M., & Vari, R. P. (2005). The family Alestidae (Ostariophysi, Characiformes): a phylogenetic analysis of a trans-Atlantic clade. *Zoological Journal of the Linnaean Society, 145*(1), 1-144.

Chapter 3: Size series of the small African fish *Petersius conserialis* (Characiformes: Alestidae)

3.1 Introduction

African tetras were initially classified with Neotropical tetras, Characidae, until Gery (1977) proposed that they should have their own family, Alestidae. The first support for monophyly of Alestidae was provided by Orti and Meyer (1997) using mitochondrial sequences, but they only included three species of Alestidae. Later research on alestid relationships agreed with Orti and Meyer's (1997) findings, supporting monophyly of Alestidae (e.g., Murray & Stewart, 2002; Hubert *et al.*, 2005; Arroyave & Stiassny, 2011). While the research agrees that Alestidae is monophyletic, continuing debate regarding relationships within the family exist.

Previously, Alestidae was separated into three tribes based principally on dental morphology: (i) Hydrocyini has caniniform teeth, (ii) Alestiini has multicuspid teeth, and (iii) Petersiini has reduced multicuspid teeth (compressed or the absence of a ‘shoulder’ on the teeth (Gery, 1995)) and a small body size (Hoedeman, 1951). One of the problems with this definition is that a reduction in tooth cusps may not be associated with phylogenetic relatedness but instead be the result of convergence due to a small body size (Murray & Stewart, 2002). For example, Murray (2004) reported changes from unicuspid dentition to multicuspid dentition in specimens of *Alestes stuhlmanni* Pfeffer associated with growth. Nzeyimana and Amiet (1992) also found that dentition varies within some species of Alestidae. A “small” body size also presents a problem as there is no accepted, formal definition and therefore is likely subjective. A thorough examination of morphological changes that occur throughout growth in specimens of Petersiini will help to identify traits that change with growth in this species, and thus allow us to better understand traits that might be convergent based only on small size.

Petersius conserialis Hilgendorf has been reported in two river systems in East Africa (Skelton, 1994). In his examination of alestid skulls, Myers (1929) restricted the genus *Petersius* to its type species, *P. conserialis* and characterized the genus based on the absence of the parietal fontanel and a larger body size compared with other petersiins. Apart from that study, little is known of *P. conserialis*.

Limited collections of *P. conserialis* are available. It is originally known from only two specimens, (i) the syntype and (ii) a second specimen from 1922 (Gery, 1995). A syntype is located at the Museum für Naturkunde in Berlin (ZMB 13535) and the second specimen at the Natural History Museum in London (1922.4.18.8). However, Murray and Stewart (2002) noted that the Canadian Museum of Nature has 15 available collections with a total of 70 specimens. Other collections are available at other museums, such as The Field Museum of Natural History in Chicago and the Museum National d'Histoire Naturelle in Paris. Despite the existence of these collections, later studies have generally not included *P. conserialis* (e.g., Hubert *et al.*, 2005; Arroyave & Stiassny, 2011) or did not have access to skeletal material for observations (e.g., Zanata & Vari, 2005). This results in a gap of understanding regarding the placement of *P. conserialis* in Alestidae.

The presence or absence of the parietal fontanelle – a fontanelle on the dorsal side of the skull that completely separates the parietals – remains unconfirmed. Poll (1967) and Gery (1995) also report the absence of a parietal fontanelle in specimens greater than 120 mm total length (TL) - although Gery (1995) did not examine specimens of *P. conserialis* but based his findings on Poll's (1967) study. Poll (1967) assessed the syntype (ZMB 13535, TL = 145 mm) and a second specimen collected in 1922 (1922.4.18.8, TL = 123 mm) for his study. However, Murray and Stewart (2002) observed a parietal fontanelle in specimens of *P. conserialis* they observed. And later work by Zanata and Vari (2005) claimed that a fontanelle was present in all specimens they examined (97.3 – 111.4 mm standard length (SL)), including the specimen from the Natural History Museum in London included in Poll's (1967) work. This conflict indicates that initial reports by Myers (1929) and Poll (1967) may have been wrong and that more research is necessary.

A second feature separating *P. conserialis* from the other species of Petersiini is their relatively large body size. Gery (1995; p. 39) included the characteristic of a small size to distinguish the Petersiini from the Alestiini, claiming that other ichthyologists refer to other petersiins as "pygmy African Characids". The placement of 'small' species together in the Petersiini remains, despite agreement throughout the literature that this tribe is likely nonmonophyletic (e.g., Poll, 1967; Murray & Stewart, 2002). Weitzman and Vari (1988) arbitrarily defined miniature fish as a species that reaches sexual maturity before 20 mm SL or doesn’t exceed 26 mm SL; however, only three species of Alestidae fit their definition. Castro (1999) proposed that small fish species should be considered as those less than 150 mm SL. No definition for a small body size has been proposed in relation to Alestidae. Here, I will use Weitzman and Vari's (1988) definition for “miniatures” and use Castro’s (1999) definition for small fishes, which includes *P. conserialis* as a small fish with the other petersiins (See Appendix A for a summary of body size terminology).

Studies have reported intraspecific variation within Alestidae (e.g., Nzeyimana & Amiet, 1992; Gery, 1995), along with changes throughout growth (Murray, 2004). Intraspecific variation is often observed throughout growth (Barriga *et al.*, 2011). The assessment of a size series may help provide further clarity on the presence or absence of the parietal fontanelle of *P. conserialis*. Further, assessing variation throughout size will allow for future comparisons with other alestids to determine possible convergences due to small body sizes.

Gery (1995) noted the difficulty in classifying *P. conserialis* due to the limited information on its cranial anatomy. Further, Zanata and Vari (2005) were unable to code a portion of skeletal features for *P. conserialis* due to no available cleared and stained material. The goal of this study is to help address these knowledge gaps by assessing the osteology of a size series of *P. conserialis*. This information may later be compared to the osteology of other alestids to determine convergences based on small body size.

3.2 Materials and Methods

3.2.1 Materials

Specimens of *Petersius conserialis* are from the Canadian Museum of Nature Fish Collection, Ottawa, Canada: catalogue number CMN F 81-0193 includes 13 alcohol preserved specimens, two double stained with alcian blue for cartilage and alizarin red S for bone, and cleared with trypsin; and catalogue number CMN F 81-0187, two double stained with alcian blue for cartilage and alizarin red S for bone and cleared with trypsin. Specimens were collected by G. M. Bernacsek and A. J. Hopson in 1979 from the Rufiji River basin in Tanzania. G. M. Bernacsek identified the specimens in 1981. I confirmed specimen identification based on a complete lateral line and upturned mouth with a prominent dentary.

3.2.2 Measurements

I collected measurements and counts for specimens according to Lunkayilakio and Vreven (2008) with the exception of transverse scale counts that were counted from the dorsal fin origin. The number of specimens included ranged from 11-14 fish, depending on the measurement taken. Measurements were made using digital calipers (0-150 mm Electronic Digital Caliper) and fin and scale counts were made using a Zeiss SteREO Discovery.V8 stereomicroscope using a Carl Zeiss 44403 6-9000 eyepiece (8x) and a Zeiss Achromat S 0.3x FWD 236 mm lens. I obtained radiographs for vertebral counts using a Bruker micro CT Skyscan 1172 (Al 0.5 mm filter, 71 kV, and 144 µA). Vertebrae were counted following the method of Brewster (1986). A summary of all measurements and meristics is available in Appendix B.

I assessed three specimens that were previously cleared and counterstained to examine skeletal features and cleared and counterstained one additional specimen (CMN F 81-0193 12) according to Taylor and Van Dyke's (1985) procedure. I took comparative photographs for osteological drawings with a Nikon DCM 1200C digital camera mounted on a Zeiss SteREO Discovery.V8 stereomicroscope with a Carl Zeiss 44403 6-9000 eyepiece (8x) and a variety of lenses (Zeiss Achromat S 0.3x FWD 236 mm; Zeiss Plan Apo S 0.63x FWD 81mm; and Zeiss Plan Apo S 1.0x FWD 60mm), with NIS Elements F package 2.20, version 5.03. Figures were processed using Adobe Photoshop CS6. Osteological terminology follows Murray (2004), with the exception of endopterygoid for mesopterygoid from Brewster (1986) and pubic processes from Prokofiev (2001).

I completed all statistical analyses using R version 3.5.2 (R Core Team, 2017). To test the distribution of the studied specimens, I calculated the skewness, kurtosis and Shapiro-Wilk test value using the package e1071 (Meyer *et al.,* 2019). Histograms and scatterplots were completed for all measurements and meristics (Appendix D). To determine allometric or isometric growth, all measurements were changed to the logarithmic form and the slopes were calculated. I created a principal component analysis (PCA) using FactoMineR (Le *et al.*, 2008), factoextra (Kassambar & Mundt, 2017), and corrplot (Wei & Simko, 2017) packages to check for correlations among characters. An exploratory PCA were conducted using all measurements and meristics. I standardized all measurements by the SL (Appendix D). Finally, I compared the length measurements of alestid species from FishBase to previously proposed definitions for miniature and small species (Froese & Pauly, 2018).

3.3 Results

3.3.1 General Body Form and External Characteristics

Petersius conserialis has a fusiform body with an upturned mouth (Fig. 3.1). The postorbital region occupies a large portion of the head (40-45% HL, mean = 43%). The body depth is approximately a third of the standard length with the greatest depth just before the dorsal fin insertion (28-31% SL, mean = 29%; Tab. 3.1). The dorsal fin insertion is just posterior to the midpoint of the standard length (53-58% SL, mean = 55% SL). The pectoral fins insert posteroventrally to the operculum and the pelvic fins insert ventrally on the body, level with the distal tips of the pectoral-fin rays. The anal-fin insertion is posterior to the distal tips of the pelvic-fin rays and behind the level of the dorsal-fin base. The last anal-fin ray inserts at the level of the insertion of the adipose fin, which is posterior on the body, just before the caudal peduncle (84-90% SL, mean = 86%). The caudal fin is forked.

Preserved specimens of *P. conserialis* are a dusky orange with translucent, white fins. Dark brown pigmentation is visible dorsally and concentrated around the base of the dorsal and adipose fins. A dark brown spot is present on the caudal peduncle. All specimens assessed for this chapter were previously preserved; therefore, no observations regarding live specimens were made. Poll (1967) described a large black spot on the caudal peduncle that extends on the medial caudal fin. In the original description, *P. conserialis* was described as silver colored with a black band along the dorsal fin base and light colored fins (Hilgendorf, 1894).

Petersius conserialis has large cycloid scales beginning just after the operculum and extending onto the caudal peduncle (Fig. 3.2). A complete lateral line (33-35 scales; Tab. 3.2) is present, beginning just behind the operculum and dropping ventrally after the first two to three scales. Measurements and meristics are summarized in Tables 1 and 2, respectively.

The measurements that were standardized by SL demonstrated a normal distribution for examined specimens (Fig. 3.3; Appendix D). All length and depth measurements are positively correlated with a slope of approximately 1.0, for example the head length and eye diameter (Fig. 3.4). There were no strong correlations (with strong defined as $r > 0.70$) found in relation to standard length and count data (Appendix D). The first two dimensions of the PCA explained approximately 40% of the variance, with both dimensions correlated with length measurements (e.g., predorsal and prepectoral distance) (Appendix D). As almost all the measurements were strongly correlated with each other (r > 0.70) no further PCA was conducted.

3.3.2 Skull

The mesethmoid has an anteromedial point and two lateral projections just posterior to it, visible in dorsal and ventral view (Fig. 3.5a & b). The posterior portion of the mesethmoid has three projections. The nasals are wide anteriorly, slimming into an elongate shape posteriorly. There is a sensory canal on the lateral portion of the nasals.

The frontals widen slightly posteriorly with the parietal fontanelle extending onto the posterior portion of the frontal. A parietal fontanelle was present in all examined specimens (*n* = 15; 40.9-91.0 mm SL). The extent that the parietal fontanelle separates the frontals depends on the size of the specimen (Fig. 3.6). Smaller specimens generally have larger fontanelles separating more of the left and right frontal compared to larger specimens. A weak negative correlation was found between the standard length and fontanelle length (measured from the anterior portion of the fontanelle where the left and right frontals meet one another in the midline to the posterior portion of the fontanelle in the supraoccipital) and between the standard length and fontanelle width (measured from the anterior edge of the parietals) (Fig. 3.7). In other words, as standard length increases the fontanelle length and width decreases. The supraorbital sensory canal extends along the length of the frontals. Anteriorly, there is a branch extending towards the nasals and one opening laterally above the middle of the orbit. There are three openings near the epiphyseal bar oriented medially and one oriented laterally. The posterior portion of the supraorbital sensory canal has two branches, one extending towards the parietal and one towards the prootic.

The parietals are fully separated by the parietal fontanelle; they are narrow medially where they are separated and widen laterally (Fig. 3.5c). The posterior portion of the supraorbital sensory canal continues from the frontal to traverse the middle of the parietal.

The supraoccipital has a notch anteriorly from the parietal fontanelle and a posterior projection. The epioccipitals are slender dorsally and expand ventrally in lateral view. The exoccipitals have a straight posterior edge and are rounded anteriorly. In ventral view, the exoccipitals and basioccipital form a large lagenar capsule as found in other characiforms (Fink & Fink, 1981). Smaller specimens have not yet fully ossified the skull bones, with cartilage prominent between bones on the posterior part of the skull, including the occipital bones, prootics and pterotics.

The pterotic has two posterior projections, with the ventral projection extending farther posteriorly. The anterior portion of the pterotic is narrow in lateral view, with the supraorbital sensory canal extending onto it from the posteroventral portion of the frontal. The prootic is large, occupying a large portion of the ventral skull. In ventral view the prootic is raised in the center and towards the pterotic and exoccipital.

The sphenotic has one ventrally oriented process. The pterosphenoids are rectangular and are visible on both sides of the parasphenoid. The orbitosphenoid comes to an anterior point in the center and has a straight edge along the posterior portion of the bone in ventral view. The medial portion of the orbitosphenoid ascends into a ridge underneath the parasphenoid in ventral view. Two pairs of foramina are found on the orbitosphenoid, anterolaterally and posterolaterally. The orbitosphenoid is approximately twice the length of the pterosphenoid in ventral view. The parasphenoid is bifurcated both anteriorly and posteriorly where it meets with the vomer and basioccipital, respectively. It extends in a straight line anteroposteriorly through the middle of the orbit, with two short lateral wings posterior to the orbit that contact the prootic.

The lateral ethmoid has a ventral projection forming the anterior edge of the orbit; the lateral ethmoid is concave dorsally in lateral view. The vomer has a straight anterior edge and curved posterior edge in ventral view.

3.3.3 Jaws and Teeth

A short ascending process is present on the premaxilla (Fig. 3.8). *Petersius conserialis* has a premaxillary pedicle, the raised ledge along the posterior extension of the premaxilla, as reported in other alestids (Roberts, 1969; Murray & Stewart, 2002). The premaxilla has two rows of multicuspid teeth; the outer row has two teeth with three cusps and the inner row has four teeth, with the first tooth having five cusps and the posterior three teeth with six cusps. The premaxillae are not connected by an interdigitating suture.

The maxilla is edentulous. It has a narrow dorsal extension and widens ventrally with a circular anteroventral edge and slanted posterior edge.

The dentaries are connected by an interdigitating suture. A small foramen for the mandibular canal is visible in the center of the dentary, just anterior to where it is overlapped by the maxilla and below a ridge (Fig. 3.8 and 3.9). The mandibular sensory canal crosses the dentary and branches anteriorly near the dentition. Multicuspid teeth, the first three with seven cusps and the fourth with five cusps, are present as a single outer row with no inner symphyseal tooth on the dentary, unlike that reported in other alestids (Murray & Stewart, 2002; Zanata & Vari, 2005). The dentary teeth progressively decrease in size from anterior to posterior. A tooth crypt is present on the anteromedial surface of the dentary, where replacement teeth are visible (Fig. 3.9).

The anguloarticular occupies the posterior half of the lower jaw. The dorsal and ventral edges of the anguloarticular are rounded, with a concave anterior edge. A small rectangular retroarticular is present on the posteroventral corner of the anguloarticular. The coronomeckelian is a small oval bone present above the mandibular sensory canal in medial view. The coronomeckelian cartilage is prominent on the medial portion of the dentary of smaller *P. conserialis* specimens but is difficult to determine in larger specimens.

3.3.4 Opercular Bones

The preopercle has two limbs forming a right angle and the sensory canal extends along both the horizontal and vertical limbs (Fig. 3.10). The sensory canal pores open ventrally along the preopercle and there is one posterior opening. The interopercle is elongate.

The opercle is semicircular, with a flat anterior edge and rounded posterior edge. The anteroventral portion of the opercle comes to a point and the dorsal portion above the facet for articulation with the hyomandibula has a straight anterior edge with a slope of 45°.

3.3.5 Suspensorium

The anterior portion of the palatine is rounded and with a slight lateral expansion (Fig. 3.11). Posteriorly, the palatine is rectangular with rounded edges. The ectopterygoid is a narrow bone with straight ventral and dorsal edges. The endopterygoid has a narrow anterior extension and widens posteriorly. On the posterior portion of the endopterygoid the dorsal surface slopes medially. The metapterygoid has an anteroventral expansion. The medial portion of the metapterygoid is narrow, widening again posteriorly. The two limbs of the quadrate form a posterior-facing 90° angle, with the horizontal limb a long narrow extension and the vertical limb forming a fan shape. This is common in other alestids (Murray, 2004). The symplectic is a long narrow bone, and the hyomandibula has a raised posterior edge. On the posterodorsal portion of the hyomandibula, a rounded condyle is present for articulation with the opercle. The hyomandibula is fan-shaped dorsally with an anterior flange that narrows into an anteroventral point.

3.3.6 Circumorbital Bones

The circumorbital series consists of eight bones, the antorbital, lacrimal (infraorbital 1), infraorbitals 2 through 5, the dermosphenotic (infraorbital 6) and the supraorbital (Fig. 3.12). The antorbital is a small triangular bone at the anterior portion of the orbit. Infraorbital 1 is a long narrow rectangle. Infraorbital 2 is narrow anteriorly and widens posteriorly. The third infraorbital is quite large and forms the posteroventral corner of the orbit. Infraorbitals 4 and 5 are rectangular. The dermosphenotic is square with an anteroventral projection. The circumorbital sensory canal is present on infraorbitals 1–6 with an opening at either end of the canal on each bone, and an additional opening on infraorbital 4. The canal is tripartite on the dermosphenotic, as is commonly reported in alestids (Murray & Stewart, 2002; Murray, 2004; Zanata & Vari, 2005). The supraorbital is long and narrow with a concave posterior edge.

3.3.7 Branchial Arches and Pharyngeal Region

The basihyal and basibranchials 1 through 3 are long narrow rectangles and are fully ossified in larger specimens (Fig. 3.13a). The hypobranchials are small square elements contacting the corresponding basibranchials. Ceratobranchials 1 through 4 are slender rods, that widen posteriorly. In contrast, ceratobranchial 5 is narrow anteriorly with a medial expansion bearing conical teeth. There are five epibranchials; epibranchials 1 and 2 are narrow rods with a projection towards the pharyngobranchials, epibranchial 3 is also a narrow rod, epibranchial 4 is a shorter element and epibranchial 5 is a small triangular bone (Fig. 3.13b). The pharyngobranchials all bear conical teeth. Pharyngobranchial 1 is fan-shaped with teeth present on the anterior portion of the bone, in the middle of the fan. Pharyngobranchial 2 is rectangular and is completely covered in teeth, whereas pharyngobranchial 3 is wide anteriorly and bifurcates posteriorly, with the teeth present only along the anteromedial portion of the bone. Finally, pharyngobranchial 4 is wide anteriorly and narrows posteriorly, with teeth only present on the anterior portion of the bone. Smaller specimens of *P. conserialis* have cartilage on the tips between the contact of the branchial elements throughout the pharyngeal series.

Gill rakers are present on the ceratobranchials and epibranchials. Smaller gill rakers are present along the hypobranchials. They are bifurcated medially, where they contact the ceratobranchials and extend as long narrow projections (Fig. 3.13c).

The dorsal and ventral hypohyals are roughly cylindrical (Fig. 3.13d). The anterior ceratohyal is wider anteriorly and posteriorly, narrowing in the middle of the bone. The posterior ceratohyal has a flat anterior and a rounded posterior edge. A groove along the midline is present on the posterior ceratohyal. The interhyal is a small, ossified rod. As in the pharyngeal apparatus, smaller specimens of *P. conserialis* have cartilage between the contact of the ceratohyals and hypohyals.

There are four branchiostegal rays. They are long, curved bones, with a dorsal projection on the proximal end. The branchiostegal rays narrow to a point at the posterior ends. The first ray is the shortest, with the remaining three getting progressively longer. The first three branchiostegal rays contact the anterior ceratohyal, whereas the fourth branchiostegal ray contacts the posterior ceratohyal.

The anterior portion of the urohyal has two bulbous projections behind which the bone narrows and then expands posterodorsally into a triangular shape along the midline of the bone with a jagged posterior edge (Fig. 3.13e). The urohyal also expands laterally, creating a triangle on each side of the posterodorsal expansion.

3.3.8 Paired Fins and Girdles

The posttemporal has a narrow dorsal point and is rounded ventrally (Fig. 3.14). The extrascapular is roughly rectangular. The supracleithrum is ovoid. The supratemporal sensory canal extends from the extrascapular across the ventral portion of the posttemporal and down the supracleithrum. The cleithrum forms approximately a 90° angle, with a vertical and horizontal arm. The anterior edge of the cleithrum is rounded and gradually rolls in lateral view. There are three postcleithra: (i) a long narrow oval substantially larger than the other two postcleithra just ventral to the supracleithrum, (ii) a small oval posterior to the cleithrum and (iii) a small oval posterior to the coracoid.

The coracoid has flat ventral and anterior edges and a curved posterior edge. In the middle of the coracoid on the dorsal edge is a rectangular projection that contacts the dorsal edge of the horizontal arm of the cleithrum (Fig. 3.14b). The mesocoracoid is narrow dorsally and widens ventrally, whereas the scapula is wide dorsally and narrows into a thin projection ventrally. The pectoral fin has one unbranched fin ray and 12-13 branched fin rays.

The pubic process of the pelvic girdle is narrow anteriorly and widens posteriorly where the fin rays attach (Fig. 3.15). The left and right pelvic girdles do not contact one other. A pelvic splint is present on the lateral edge of the pelvic girdle. The pelvic fin has one unbranched fin ray and 8-9 branched fin rays. Smaller specimens have cartilage remaining in the pectoral and pelvic fin radials.

3.3.9 Weberian Apparatus and Vertebral Column

The Weberian apparatus is a modification to the first four vertebrae in Characiformes - and to the first four or five vertebrae in other ostariophysan fishes - that enhances hearing. The neural complex has a wide base dorsal to vertebrae 2 through 4, with an anterodorsal projection (Fig. 3.16). The tripus is ventral to vertebrae 2 through 4. It is triangular with the dorsal most corner just under the transverse process of vertebra 4. Posteromedially, the tripus slopes towards the posterior edge of vertebra 4. The intercalarium is elongate and underlies the transverse process of vertebra 3. The triangular scaphium is above vertebrae 2. The claustrum is a small, oval bone, overlying the scaphium.

The vertebral column has a total of 37-38 vertebrae; there are 16-18 abdominal vertebrae, 17-20 caudal vertebrae, and 3-4 transitional vertebrae, following the definition of Brewster (1986).

Specimens of *P. conserialis* have epineurals beginning immediately posterior to the Weberian apparatus (vertebra 5). The epipleurals are associated with the haemal spines. Both the epineurals and epipleurals end at preural 5. Anterior ribs have an anteroventral flange, except for the last three ribs of the anterior vertebrae in which the flange is reduced or absent.

3.3.10 Dorsal and Anal Fins and Supports

The dorsal fin is positioned posteriorly on the body (predorsal length is 53-58% SL, mean = 55% SL). There are two unbranched dorsal-fin rays and 8 branched dorsal-fin rays in all examined specimens. The first unbranched fin ray is approximately half the length of the second unbranched dorsal-fin ray. The remaining fin rays decrease progressively in size. The dorsal fin has a relatively small base (9-14% SL, mean = 11% SL) and is falcate in shape.

The falcate anal fin begins just posterior to the distal tips of the pelvic fin rays (preanal length is 71-76% SL, mean = 74% SL). There are 3 unbranched fin rays, and 18-20 branched fin rays. The first unbranched fin ray is substantially shorter than the second. The first branched fin ray is the longest, with the remaining fin rays gradually decreasing in size.

3.3.11 Caudal Fin and Skeleton

The fused first ural and first preural centrum bears a large urostyle (Fig. 3.17). A slender uroneural is present lying along the ventral edge of the posterior portion of the urostyle. The uroneural gets longer as body size increases, initially present only at the posterior end of the urostyle, and shorter than hypural 6, and in larger specimens extending farther anteroventrally, becoming the same length as the longer hypurals (Fig. 3.18). There are three epurals, all elongate and approximately the same size. The parhypural bears an anterior flange proximally and is fused with the compound centrum (pu1+u1).

There are six autogenous hypurals. Hypural 1 has a narrow anterior edge that widens to form a triangle and is the largest. Hypurals 2 through 6 are long and narrow. A large diastema is present between hypural 2 and 3. Hypurals 3 through 6 gradually decrease in size with hypural

3 being the largest. Smaller specimens retain cartilaginous distal tips on the hypurals and parhypural, but larger specimens have a fully ossified caudal skeleton.

The neural and haemal spines on preural centrum 2 have anterior flanges. Two neural spines are present on preural centrum 2 of cleared and stained specimens figured here (Fig. 18). However, CT scan images and previously taken radiographs for specimens of *P. conserialis* (CMN F 81-0193) show variation in this number (Fig. 19). Vertebrae anterior to the preural centra have long narrow neural and haemal spines with no additional expansions. The general osteology of the caudal fin is similar between larger and smaller specimens with the exception of the ossification of the hypurals and the anteroventral growth of the uroneural. *Petersius conserialis* has a forked caudal fin that is approximately a fifth of the total length (19-27% TL, mean = 23%).

3.4 Discussion

This size series of *Petersius conserialis* covers a range of 40.9 to 91.0 mm standard length (SL) (54.1 – 115.0 mm total length (TL)). While Murray and Stewart (2002) included specimens of *P. conserialis* in their research and did not report the standard length, the specimens they assessed were the same as those I examined (CMN 81-0187, maximum standard length = 91 mm). The specimens in Zanata and Vari's (2005, p. 22) research were larger, with a standard length of 101.8 mm and 111.4 mm - and all had a parietal fontanelle, although significantly reduced in larger specimens. All of these specimens are smaller than the maximum reported total length of 145 mm (Poll, 1967). However, one of the specimens of *P. conserialis* that Zanata and Vari (2005) assessed was the specimen from 1922 referenced in Poll (1967) and Gery's (1995) work as not having a parietal fontanelle (97.3 mm SL from the British Museum of Natural History; 1922.4.18.8). No recent studies have examined the syntype.

Most studies in the past 20 years have excluded *P. conserialis* from analyses, probably because of limited specimen availability, with the exception of two phylogenetic studies: (i) Murray and Stewart (2002) and (ii) Zanata and Vari (2005). While older studies included *P. conserialis*, they concentrated on skull characteristics and classifications (e.g., Myers, 1929; Hoedeman, 1951; Gery, 1995). However, Poll (1967) included some counts in his work, which are compared with the results found here and are within the same range (Tab. 3.3).

The measurements recorded in this study are normally distributed (Appendix D). Measurements all had a slope of approximately 1.0, suggesting isometric scaling of body size. Differences were observed in the osteology throughout the size series.

3.4.1 Osteological Changes in a Size Series

The most obvious change to the skeleton throughout a series of sizes was the amount of ossification. The smallest cleared and stained specimen (specimen number 12, CMN F 81-0193, 40.91 mm SL) retained a considerable amount of cartilage in comparison to the largest cleared and stained specimen (specimen number 2, CMN F 81-0187, 70.41 mm SL) (Fig 3.18). The smallest specimen of *P. conserialis* had cartilage between the sutures of the skull bones, particularly along the posterior portion of the skull. Mattox *et al.* (2014) assessed the ossification sequence of a basal characid for comparisons to other characids and reported that the posterior skull bones started to ossify first (basioccipital and exoccipital), along with the frontals and parasphenoid. This study did not assess the ossification sequence throughout ontogeny but the continual presence of cartilage along the sutures of the posterior skull bones contradicts the findings of Mattox *et al.* (2014). Other studies have found a consistent pattern with the anterior portion of the skull, and bones involved with feeding, ossifying first (e.g., *Seriola dumerili* in Liu, 2001 and *Hippocampus hippocampus* in Novelli *et al.*, 2017). *Petersius conserialis* may have a similar ossification sequence in which anterior skull bones and those involved with feeding are ossifying earlier than the posterior skull elements.

Cartilage was also present between the pharyngeal bones, the radials of the pectoral and pelvic fins and the caudal fin in the smallest specimen. Larger specimens presented less cartilage in comparison.

3.4.2 The Parietal Fontanelle

The presence or absence of a parietal fontanelle in specimens of *P. conserialis* has been debated. Original work described no parietal fontanelle in larger specimens (145 mm TL) (e.g., Myers, 1929; Hoedeman, 1951; Poll, 1967) and recent studies have described the presence of a parietal fontanelle in smaller specimens (≤ 135 mm TL) (e.g., Murray & Stewart, 2002; Zanata & Vari 2005)).

I found a parietal fontanelle in all examined specimens (40.9 – 91.0 mm SL) and reported a weak negative correlation and negative slope between the size of the fontanelle and standard length (Fig. 7). The fontanelle may eventually be lost as body size increases as this analysis only included four specimens resulting in a weak, nonsignificant correlation (r = -0.31, *p* = 0.69). Based on recent observations of specimens of *P. conserialis* (e.g., Murray & Stewart, 2002; Zanata & Vari, 2005) and those made here, the absence of the parietal fontanelle should not be used as a diagnostic character for this genus. A reassessment of the syntype and additional larger specimens would help verify these observations. While Zanata and Vari (2005) did reassess the larger specimen from 1922 reported to lack a parietal fontanelle in Poll (1967) and observed that there is a fontanelle, they did not assess the syntype. Unfortunately, access to the syntype was not possible for this thesis chapter.

Petersius was previously considered to be monotypic, with the genus having been established based on the absence of the parietal fontanelle (and a larger body size compared to other small alestids) (Myers, 1929). In addition to the demonstrated presence of the fontanelle in *Petersius* in past studies and here, the presence or absence of a parietal fontanelle has not been considered as a generic feature in other characiforms (Howes, 1982). Therefore, the previous removal of other “dwarf” alestid taxa from *Petersius* to other genera based predominantly on the purported condition of the fontanelle, should be re-examined in light of this information.

3.4.3 “Dwarf” Status

A second feature used to distinguish specimens of *Petersius* from other members of Petersiini was its relatively large body size (Gery, 1995). *Petersius conserialis* was considered to be a “peculiar large form” (Myers, 1929; p. 5); however, conflicting definitions have been provided for small taxa (Appendix A). *Petersius conserialis* attains and adult size that is too large for most of the previously proposed definitions, with the exception of that proposed by Castro (1999) for a small fish (less than 150 mm SL) (Fig. 3.20). However, classifying groups based on body size may be subjective, particularly if no obvious bimodal distribution in size exists (as observed in alestids; Fig. 3.20).

3.4.4 Conclusions

The parietal fontanelle appears to demonstrate negative allometric growth, although a higher sample size is needed to confirm this. The uroneural appears to increase in size as body size increases, extending anteroventrally along the urostyle. Other measurements of the size series of *P. conserialis* appears to display isometric growth. The overall shape of the bones remained consistent regardless of overall body size, with the extent of cartilage varying throughout the size series. The skull bone sutures, pectoral and pelvic fin radials and caudal fin bones have larger amounts of cartilage present in smaller specimens of *P. conserialis*. This study agrees with recent studies that the parietal fontanelle is present in at least smaller members of *P. conserialis*. Finally, *P. conserialis* does not conform with any previously proposed definitions of dwarf or miniature but does meet the criterion (less than 150 mm SL) of small fishes outlined by Castro (1999).

3.5 Tables

Table 3.1. Measurements and ratios for *Petersius conserialis,* CMN F 81-0193, from the Rufiji River, Tanzania (*n* = 14).

	Range	**Mean**	**SD**
Standard length (SL mm)	40.9 – 91.0	58.2	14.6
Total length (TL m)	54.1 – 115.0	74.9	17.2
SL:TL	0.74 – 0.81	0.77	0.02
Body depth SL^{-1}	0.28 – 0.31	0.29	0.01
Head length (HL mm) SL^{-1}	0.27 – 0.30	0.28	0.01
Head depth SL^{-1}	0.14 – 0.18	0.16	0.01
Eye diameter HL^{-1}	0.27 – 0.36	0.31	0.02
Interorbital distance HL^{-1}	0.19 – 0.25	0.22	0.02
Snout length HL^{-1}	0.23 – 0.30	0.27	0.02
Caudal peduncle depth:Caudal peduncle length	0.61 – 0.84	0.71	0.08
Preadipose length SL^{-1}	0.84 – 0.90	0.86	0.01
Predorsal length SL^{-1}	0.53 – 0.58	0.55	0.01
Preanal length SL^{-1}	0.71 – 0.76	0.74	0.02
Prepelvic length SL^{-1}	0.47 – 0.54	0.50	0.02
Prepectoral length SL^{-1}	0.28 – 0.33	0.30	0.01
Dorsal fin base SL^{-1}	0.09 – 0.14	0.11	0.02
Anal fin base SL^{-1}	0.17 – 0.21	0.19	0.01

Table 3.2. Meristics for *Petersius conserialis*, CMN F 81-0193, from the Rufiji River, Tanzania. The number of specimens that showed each count is given in brackets.

Number of	**Sample Size**				
Dorsal-fin rays	14	10 (14)			
Anal-fin rays	14	21 (3)	22 (8)	23 (3)	
Abdominal vertebrae	12	16 (5)	17 (6)	18 (1)	
Transitional vertebrae	12	3 (9)	4 (3)		
Caudal vertebrae	12	17 (2)	18 (6)	19 (3)	20 (1)
Total vertebrae	12	37 (1)	38 (9)	39 (3)	
Lateral line scales	13	33 (4)	34 (4)	35 (5)	
Transverse scales	11	9 (5)	10 (5)	11 (1)	
Gill rakers	14	17 (1)	18 (7)	19 (5)	20 (1)

Table 3.3. Comparison of measurements from this study to Poll's (1967) study. Roman numerals refer to unbranched fin rays and Arabic numerals refer to branched fin rays.

Measurement	**Current Study**	**Poll (1967)**
Dorsal Fin Rays	II, 8	II,8
Anal Fin Rays	III,18 – III,20	III,19
Gill Rakers	17 – 20	20
Lateral Line Scales	33 – 35	34
Transverse Scales	9 – 11	10

3.6 Figures

Figure 3.1. Photograph of *Petersius conserialis*, CMN F 81-0193, smallest specimen = specimen number 12, SL = 40.9 mm, largest specimen = specimen number 2, SL = 91.0 mm. Scale bar = 5 mm.

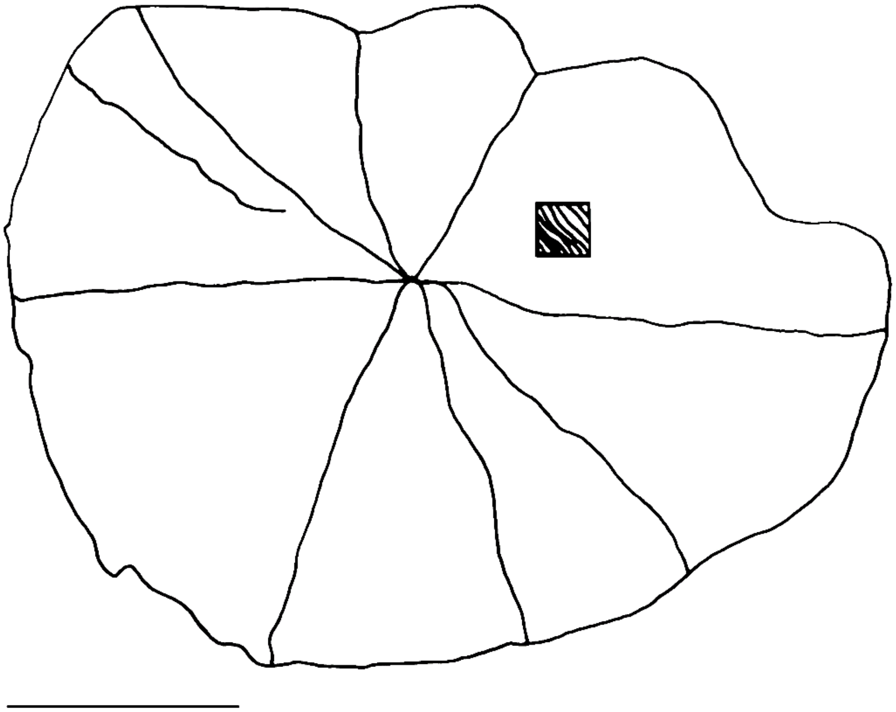

Figure 3.2. Drawing of scale of *Petersius conserialis* CMN F 81-0187, specimen number 1, SL = 56.3 mm. The circuli are drawn in the box. Scale bar = 1mm.

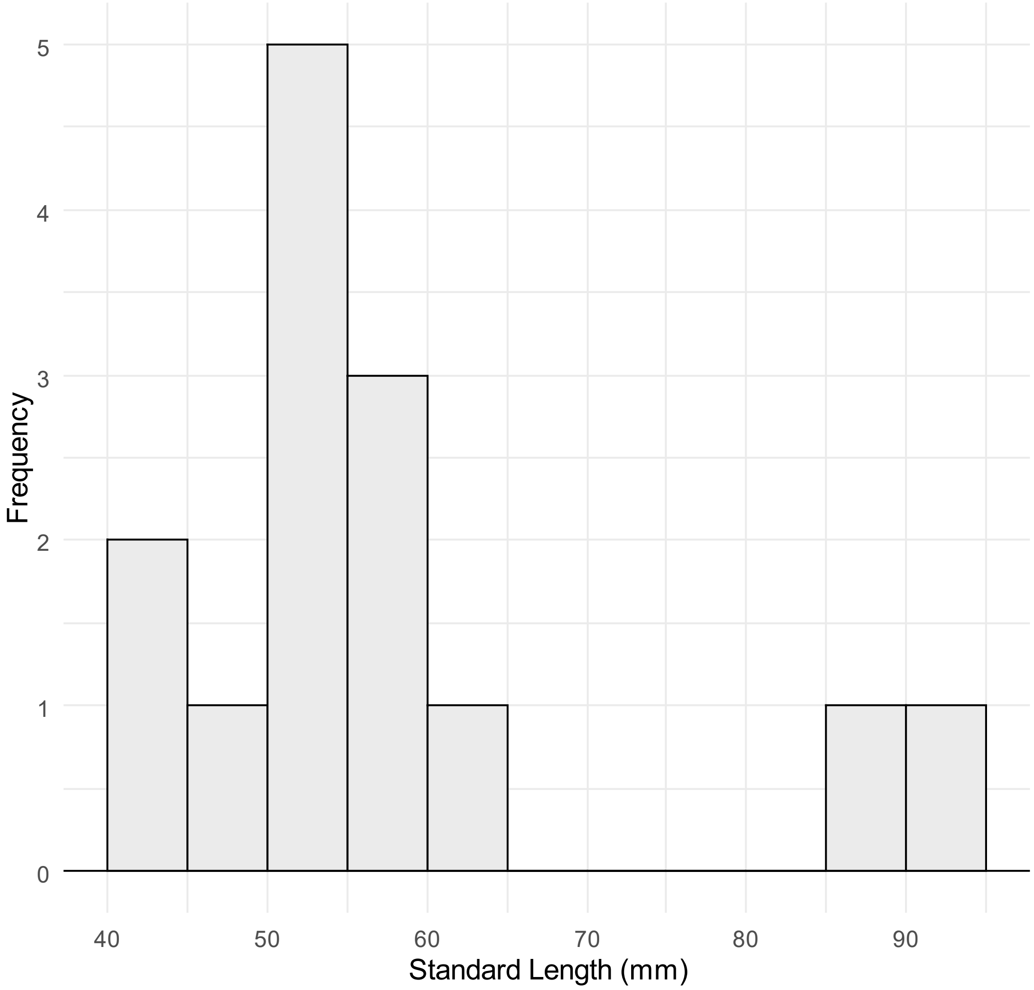

Figure 3.3. Histogram of standard length for *Petersius conserialis*, CMN F 81-0193. Histograms for remaining measurements are available in Appendix D.

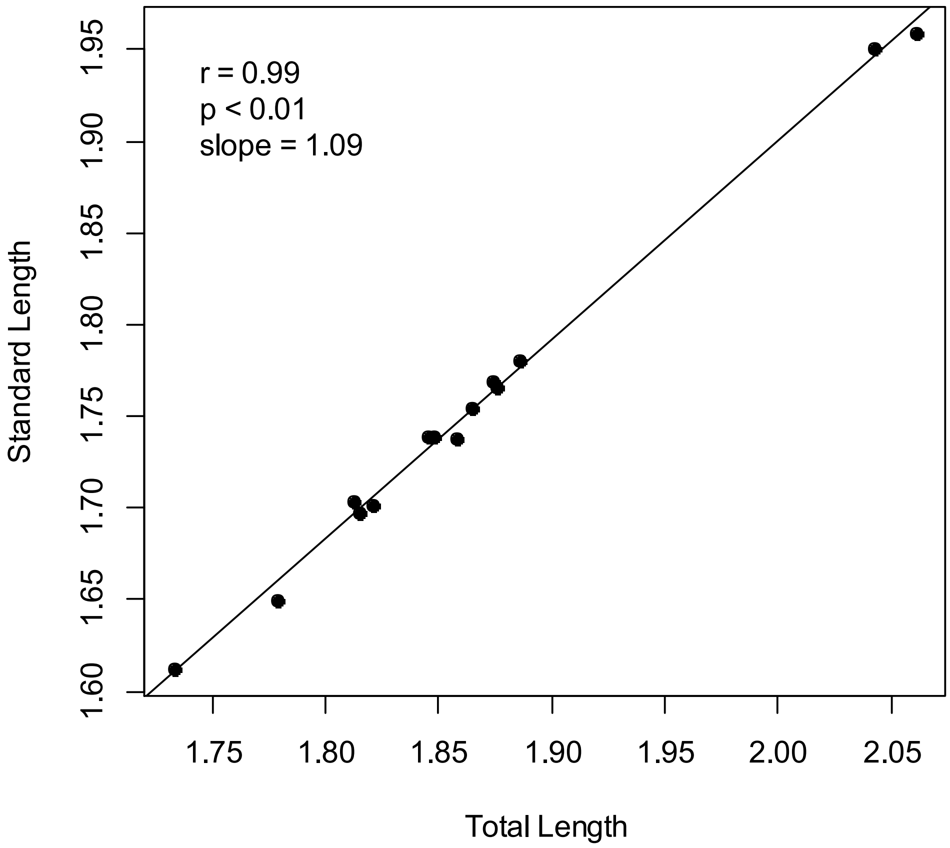

Figure 3.4. Scatterplot of standard length in relation to total length in *Petersius conserialis* CMN F 81-0193 (*n* = 14) using logarithmic data. Pearson correlation and slope values are in the respective top left corners. Scatterplots for remaining measurements are available in Appendix D.

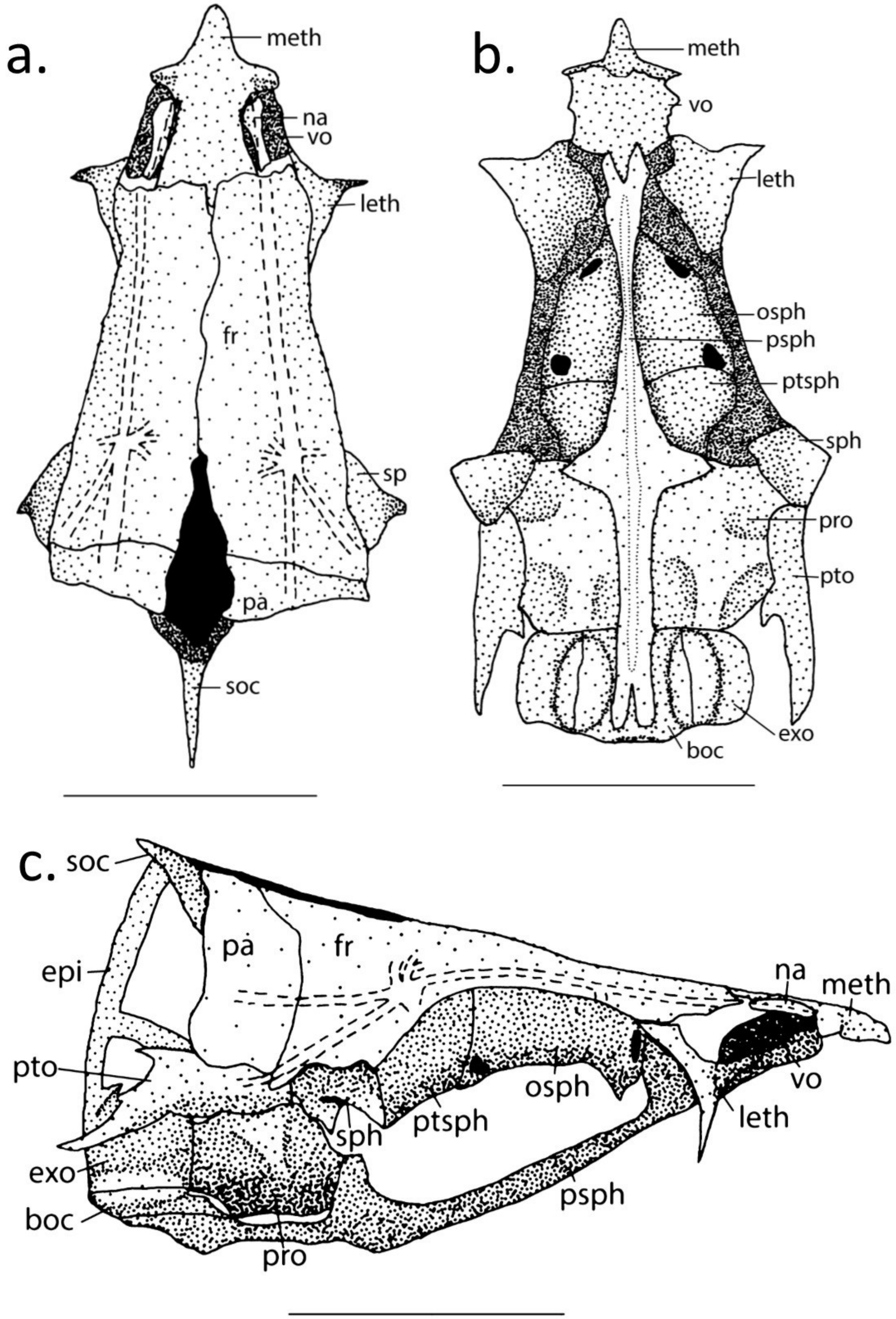

Figure 3.5. Drawing of the skull of *Petersius conserialis* CMN F 81-0187, specimen number 1, SL = 56.3 mm, (a) dorsal, (b) ventral, and (c) lateral views. Scale bar = 5 mm.

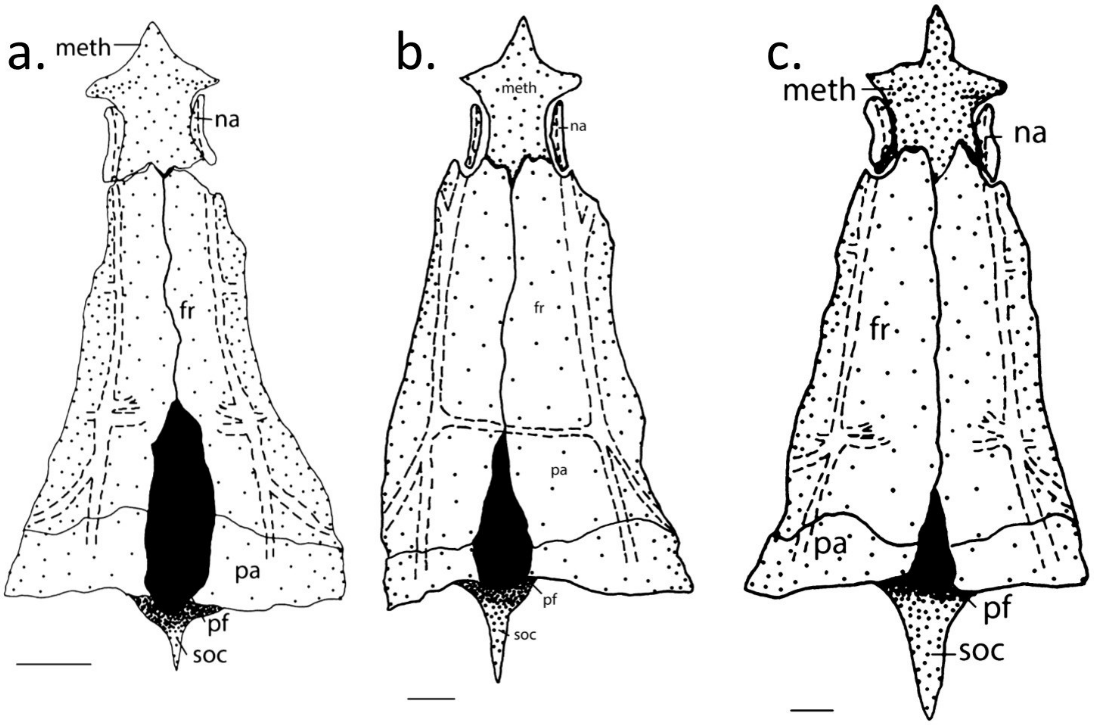

Figure 3.6. Drawings of the skulls of a size series of *Petersius conserialis* to show the difference in size of the parietal fontanelle, (a) specimen number = 12, SL = 40.9 mm, CMN F 81-0193, (b) specimen number = 1, SL = 56.3, CMN F 81-0187, (c) specimen number = 2, SL = 70.4, CMN F 81-0187. Scale bar = 1 mm.

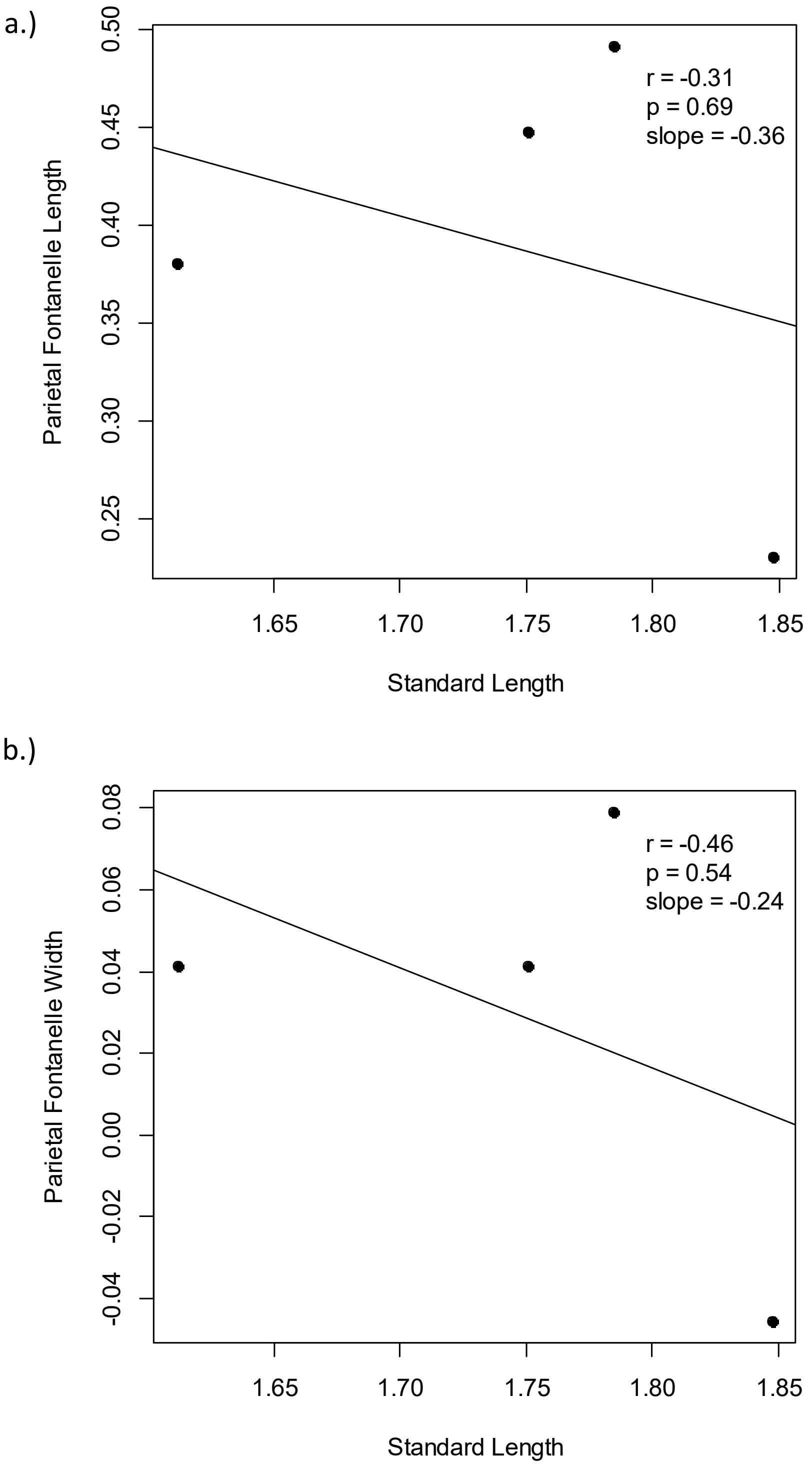

Figure 3.7. Negative slope and correlation between (a) standard length and fontanelle length, and (b) standard length and fontanelle width in *Petersius conserialis*, CMN F 81-0187 (*n* = 2) and CMN F 81-0193 (*n* = 2). Pearson's correlation and slope value in top right corner.

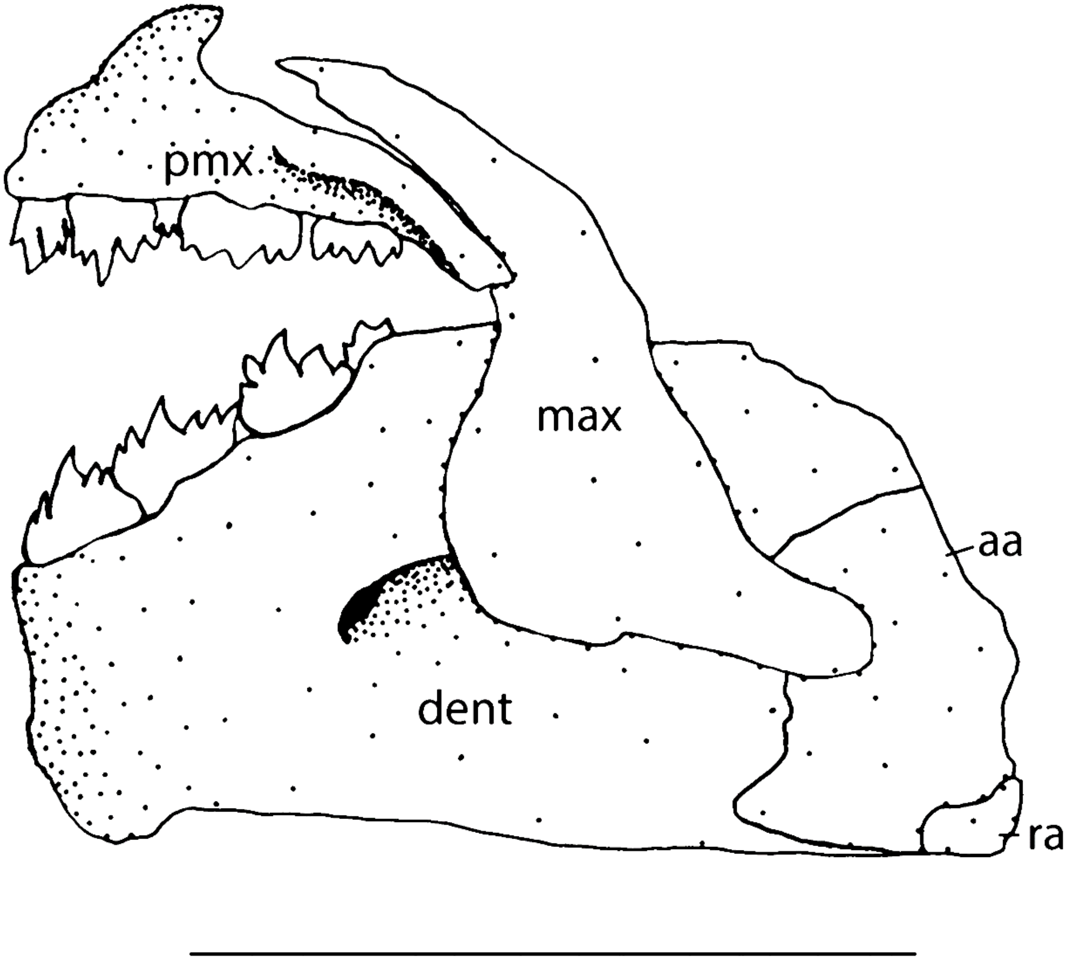

Figure 3.8. Drawing of the left jaws laterally of *Petersius conserialis* CMN F 81-0187, specimen number 1, SL = 56.3 mm. Scale bar = 5 mm.

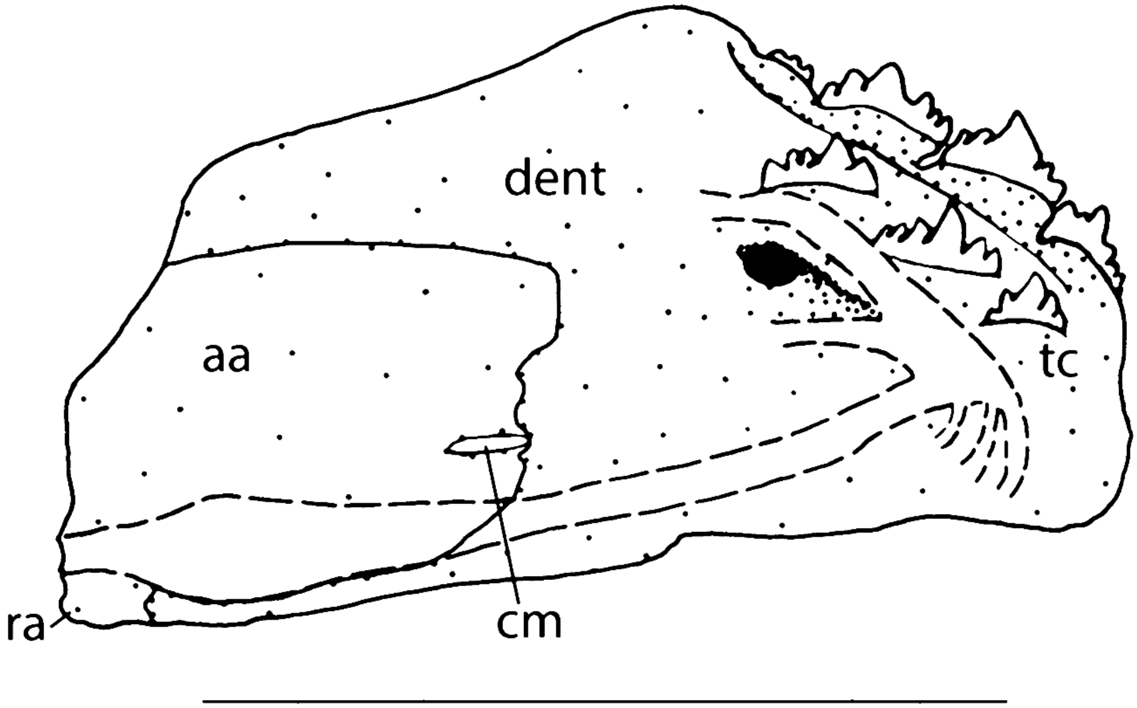

Figure 3.9. Drawing of the left dentary bone medially, featuring the tooth crypt of *Petersius conserialis* CMN F 81-0187, specimen number 1, 56.3 mm SL. Scale bar = 5 mm.

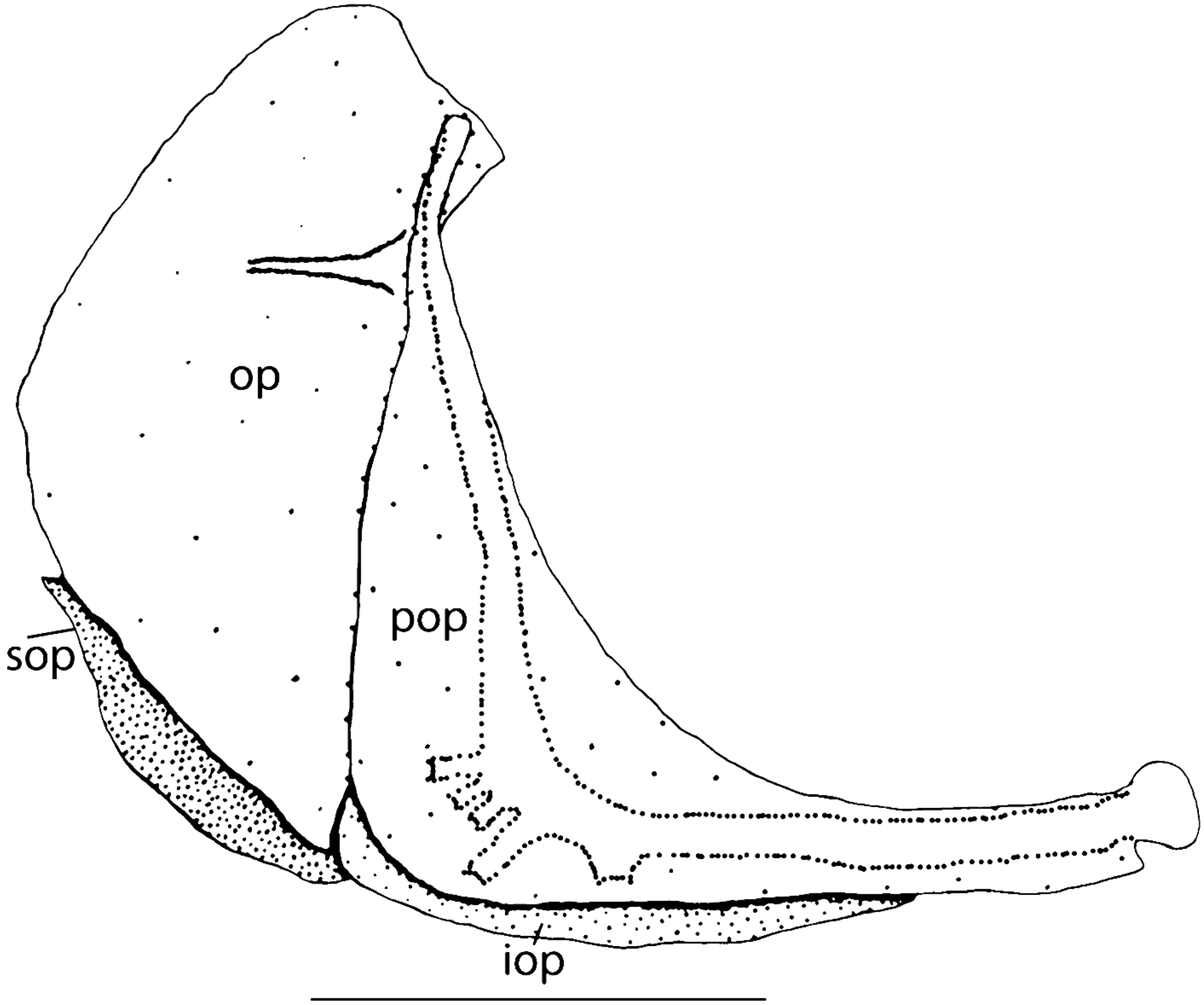

Figure 3.10. Drawing of the opercular series of *Petersius conserialis* CMN F 81-0187, specimen number 1, 56.3 mm SL. Scale bar = 5 mm.

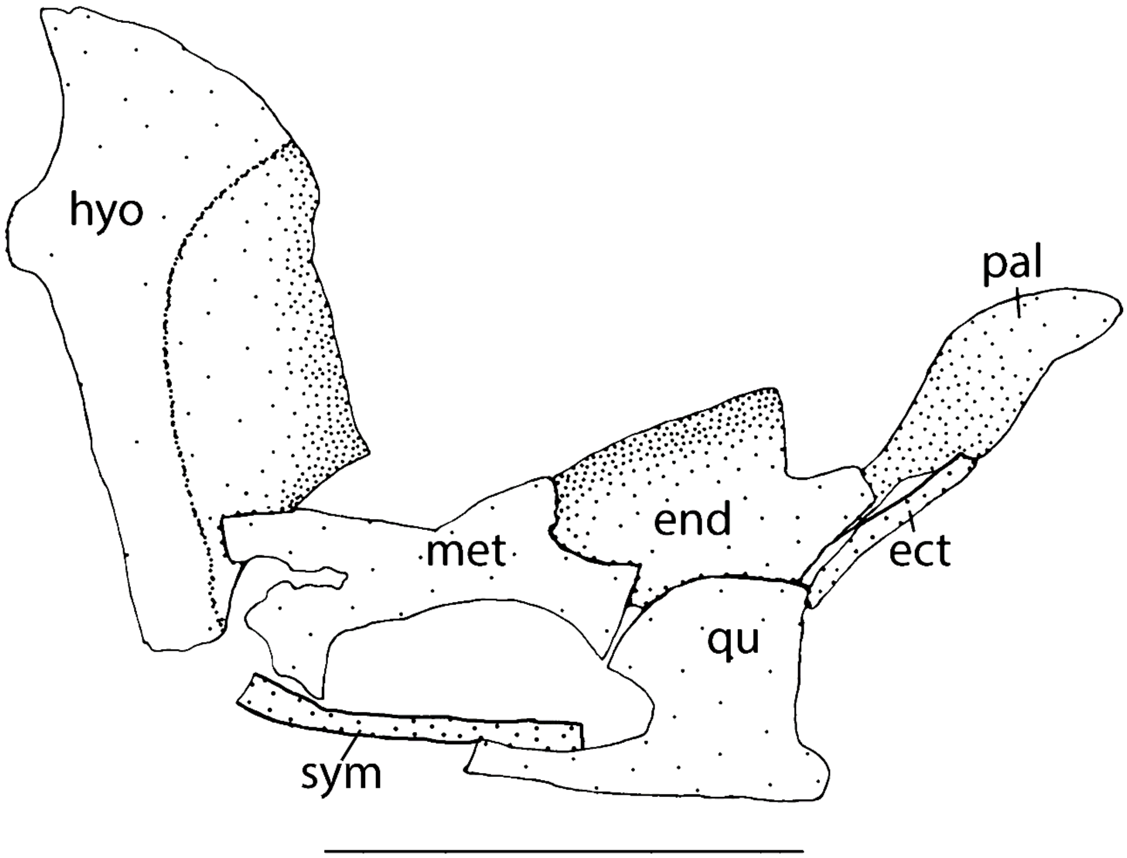

Figure 3.11. Drawing of the suspensorium of *Petersius conserialis* CMN F 81-0187, specimen number 1, 56.3 mm SL in lateral view. Scale bar = 5 mm.

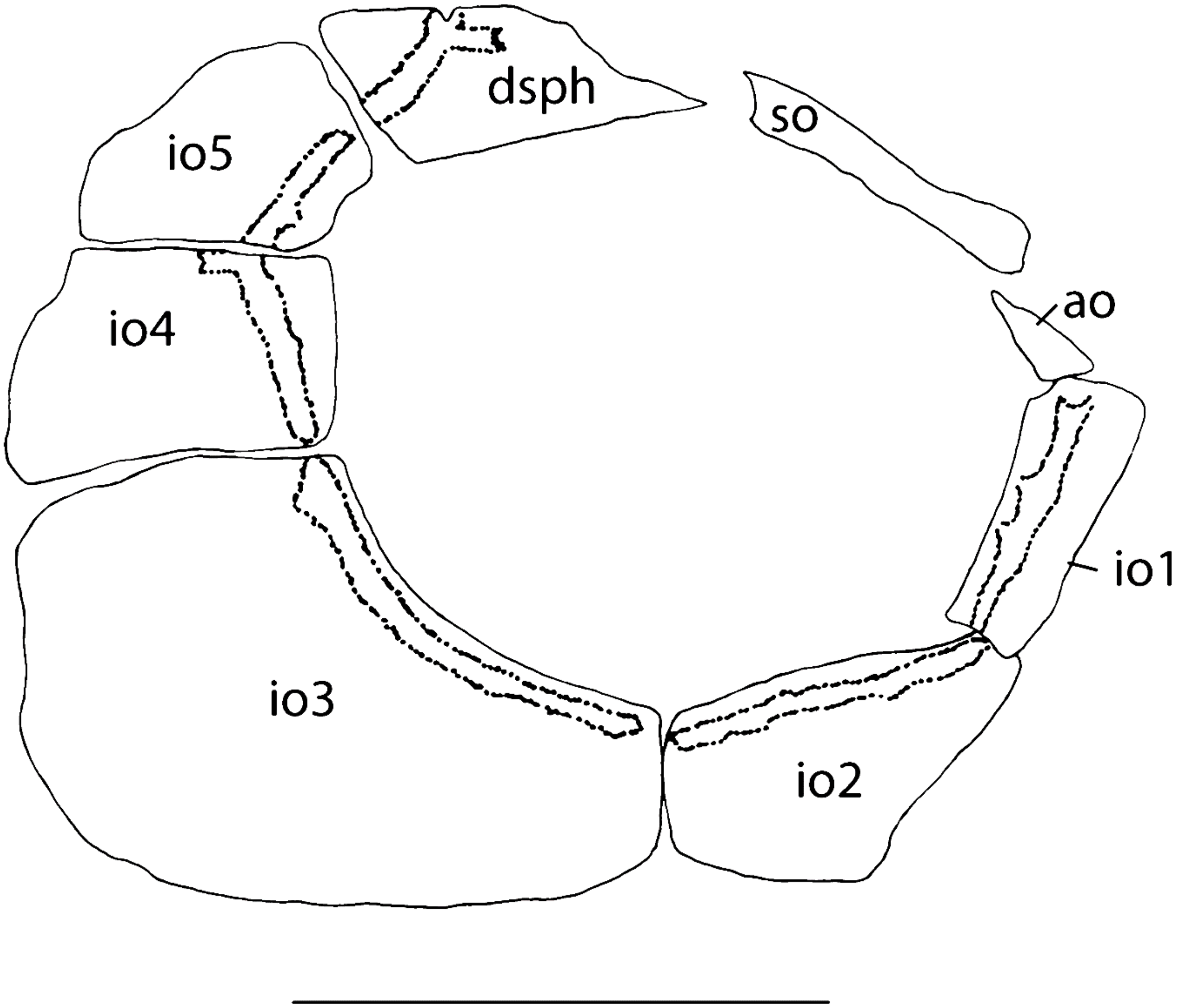

Figure 3.12. Drawing of the circumorbital series of *Petersius conserialis*, CMN F 81-0187, specimen number 1, 56.3 mm SL. Scale bar = 5 mm.

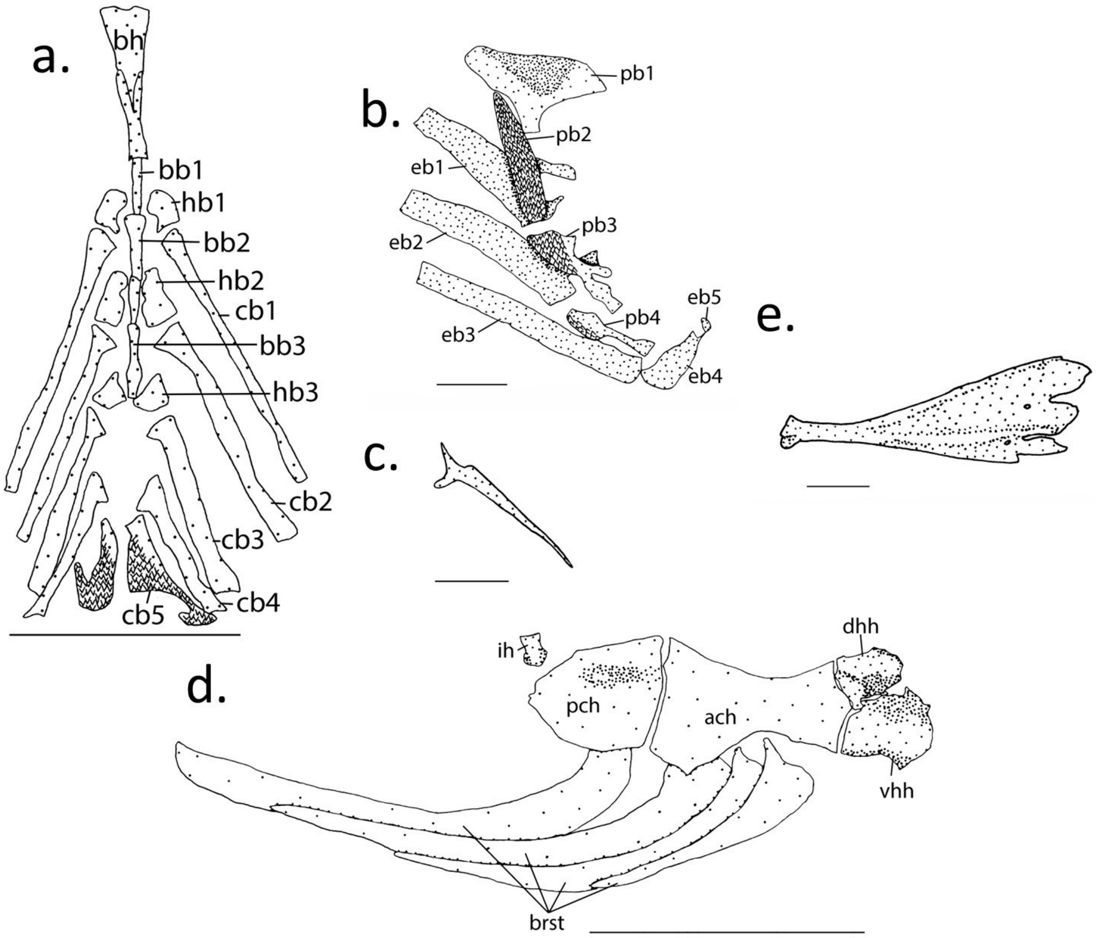

Figure 3.13. Drawing of the branchial arches and pharyngeal region of *Petersius conserialis* CMN F 81-0187, specimen number 1, 56.3 mm SL, (a) lower pharyngeal bones, (b) upper pharyngeal bones, (c) gill raker, (d) ceratohyal, and (e) urohyal. Scale bar for a and d = 5 mm, scale bar for b, c and e = 1 mm.

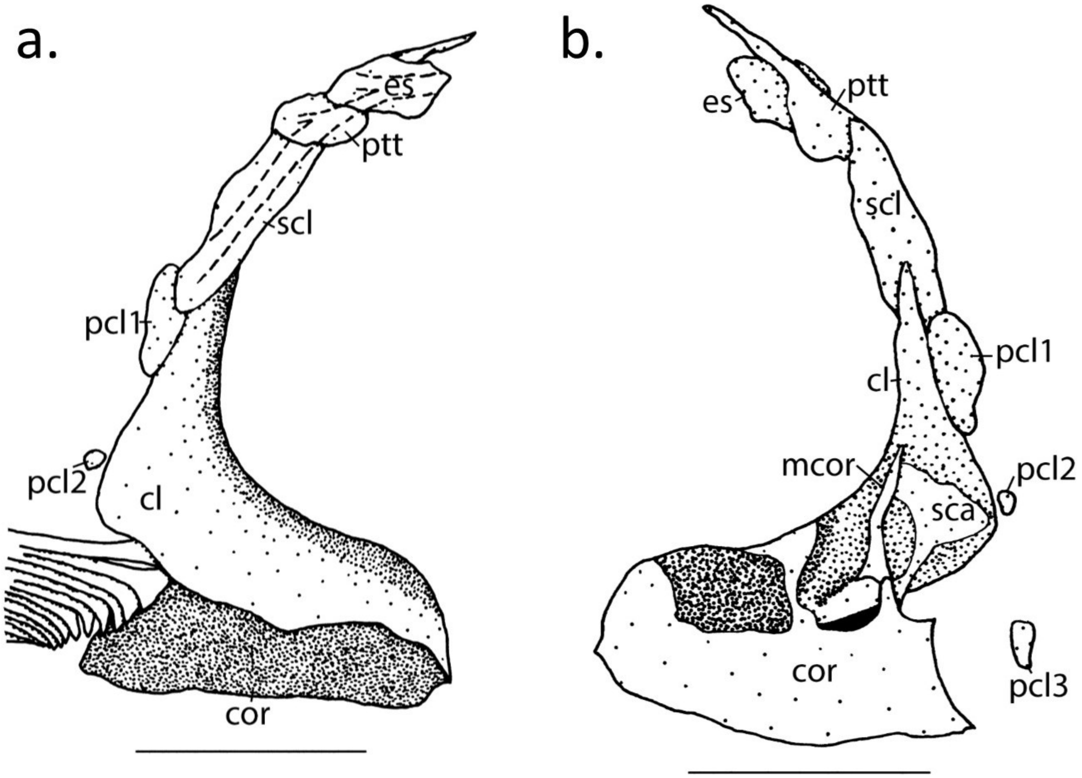

Figure 3.14. Drawing of the right pectoral girdle of *Petersius conserialis* CMN F 81-0187, specimen number 1, 56.3 mm SL, in (a) lateral and (b) medial view. Scale bar = 5 mm.

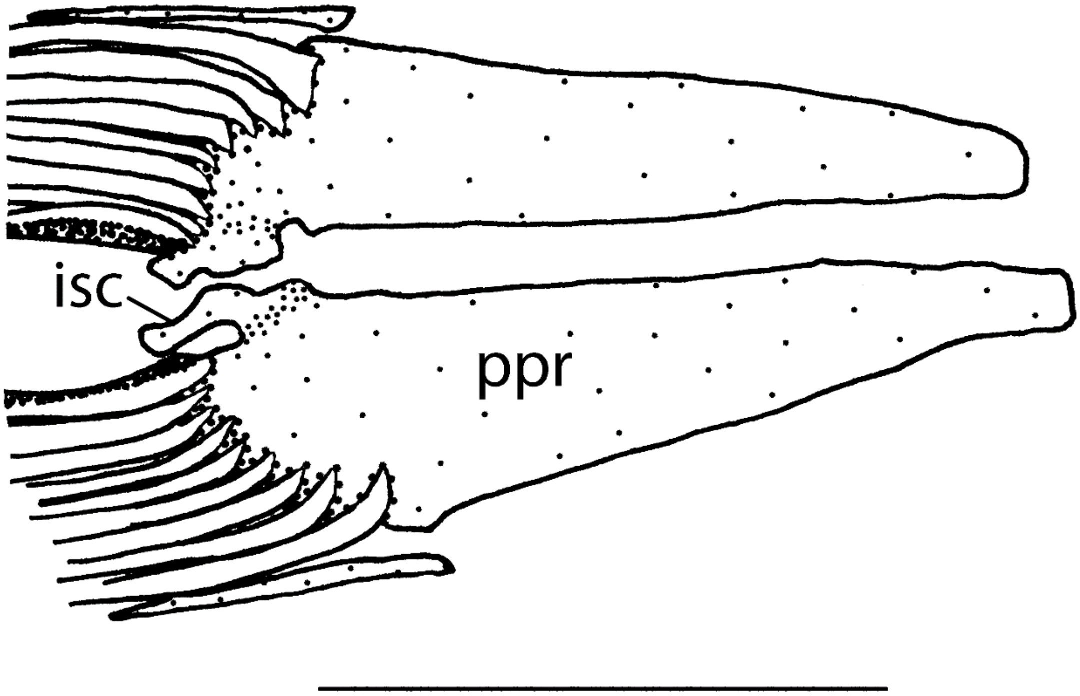

Figure 3.15. Drawing of the pelvic girdle of *Petersius conserialis*, CMN F 81-0193, specimen number 15, 60.9 mm SL in ventral view. Scale bar = 5 mm.

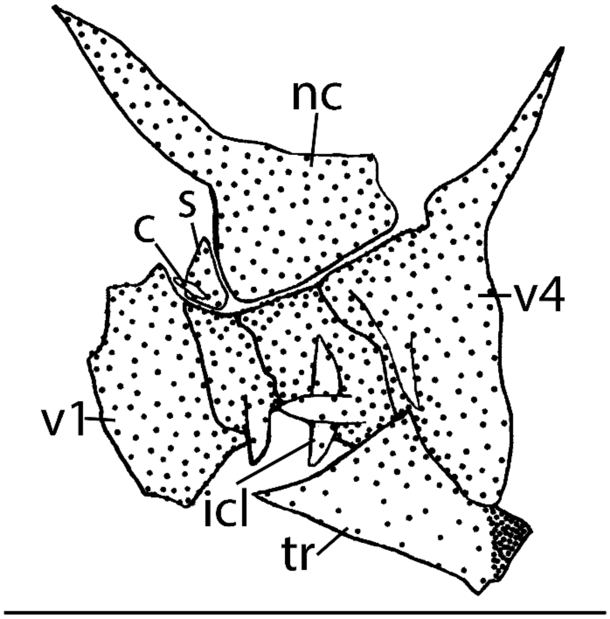

Figure 3.16. Drawing of the Weberian apparatus of *Petersius conserialis* CMN F 81-0193, specimen number 15, 60.9 mm SL. Scale bar = 5 mm.

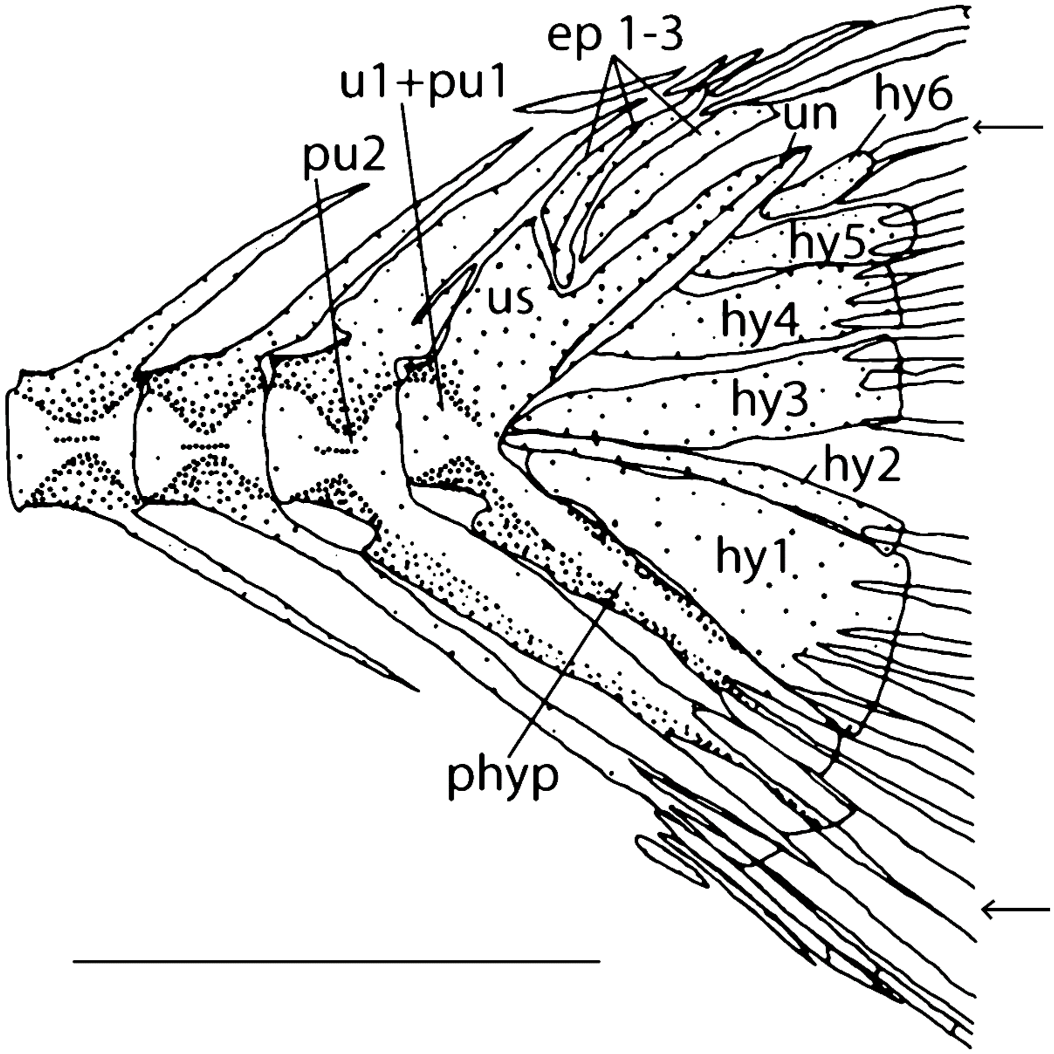

Figure 3.17. Drawing of the caudal fin of *Petersius conserialis* CMN F 81-0187, specimen number 2, 70.4 m SL. Arrows indicate first (unbranched) principal fin ray. Scale bar = 5 mm

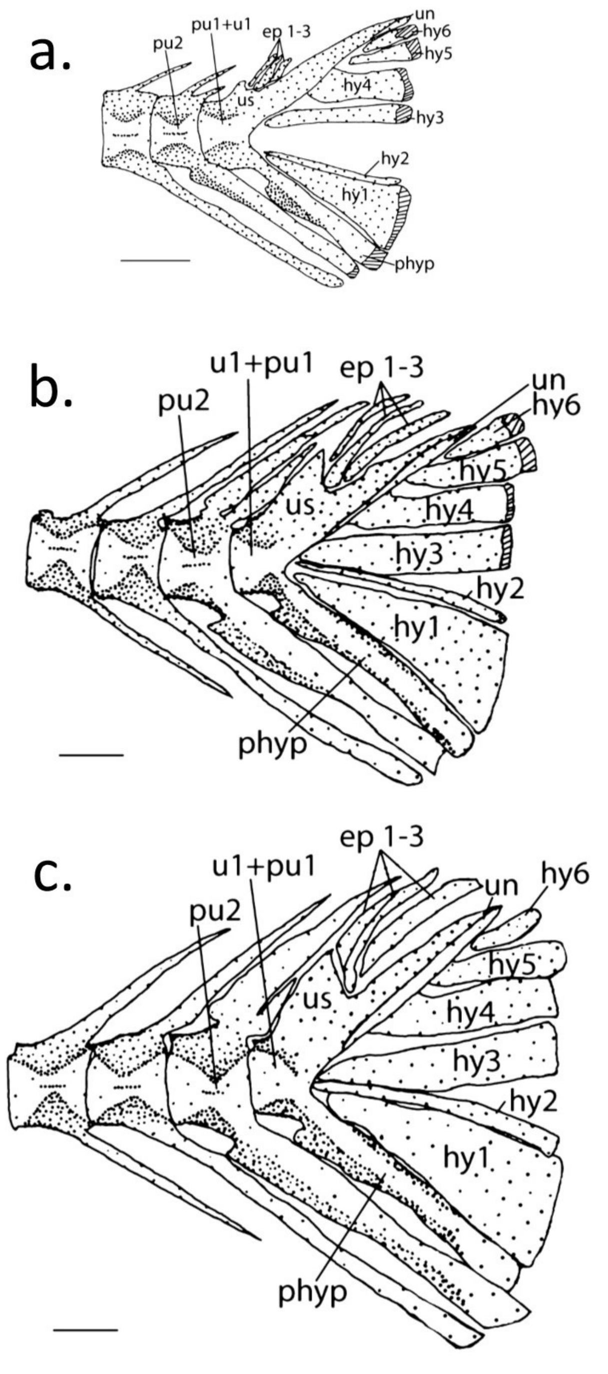

Figure 3.18. Drawing of the caudal fins of a size series of *Petersius conserialis*, (a) CMN F 81-0187, specimen 2, 70.4 mm SL, (b) CMN F 81-0193, specimen number 15, 60.9 mm SL, (c) CMN F 81-0187, specimen 2, 70.4 mm SL x. Hatching represents cartilage. Scale bar = 1 mm.

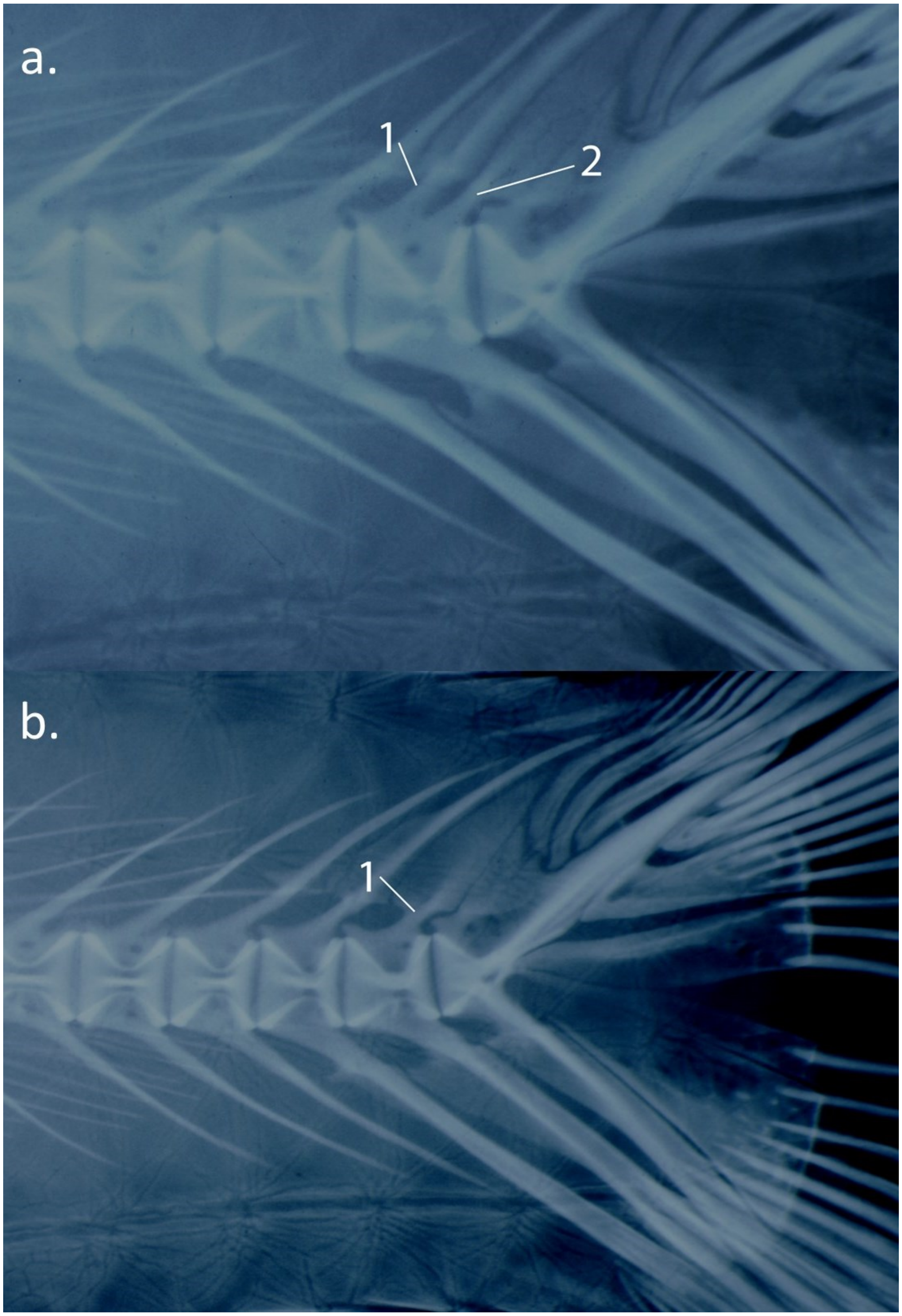

Figure 3.19. Radiographs of the caudal skeleton of *Petersius conserialis*, CMN F 81-0187 with unidentified specimen numbers. Demonstrating the different number of neural spines present on preural 2.

a.

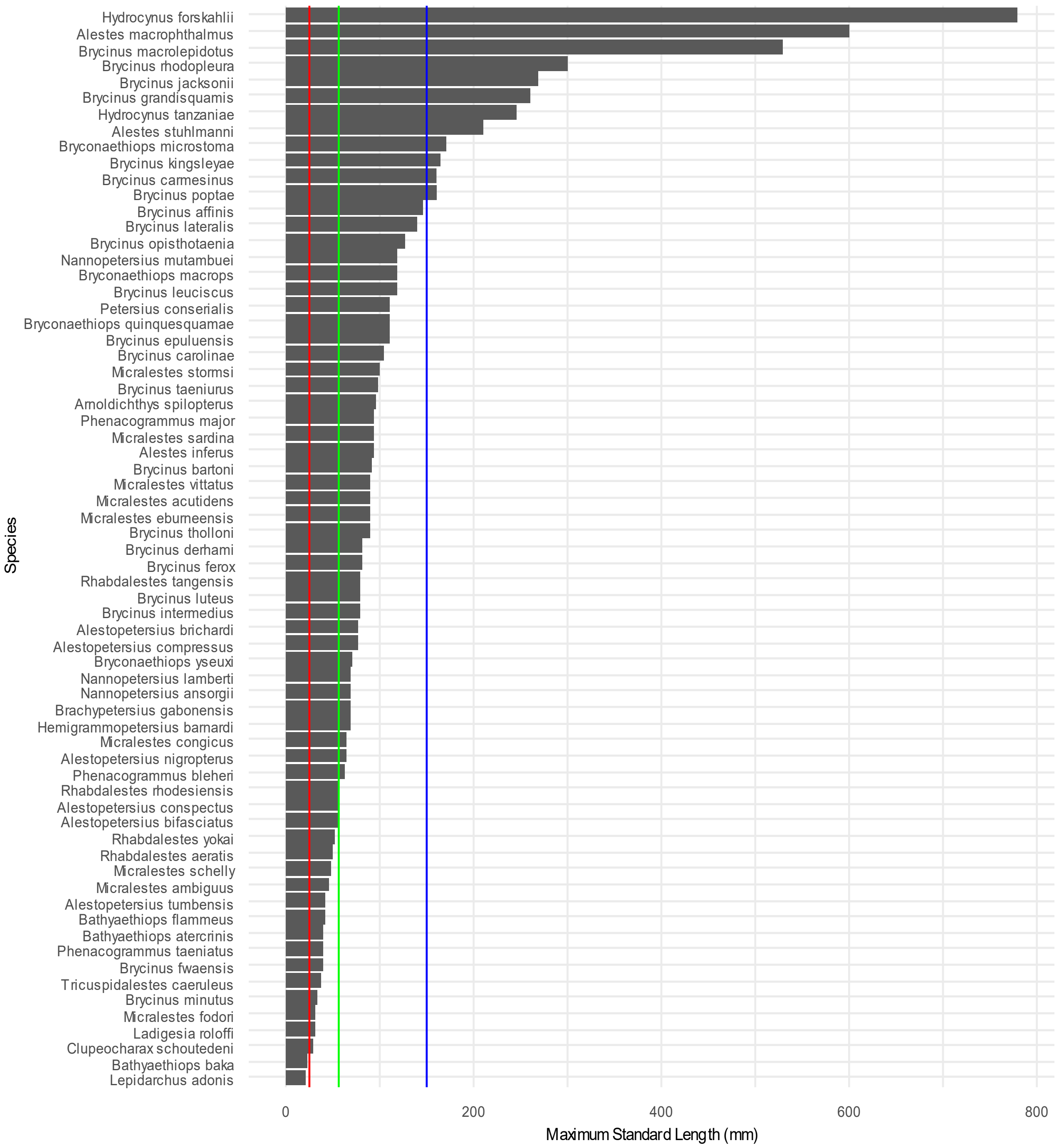
Hydrocynus forskahlii
Alestes macrophthalmus
Brycinus macrolepidotus
Brycinus rhodopleura
Brycinus jacksonii
Brycinus grandisquamis
Hydrocynus tanzaniae
Alestes stuhlmanni
Bryconaethiops microstoma
Brycinus kingsleyae
Brycinus carmesinus
Brycinus poptae
Brycinus affinis
Brycinus lateralis
Brycinus opisthotaenia
Nannopetersius mutambuei
Bryconaethiops macrops
Brycinus leuciscus
Petersius conserialis
Bryconaethiops quinquesquamae
Brycinus epuluensis
Brycinus carolinae
Micralestes stormsi
Brycinus taeniurus
Arnoldichthys spilopterus
Phenacogrammus major
Micralestes sardina
Alestes inferus
Brycinus bartoni
Micralestes vittatus
Micralestes acutidens
Micralestes eburneensis
Brycinus tholloni
Brycinus derhami
Brycinus ferox
Rhabdalestes tangensis
Brycinus luteus
Brycinus intermedius
Alestopetersius brichardi
Alestopetersius compressus
Bryconaethiops yseuxi
Nannopetersius lamberti
Nannopetersius ansorgii
Brachypetersius gabonensis
Hemigrammopetersius barnardi
Micralestes congicus
Alestopetersius nigropterus
Phenacogrammus bleheri
Rhabdalestes rhodesiensis
Alestopetersius conspectus
Alestopetersius bifasciatus
Rhabdalestes yokai
Rhabdalestes aeratis
Micralestes schelly
Micralestes ambiguus
Alestopetersius tumbensis
Bathyaethiops flammeus
Bathyaethiops atercrinis
Phenacogrammus taeniatus
Brycinus fwaensis
Tricuspidalestes caeruleus
Brycinus minutus
Micralestes fodori
Ladigesia roloffi
Clupeocharax schoutedeni
Bathyaethiops baka
Lepidarchus adonis
Species
0
200
400
600
800
Maximum Standard Length (mm)

b.

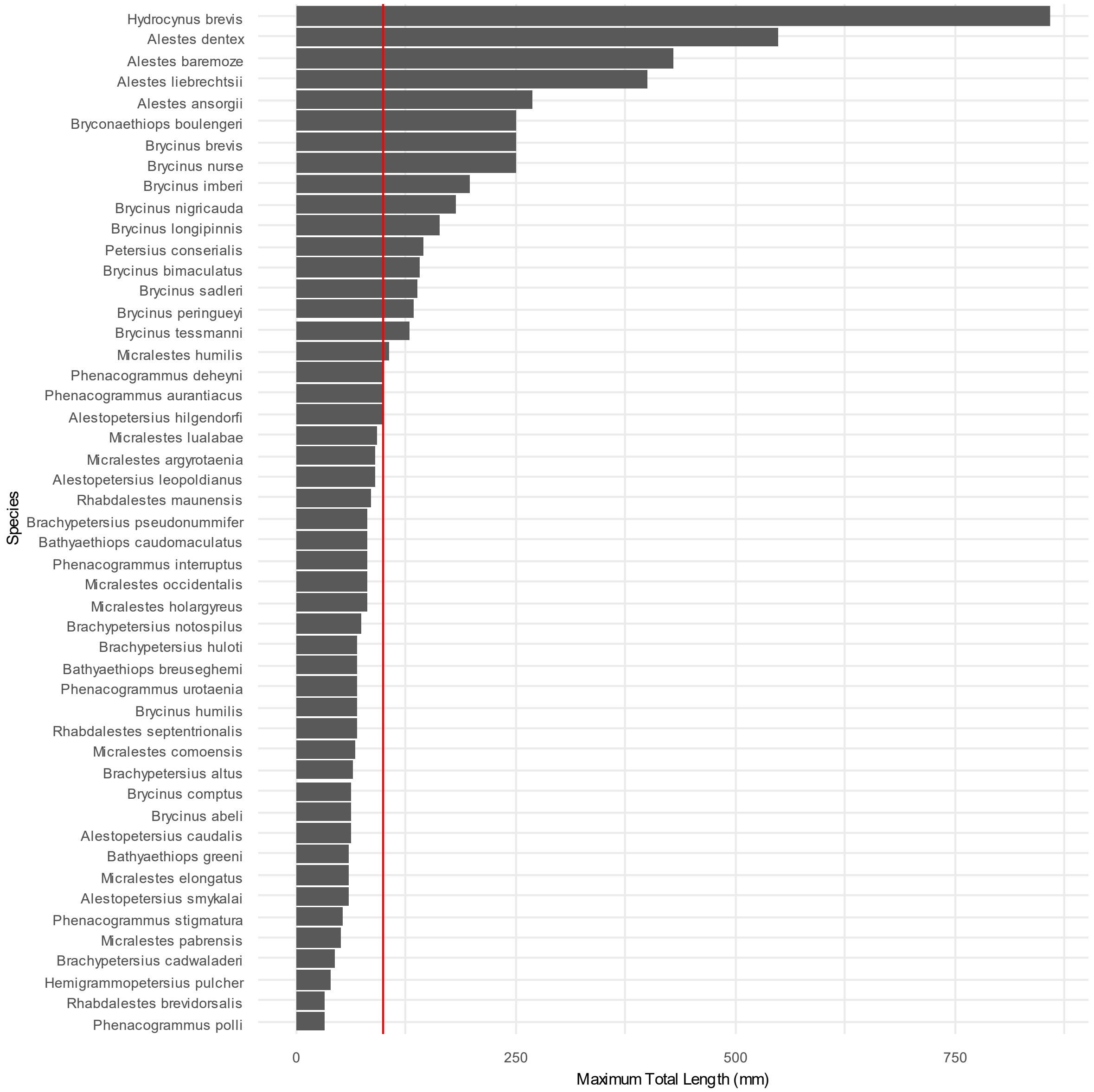

Figure 3.20. Length measurements as reported in FishBase (Froese & Pauly, 2018). (A) Maximum standard length (SL) measurements for 67 of 119 alestid species, the red line represents 26 mm SL (Weitzman and Vari's (1988) definition for miniature), the green line represents the smallest quarter of alestid species, 57 mm SL (Purvis and Harvey's (1996) definition), and the blue line represents 150 mm SL (Castro's (1999) definition for small fish). (B) Maximum total length measurements for 49 of 119 alestid species, the red line represents fish under 100 mm TL (Lindsey's (1966) definition).

3.7 References

Arroyave, J., & Stiassny, M. L. J. (2011). Phylogenetic relationships and the temporal context for the diversification of African characins of the family Alestidae (Ostariophysi: Characiformes): Evidence from DNA sequence data. *Molecular Phylogenetics and Evolution, 60*(3), 385-397.

Barriga, J. P., Battini, M. Á., García-Asorey, M., Carrea, C., Macchi, P. J., & Cussac, V. E. (2011). Intraspecific variation in diet, growth, and morphology of landlocked *Galaxias maculatus* during its larval period: the role of food availability and predation risk. *Hydrobiologia, 679*(1), 27-41.

Brewster, B. (1986). A review of the genus *Hydrocynus* Cuvier 1819 (Teleostei: Characiformes). *Bulletin of the British Museum Natural History (Zoology), 50*(3), 163-206.

Castro, R. M. C. (1999). Evolucao da ictiofauna de riachos Sul-Americanos: Padroes gerais e possiveis processos causais. In R. Mazzoni & P. R. Peres-Neto (Eds.), *Ecologia de Peizes de Riachos* (Vol. 6, pp. 139-155). Rio de Janeiro, Brazil.

Fink, S. V., & Fink, W. L. (1981). Interrelationships of the ostariophysan fishes (Teleostei). *Zoological Journal of the Linnaean Society, 72*(4), 297-353.

Froese, R., & Pauly, D. (2018). FishBase. *World Wide Web electronic publication.* Retrieved from www.fishbase.org

Gery, J. (1977). *Characoids of the World*. USA: T.F.H. Publications, Inc. Ltd.

Gery, J. (1995). Description of new or poorly known Alestinae (Teleostei: Characiformes: Alestidae) from Africa, with a note on the generic concept in the Alestinae. *Journal of Ichthyology and Aquatic Biology, 1*(4), 37-64.

Hilgendorf. (1894). Neue Characinidengattung, *Petersius*, aus dem Kinganiflusse. *Sitzungs-Berichte der Gesellschaft Naturforschender Freunde zu Berlin*, 172.

Hoedeman, J. J. (1951). Studies on African Characid Fishes. The tribe Alestidi. *Beaufortia, 3*, 1-8.

Howes, G. J. (1982). Review of the genus *Brycon* (Teleostei: Characoidei). *Bulletin of the British Museum of Natural History (Zoology), 43*(1), 1-47.

Hubert, N., Bonillo, C., & Paugy, D. (2005). Early divergence among the Alestidae (Teleostei, Ostariophyses, Characiformes): Mitochondrial evidences and congruence with morphological data. *Animal Biology and Pathology, 328* (5), 477-491.

Kassambar, A., & Mundt, F. (2017). factoextra: Extract and visualize the results of multivariate data analyses (Version R package version 1.0.5). Retrieved from https://CRAN.R-project.org/package=factoextra

Le, S., Josse, J., & Husson, F. (2008). FactoMineR: An R package for multivariate analysis. *Journal of Statistical Software, 15*(1), 1-18.

Lindsey, C. C. (1966). Body sizes of poikilotherm vertebrates at different latitudes. *Evolution, 20*(4), 456-465.

Liu, C. H. (2001). Early osteological development of the yellow tail *Seriola dumerili* (Pisces: Carangidae). *Zoological Studies, 40*(4), 289-298.

Lunkayilakio, S. W., & Vreven, E. (2008). *Nannopetersius mutambuei* (Characiformes: Alestidae), a new species from the Inkisi River basin, Lower-Congo. *Ichthyological Exploration of Freshwaters, 19*(4), 367-376.

Mattox, G. M. T., Britz, R., & Toledo-Piza, M. (2014). Skeletal development and ossification sequence of the characiform *Salminus brasiliensis* (Ostariophysi: Characidae). *Ichthyological Exploration of Freshwaters, 25*(2), 103-158.

Meyer, D., Dimitriadou, E., Hornik, K., Weingessel, A., and Leisch, F. (2019). e1071: Misc Functions of the Department of Statistics, Probability Theory Group (Formerly:E1071), TU Wien. R package version 1.7-3. https://CRAN.R-project.org/package=e1071.

Murray, A. M. (2004). Osteology and morphology of the characiform fish *Alestes stuhlmannii* Pfeffer, 1896 (Alestidae) from the Rufiji River basin, East Africa. *Journal of Fish Biology, 65*(5), 1412-1430.

Murray, A. M., & Stewart, K. M. (2002). Phylogenetic relationships of the African genera *Alestes* and *Brycinus* (Teleostei, Characiformes, Alestidae). *Canadian Journal of Zoology-Revue Canadienne De Zoologie, 80*(11), 1887-1899.

Myers, G. S. (1929). Cranial differences in the African characin fishes of the genera *Alestes* and *Brycinus*, with notes on the arrangement of the genera. *American Museum Novitates, 342*, 1-7.

Novelli, B., Otero-Ferrer, F., Socorro, J. A., Caballero, M. J., Segade-Botella, A., & Dominguez, L. (2017). Development of short-snouted seahorse (*Hippocampus hippocampus*, L. 1758):

osteological and morphological aspects. *Fish Physiology and Biochemistry, 43*(3), 833-848.

Nzeyimana, F., & Amiet, J. (1992). Redescription, affinites et distribution au cameroun de *Brachypetersius altus* (Boulenger, 1899) (Characidae, Petersiini). *Cybium, 16*(1), 31-42.

Orti, G., & Meyer, A. (1997). The radiation of characiform fishes and the limits of resolution of mitochondrial ribosomal DNA sequences. *Systematic Biology, 46*(1), 75-100.

Poll, M. (1967). Revision des Characidae nains Africains. *Annales du Musee Royal de l'Afrique Centrale Tervurum serie in-8 Sciences Zoologiques, 162*, 1-158.

Prokofiev, A. M. (2001). A new genus of Neoscopelidae for *Eomyctophum gracile* Daniltshenko from the Middle Eocene of Georgia (Pisces: Osteichthyes: Myctophiformes). *Zoosystematica Rossica, 10*(1), 215 - 218.

Purvis, A., & Harvey, P. H. (1996). Miniature mammals: life-history strategies and macroevolution. In P. J. Miller (Eds.), *Miniature Vertebrates: The Implications of Small Body Size*. Oxford: Clarendon Press.

R Core Team (2017). R: A language and environment for statistical computing (Version 3.4.3). Vienna, Austria. Retrieved from https://www.R-project.org/

Roberts, T. R. (1969). Osteology and relationships of characoid fishes, particularly the genera *Hepsetus*, *Salminus*, *Hoplias*, *Ctenolucius*, and *Acestrorhynchus*. *Proceedings of the California Academy of Sciences, 36*(15), 391-500.

Skelton, P. H. (1994). Diversity and distribution of freshwater fishes in East and Southern Africa. *Annales du Musee Royale de l'Afrique Centrale, Sciences Zoologiques, 275*, 95-131.

Taylor, W. R., & Van Dyke, G. C. (1985). Revised procedure for staining and clearing small fishes and other vertebrates for bone and cartilage study. *Cybium, 9*(2), 107-119.

Wei, T., & Simko, V. (2017). R package "corrplot": Visualization of a Correlation Matrix (Version 0.84). Retrieved from https://github.com/taiyun/corrplot

Weitzman, S. H., & Vari, R. P. (1988). Miniaturization in South American freshwater fishes; An overview and discussion. *Proceedings of the Biological Society of Washington, 101*(2), 444-465.

Zanata, A. M., & Vari, R. P. (2005). The family Alestidae (Ostariophysi, Characiformes): a phylogenetic analysis of a trans-Atlantic clade. *Zoological Journal of the Linnaean Society, 145*(1), 1-144.

Chapter 4: Miniaturization of African alestids: A comparison of miniature species to juveniles of mid-sized species

4.1 Introduction

Miniaturization is a decrease in body size over evolutionary size that results in morphological, physiological, or behavioral changes (Hanken & Wake, 1993). This phenomenon is commonly reported throughout vertebrate taxa (e.g., Hanken & Wake, 1993; Yeh, 2002; Masters *et al.*, 2014) and is prevalent within teleosts (e.g., Carnevale, 2008; Britz & Conway, 2009; Bloom *et al.*, 2020). Various researchers have attempted to define small and miniature fishes (e.g., Lindsey, 1966; Purvis & Harvey, 1996; Castro, 1999); however, Weitzman and Vari's (1988) definition for miniature fishes continues to persist in the literature. A miniature fish either (i) reaches sexual maturity at sizes less than 20 mm standard length (SL) or (ii) never exceeds 26 mm SL (Weitzman & Vari, 1988). A key feature of their definition is the loss or reduction of features such as skeletal elements or the latero-sensory system (Weitzman & Vari, 1988). Two types of miniaturization in fishes have since been identified: (i) proportional dwarfs or smaller forms of their larger-bodied relatives, and (ii) developmentally truncated taxa or miniatures that retain juvenile traits (Britz & Conway, 2009). Both types are reported to have independently evolved numerous times within ostariophysans (e.g., Ruber *et al.*, 2007; De Santana & Crampton, 2011; Dutra *et al.*, 2012).

Ostariophysi is a group of fish classified by the presence of a Weberian apparatus, a modification to the first four or five anterior vertebrae that enhances hearing, and is comprised of four orders; (i) Gymnotiformes, (ii) Siluriformes, (iii) Cypriniformes, and (iv) Characiformes (Nelson, 2006). Characiformes – tetras, piranhas, and their relatives – inhabit South America and Africa (Nelson, 2006). These freshwater fishes demonstrate a wide diversity with over 2000 species described, and more are continually being described (Oliveira *et al.*, 2011). An asymmetrical distribution is found in Characiformes, with just over 200 characiform species residing in Africa and over 1800 characiform species described from the Neotropics (Oliveira *et al.*, 2011).

South American characiforms have an extensive diversity of miniature fish, with 87 species documented as of 2014 (Toledo-Piza *et al.*, 2014), compared with African characiforms with only five recorded as of 2006 (Conway & Moritz, 2006). Both counts have continued to rise with more miniatures described in recent years (e.g., Moritz & Schliewan, 2016; Pastana *et al.*, 2017; da Graca *et al.*, 2019). The sheer number of miniature characiform fishes in South America has led to a solid foundation of research (e.g., Netto-Ferreira *et al.*, 2013; Toledo-Piza *et al.*, 2014; Mattox *et al.*, 2016), whereas limited research has been conducted on African counterparts (some exceptions include: Poll, 1967; Murray & Stewart, 2002; Hubert *et al.*, 2005; Zanata & Vari, 2005; Moritz & Schliewan, 2016).

Alestidae is one of only four African characiform families and one of the two African characiform families known to contain miniatures (Conway & Moritz, 2006; Moritz and Schliewan, 2016). Alestids exhibit a pronounced diversity in body size, including the previously mentioned miniatures (< 26 mm SL) to giants such as *Hydrocynus goliath* Boulenger that reach up to 1300 mm SL (Hubert *et al.*, 2005). Previous phylogenetic hypotheses indicate multiple independent miniaturization events occurred in Alestidae (Hubert *et al.*, 2005; Zanata & Vari, 2005), suggesting small body sizes or miniaturization may present a potential advantage to those species.

Miniature alestids display a gradual decrease in body size, with increased reductions and losses of features, in a phylogenetic context (Zanata & Vari, 2005). *Hemigrammopetersius barnardi* (Herre), while not a true miniature fish as it has a maximum reported SL of 70 mm (Eccles, 1992), demonstrates morphological reductions and losses with a decreased body size in a phylogenetic context (Zanata & Vari, 2005). This chapter will compare the osteology of *H. barnardi*, a proportionally small fish, to two other alestid species: (i) a traditionally classified larger petersiin, *Petersius conserialis* Hilgendorf, which reaches a maximum total length (TL) of 145 mm (Poll, 1967) and (ii) juvenile specimens of *Alestes dentex* (Linnaeus), which attain a much larger adult size at a maximum TL of 550 mm (Paugy, 1990b).

Previous studies (e.g., Johnson & Brothers, 1993; Britz & Conway, 2009; Franz-Odendaal & Adriaens, 2014) have successfully compared the osteology of miniatures to juveniles of species that attain a larger body-size to determine potential synapomorphies that are present during earlier developmental stages of larger relatives. The comparison of the osteology of an almost miniature alestid, *H. barnardi*, to a full grown larger alestid, *P. conserialis*, and a juvenile alestid of a species that reaches a larger adult size, *A. dentex,* will identify potential convergent characters resulting from a decrease in body size that are not indicative of evolutionary relationships as implied by traditional classification systems in alestids (e.g., Poll, 1967; Gery, 1977, 1995). A review on potential costs and benefits of miniaturization in general is included in the discussion of this chapter.

4.2 Materials and Methods

4.2.1 Materials Examined

Alestes dentex: USNM 229863, 3 cleared and stained (c&s), 3 jaw skeletons, Sokoto-Rima Floodplain, Sokoto, Nigeria, 43.2 – 62.7 mm SL.

Hemigrammopetersius barnardi: CMN F 81-0188, 157 alcohol preserved, three c&s, Rufiji River, west end of Lake Ruwe, Tanzania, 19.2 – 34.9 mm SL.

Petersius conserialis: CMN F 81-0193, 13 alcohol preserved, 2 c&s, Rufiji River, Tanzania, 40.9 – 91 mm SL, CMN F 81-0187, 2 c&s, Rufiji River, Tanzania, 56.3 – 70.4 mm SL.

4.2.2 Methods

Specimens were previously cleared and counterstained for bone and cartilage according to Taylor and Van Dyke's (1985) procedure. I took comparative photographs for osteological drawings using a Nikon DXM 1200C digital camera mounted on a Zeiss Stereo Discovery .V8 stereomicroscope with a Carl Zeiss 44403 6-9000 eyepiece (8x) and a variety of lenses (Zeiss Achromat S 0.3x FWD 236 mm, Zeiss Plan Apo S 0.63x FWD 81 mm, and Zeiss Plan Apo S 1.0x FWD 60 mm), with NIS-Elements F package 2.20, version 5.03. I processed figures using Adobe Photoshop CS6. Osteological terminology follows Murray (2004), with the exception of endopterygoid for mesopterygoid from Brewster (1986) and pubic processes from Prokofiev (2001).

4.3 Osteological Comparisons

The smallest examined specimen of *Alestes dentex* (SL = 43.2 mm) is not fully ossified where the ribs contact the vertebrae (Fig 4.1). The absence of complete ossification at the point of contact between the ribs and the anterior vertebrae, combined with the fact that adult specimens of *A. dentex* reach a maximum of 550 mm TL (Paugy, 1990b), indicates that the three examined specimens of *A. dentex* (SL = 43.2 – 62.7 mm) likely represent juveniles, even though sexual maturity of these individuals cannot be determined. Examined specimens of *Hemigrammopetersius barnardi* and *Petersius conserialis* are assumed to be adults as no cartilage persists along the vertebrae and ribs.

4.3.1 Skull

In all examined species the anterior end of the mesethmoid has a distinct raised medial process, with well-developed lateral projections just behind it (Fig. 4.2). Specimens of *H. barnardi* and *P. conserialis* have three posterior pointed projections, with a longer middle one that separates the left and right frontals. In comparison, *A. dentex* has only a single large posteromedial process – also separating the left and right frontals – but no other posterior projections. All three species have long, narrow nasals, with the supraorbital sensory canal extending along the lateral edge of the bone. The lateral ethmoid has a ventral projection and a concave posterior edge in all species

The frontals of all species expand posteriorly. The supraorbital sensory canal extends anteriorly to posteriorly across the frontal and is less extensive in specimens of *H. barnardi* with three openings along the posterior portion of the skull (one at level with the epiphyseal bar, one extending onto the ventral edge of the parietal and one extending onto the anterior edge of the pterotic), in comparison to *A. dentex* and *P. conserialis* which have five and six openings, respectively (Fig. 4.3). *Alestes dentex* has a dorsal and ventral opening of the supraorbital sensory canal at level with the epiphyseal bar and three openings extending posteriorly towards the parietal and pterotic, whereas *P. conserialis* has three dorsal and one ventral opening at level with the epiphyseal bar and two extending posteriorly towards the parietal and pterotic. A parietal fontanelle fully separates the left and right parietals in all species. The parietal fontanelle extends anterior to the epiphyseal bar in *A. dentex* and *H. barnardi*, unlike specimens of *P. conserialis* in which the relative length of the parietal fontanelle decreases as body size increases (the smallest examined specimen, CMN F 81 0193 #12, 40.9 mm SL, has the parietal fontanelle extending anterior to the epiphyseal bar as observed in *A. dentex* and *H. barnardi*, whereas in the largest examined specimen, CMN F 81-0187 #2, 70.4 mm SL, the parietal fontanelle ends posterior to the epiphyseal bar). The supraorbital sensory canal crosses from the frontal to the parietal in all species. The parietal narrows ventrally in *A. dentex* and *H. barnardi*, compared to *P. conserialis*, in which the parietal widens ventrally.

The posterior edge of the parietal fontanelle is formed by a deep, v-shaped notch in the supraoccipital in all three species. The supraoccipital of larger specimens of *H. barnardi* and *P. conserialis* is fully ossified, in comparison with juvenile specimens of *A. dentex*, and small specimens of *H. barnardi* (31.2 mm SL) and *P. conserialis* (40.9 mm SL) that still have cartilage along the ventral edge of the supraoccipital. Appendix E summarizes the presence and absence of cartilage in endochondral bones found in all specimens.

The parasphenoid of *A. dentex* and *H. barnardi* is ventrally depressed, as is common in other alestids and characids (Zanata & Vari, 2005). The parasphenoid of *P. conserialis* runs in a straight line through the center of the orbit (Fig. 4.3). Anteriorly, the parasphenoid is forked and contacts the vomer, and posteriorly it contacts the basioccipital. The lateral wings of the parasphenoid contact the prootics. The orbitosphenoid has a medial ridge that comes to an anteromedial point in all three species. Specimens of *H. barnardi* and *P. conserialis* have two pairs of foramina on the orbitosphenoid, an anterolateral and posterolateral pair. This is unlike *A. dentex*, in which there is a single pair of anterolateral foramina on the orbitosphenoid. Cartilage persists between the orbitosphenoid and pterosphenoid in two juveniles of *A. dentex* (43.2- and 62.7-mm SL) and a specimen of *H. barnardi* (31.2 mm SL). The sphenotic has one ventral projection in all specimens.

The prootic of *H. barnardi* is rounded with a small anterior foramen. *Alestes dentex* has two anterior foramina on the prootic and *P. conserialis* has one large anterior foramen with three small foramina along the medial edge of the prootic near the parasphenoid. The prootic is not fully ossified along the edges in smaller specimens of *H. barnardi* (31.2 mm SL) and *A. dentex* (43.2 mm SL). *Alestes dentex* and *P. conserialis* have a raised expansion on the prootic in ventral view that extends laterally towards the pterotic and posteriorly towards the basioccipital.

The pterotic retains cartilage in smaller specimens of all species (*A. dentex* 43.2 – 62.7 mm SL, *H. barnardi* 31.2 – 32.7 mm SL, and *P. conserialis* 40.9 mm SL). Rounded edges of the pterotic and poorly defined posterior projections are found in *H. barnardi*, compared to *A.*

dentex and *P. conserialis*, which have well-developed pointed posterior projections. The pterotic of *A. dentex* also has a dorsal projection separating the ventral portion of the frontal and parietal (Fig. 4.3).

The edges of the epioccipital retain cartilage in small specimens (*A. dentex* 43.2 – 62.7 mm SL*, H. barnardi* 26.2 – 31.2 mm SL, and *P. conserialis* 40.9 mm SL). The exoccipital and basioccipital form a large lagenar capsule in ventral view for all three species, as reported in other characiforms (Fink & Fink, 1981). Smaller specimens of *A. dentex* (43.2 mm SL) and *H. barnardi* (31.2 mm SL) retain cartilage along the edge of the exoccipital, which is fully ossified in larger specimens (≥ 55.8 mm SL and ≥ 32.7 mm SL, respectively). The exoccipital of all specimens of *P. conserialis* (40.9 – 70.4 mm SL) is fully ossified.

4.3.2 Jaws and Teeth

All three species have a premaxillary pedicle and a short ascending process on the premaxilla (Fig. 4.4). Two rows of multicuspid teeth are present on the premaxilla. *Hemigrammopetersius barnardi* and *P. conserialis* have two outer premaxillary teeth (only one is visible *P. conserialis* in Fig. 4.4e, f because the second has been lost) and four inner premaxillary teeth. In contrast, *A. dentex* has three outer and four inner premaxillary teeth. The number of tooth cusps differs among the species. *Hemigrammopetersius barnardi* has three cusps on the outer premaxilla teeth and three to five cusps on the inner premaxillary teeth. *Petersius conserialis* has three cusps on the outer premaxillary teeth and five to seven cusps on the inner premaxillary teeth. Finally, *A. dentex* has three to four cusps on the outer premaxillary teeth and five to seven cusps on the inner premaxillary teeth (Table 4.1).

No teeth are present on the maxilla, as is normal in alestids (Gery, 1977). A “paddle-like” maxilla, as described by Gery (1977, p. 18), is a common feature in Alestinae (subfamily *sensu* Roberts (1969) that includes all alestid genera with the exception of *Hydrocynus*) that distinguishes them from their New World counterparts, Characidae, and is found in all species examined here.

The dentary of *A. dentex* and *P. conserialis* is rectangular in shape in lateral view in comparison with *H. barnardi* (Fig. 4.5). Specimens of *H. barnardi* and *P. conserialis* have four multicuspid dentary teeth and no inner dentary tooth, in contrast to specimens of *A. dentex* that have four outer multicuspid dentary teeth and an inner symphyseal tooth. The multicuspid dentary teeth of *A. dentex* and *H. barnardi* bear three to five cusps, whereas *P. conserialis* has five to seven cusps on the dentary teeth. The teeth gradually decrease in size from anterior to posterior in all three species.

The anguloarticular of *H. barnardi* has a rounded anterodorsal projection with a rectangular anteroventral projection that extends across the posterior half of the dentary. In comparison, the anguloarticular of *A. dentex* and *P. conserialis* has multiple pointed projections extending across the posterior half of the dentary.

4.3.3 Opercular Bones

No distinguishable differences were observed in the shape of the bones of the opercular series or the corresponding sensory canals among examined species. Chapters 2 and 3 of this thesis describe the opercular bones in *H. barnardi* and *P. conserialis*, respectively.

4.3.4 Suspensorium

All specimens of *H. barnardi* (26.2 – 38.6 mm SL) retain cartilage along the dorsal edge of the hyomandibula, and smaller specimens (≤ 31.2 mm SL) also retain cartilage along the ventral edge of the hyomandibula. Specimens of both *A. dentex* and *P. conserialis* have cartilage along the dorsal edge of the hyomandibula. All specimens of *A. dentex* and *H. barnardi* have cartilage caps on the anterior and posterior ends of the symplectic, which is a long narrow bone, in contrast to larger specimens of *P. conserialis* (56.3 – 70.4 mm SL) that have a fully ossified symplectic. All specimens retain cartilage between the quadrate and metapterygoid and along the anterior edge of the palatine where it contacts the premaxilla.

4.3.5 Circumorbital Series

A notable difference among the three species is found in the circumorbital series. *Hemigrammopetersius barnardi* has lost the supraorbital bone, unlike *A. dentex* and *P. conserialis*, which both have a supraorbital (Fig. 4.6). *Alestes dentex* has a rounded supraorbital with pointed anterior and posterior ends and *P. conserialis* has a rectangular supraorbital. The antorbital of *H. barnardi* has rounded corners compared with the triangular antorbital observed in *A. dentex* and *P. conserialis*. Furthermore, *H. barnardi* only has two openings of the circumorbital sensory canal on the dermosphenotic (infraorbital 6), compared to the three present on the dermosphenotic of *A. dentex* and *P. conserialis. Petersius conserialis* also has a sensory canal opening between infraorbitals 4 and 5, which is not present in the other two species.

4.3.6 Branchial Arches and Pharyngeal Region

The presence of conical teeth on elements of the hyoid arch varies among species. Ceratobranchial 5 bears prominent teeth in all three species but only *A. dentex* and *P. conserialis* have teeth on the pharyngobranchials. *Alestes dentex* also has teeth on some epibranchials.

Cartilage remains present between the elements of the pharyngeal apparatus of *H. barnardi* (basihyal, basibranchials, hypobranchials, ceratobranchials, pharyngobranchials, and epibranchials). Small specimens of *A. dentex* and *P. conserialis* also retain cartilage between the elements of the pharyngeal apparatus. In contrast, larger specimens of *A. dentex* (55.8 mm SL) have fully ossified basibranchials and hypobranchials and larger specimens of *P. conserialis* (70.4 mm SL) have fully ossified basibranchials. All specimens retain cartilage between the posterior and anterior ceratohyals, the dorsal and ventral hypohyals, and on either end of the interhyal.

The urohyal in all species is tripartite in cross section, as described by Zanata and Vari (2005). The posterior edge of the urohyal is noticeably different among the species (Fig. 4.7). The urohyal of *P. conserialis* has a jagged posterior edge with two posteriorly positioned foramina visible in lateral view, unlike the smooth rounded posterior edge of the urohyal of *A. dentex* and *H. barnardi.* The urohyal of *H. barnardi* has a concave posterior edge, whereas the urohyal of *A. dentex* is expanded posterodorsally and the posteroventral corner is constricted anteriorly.

4.3.7 Paired Fins and Girdles

A long narrow posttemporal, with a dorsal projection, is present in all specimens. The supratemporal sensory canal runs the length of the posttemporal in *A. dentex* and *P. conserialis* but is restricted to the ventral corner of the posttemporal in *H. barnardi.* A long, ovoid supracleithrum has a distinct pointed dorsal projection in *A. dentex* and *P. conserialis*, compared with a more rounded dorsal projection in *H. barnardi*.

The dorsal- and anterior-oriented arms of the cleithrum in all three species forms a 90° angle opening anteriorly. The supratemporal sensory canal continues from the posttemporal to the supracleithrum and ventrally to the dorsal arm of the cleithrum. In *A. dentex*, the sensory canal does not continue onto the ventral, horizontal arm of the cleithrum, but in *H. barnardi* and *P. conserialis* the canal continues approximately halfway along the ventral arm. *Hemigrammopetersius barnardi* has two, small, circular postcleithra, whereas *A. dentex* and *P. conserialis* have three postcleithra. *Alestes dentex* and *P. conserialis* have a comparably larger, ovoid first postcleithrum than that of *H. barnardi*. Postcleithra 2 and 3 in specimens of *A. dentex* and *P. conserialis* are small, circular bones.

Alestes dentex and *H. barnardi* have one large dorsal concavity in the coracoid with a small foramen ventral to the concavity (Fig. 4.8). This is unlike *P. conserialis* that has two dorsal concavities in the coracoid and no foramen. The ventral edge of the mesocoracoid in *A. dentex* retain cartilage, whereas the mesocoracoid of *H. barnardi* and *P. conserialis* is fully ossified. The dorsal edge of the scapula in the juveniles of *A. dentex* (43.2 – 62.7 mm SL) and a smaller specimen of *P. conserialis* (60.9 mm SL) retains cartilage. The remainder of examined specimens of *P. conserialis* and all examined specimens of *H. barnardi* are fully ossified where the scapula contacts the coracoid.

The fin radials of the specimens of *A. dentex* and the smallest specimen of *P. conserialis* (40.9 mm SL) remain partly cartilaginous. The number of pectoral fin rays differs among examined specimens. All three species have one unbranched pectoral fin ray, but *H. barnardi* possesses eight to nine branched pectoral-fin rays, *A. dentex* has nine to ten branched pectoral-fin rays, and *P. conserialis* has 12 to 13 branched pectoral-fin rays (Table 4.2).

The general shape of the pelvic girdle is consistent among species, with the exception of the ischiac process. The left and right ischiac processes of *H. barnardi* contact each other anteriorly, in contrast to *A. dentex* and *P. conserialis* in which the ischiac processes do not touch one another (Fig. 4.9). The pelvic fin ray count is comparable among the species, with one unbranched fin ray and seven to nine branched fin rays (Table 2). All specimens of *A. dentex*

(43.2 – 62.7 mm SL), the smallest specimen of *H. barnardi* (26.2 mm SL), and smaller specimens of *P. conserialis* (40.9 – 60.9 mm SL) possess cartilage on the pelvic fin radials. Specimens of *A. dentex* have cartilage along the posterolateral edge of the pelvic girdle and smaller specimens of *P. conserialis* (40.9 – 60.9 mm SL) have cartilage along the pelvic splint.

4.3.8 Weberian Apparatus and Vertebral Column

The neural crest of *A. dentex* and *H. barnardi* retains cartilage along the ventral edge in smaller specimens (43.2 – 55.8 mm SL and 26.2 – 31.2 mm SL, respectively), with cartilage along the dorsal edge of the neural crest in one specimen of *H. barnardi* (31.2 mm SL). The tripus has cartilage along the dorsal edge in one specimen of *H. barnardi* (31.2 mm SL) and *P. conserialis* (60.9 mm SL). All other elements of the Weberian apparatus are fully ossified in specimens.

Different vertebral morphologies are observed in the different species (Fig. 4.10). Long prezygapophyses on the anterior vertebrae that gradually decrease in size and are substantially smaller on the caudal vertebrae are present in all specimens. However, *A. dentex* demonstrates exceptionally long prezygapophyses, with the anterior edge extending past the posterior edge of the preceding vertebra, compared with *H. barnardi* and *P. conserialis*, in which the anterior edge of the prezygapophysis does not reach anteriorly to extend past the posterior edge of the preceding vertebra.

The anterior ribs of all three species have a dorsal flange that gradually decreases in size posteriorly, becoming absent on the last three ribs. The forked epineurals of *A. dentex* begin immediately posterior to the skull and continue to preural 5. *Hemigrammopetersius barnardi* and *P. conserialis* have small thin epineurals that are not forked. The epineurals of *H. barnardi* begin on vertebra 9 or 10, and the epineurals of *P. conserialis* begin on vertebra 5, just posterior to the Weberian apparatus, both continue to preural 5. The epiplurals are associated with the haemal spines and cease at preural 5 in all specimens.

4.3.9 Dorsal and Anal Fins and Supports

The falcate dorsal and anal fins in the three species have few notable differences. Chapters 2 and 3 of this thesis describe these fins for *H. barnardi* and *P. conserialis*. Varying anal-fin ray counts are summarized in Table 2.

4.3.10 Caudal Fin and Skeleton

The major difference of the caudal skeleton among species was the degree of ossification (Appendix E). Epurals 2 and 3 have cartilage along the edges in all specimens of *H. barnardi* (26.2 – 38.6 mm SL). Only the distal ends of all three epurals in the smallest specimen of *A. dentex* (43.2 mm SL) and the smallest specimen of *P. conserialis* (40.9 mm SL) are cartilaginous. The remaining specimens of *A. dentex* possess cartilage on the distal end of epural 3, with epurals 1 and 2 being fully ossified. While specimens of *A. dentex* and *H. barnardi* have a long, narrow oval uroneural, the uroneural of *P. conserialis* changes with body size (as described in chapter 3 where smaller specimens have a small uroneural that progressively increases in size with an increase in body size).

4.4 Osteological Comparisons of Specimens to those Previously Described in the Literature

The comparisons made above among the three species of alestid display similarities and differences to other alestids previously described. The mesethmoid of *Alestes stuhlmanni* Pfeffer, described by Murray (2004), is comparable to the mesethmoid of *A. dentex* described here, with a single median posterior projection separating the left and right frontal in dorsal view (Murray, 2004:fig. 2; Fig 4.2). This is in contrast to the mesethmoids of *Hemigrammopetersius barnardi* and *Petersius conserialis*, which have three posterior projections. While most characiforms have a straight parasphenoid, Characidae and Alestidae generally have a parasphenoid that curves ventrally (Zanata & Vari, 2005), such as that figured for *A. dentex* and *H. barnardi* here (Fig. 4.3). *Petersius conserialis* has a straight parasphenoid. Zanata and Vari (2005) emphasized a difference of opinions in coding the curvature of the parasphenoid for the alestid genus *Hydrocynus* between Brewster (1986) and Murray and Stewart (2002), but overlooked the straight parasphenoid present in *P. conserialis* and coded it as ventrally depressed (their character 41).

The absence or reduction of the frontoparietal fontanelle is convergent throughout characiforms, making the absence or presence of the frontoparietal fontanelle a poor indicator of evolutionary relationships (Howes, 1982; Zanata & Vari, 2005). The extent of the frontoparietal fontanelle can vary within genera, as observed in *Alestes* (Vari, 1995).The three alestids here all have a frontoparietal fontanelle, despite previous studies describing the absence of the parietal fontanelle in *P. conserialis* (Myers, 1929; Poll, 1967; Gery, 1995). Zanata and Vari (2005) observed that the size of the frontoparietal fontanelle varies in at least some alestids depending on the stage of development. This is consistent with the described decrease in length and width of the frontoparietal fontanelle in *P. conserialis* (Chap. 3).

Dental features were used for the non-monophyletic tribal classification scheme for Alestidae presented by Hoedeman (1951). The juvenile specimens of *A. stuhlmanni* examined by Murray (2004) have unicuspid dentition (SL = 15.5 mm, CMN 81-0193 #5) that transitions to multicuspid dentition (SL ≥ 37.0 mm, CMN 81-0177 #11) as specimens grow. All examined specimens of *A. dentex* here have multicuspid dentition, possibly because all were larger than the *A. stuhlmanni* with unicuspid dentition examined by Murray (2004); whether or not smaller individuals of *A. dentex* have unicuspid dentition is unknown. The small-bodied alestids examined here all had multicuspid dentition, even in the smallest individuals. The recently described miniature alestid, *Bathyaethiops baka* Moritz and Schliewan, has comparably similar dentition to other small alestids (including those here), with two outer and four inner multicuspid premaxillary teeth and four outer multicuspid dentary teeth with no inner symphyseal tooth (Moritz & Schliewan, 2016). This differs from the miniature alestid, *Lepidarchus adonis* Roberts*,* and a small-bodied alestid, *Clupeocharax schoutedeni* Pellegrin*,* which have unicuspid dentition that are considered to be related to their small size (Roberts, 1966; Zanata & Vari, 2005). *Bathyaethiops flammeus* Moritz and Schliewan is a larger-bodied species that was described at the same time as *B. baka*, but has an inner symphyseal dentary tooth (Moritz & Schliewan, 2016). While Moritz and Schliewan (2016) provided only limited osteological descriptions for their new species, they did propose certain features in *B. baka* to be reductions correlated with their small size, such as the absence of an inner symphyseal tooth. The absence of an inner symphyseal dentary tooth is a potential independent reduction resulting from decreasing body size, as it is also observed in the smaller specie here, *H. barnardi* and *P. conserialis*.

The loss of bones in the circumorbital series is commonly reported in miniature Characiformes (e.g., Malabarba & Weitzman, 2003; Azevedo, 2010; Marinho, 2017), with small-bodied alestids as no exception (Zanata & Vari, 2005). *Hemigrammopetersius barnardi* provides an example of a small-bodied alestid that has lost the supraorbital. According to Zanata and Vari's (2005:fig. 43) phylogenetic hypothesis, loss of the supraorbital appears to have occurred in at least two clades (their clades 23 and 37). Frequent independent losses of circumorbital elements among characiform species associated with decreasing body sizes indicates caution must be exercised when using loss of circumorbital elements for determining broader evolutionary relationships.

Postcranial losses and reductions associated with decreasing body sizes are also described in alestids. For example, *H. barnardi* does not have a third postcleithrum. Zanata and Vari (2005) report the loss of the third postcleithrum in two other small alestid species, *C. schoutedeni* (a specimen with a SL = 29 mm) and *Rhabdalestes rhodesiensis* Ricardo-Bertram (a specimen with a SL = 57 mm reported by Zamba & Vreven, (2008)). The anterior portions of the ischiac processes of the pelvic girdle contact each other in *A. dentex* (Fig. 9); however, Zanata and Vari (2005) mentioned contact between the anterior portions of the ischiac processes in larger specimens of *A. dentex* that they examined (139.4 – 187.3 mm SL). This observed difference may occur because the pelvic processes are not yet fully ossified in the specimens I examined. Mattox *et al.* (2014) reports that the pelvic girdle is among the last bones to ossify in a basal characid.

Finally, a reduction to the laterosensory system is frequently reported in miniatures (Weitzman & Vari, 1988; Hanken & Wake, 1993). I observed reductions to the sensory canal system in *H. barnardi* in comparison with the larger-bodied alestids assessed. The supraorbital sensory canal does not extend onto the parietal and the anterodorsal branch of the dermosphenotic portion of the canal is lost in *H. barnardi*; this was also observed by Zanata and Vari (2005, p. 70 and appendix 2, respectively). *Hemigrammopetersius barnardi* has fewer openings of the supraorbital sensory canal in comparison to *A. dentex* and *P. conserialis* (Fig. 4.3) and also fewer than in *A. stuhlmanni* as figured in Murray (2004:fig. 2). The supratemporal sensory canal is also restricted to the ventral corner of the posttemporal in *H. barnardi* unlike the condition in *A. dentex* and *P. conserialis* in which the sensory canal extends across the length of the bone. These findings provide further support for the reduction of the laterosensory system and loss of bony elements that often accompanies a decrease in body size, or miniaturization in fishes (Weitzman & Vari, 1988).

4.4.1 Ontogenetic Osteological Comparisons

To the best of my knowledge no ossification sequence has been documented for a species of Alestidae. Ontogenetic development of ossification sequences has been reported in some characids (e.g., Bertmar, 1959; Vandewalle *et al.*, 2005; Walter, 2013; Mattox *et al.*, 2014, 2016) and these can be used to provide a foundation for future comparisons with other Characiformes. Almost all of these studies examined species of Characidae, with the exception of Bertmar's (1959) work on *Hepsetus odoe* (Bloch)*,* an African species in the family Hepsetidae, which focused on the embryological development of cranial cartilages. Mabee *et al.* (2000) reported little variation in the ossification sequence during early stages of development but found increased variation towards the end of development, suggesting that features that occur towards the end of development are most susceptible to heterochronic changes. In this section, I will use Mattox *et al.*'s (2014) extensive description of the skeletal development of *Salminus brasiliensis* (Cuvier)*,* a basal characid (maximum SL of 1000 mm), to compare with the observations I made above regarding the pattern of ossification in the examined alestids.

Mattox *et al.* (2014) reported postcranial, jaw, suspensorium, pharyngeal and posterior skull bones as the last to ossify, with the supraorbital being the last bone of the entire body to begin ossifying. The supraorbital is frequently lost in species of Characiformes (e.g., Malabarba & Weitzman, 2003; Azevedo, 2010; Marinho, 2017). This suggests that the loss of the supraorbital in *H. barnardi* may be due to developmental truncated development.

A later study assessing the osteology of skeletal elements in a miniature characid genus, *Priocharax*, by Mattox *et al.* (2016) found that *Priocharax* sp. (12.5 – 14.7 mm SL) was missing 18 bones throughout the body in comparison to *S. brasiliensis*, most of which developed later in ontogeny. For example, the loss of one of three postcleithra, suggesting that the loss of the third postcleithrum in *H. barnardi* is the result of truncation. Mattox *et al.* (2016) reported that particular laterosensory canals that are usually present in adult characids are not present in miniatures. The simplification of the laterosensory system described in *H. barnardi* in comparison with other larger-bodied alestids, supports the presence of minor developmental truncation due to a decreasing body size. Studies on the ossification sequences of alestids throughout ontogeny will be helpful in determining potential truncation that influences body size differences (Mattox *et al.*, 2014) and characters that result from decreasing adult body size.

4.5 Discussion

4.5.1 Dentition in Alestidae

Species of Alestidae exhibit a wide variety of dentition. This variation was previously used for classifying members of the family (Hoedeman, 1951; Poll, 1967; Gery 1995). Three tribes were proposed for Alestidae using dental characteristics: (i) Hydrocynini with caniniform teeth, (ii) Alestini with multicuspid teeth, and (iii) Petersiini with reduced multicuspid teeth (Paugy, 1990b) or an “absence of the pair of shoulders” on their teeth (Gery, 1995, p. 39). This classification scheme has since been shown to be artificial due to the lack of support for each tribe based on cladistic studies (e.g., Murray & Stewart, 2002; Zanata & Vari, 2005; Arroyave & Stiassny, 2011).

4.5.1.1 Variation in Dentition

Most alestids have tri- or multicuspid teeth (Zanata & Vari, 2005). Unicuspid teeth are thought to be secondarily derived in the genus *Hydrocynus* (Brewster, 1986). Small-bodied and miniature species, such as *Clupeocharax* and *Lepidarchus,* also have unicuspid teeth; however, these are likely a reduction caused by their small size of the multicuspid teeth found in closely related taxa (Roberts, 1966; Murray & Stewart, 2002; Zanata & Vari, 2005).

The variation observed among and within alestid species with multicuspid dentition has presented problems with classification beyond the artificial tribal scheme. For example, two petersiin genera, *Alestopetersius* and *Duboisialestes*, were recently synonymized by Munene and Stiassny (2012). Having originally been separated by Poll (1967) using dental morphology, Munene and Stiassny (2012) noted that no modern phylogenetic analysis has yet to produce a monophyletic grouping of the species of *Alestopetersius* because *Dubioisialestes* is continually nested within *Alestopetersius* (e.g., Zanata & Vari, 2005; Arroyave & Stiassny, 2011).

Beyond variation in tooth morphology, variation has also been reported among species in the spacing of teeth. Poor spacing between the inner and outer premaxillary tooth rows of *Hemigrammopetersius barnardi* make it difficult to clearly distinguish between the two rows.

Zanata and Vari (2005) described this in a clade of smaller-bodied alestids, containing genera *Hemigrammopetersius, Virilia,* and *Rhabdalestes*. Larger-bodied alestids, such as *Alestes dentex* and *Petersius conserialis*, have two clearly distinguished tooth rows on the premaxilla, with the exception of the three rows described in *Bryconalestes* (Zanata & Vari, 2005). A high amount of variation in tooth morphology, number of teeth and their placement is reported throughout alestids and caution should be used when assessing dental characters for the purpose of determining evolutionary relationships.

4.5.1.2 Ancestral Dental Condition

Both multicuspid (e.g., Myers, 1958) and unicuspid (e.g., Lawson & Manly, 1973; Fink & Fink, 1981) teeth have been hypothesized as primitive in characiforms. Overwhelming support for unicuspid teeth as the primitive condition in alestids has since emerged. Roberts (1967, 1969) described the multicuspid teeth found in Alestidae to be composed of single conical elements. Studies assessing juvenile alestids have provided further support for this. Brewster's (1986) study on *Hydrocynus* found small, juvenile specimens to have conical teeth that later fused into tricuspid dentition (with the middle cusp later overtaking the other two resulting in secondarily-derived unicuspid dentition). Murray (2004) described juvenile specimens of *A. stuhlmanni* with unicuspid teeth (SL ≤ 15.5 mm) that later develop into multicuspid teeth with growth (SL ≥ 37.0 mm).

The unicuspid dentition described in the miniature alestid, *Lepidarchus*, and the small alestid, *Clupeocharax*, is likely due to their small size (e.g., Poll, 1967; Gery, 1995; Zanata & Vari, 2005). It has been suggested that the reduced multicuspid dentition observed in petersiins – the absence of “shoulders”, lack of labio-lingual thickening, and the absence of inner symphyseal dentary teeth – may be the result of a decrease in body size and not indicative of relatedness (Gery, 1995).

4.5.2 Miniaturization

Miniaturization is hypothesized to have independently evolved at least twice in Alestidae, as well as gigantism (Hubert *et al.*, 2005; Zanata & Vari, 2005), thus it is an interesting group in which to study the evolution of pronounced body size differences. In their evaluation of South American miniatures, Weitzman and Vari (1988) also estimated the number of miniature African fishes, including two species of Alestidae, *Lepidarchus adonis* and *Micralestes pabrensis* (Roman), previously classified within the genus *Virilia*. Conway and Moritz (2006) established the first list of miniature African species, but only list a single alestid, *L. adonis*, because they meticulously followed Weitzman and Vari's (1988) criterion that miniatures do not exceed 26 mm SL and *V. pabrensis* had since been documented to reach a maximum of 52 mm SL (Paugy, 1990a). However, *V. pabrensis* still meets the second criterion of Weitzman and Vari's (1988) arbitrary definition and reaches sexual maturity at 18 mm SL (Zanata & Vari, 2005, p. 2). One new miniature alestid has been described since the release of Conway and Moritz's (2006) list, *Bathyaethiops baka* Moritz and Schliewan, bringing the number to a total of three miniature alestids. Only a few morphological losses and reductions are reported in miniature alestids; hence, they are designated as proportional dwarfs.

In order to assess potential losses and reductions of osteological features associated with decreasing body size, a phylogenetic framework is required. Previously proposed phylogenetic hypotheses of Alestidae – that include miniature species – suggest at least two independent miniaturization events (Hubert *et al.*, 2005; Zanata & Vari, 2005). The phylogenetic tree of Zanata and Vari's (2005:Fig. 43) has the most extensive species coverage (including two of three miniature species) and uses morphological characters to help assess potential reduced or absent features identified in other alestid specie, therefore, it is used here. The use of molecular trees to trace morphological features or plot body size to confidently establish body size decreases would be beneficial in future studies. Zanata and Vari's (2005:Fig. 43) most parsimonious tree (simplified in Fig. 4.11 here) suggests two independent miniaturization events (clades 23 and 37). The species most closely related to the two miniatures included in Zanata and Vari's (2005) tree, *Lepidarchus adonis* and *V. pabrensis* (i.e., *Ladigesia, Tricuspidalestes, Clupeocharax, Hemigrammopetersius* and *Rhabdalestes*), demonstrate progressive reductions such as having an incomplete lateral line or an absence of cranial skeletal elements. *Hemigrammopetersius barnardi*, whose morphology I describe in chapter 2, is closely related to the miniature *V. pabrensis* according to Zanata and Vari’s (2005) analysis (clade 23) and presents some reduced features potentially due to a decreasing body size. The loss of the supraorbital and reductions in the laterosensory system I observed in *H. barnardi* are also reported in closely related genera (i.e., *Rhabdalestes* and *Virilia*) according to Zanata and Vari's (2005: Fig. 43) phylogenetic tree. This suggests that features that develop towards the end of development are influenced by truncation and are apparent in both small-bodied alestids and miniatures.

4.5.2.1 Miniaturization in Alestidae

A goal of my thesis was to assess the effect of small size on morphological features. Due to specimen availability I did not have the opportunity to examine true miniatures according to Weitzman and Vari's (1988) definition. However, *H. barnardi* was an excellent species to examine and compare to juvenile alestids that reach a larger size because it exhibits select reductions and bone losses commonly found in miniatures and is a close relative to a true miniature according to Zanata and Vari's (2005) phylogenetic hypothesis These include the loss of the supraorbital, postcleithrum 3, reduced complexity of the laterosensory system, and fewer intermuscular bones in comparison with larger alestids. These reported losses and reductions are also present in the true miniature *V. pabrensis* from the same clade (Zanata & Vari, 2005, clade 23). True miniatures in Alestidae are described with increased osteological losses and reductions (e.g., *L. adonis* has lost the antorbital, supraorbital, third to sixth infraorbitals, nasal, intercalar, extrascapular, and postcleithrum 1) compared to close smaller-bodied relatives. The bones most frequently lost or reduced in miniature and small species are those that develop towards the end of development, suggesting developmental truncation influences these reductions (Mattox *et al.*, 2014, 2016).

Incomplete lateral lines and simplified laterosensory systems are commonly reduced in miniatures. I found a reduction to the laterosensory system of the small-bodied alestid, *H. barnardi*. The reduction of the laterosensory system progressively increases in closely related fish according to Zanata and Vari's (2005) phylogenetic hypothesis, with *V. pabrensis* exhibiting even less development of the laterosensory system in comparison to *H. barnardi*.

Miniature alestids are proportional dwarfs because the described morphological losses and reductions are limited in comparison with the high numbers reported in developmentally truncated teleosts (e.g., Britz & Conway, 2009; Mattox *et al.*, 2014). The following sections will consider the functional limitations of miniaturization and potential advantages of being small for teleosts in general.

4.5.2.2 Limits of Miniaturization in Fishes

Mattox *et al.* (2016) discussed the developmental truncation of the characid, *Priocharax* sp. In comparison with other characids, *Priocharax* sp. is missing 18 of 147 bones described in *S. brasiliensis*, most of which ossify at the end of ontogeny (Mattox *et al.*, 2016). Other developmentally truncated miniature teleosts have been described with even more bone losses than those reported in *Priocharax* sp. For example, *Paedocypris* sp., a miniature cyprinid, is hypothesized to represent the smallest possible size range (10 – 12 mm SL) for an adult vertebrate (Britz & Conway, 2009), with 41 bones either lost or remaining cartilaginous. Even with the high level of developmental truncation, the Weberian apparatus of *Paedocypris* is relatively large compared to the rest of the skeleton, suggesting a lower size limit to its functionality (Britz & Conway, 2009). While certain bones of the Weberian apparatus are reduced (the intercalarium and the claustrum, which are those reported to be altered in other small Cypriniformes, (Bird and Hernandez, 2007)) the bones that are key in sound transmission, such as the tripus, which detects initial sound-pressure waves, are not reduced in size (Britz & Conway, 2009).

Due to biological differences across different species it is difficult to establish a precise definition or a critical size for miniaturized species (Hanken & Wake, 1993). This makes definitively establishing the limits of miniaturization difficult. Conway *et al.* (2017) states that anatomical changes due to miniaturization remain poorly studied and contribute to ambiguous conclusions regarding the influence of miniaturization on morphology. In contrast, numerous ideas have been proposed regarding the evolutionary advantages for miniaturization and small-body sizes in fish.

4.5.2.3 Why be Small? Potential Adaptive Advantages of Miniaturization in Fishes

Ecological interactions play a paramount role in most theories on the evolution of small body sizes in fishes. Small taxa require fewer resources to maintain their metabolic rate (Peters, 1992; Brandl *et al.*, 2018). This allows small and miniature species to take advantage of low resource environments that would not support larger taxa (Peters, 1992). For example, small-bodied fishes may take advantage of food resources that are unavailable to larger fishes or other organisms (Castro, 1999; Brandl *et al.*, 2018).

The capacity to inhabit physically smaller niches may reduce competition or promote predator avoidance (Yeh, 2002; Brandl *et al.*, 2018; Bloom *et al.*, 2020). Small fishes are often reported in complex ecosystems with slow-flowing waters (Weitzman & Vari, 1988; Castro, 1999). Weitzman and Vari (1988) discussed how acidic waters in South America may lead to the reduction of the laterosensory system in miniatures, and report that most small-bodied and miniature fish are found in slow-flowing shallow waters as they would likely struggle in fast-moving currents. Being small would allow species to hide in small places that are unreachable by larger predators (Castro, 1999). Alternatively, the energy a predator may have to spend in pursuing a small or miniature fish may not be cost effective (Miller, 1994).

Finally, small species generally produce more offspring in shorter periods of time, have early sexual maturity and the ability to rapidly occupy new habitats or those that were reduced due to environmental fluctuations (Gould, 1977; Castro, 1999; Yeh, 2002; Azevedo, 2010). Although variation is observed in the reproductive strategies of small fish (Azevedo, 2010), the ability to quickly reproduce would allow small-bodied fishes to quickly occupy new ecosystems, such as floodplains or streams (Castro, 1999).

A combination of rapid-reproductive strategies, decreased predation, and the ability to exploit smaller niches and environments with fewer resources has likely contributed to the success of small-bodied fish. In comparison with South American miniatures, the habitat and ecology of many alestids is still poorly understood. For the alestid species that have been assessed in my thesis, *H. barnardi* resides in the weedy areas of lakes and affluent rivers (Konings *et al.*, 2018), whereas *A. dentex* resides along lake shores and in the lower reaches of rivers (Akinyi *et al.*, 2010). Although Hanssens & Snoeks (2006) reported that no habitat information is available for *P. conserialis*, Copley (1958) indicated they are found in shoals and shallow, faster-flowing water. In general, small-bodied alestids have been documented to use floodplains to spawn, allowing them to escape predation of larger fish that do not occupy these environments (IUCN, 2020). The use of temporary water bodies like floodplains for spawning selects for rapid-reproductive strategies that are reported in smaller fish and supports the concept that small fish can quickly inhabit new environments with potentially limited resources (Castro, 1999).

4.5.3 Conclusion

I found that developmental truncation results in the loss of select features in small-bodied alestids. These include modifications in dentition, reductions to the laterosensory system, and a loss of bony elements in the circumorbital series and pectoral girdle. Therefore, caution should be exercised when using these features, or features that develop late in development, for indicating evolutionary relationships as they are likely to be the first features that are truncated with a decreasing body size.

4.6 Tables

Table 4.1. Comparison of tooth and cusp counts for examined species.

	Premaxilla Outer Row Number of		Premaxilla Inner Row Number of		Dentary Outer Row Number of		Dentary Inner Row Number of	
	Teeth	Cusps	Teeth	Cusps	Teeth	Cusps	Teeth	Cusps
Alestes dentex	3	3-4	4	5-7	4	3-5	1	1
Hemigrammopetersius barnardi	2	3	4	3-5	4	3-5	0	-
Petersius conserialis	2	3	4	5-7	4	5-7	0	-

Table 4.2. Comparison of fin ray count for examined species.

	Sample size	Pectoral-fin rays		Pelvic-fin rays		Dorsal-fin rays		Anal-fin rays	
		Unbranched	Branched	Unbranched	Branched	Unbranched	Branched	Unbranched	Branched
Alestes dentex	3	1	10	1	8	2	8	3	24 – 27
Hemigrammopetersius barnardi	156	1	8 – 9	1	7 - 8	2	7 - 8	3	15 – 18
Petersius conserialis	14	1	12 - 13	1	8 - 9	2	8	2	18 - 20

4.7 Figures

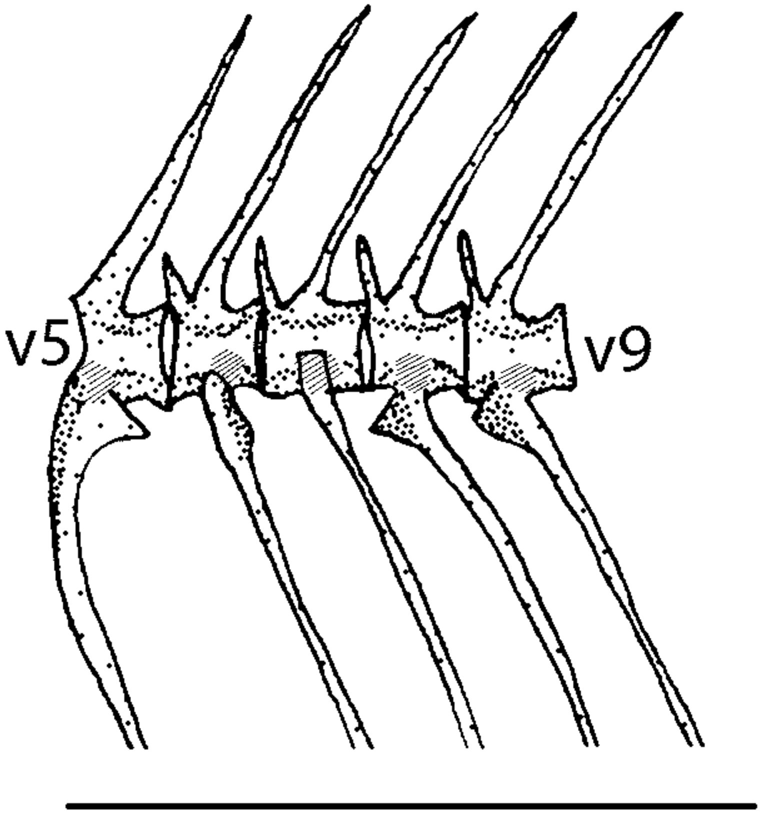

Figure 18. Drawing of vertebrae 5 – 9 of *Alestes dentex* USNM 229863, specimen number 4, SL = 43.2 mm. Smallest examined specimen of *A. dentex* with cartilage still present where ribs attach to vertebrae. Hatching represents cartilage. Scale bar = 5 mm.

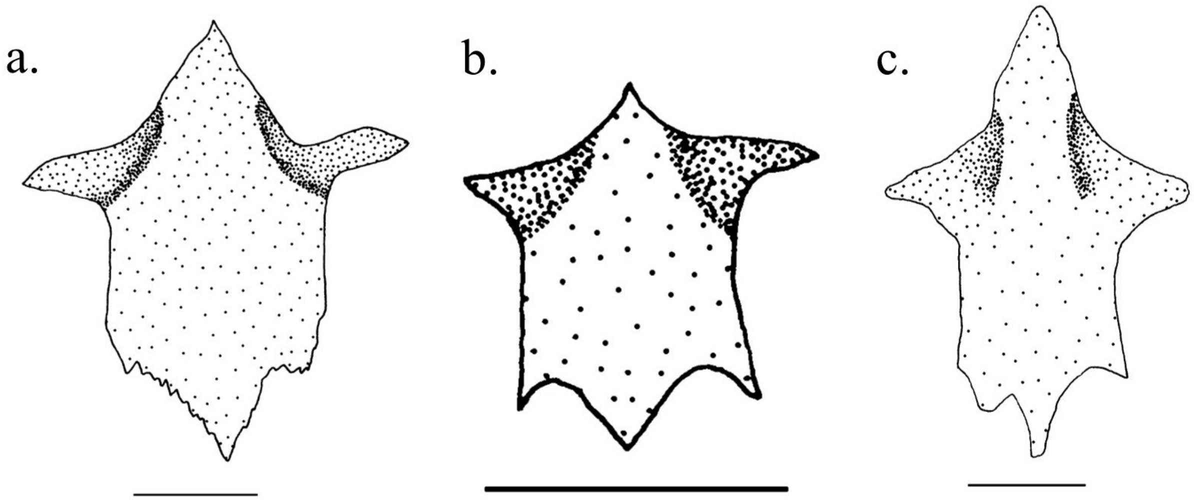

Figure 4.2. Drawing of the mesethmoid of (a) *Alestes dentex* USNM 229863, specimen number 5, SL = 55.8 mm, (b) *Hemigrammopetersius barnardi*, CMN F 81-0188, specimen number 106, SL = 31.2 mm, and (c) *Petersius conserialis* CMN F 81-0187, specimen number 1, SL = 56.3 mm in dorsal view. Scale bar = 1 mm.

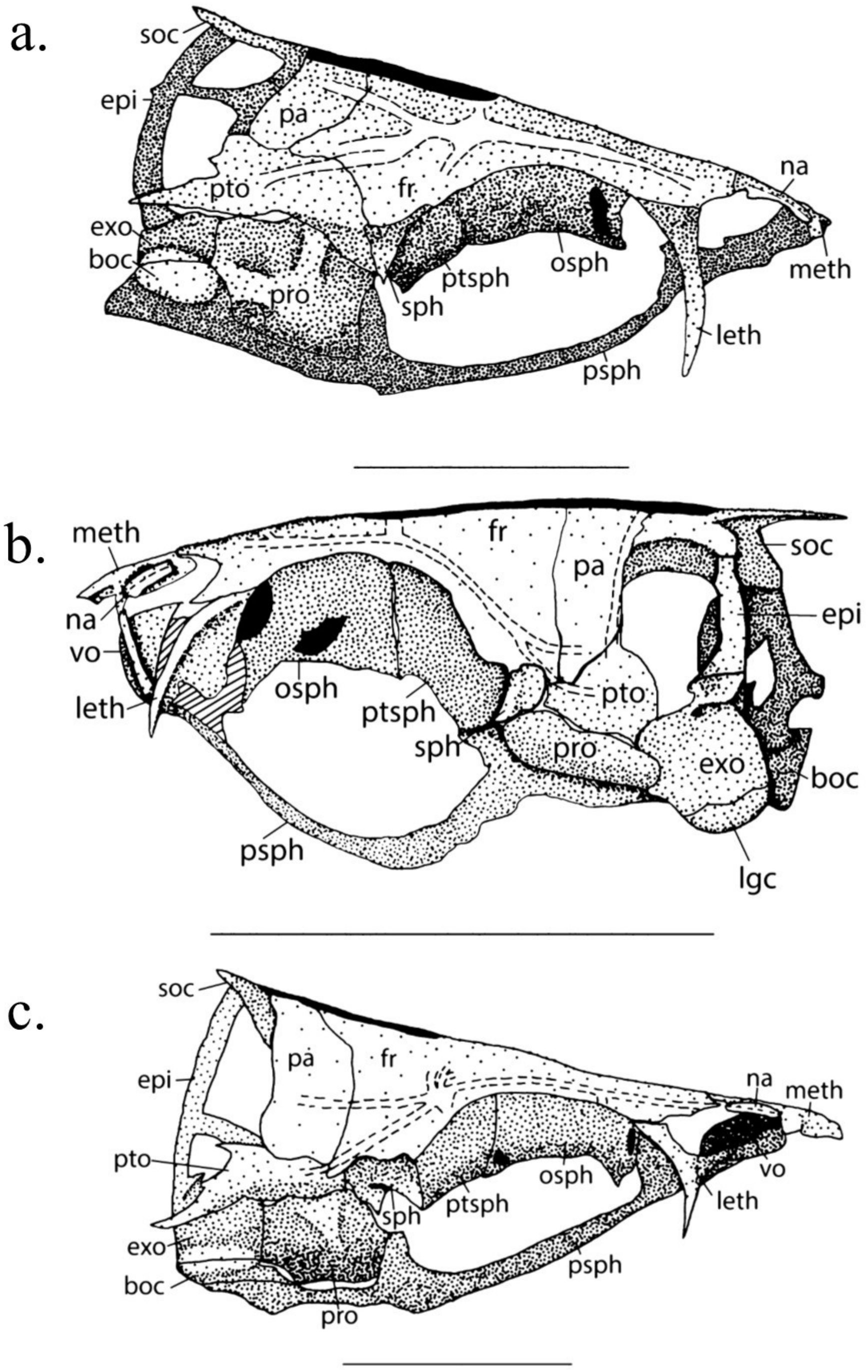

Figure 19. Drawing of the skull of (a) *Alestes dentex* USNM 229863, specimen number 5, SL = 55.8 mm, (b) *Hemigrammopetersius barnardi*, CMN F 81-0188, specimen number 106, SL = 31.2 mm, and (c) *Petersius conserialis* CMN F 81-0187, specimen number 1, SL = 56.3 mm in lateral view. Hatching represents cartilage. Scale bar = 5 mm.

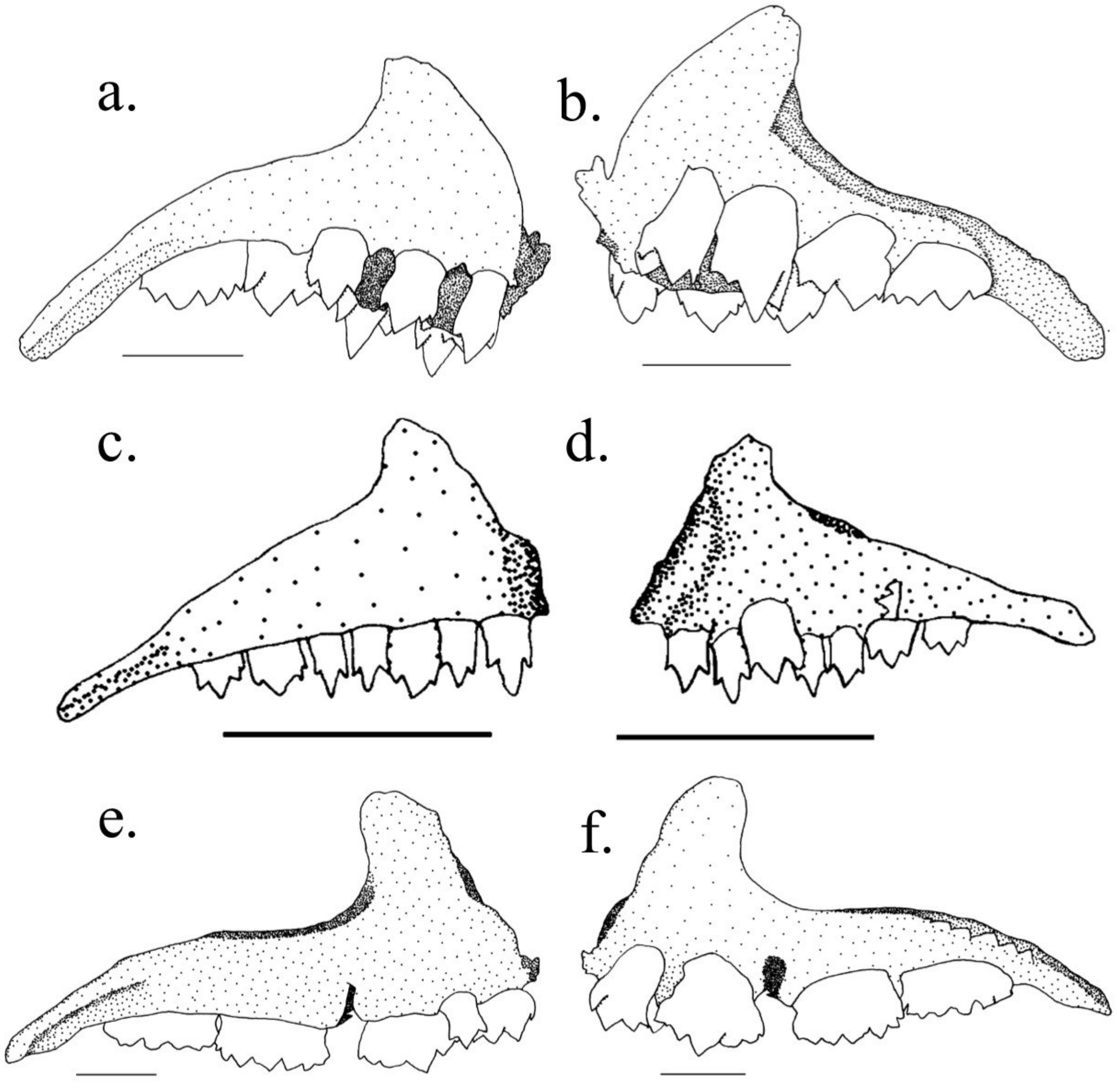

Figure 20. Drawing of the right premaxilla of *Alestes dentex* USNM 229863, specimen number = 2, in (a) lateral and (b) medial views; right premaxilla of *Hemigrammopetersius barnardi* CMN F 81-0188, specimen number = 106, SL = 31.2 mm, in (c) lateral and (d) medial views; right premaxilla of *Petersius conserialis* CMN F 81-0187, specimen number = 1, in (e) lateral and (f) medial views. Scale bar = 1 mm.

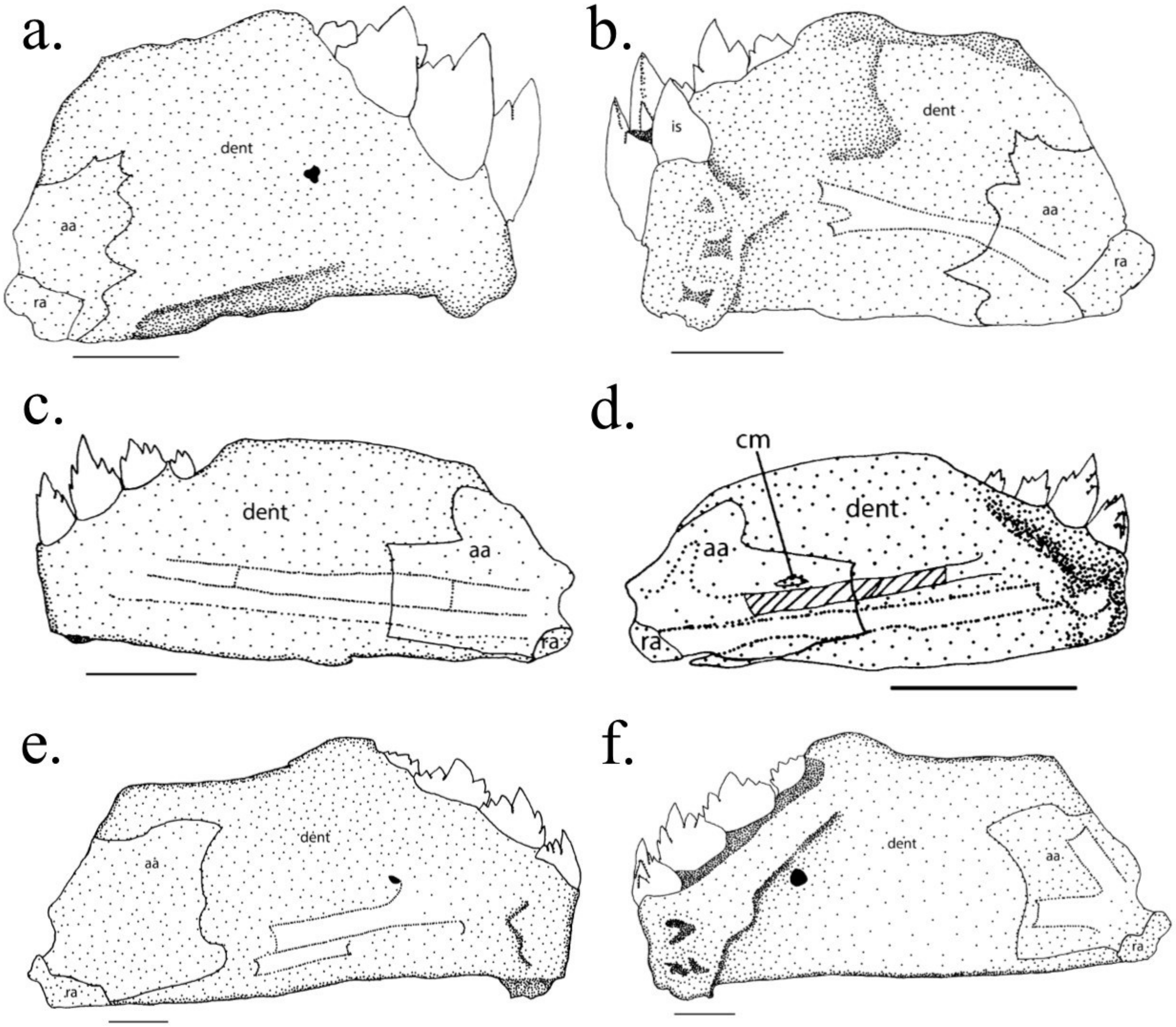

Figure 215. Drawing of the right dentary of *Alestes dentex* USNM 229863, specimen number = 2, in (a) lateral and (b) medial views; left dentary of *Hemigrammopetersius barnardi* CMN F 81-0188, specimen number = 106, SL = 31.2 mm, in (c) lateral and (d) medial views; right dentary of *Petersius conserialis* CMN F 81-0187, specimen number = 1, in (e) lateral and (f) medial views. Hatching represents cartilage. Scale bar = 1 mm.

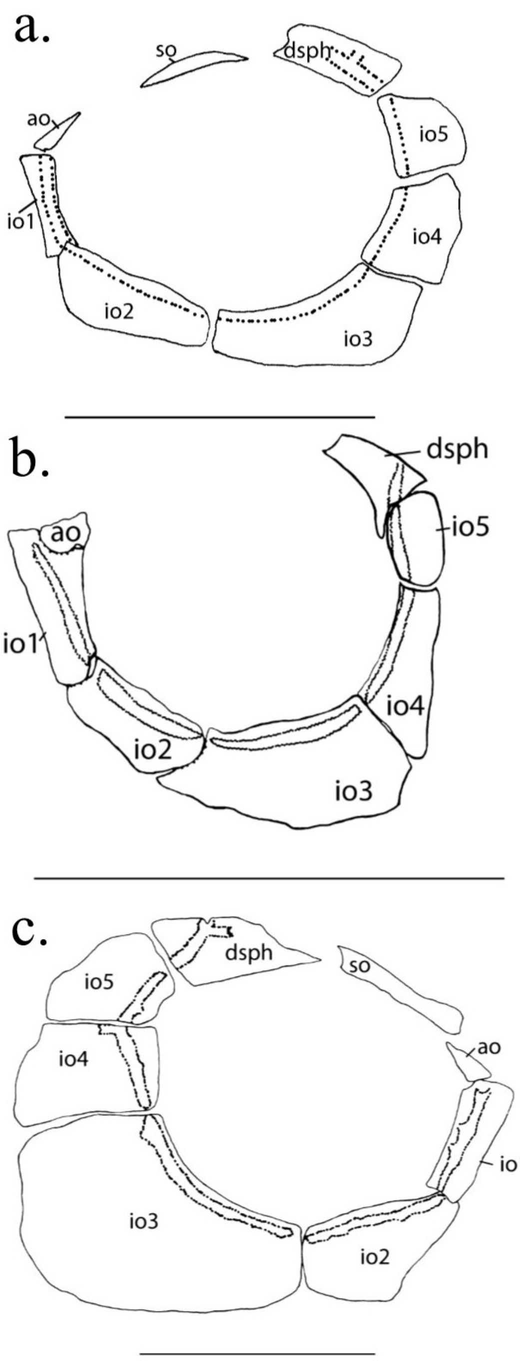

Figure 22. Drawing of the (a) left circumorbital series of *Alestes dentex* USNM 229863, specimen number 4, SL = 43.2 mm, (b) left circumorbital series of *Hemigrammopetersius barnardi* CMN F 81-0188, specimen number 4, SL = 32.7 mm, (c) right circumorbital series of *Petersius conserialis* CMN F 81-0187, specimen number 1, SL = 56.3 mm. Scale bar = 5 mm.

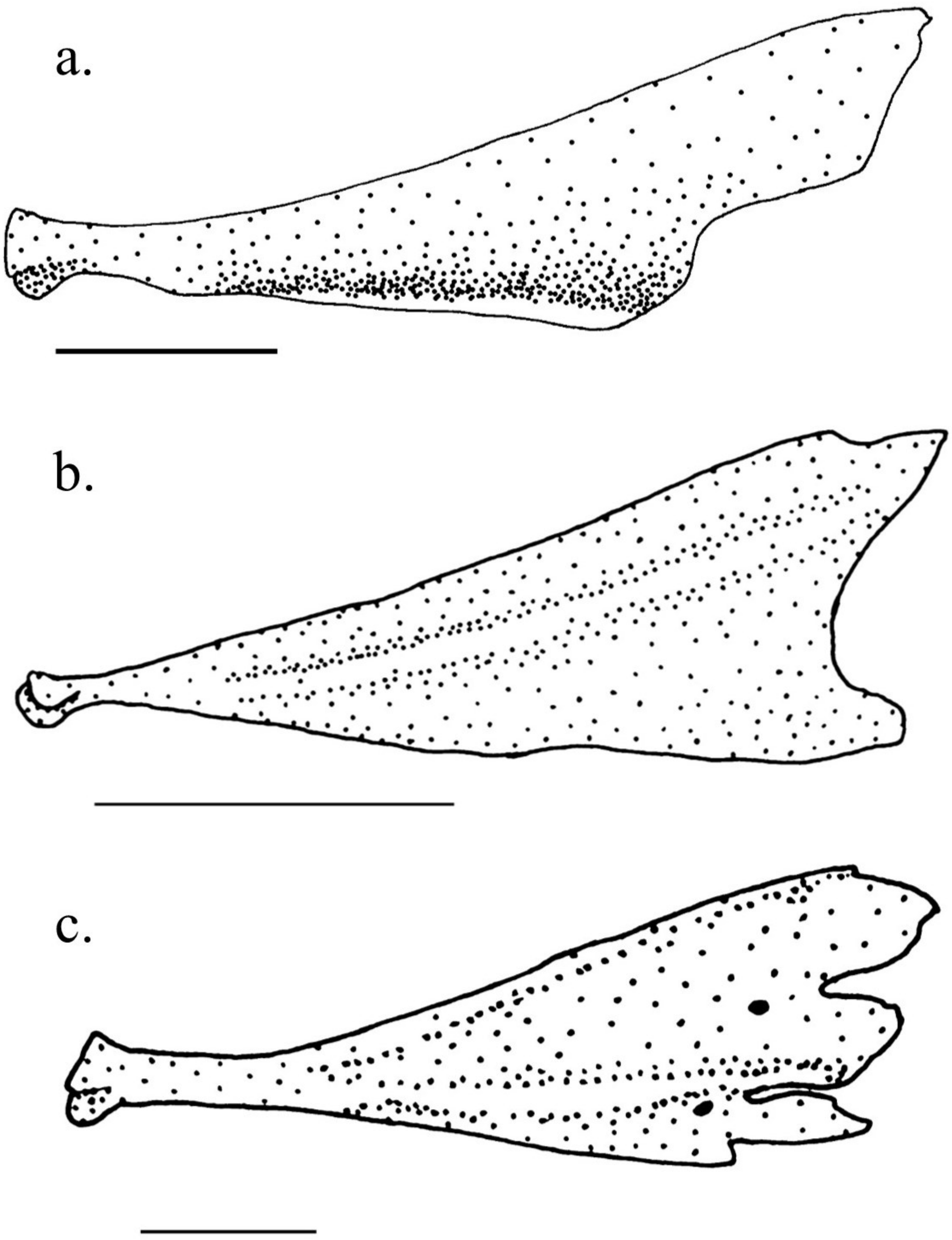

Figure 23.7. Drawing of the urohyal of (a) *Alestes dentex* USNM 229863, specimen number 5, SL = 55.8 mm, (b) *Hemigrammopetersius barnardi* CMN F 81-0188, specimen number = 106, SL = 31.2 mm, and (c) *Petersius conserialis* CMN F 81-0187, specimen number = 1, SL = 56.3 mm. Scale bar = 1 mm.

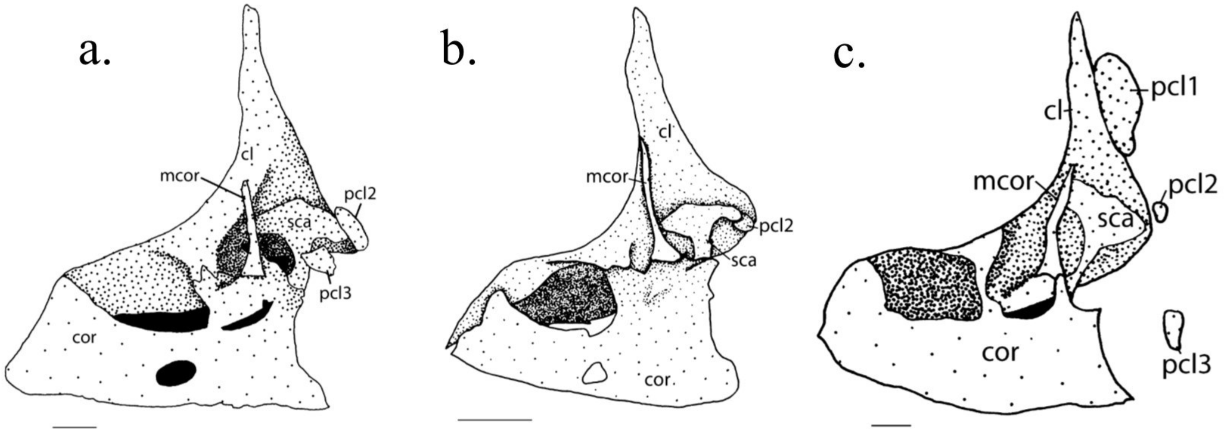

Figure 24. Drawing of the right median pectoral girdle of (a) *Alestes dentex* USNM 229863, specimen number = 5, SL = 55.8 mm, (b) *Hemigrammopetersius barnardi* CMN F 81-0188, specimen number = 106, SL = 31.2 mm, (c) *Petersius conserialis* CMN F 81-0187, specimen number = 1, SL = 56.3 mm. Scale bar = 1 mm.

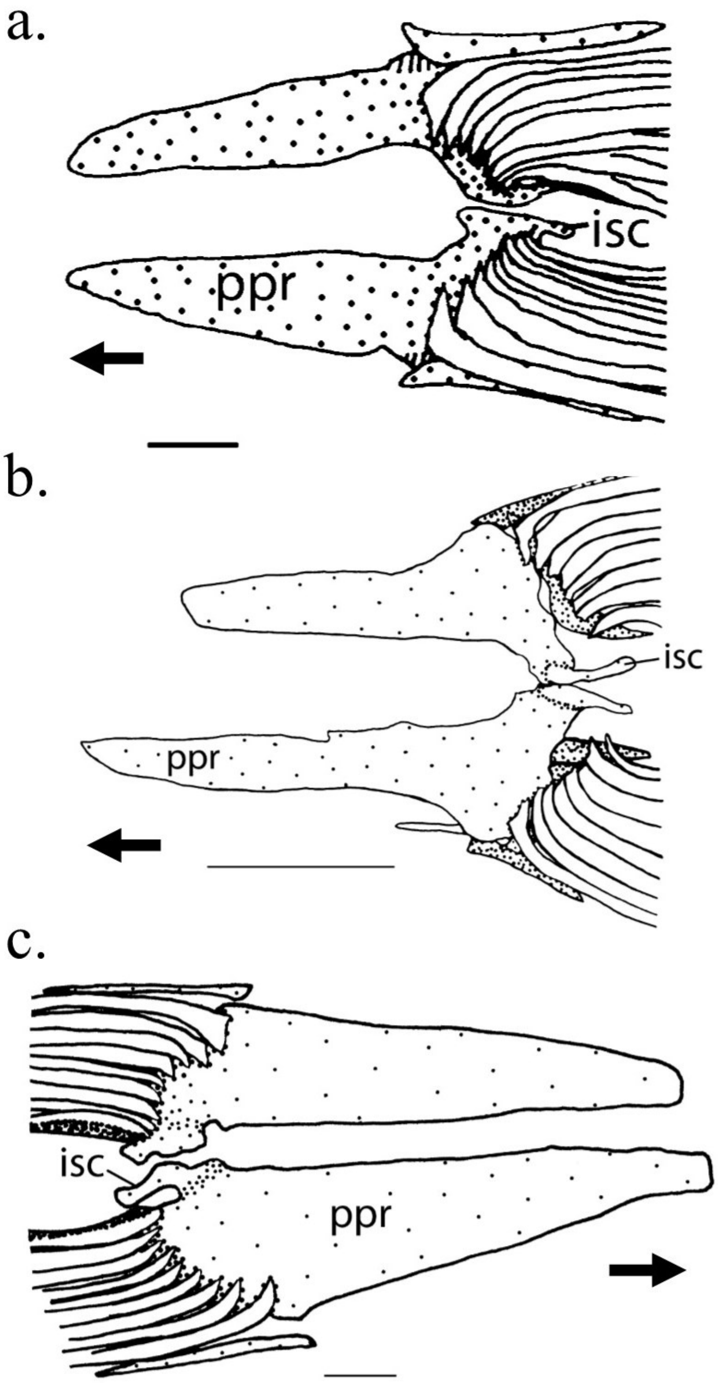

Figure 25. Drawing of the ventral pelvic girdle of (a) *Alestes dentex* USNM 229863, specimen number = 6, SL = 62.7 mm, (b) *Hemigrammopetersius barnardi* CMN F 81-0188, specimen number = 106, SL = 31.2 mm, (c) *Petersius conserialis* CMN F 81-0193, specimen number = 15, SL = 60.9 mm. Scale bar = 1 mm. Arrows point anterior.

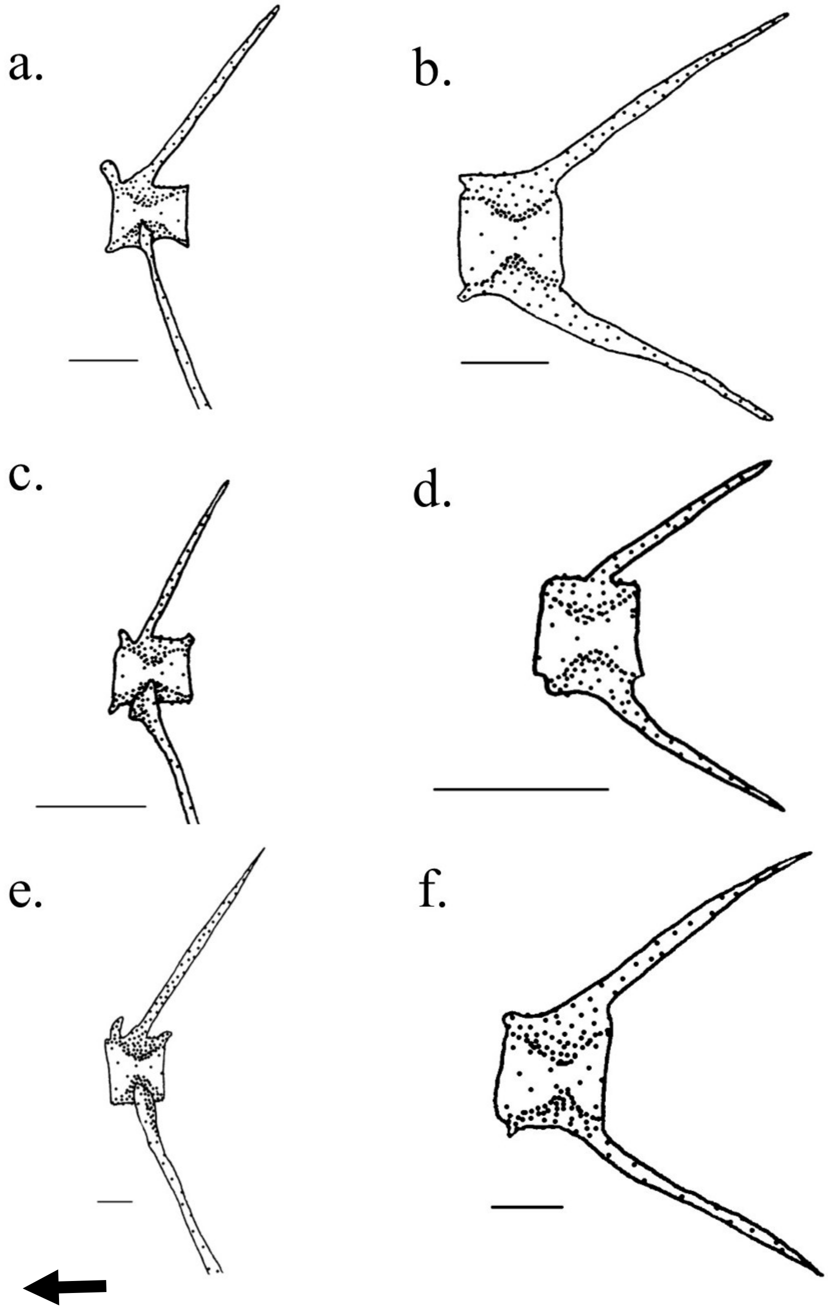

Figure 26. Drawing of the sixth abdominal vertebra (a, c, e) and fourth preural vertebra (b, d, f) of (a, b) *Alestes dentex* USNM 229863, specimen number = 6, SL = 62.7 mm, (c, d) *Hemigrammopetersius barnardi* CMN F 81-0188, specimen number = 3, SL = 26.2 mm, (e, f) *Petersius conserialis* CMN F 81-0187, specimen number = 2, SL = 70.4 mm. Scale bars = 1 mm. Arrow points anterior.

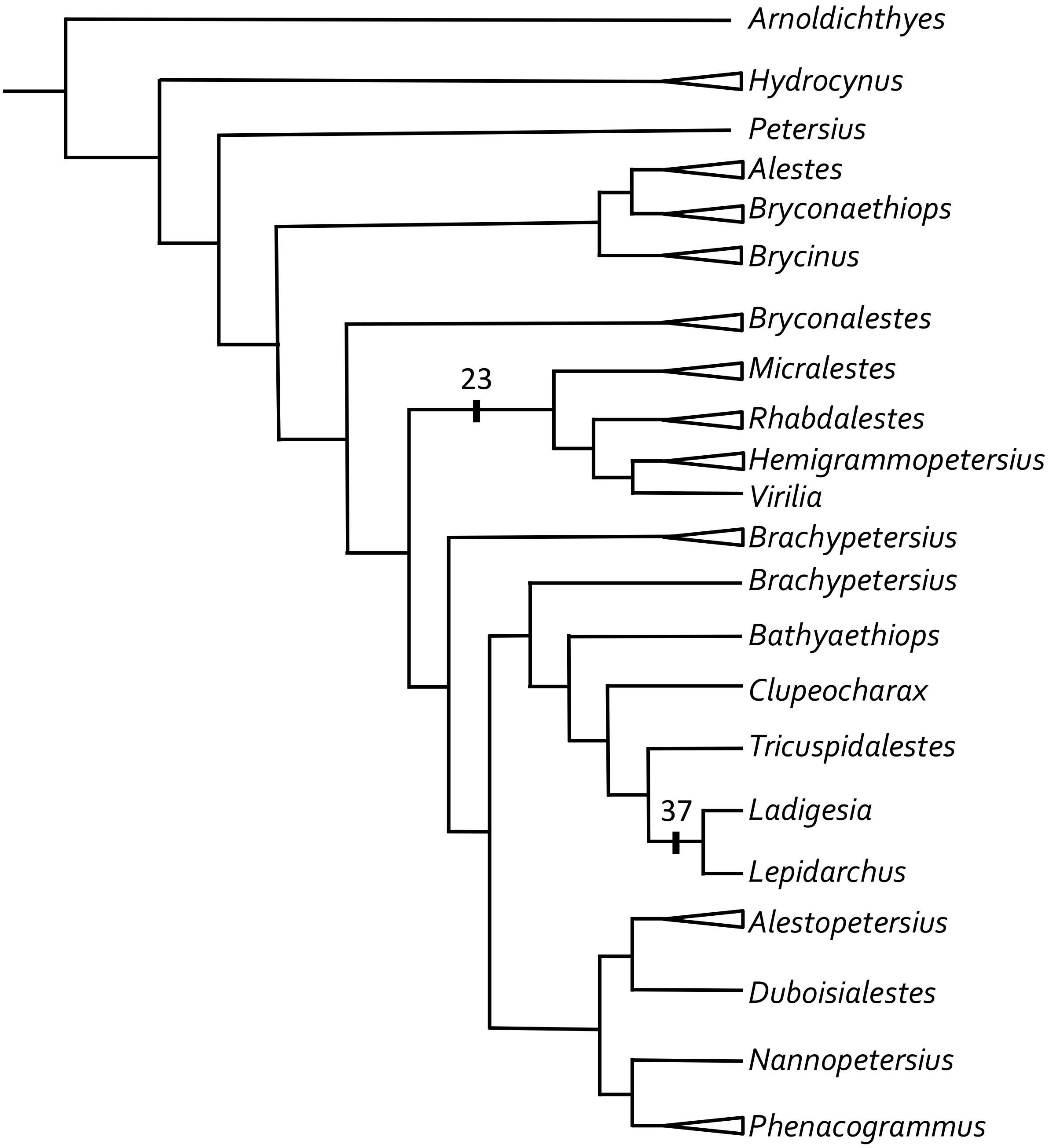

Figure 4.11. Phylogenetic hypothesis of Alestidae modified from Zanata and Vari (2005). Clades 23 and 37 from Zanata and Vari's (2005) phylogenetic tree are indicated on the tree by their representative numbers.

4.8 References

Akinyi, E., Azeroual, A., Entsua-Mensah, M., Getahun, A., P., L., & Twongo, T. (2010). *Alestes dentex*. The IUCN Red List of Threatened Species. Retrieved from https://www.iucnredlist.org/species/182128/7810513

Arroyave, J., & Stiassny, M. L. J. (2011). Phylogenetic relationships and the temporal context for the diversification of African characins of the family Alestidae (Ostariophysi: Characiformes): Evidence from DNA sequence data. *Molecular Phylogenetics and Evolution, 60*(3), 385-397.

Azevedo, M. A. (2010). Reproductive characteristics of characid fish species (Teleostei, Characiformes) and their relationship with body size and phylogeny. *Iheringia Serie Zoologia, 100*(4), 469-482.

Bertmar, G. (1959). On the ontogeny of the chondral skull in Characidae, with a discussion on the chondrocranial base and the visceral chondrocranium in fishes. *Acta Zoologica*, 203 - 364.

Bird, N. C., & Hernandez, L. P. (2007). Morphological variation in the Weberian apparatus of Cypriniformes. *Journal of Morphology*, *268*(9), 739-757.

Bloom, D. D., Kolmann, M., Foster, K., & Watrous, H. (2020). Mode of miniaturisation influences body shape evolution in New World anchovies (Engraulidae). *Journal of Fish Biology, 96*(1), 194-201.

Brandl, S. J., Goatley, C. H. R., Bellwood, D. R., & Tornabene, L. (2018). The hidden half: ecology and evolution of cryptobenthic fishes on coral reefs. *Biological Reviews of the Cambridge Philosophical Society, 93*(4), 1846-1873.

Brewster, B. (1986). A review of the genus *Hydrocynus* Cuvier 1819 (Teleostei: Characiformes). *Bulletin of the British Museum Natural History (Zoology), 50*(3), 163-206.

Britz, R., & Conway, K. W. (2009). Osteology of *Paedocypris*, a miniature and highly developmentally truncated fish (Teleostei: Ostariophysi: Cyprinidae). *Journal of Morphology, 270*(4), 389-412.

Carnevale, G. (2008). Miniature deep-sea hatchetfish (Teleostei : Stomiiformes) from the Miocene of Italy. *Geological Magazine, 145*(1), 73-84.

Castro, R. M. C. (1999). Evolucao da ictiofauna de riachos Sul-Americanos: Padroes gerais e possiveis processos causais. In R. Mazzoni & P. R. Peres-Neto (Eds.), *Ecologia de Peixes de Riachos* (Vol. 6, pp. 139-155). Rio de Janeiro, Brazil.

Conway, K. W., Kubicek, K. M., & Britz, R. (2017). Morphological novelty and modest developmental truncation in *Barboides*, Africa's smallest vertebrates (Teleostei: Cyprinidae). *Journal of Morphology, 278*(6), 750-767.

Conway, K. W., & Moritz, T. (2006). *Barboides britzi*, a new species of miniature cyprinid from Benin (Ostariophysi : Cyprinidae), with a neotype designation for *Barboides gracilis*. *Ichthyological Exploration of Freshwaters, 17*(1), 73-84.

Copley, H. (1958). *Common freshwater fishes of East Africa*. H. F. & G. Witherby LTD, 5 Warwick Court London.

da Graca, W. J., Ota, R. R., & Domingues, W. M. (2019). A new species of miniature *Characidium* (Characiformes: Crenuchidae) from the upper Rio Paraguay basin, Mato Grosso state, Brazil. *Journal of Fish Biology, 95*(6), 1480-1485.

De Santana, C. D., & Crampton, W. G. R. (2011). Phylogenetic interrelationships, taxonomy, and reductive evolution in the Neotropical electric fish genus *Hypopygus* (Teleostei, Ostariophysi, Gymnotiformes). *Zoological Journal of the Linnaean Society, 163*(4), 1096-1156.

Dutra, G. M., Wosiacki, W. B., & de Pinna, M. C. C. (2012). *Trichomycterus anhanga*, a new species of miniature catfish related to *T. hasemani* and *T. johnsoni* (Siluriformes: Trichomycteridae) from the Amazon basin, Brazil. *Neotropical Ichthyology, 10*(2), 225-231.

Eccles, D. H. (1992). *FAO species identification sheets for fishery purposes. Field guide to the freshwater fishes of Tanzania. Prepared and published with the support of the United Nations Development Programme (project URT/87/016).* Rome: FAO.

Fink, S. V., & Fink, W. L. (1981). Interrelationships of the ostariophysan fishes (Teleostei). *Zoological Journal of the Linnaean Society, 72*(4), 297-353.

Franz-Odendaal, T. A., & Adriaens, D. (2014). Comparative developmental osteology of the seahorse skeleton reveals heterochrony amongst *Hippocampus* sp and progressive caudal fin loss. *EvoDevo, 5*, 1-11.

Gery, J. (1977). *Characoids of the World*. USA: T.F.H. Publications, Inc. Ltd.

Gery, J. (1995). Description of new or poorly known Alestinae (Teleostei: Characiformes: Alestidae) from Africa, with a note on the generic concept in the Alestinae. *Journal of Ichthyology and Aquatic Biology, 1*(4), 37-64.

Gould, S. J. (1977). *Ontogeny and Phylogeny*. Cambridge, Massachusetts: Belknap Press.

Hanken, J., & Wake, D. B. (1993). Miniaturization of body-size - organismal consequences and evolutionary significance. *Annual Review of Ecology and Systematics, 24*, 501-519.

Hanssens, M., & Snoeks, J. (2006). *Petersius conserialis*. The IUCN Red List of Threatened Species. Retrieved from https://www.iucnredlist.org/species/60326/12350116.

Hoedeman, J. J. (1951). Studies on African Characid Fishes. The tribe Alestidi. *Beaufortia, 3*, 1-8.

Howes, G. J. (1982). Review of the genus *Brycon* (Teleostei: Characoidei). *Bulletin of the British Museum Natural History (Zoology), 43*(1), 1-47.

Hubert, N., Bonillo, C., & Paugy, D. (2005). Early divergence among the Alestidae (Teleostei, Ostariophyses, Characiformes): Mitochondrial evidences and congruence with morphological data. *Animal Biology and Pathology, 328*(5), 477-491.

International Union for Conservation of Nature (IUCN). 2020. *The IUCN Red List of Threatened Species.* Version 2019-3. Retrieved from www.iucnredlist.org.

Johnson, G. D., & Brothers, E. B. (1993). *Schindleria*: A paedomorphic goby (Teleostei: Gobioidei). *Bulletin of Marine Science, 52*(1), 441-471.

Konings, A., Bills, R., Hanssens, M., Kazembe, J., & Tweddle, D. (2018). *Hemigrammopetersius barnardi. The IUCN Red List of Threatened Species* 2018:e. Retrieved from https://www.iucnredlist.org/species/63238/3124598

Lawson, R., & Manly, B. F. J. (1973). Tooth growth and replacement in *Ctenolucius hujeta*, a Neotropical characoid fish. *Journal of Morphology, 141*(4), 383-394.

Lindsey, C. C. (1966). Body sizes of poikilotherm vertebrates at different latitudes. *Evolution, 20*(4), 456-465.

Mabee, P. M., Olmstead, K. L., & Cubbage, C. C. (2000). An experimental study of intraspecific variation, developmental timing, and heterochrony in fishes. *Evolution, 54*(6), 2091-2106.

Malabarba, L. R., & Weitzman, S. H. (2003). Description of a new genus with six new species from Southern Brazil, Uruguay and Argentina, with a discussion of a putative Characid clade (Teleostei: Characiformes: Characidae). *Comun. Mus. Ciene. Tecnol. PUCRS. Ser. Zool. Porto Alegre, 16*(1), 67-151.

Marinho, M. M. F. (2017). Comparative development in *Moenkhausia pittieri* and *Paracheirodon innesi* (Ostariophysi: Characiformes) with comments on heterochrony and miniaturization in the Characidae. *Journal of Fish Biology, 91*(3), 851-865.

Masters, J. C., Genin, F., Silvestro, D., Lister, A. M., & DelPero, M. (2014). The red island and the seven dwarfs: body size reduction in Cheirogaleidae. *Journal of Biogeography, 41*(10), 1833-1847.

Mattox, G. M. T., Britz, R., & Toledo-Piza, M. (2014). Skeletal development and ossification sequence of the characiform *Salminus brasiliensis* (Ostariophysi: Characidae). *Ichthyological Exploration of Freshwaters, 25*(2), 103-158.

Mattox, G. M. T., Britz, R., & Toledo-Piza, M. (2016). Osteology of *Priocharax* and remarkable developmental truncation in a miniature Amazonian fish (Teleostei: Characiformes: Characidae). *Journal of Morphology, 277*(1), 65-85.

Miller, P. J. (1994). *Miniature Vertebrates: The Implications of Small Body Size*. Oxford: Clarendon Press.

Moritz, T., & Schliewan, U. K. (2016). Description of two new *Bathyaethiops* species (Teleostei: Alestidae) from the Congo basin. *Zoo Taxa, 4117*(4), 476-490.

Munene, J. J. M. M., & Stiassny, M. L. J. (2012). A new *Alestopetersius* (Characiformes: Alestidae) from the Kwilu River (Kasai basin) of central Africa; with a phylogeny for the genus and synonymy of *Duboisialestes*. *Zootaxa, 3166*(3166), 59-68.

Murray, A. M. (2004). Osteology and morphology of the characiform fish *Alestes stuhlmannii* Pfeffer, 1896 (Alestidae) from the Rufiji River basin, East Africa. *Journal of Fish Biology, 65*(5), 1412-1430.

Murray, A. M., & Stewart, K. M. (2002). Phylogenetic relationships of the African genera *Alestes* and *Brycinus* (Teleostei, Characiformes, Alestidae). *Canadian Journal of Zoology-Revue Canadienne De Zoologie, 80*(11), 1887-1899.

Myers, G. S. (1929). Cranial differences in the African characin fishes of the genera *Alestes* and *Brycinus*, with notes on the arrangement of the genera. *American Museum Novitates, 342*, 1-7.

Myers, G. S. (1958). Trends in the evolution of teleostean fishes. *Standford Ichthyological Bulletin, 7*, 27-30.

Nelson, J. S. (2006). *Fishes of the World* (Fourth ed.). Hoboken, New Jersey: John Wiley & Sons, Inc.

Netto-Ferreira, A. L., Birindelli, J. L. O., de Sousa, L. M., Mariguela, T. C., & Oliveira, C. (2013). A new miniature characid (Ostariophysi: Characiformes: Characidae), with phylogenetic position inferred from morphological and molecular data. *Plos One, 8*(1), 1-7.

Oliveira, C., Avelino, G. S., Abe, K. T., Mariguela, T. C., Benine, R. C., Orti, G., Vari, R. P., & Correa e Castro, R. M. (2011). Phylogenetic relationships within the speciose family Characidae (Teleostei: Ostariophysi: Characiformes) based on multilocus analysis and extensive ingroup sampling. *BMC Evolutionary Biology, 11*(275), 1-25.

Pastana, M. N. L., Dagosta, F. C. P., & Esguicero, A. L. H. (2017). A new sexually dichromatic miniature *Hyphessobrycon* (Teleostei: Characiformes: Characidae) from the Rio Formiga, upper Rio Juruena basin, Mato Grosso, Brazil, with a review of sexual dichromatism in Characiformes. *Journal of Fish Biology*, *91*(5), 1301-1318.

Paugy, D. (1990a). Characidae. In C. Leveque, D. Paugy, & G. G. Teugels (Eds.), *Faune des poissons d'eaux douces et saumatres de l'Afrique de l'Ouest* (Vol. XXVIII, pp. 195 - 236). Musee Royal de l'Afrique Centrale, Tervuren et O.R.S.T.O.M., Paris: Tome I. Coll. Faune Tropicale n.

Paugy, D. (1990b). Note a propos des Petersiini (Teleostei: Characidae) d'Afrique occidentale. *Ichthyological Exploration of Freshwaters, 1*(1), 75-84.

Peters, R. H. (1992). Lessons from the size efficiency hypothesis II. The mire of complexity. *Hydrobiologia, 235/236*, 435-455.

Poll, M. (1967). Revision des Characidae nains Africains. *Annales du Musee Royal de l'Afrique Centrale Tervurum serie in-8 Sciences Zoologiques, 162*, 1-158.

Prokofiev, A. M. (2001). A new genus of Neoscopelidae for *Eomyctophum gracile* Daniltshenko from the Middle Eocene of Georgia (Pisces: Osteichthyes: Myctophiformes). *Zoosystematica Rossica, 10*(1), 215-218.

Purvis, A., & Harvey, P. H. (1996). Miniature mammals: life-history strategies and macroevolution. In P. J. Miller (Eds.), *Miniature Vertebrates: The Implications of Small Body Size*. Oxford: Clarendon Press.

Roberts, T. R. (1966). Description and osteology of *Lepidarchus adonis*, a remarkable new characid fish from West Africa. *Standford Ichthyological Bulletin, 8*, 209-227.

Roberts, T. R. (1967). Tooth formation and replacement in characoid fishes. *Standford Ichthyological Bulletin, 8*, 231-247.

Roberts, T. R. (1969). Osteology and relationships of characoid fishes, particularly the genera *Hepsetus*, *Salminus*, *Hoplias*, *Ctenolucius*, and *Acestrorhynchus*. *Proceedings of the California Academy of Sciences, 36*(15), 391-500.

Ruber, L., Kottelat, M., Tan, H. H., Ng, P. K. L., & Britz, R. (2007). Evolution of miniaturization and the phylogenetic position of *Paedocypris*, comprising the world's smallest vertebrate. *BMC Evolutionary Biology, 7*(1), 1-10.

Taylor, W. R., & Van Dyke, G. C. (1985). Revised procedure for staining and clearing small fishes and other vertebrates for bone and cartilage study. *Cybium, 9*(2), 107-119.

Toledo-Piza, M., Mattox, G. M. T., & Britz, R. (2014). *Priocharax nanus*, a new miniature characid from the rio Negro, Amazon basin (Ostariophysi: Characiformes), with an updated list of miniature Neotropical freshwater fishes. *Neotropical Ichthyology, 12*(2), 229-246.

Vandewalle, P., Germeau, G., Besancenet, P., Parmentier, E., & Baras, E. (2005). Early development of the head skeleton in *Brycon moorei* (Pisces, Ostariophysi, Characidae). *Journal of Fish Biology, 66*(4), 996-1024.

Vari, R. P. (1995). The Neotropical fish family Ctenoluciidae (Teleostei: Ostariophysi: Characiformes): Supra and intrafamilial phylogenetic relationships, with a revisionary study. *Smithosonian Contributions to Zoology, 564*, 1-108.

Walter, B. E. (2013). Cranial skeletogenesis and osteology of the redeye tetra *Moenkhausia sanctaefilomenae*. *Journal of Fish Biology, 82*(1), 69-95.

Weitzman, S. H., & Vari, R. P. (1988). Miniaturization in South American freshwater fishes; An overview and discussion. *Proceedings of the Biological Society of Washington, 101*(2), 444-465.

Yeh, J. (2002). The effect of miniaturized body size on skeletal morphology in frogs. *Evolution, 56*(3), 628-641.

Zamba, A. I., & Vreven, E. (2008). *Rhabdalestes yokai* (Characiformes: Alestidae), a new species from the Lefini and Sangha River basins (Congo River basin), Africa. *Ichthyological Exploration of Freshwaters, 19*(4), 377-384.

Zanata, A. M., & Vari, R. P. (2005). The family Alestidae (Ostariophysi, Characiformes): a phylogenetic analysis of a trans-Atlantic clade. *Zoological Journal of the Linnaean Society, 145*(1), 1-144.

Chapter 5: Conclusion

In this thesis I described the osteology of three alestids: (i) *Hemigrammopetersius barnardi* (Herre), (ii) *Petersius conserialis* Hilgendorf, and (iii) *Alestes dentex* (Linnaeus). A lack of thorough osteological descriptions for small and miniature characiforms is apparent in the literature (some exceptions include Toledo-Piza *et al.*, 2014; Mattox *et al.*, 2016; Marinho, 2017; Pastana *et al.*, 2017; Darlim & Marinho, 2018). The comprehensive osteological descriptions provided here, particularly for the small-bodied alestid *H. barnardi*, which reaches a maximum standard length (SL) of 70 mm (Eccles, 1992), provides a foundation for future comparisons to other species of Alestidae. Identified morphological differences between *H. barnardi* and small individuals of *A. dentex*, which reaches a maximum total length (TL) of 550 mm (Paugy, 1990), will help identify potential truncated features resulting from a phylogenetic decrease in body size.

Miniaturization and small body sizes are often accompanied by a variety of features such as morphological novelties, losses and reductions to structural features, hyperossification, and increased intraspecific variation (Hanken & Wake, 1993; Frobisch & Schoch, 2009). My first objective was to assess the intraspecific variation in a sample (*n* = 161) of a small alestid, *H. barnardi*. A thorough osteological description was conducted for comparisons to other alestid species to identify potential morphological reductions and losses. The second objective was the description of the osteology of a relatively unknown species of Alestidae, *P. conserialis*. Due to several factors such as limited specimen availability (e.g., Zanata & Vari, 2005), and discrepancies in the literature regarding cranial morphology (e.g., Myers, 1929; Poll, 1967; Zanata & Vari, 2005), little is known regarding the osteology of *P. conserialis*. Britz and Conway (2009) recommended the comparison of full-grown miniatures to juveniles of mid-sized taxa to determine homoplastic features that result from a phylogenetic body size decrease. Therefore, the last objective of my thesis was to compare the small-bodied alestid, *H. barnardi*, to *P. conserialis,* and juvenile alestids of a species that attains a larger adult size, *A. dentex*, to identify possible convergent features that result from a phylogenetic decrease in body size and are not indicative of evolutionary relationships.

5.1 Summary of Findings

Intraspecific variation is reported to increase among miniature species (Hanken & Wake, 1993; Frobisch & Schoch, 2009). Few studies have assessed intraspecific variation within Alestidae (some exceptions include Nzeyimana & Amiet, 1992; Murray, 2004). The second chapter of my thesis assesses intraspecific variation of a sample of specimens of *H. barnardi*. I found a right-skewed distribution of measurements suggesting the examined specimens of *H. barnardi* had relatively smaller body sizes with only a few specimens reaching larger body sizes (the maximum SL here was 34.9 mm compared with the maximum reported SL of 70 mm (Eccles, 1992). The measurements and counts reported here were comparable with those presented in previous papers for other specimens of *H. barnardi*. The greatest variation was in the reported number of anal-fin rays (18 – 21; *n* = 158) and lateral line scales (7 – 12; *n* = 120), with less variation found among fin ray, scale, vertebral, and gill raker counts. Two of the specimens did not have an adipose fin, the loss of which has been associated with developmental truncation in characiforms (Pastana *et al.*, 2017) and is common in miniature and small characiforms (Dagosta *et al.*, 2014; Marinho, 2017). The loss of the adipose fin in two specimens of *H. barnardi*, however, may not be due to a reduced adult size and is potentially the result of intraspecific variation, as Murray (2004) reported one specimen in a sample (*n* = 143) of *A. stuhlmanni* also to not have an adipose fin.

The osteological description of *H. barnardi* provided here creates a foundation for future comparisons with other small alestids (and characiforms). Select morphological features were identified as lost or reduced in *H. barnardi* (i.e., the supraorbital, postcleithrum 3, simplified projections on the posterior of the pterotic, and simplification of the latero-sensory system). Finally, potential sexual dimorphism of the anal fin was described, and although the sex of the specimens could not be confirmed, the thickening of the anterior branched anal-fin rays in males was identified as noted by Zanata and Vari (2005).

The size series of *P. conserialis* provided much needed information on the osteology of this species and clarification on the debated presence or absence of the parietal fontanelle. Myers (1929) originally established *Petersius* as monotypic on the basis of the absence of a parietal fontanelle, the absence of which was later corroborated by Poll (1967). Gery (1995) maintained this classification and noted the lack of a fontanelle based on Poll (1967) but did not assess any specimens himself. Recent studies have reported the presence of a fontanelle (Murray & Stewart, 2002; Zanata & Vari, 2005) but in smaller specimens than those previously assessed; Poll (1967) assessed specimens of *P. conserialis* with a maximum TL of 145 mm; Zanata and Vari (2005) assessed specimens of *P. conserialis* with a maximum SL of 111.4 mm. However, one of the specimens that Poll (1967) examined was also examined by Zanata and Vari (2005), who found a small parietal fontanelle still present. Here, I found a weak negative trend for the gradual decrease in the length and width of the parietal fontanelle with an increase in body size, suggesting that while the fontanelle may fully close in larger specimens, it is present in smaller specimens (54.1 – 115.0 TL). While the parietal fontanelle exhibits negative growth, other features of *P. conserialis* appear to demonstrate isometric growth.

Petersius conserialis is relatively large in comparison with other Petersiini (dwarf alestids). It does not fit the criteria previously proposed for definitions of dwarf or miniature fishes (e.g., Lindsey, 1966; Weitzman & Vari, 1988; Miller, 1994), showing the lack of a clear definition of these terms in reference to *P. conserialis* in previous publications (e.g., Myers, 1929; Poll, 1967). I suggest that *P. conserialis* is not a proportional dwarf, but may continue to be considered a small alestid according to Castro's (1999) definition of small fish being less than 150 mm SL.

The final objective was to compare the osteology of *H. barnardi* to *P. conserialis*, and juveniles of *A. dentex* to identify potential morphological features that result from a phylogenetic decrease in body size and are not indicative of evolutionary relationships. Some osteological features were identified as potential truncations that are likely convergent within small and miniature species of Alestidae based on the examined specimens here and comparisons to previous literature.

5.2 Morphological Features Influenced by Small Body Size

Previous artificial classification systems for Alestidae were established based predominantly on dental morphologies (Hoedeman, 1951; Poll, 1967; Roberts, 1969). However, dentition has been reported to greatly vary among species (Poll, 1967; Zanata & Vari, 2005) and throughout growth (Brewster, 1986; Murray, 2004) in Alestidae. Roberts (1966) suggested that the unicuspid dentition in the miniature *Lepidarchus adonis* Roberts and small alestid

Clupeocharax schoutedeni Pellegrin is likely due to their small size and is not indicative of evolutionary relationships. The presence or absence of the inner dentary symphyseal tooth has also been considered the result of decreasing body size and not to indicate evolutionary relationships (Poll, 1967; Mamonekene & Stiassny, 2012). The spacing of the tooth rows on the premaxilla are poorly defined in *H. barnardi* in comparison with other alestids, as is also found in other small-bodied alestids (Zanata & Vari, 2005). Therefore, due to the variation of dental morphology in Alestidae and the reported changes with growth (Roberts, 1969; Brewster, 1986) caution should be used when using dental characters to determine evolutionary relationships.

Loss or reduction of osteological elements that develop towards the end of development may be the result of truncation. I found that several morphological features were reduced and absent in *H. barnardi*. The supraorbital, which is the last element to develop in a basal characid, *Salminus brasilis* (Cuvier), according to Mattox *et al.* (2014), is lost in *H. barnardi*. The loss of bones from the circumorbital series is common in miniature characiforms (e.g., Malabarba & Weitzman, 2003; Azevedo, 2010; Marinho, 2017), and according to Zanata and Vari's (2005) phylogenetic hypothesis the loss of the supraorbital has independently occurred twice in Alestidae. *Hemigrammopetersius barnardi* has also lost postcleithrum 3, which also develops towards the end of ontogeny (Mattox *et al.*, 2014). The loss of bones that are the last to develop in small and miniature fishes may be the result of truncation and therefore, these should be used with caution for building phylogenies.

Reductions to the lateral line system were also described for *H. barnardi* in comparison with other alestids. These include an incomplete lateral line, the loss of the anterodorsal branch of the circumorbital sensory canal on the dermosphenotic, and reductions to the supraorbital sensory canal in comparison with *P. conserialis* and *A. dentex*. These features should either be removed from phylogenetic hypotheses or also used with caution as they potentially have evolved independently in small species.

5.3 “Miniature” and “Small-Body Size” in Fishes

Previous researchers have proposed definitions for miniature and small body sizes in fishes, as previously discussed (e.g., Lindsey, 1966; Weitzman & Vari, 1988; Miller, 1994; Castro, 1999). All these definitions are relatively arbitrary with the largest emphasis not on a size criterion but on the presence of reduced morphological features. I chose to use Weitzman and Vari's (1988) definition for **miniature** fishes (less than 26 mm SL or reach sexual maturity by 20 mm SL) for the purposes of this thesis. Based on their definition, three species of Alestidae may be considered miniatures (i.e., *Lepidarchus adonis, Bathyaethiops baka* Moritz and Schliewan*,* and *Micralestes pabrensis* (Roman)). Castro (1999) defined **small** fishes as those less than 150 mm SL, which includes all Petersiini taxa as traditionally classified, including *P. conserialis*, the "peculiar large form" as described by Myers (1929: p. 5). This definition for small fishes was used here, classifying both *H. barnardi* and *P. conserialis* as small.

5.4 Limitations

A limitation of this thesis was the use of cleared and stained specimens to assess sexual dimorphism and the size series because there was no available method to sex or age previously cleared and stained specimens. Using specimens of *H. barnardi* is a potential limitation for assessing a miniaturization within the group as they are not a true miniature according to Weitzman and Vari's (1988) definition. Although, as *H. barnardi* exhibits a phylogenetic decrease in body size according to Zanata and Vari's (2005) analysis, they suffice as example specimens to assess potential morphological reductions and absences in small alestid species. Further, as no information is available on when *H. barnardi* reaches sexual maturity, to the best of my knowledge, *H. barnardi* may be a miniature and attain sexual maturity by 20 mm SL.

My thesis focused on morphological features in small and miniature alestids and I drew conclusions regarding potential reductions and absences as a result of decreasing body size. An oversight in my thesis was that I did not consider molecular data. The use of a molecular phylogeny would have allowed me to trace characters that were identified as reduced or absent to determine if they are homoplastic in small alestids. Further, the addition of using a phylogeny to trace the maximum body sizes of current alestid taxa would have allowed me to determine if a true phylogenetic decrease in body size was occurring and assess trends that occur in body size throughout Alestidae.

5.5 Future Research

There are numerous directions for future research on miniaturization in Alestidae and to address the limitations of my thesis. To confidently determine sexual dimorphism, specimens may be sexed using dissection or histology (e.g., West, 1990; Saborido-Rey & Junquera, 1998), prior to clearing and staining to assess sexual dimorphism of skeletal features. The use of scales, otoliths, or some bony structures may have been used to more accurately determine age estimates in order to more confidently determine the age of specimens throughout the size series. Further, the assessment of an ossification sequence of a basal alestid species (e.g., *Arnoldichthys spilopterus* according to Zanata and Vari (2005) and Calcagnotto *et al.* (2005) or a *Brycinus* sp. According to Calcagnotto *et al.* (2005) and Hubert *et al.* (2005)) will allow a more confident identification of features that develop at the end of developmental, which will be useful for determining potentially truncated features in small and miniature alestid taxa. I believe that a thorough description of the osteology of a true miniature alestid according to Weitzman and Vari's (1988) definition will allow the identification of additional morphological features influenced by a phylogenetic body size decrease and help corroborate those identified here.

Further, the body sizes of current alestid species could be plotted on a phylogenetic hypothesis to confidently address phylogenetic decreases in body size and miniaturization events throughout the family. A molecular phylogenetic hypothesis may also be used to trace potential morphological features that are identified as reduced or absent in small and miniature alestids to assess if they are convergently occurring in Alestidae with independent decreases in body size. The confident determination of truncated morphological features in Alestidae will allow those features to be excluded from future phylogenetic analyses and allow more robust hypotheses to be developed regarding relationships in Alestidae.

5.6 References

Azevedo, M. A. (2010). Reproductive characteristics of characid fish species (Teleostei, Characiformes) and their relationship with body size and phylogeny. *Iheringia Serie Zoologia, 100*(4), 469-482.

Brewster, B. (1986). A review of the genus *Hydrocynus* Cuvier 1819 (Teleostei: Characiformes). *Bulletin of the British Museum of Natural History (Zoology), 50*(3), 163-206.

Britz, R., & Conway, K. W. (2009). Osteology of *Paedocypris*, a Miniature and Highly Developmentally Truncated Fish (Teleostei: Ostariophysi: Cyprinidae). *Journal of Morphology, 270*(4), 389-412.

Castro, R. M. C. (1999). Evolucao da ictiofauna de riachos Sul-Americanos: Padroes gerais e possiveis processos causais. In R. Mazzoni & P. R. Peres-Neto (Eds.), *Ecologia de Peixes de Riachos* (Vol. 6, pp. 139-155). Rio de Janeiro, Brazil.

Dagosta, F. C. P., Marinho, M. M. F., & Camelier, P. (2014). A new species of *Hyphessobrycon* Durbin (Characiformes: Characidae) from the middle Rio Sao Francisco and upper and middle Rio Tocantins basins, Brazil, with comments on its biogeographic history. *Neotropical Ichthyology, 12*(2)*,* 365-375.

Darlim, G., & Marinho, M. M. F. (2018). *Moenkhausia lepidura* (Kner, 1858) (Charciformes, Characidae): osteology and relationships. *Biota Neotropica, 18*(4), 1-13.

Eccles, D. H. (1992). *FAO species identification sheets for fishery purposes. Field guide to the freshwater fishes of Tanzania. Prepared and published with the support of the United Nations Development Programme (project URT/87/016).* Rome: FAO.

Frobisch, N. B., & Schoch, R. R. (2009). Testing the impact of miniaturization on phylogeny: Paleozoic dissorophoid amphibians. *Systematic Biology, 58*(3), 312-327.

Gery, J. (1995). Description of new or poorly known Alestinae (Teleostei: Characiformes: Alestidae) from Africa, with a note on the generic concept in the Alestinae. *Journal of Ichthyology and Aquatic Biology, 1*(4), 37-64.

Hanken, J., & Wake, D. B. (1993). Miniaturization of body-size - organismal consequences and evolutionary significance. *Annual Review of Ecology and Systematics, 24*, 501-519.

Hoedeman, J. J. (1951). Studies on African Characid Fishes. The tribe Alestidi. *Beaufortia, 3*, 1-8.

Lindsey, C. C. (1966). Body sizes of poikilotherm vertebrates at different latitudes. *Evolution, 20*(4), 456-465.

Malabarba, L. R., & Weitzman, S. H. (2003). Description of a new genus with six new species from Southern Brazil, Uruguay and Argentina, with a discussion of a putative Characid clade (Teleostei: Characiformes: Characidae). *Comun. Mus. Ciene. Tecnol. PUCRS. Ser. Zool. Porto Alegre, 16*(1), 67-151.

Mamonekene, V., & Stiassny, M. L. J. (2012). A new *Bathyaethiops* (Characiformes: Alestidae) from the Lékoumou River (Kouilou-Niari Basin) in the Republic of Congo; First record of the genus in the Lower Guinean Ichthyofaunal Province. *Copeia, 2012*(3), 478-483.

Marinho, M. M. F. (2017). Comparative development in *Moenkhausia pittieri* and *Paracheirodon innesi* (Ostariophysi: Characiformes) with comments on heterochrony and miniaturization in the Characidae. *Journal of Fish Biology, 91*(3), 851-865.

Mattox, G. M. T., Britz, R., & Toledo-Piza, M. (2014). Skeletal development and ossification sequence of the characiform *Salminus brasiliensis* (Ostariophysi: Characidae). *Ichthyological Exploration of Freshwaters, 25*(2), 103-158.

Mattox, G. M. T., Britz, R., & Toledo-Piza, M. (2016). Osteology of *Priocharax* and remarkable developmental truncation in a miniature Amazonian fish (Teleostei: Characiformes: Characidae). *Journal of Morphology, 277*(1), 65-85.

Miller, P. J. (1994). *Miniature Vertebrates: The Implications of Small Body Size*. Oxford: Clarendon Press.

Murray, A. M. (2004). Osteology and morphology of the characiform fish *Alestes stuhlmannii* Pfeffer, 1896 (Alestidae) from the Rufiji River basin, East Africa. *Journal of Fish Biology, 65*(5), 1412-1430.

Murray, A. M., & Stewart, K. M. (2002). Phylogenetic relationships of the African genera *Alestes* and *Brycinus* (Teleostei, Characiformes, Alestidae). *Canadian Journal of Zoology-Revue Canadienne De Zoologie, 80*(11), 1887-1899.

Myers, G. S. (1929). Cranial differences in the African characin fishes of the genera *Alestes* and *Brycinus*, with notes on the arrangement of the genera. *American Museum Novitates, 342*, 1-7.

Nzeyimana, F., & Amiet, J. (1992). Redescription, affinites et distribution au cameroun de *Brachypetersius altus* (Boulenger, 1899) (Characidae, Petersiini). *Cybium, 16*(1), 31-42.

Pastana, M. N. L., Dagosta, F. C. P., & Esguicero, A. L. H. (2017). A new sexually dichromatic miniature *Hyphessobrycon* (Teleostei: Characiformes: Characidae) from the Rio Formiga, upper Rio Juruena basin, Mato Grosso, Brazil, with a review of sexual dichromatism in Characiformes. *Journal of Fish Biology*, *91*(5), 1301-1318.

Paugy, D. (1990). Note a propos des Petersiini (Teleostei: Characidae) d'Afrique occidentale. *Ichthyological Exploration of Freshwaters, 1*(1), 75-84.

Poll, M. (1967). Revision des Characidae nains Africains. *Annales du Musee Royal de l'Afrique Centrale Tervurum serie in-8 Sciences Zoologiques, 162*, 1-158.

Roberts, T. R. (1966). Description and osteology of *Lepidarchus adonis*, a remarkable new characid fish from West Africa. *Standford Ichthyological Bulletin, 8*, 209-227.

Roberts, T. R. (1969). Osteology and relationships of characoid fishes, particularly the genera *Hepsetus*, *Salminus*, *Hoplias*, *Ctenolucius*, and *Acestrorhynchus*. *Proceedings of the California Academy of Sciences, 36*(15), 391-500.

Saborido-Rey, F. & Junquera, S. (1998). Histological assessment of variations in sexual maturity of cod (*Gadus morhua* L.) at the Flemish Cap (north-west Atlantic). *ICES Journal of Marine Science, 55*, 515-521.

Toledo-Piza, M., Mattox, G. M. T., & Britz, R. (2014). *Priocharax nanus*, a new miniature characid from the rio Negro, Amazon basin (Ostariophysi: Characiformes), with an updated list of miniature Neotropical freshwater fishes. *Neotropical Ichthyology, 12*(2), 229-246.

Weitzman, S. H., & Vari, R. P. (1988). Miniaturization in South American freshwater fishes; An overview and discussion. *Proceedings of the Biological Society of Washington, 101*(2), 444-465.

West, G. (1990). Methods of assessing ovarian development in fishes: a review. *Australian Journal of Marine and Freshwater Research, 41*, 199-222.

Zanata, A. M., & Vari, R. P. (2005). The family Alestidae (Ostariophysi, Characiformes): a phylogenetic analysis of a trans-Atlantic clade. *Zoological Journal of the Linnaean Society, 145*(1), 1-144.

Bibliography

Akinyi, E., Azeroual, A., Entsua-Mensah, M., Getahun, A. P. L., & Twongo, T. (2010). *Alestes dentex*. The IUCN Red List of Threatened Species. Retrieved from https://www.iucnredlist.org/species/182128/7810513

Arroyave, J., & Stiassny, M. L. J. (2011). Phylogenetic relationships and the temporal context for the diversification of African characins of the family Alestidae (Ostariophysi: Characiformes): Evidence from DNA sequence data. *Molecular Phylogenetics and Evolution, 60*(3), 385-397.

Azevedo, M. A. (2010). Reproductive characteristics of characid fish species (Teleostei, Characiformes) and their relationship with body size and phylogeny. *Iheringia Serie Zoologia, 100*(4), 469-482.

Barlow, G. W. (1961). Causes and significance of morphological variation in fishes. *Systematic Zoology, 10*(3), 105-117.

Barriga, J. P., Battini, M. A., Garcia-Asorey, M., Carrea, C., Macchi, P. J., & Cussac, V. E. (2011). Intraspecific variation in diet, growth, and morphology of landlocked *Galaxias maculatus* during its larval period: The role of food availability and predation risk. *Hydrobiologia, 679*(1), 27-41.

Bertmar, G. (1959). On the ontogeny of the chondral skull in Characidae, with a discussion on the chondrocranial base and the visceral chondrocranium in fishes. *Acta Zoologica,* 203-364.

Bird, N. C., & Hernandez, L. P. (2007). Morphological variation in the Weberian apparatus of Cypriniformes. *Journal of Morphology*, *268*(9), 739-757.

Bloom, D. D., Kolmann, M., Foster, K., & Watrous, H. (2020). Mode of miniaturisation influences body shape evolution in New World anchovies (Engraulidae). *Journal of Fish Biology, 96*(1), 194-201.

Brandl, S. J., Goatley, C. H. R., Bellwood, D. R., & Tornabene, L. (2018). The hidden half: ecology and evolution of cryptobenthic fishes on coral reefs. *Biological Reviews of the Cambridge Philosophical Society, 93*(4), 1846-1873.

Braun, C. B., & Grande, T. (2008). Evolution of peripheral mechanisms for the enhancement of sound reception. In J. F. Webb, R. R. Fay, & A. N. Popper (Eds.), *Fish Bioacoustics* (pp. 99-144). New York: Springer.

Brewster, B. (1986). A review of the genus *Hydrocynus* Cuvier 1819 (Teleostei: Characiformes). *Bulletin of the British Museum of Natural History (Zoology), 50*(3), 163-206.

Britz, R., & Conway, K. W. (2009). Osteology of *Paedocypris*, a miniature and highly developmentally truncated fish (Teleostei: Ostariophysi: Cyprinidae). *Journal of Morphology, 270*(4), 389-412.

Britz, R., & Conway, K. W. (2016). *Danionella dracula*, an escape from the cypriniform bauplan via developmental truncation? *Journal of Morphology, 277*(2), 147-166.

Buckup, P. A. (1998). Relationships of the Characidiinae and phylogeny of characiform fishes (Teleostei: Ostariophysi). In L. R. Malabarba, R. E. Reis, R. P. Vari, Z. M. S. Lucena, & C. A. S. Lucena (Eds.), *Phylogeny and Classification of Neotropical Fishes* (pp. 123-144). Porto Alegre, Brasil: EDIPUCRS.

Calcagnotto, D., Schaefer, S. A., & DeSalle, R. (2005). Relationships among characiform fishes inferred from analysis of nuclear and mitochondrial gene sequences. *Molecular Phylogenetics and Evolution, 36*(1), 135-153.

Carnevale, G. (2008). Miniature deep-sea hatchetfish (Teleostei: Stomiiformes) from the Miocene of Italy. *Geological Magazine, 145*(1), 73-84.

Castro, R. M. C. (1999). Evolucao da ictiofauna de riachos Sul-Americanos: Padroes gerais e possiveis processos causais. In R. Mazzoni & P. R. Peres-Neto (Eds.), *Ecologia de Peixes de Riachos* (Vol. 6, pp. 139-155). Rio de Janeiro, Brazil.

Chakrabarty, P., Faircloth, B. C., Alda, F., Ludt, W. B., McMahan, C. D., Near, T. J., Dornburg, A., Albert, J. S., Arroyave, J., Stiassny, M. L. J., Sorenson, L., & Alfaro, M. E. (2017). Phylogenomic systematics of ostariophysan fishes: ultraconserved elements support the surprising non-monophyly of Characiformes. *Systematic Biology, 66*(6), 881-895.

Chardon, M., & Vandewalle, P. (1997). Evolutionary trends and possible origin of the Weberian apparatus. *Netherlands Journal of Zoology, 47*(4), 383-403.

Conway, K. W., Kubicek, K. M., & Britz, R. (2017). Morphological novelty and modest developmental truncation in *Barboides*, Africa's smallest vertebrates (Teleostei: Cyprinidae). *Journal of Morphology, 278*(6), 750-767.

Conway, K. W., & Moritz, T. (2006). *Barboides britzi*, a new species of miniature cyprinid from Benin (Ostariophysi : Cyprinidae), with a neotype designation for *Barboides gracilis*. *Ichthyological Exploration of Freshwaters, 17*(1), 73-84.

Copley, H. (1958). *Common freshwater fishes of East Africa*. H. F. & G. Witherby LTD, 5 Warwick Court London.

Dagosta, F. C. P., Marinho, M. M. F., & Camelier, P. (2014). A new species of *Hyphessobrycon* Durbin (Characiformes: Characidae) from the middle Rio Sao Francisco and upper and middle Rio Tocantins basins, Brazil, with comments on its biogeographic history. *Neotropical Ichthyology, 12*(5)*,* 365-375.

da Graca, W. J., Ota, R. R., & Domingues, W. M. (2019). A new species of miniature *Characidium* (Characiformes: Crenuchidae) from the upper Rio Paraguay basin, Mato Grosso state, Brazil. *Journal of Fish Biology, 95*(6), 1480-1485.

Darlim, G., & Marinho, M. M. F. (2018). *Moenkhausia lepidura* (Kner, 1858) (Characiformes, Characidae): osteology and relationships. *Biota Neotropica, 18*(4), 1-13.

De Santana, C. D., & Crampton, W. G. R. (2011). Phylogenetic interrelationships, taxonomy, and reductive evolution in the Neotropical electric fish genus *Hypopygus* (Teleostei, Ostariophysi, Gymnotiformes). *Zoological Journal of the Linnaean Society, 163*(4), 1096-1156.

Douglas, M. E. (1987). An ecomorphological analysis and niche packing and niche dispersion in stream fish clades. In W. J. Matthews & D. C. Heins (Eds.), *Community and evolutionary ecology of North American stream fishes* (p. 144 - 149). University of Oklahoma Press: Norman.

Dutra, G. M., Wosiacki, W. B., & de Pinna, M. C. C. (2012). *Trichomycterus anhanga*, a new species of miniature catfish related to *T. hasemani*and *T. johnsoni* (Siluriformes: Trichomycteridae) from the Amazon basin, Brazil. *Neotropical Ichthyology, 10*(2), 225-231.

Eccles, D. H. (1992). *FAO species identification sheets for fishery purposes. Field guide to the freshwater fishes of Tanzania. Prepared and published with the support of the United Nations Development Programme (project URT/87/016).* Rome: FAO.

Fink, S. V., & Fink, W. L. (1981). Interrelationships of the ostariophysan fishes (Teleostei). *Zoological Journale of the Linnaean Society, 72*(4), 297-353.

Franz-Odendall, T. A., & Adriaens, D. (2014). Comparative developmental osteology of the seahorse skeleton reveals heterochrony amongst *Hippocampus* sp and progressive caudal fin loss. *EvoDevo, 5*, 1-11.

Fricke, R., Eschmeyer, W. N., & van der Laan, R. E. (2019). Eschmeyer's catalogue of fishes: Genera, species, references. California Academy of Sciences. Retrieved from http://researcharchive.calacademy.org/research/ichthyology/catalog/fishcatmain.asp

Fricke, R., Eschmeyer, W. N., & Fong, J. D. (2020). Species by family/subfamily. Retrieved from http://researcharchive.calacademy.org/research/ichthyology/catalog/SpeciesByFamily.asp

Frobisch, N. B., & Schoch, R. R. (2009). Testing the impact of miniaturization on phylogeny: Paleozoic dissorophoid amphibians. *Systematic Biology, 58*(3), 312-327.

Froese, R., & Pauly, D. (2018). FishBase. *World Wide Web electronic publication*. Retrieved from www.fishbase.org

Gery, J. (1977). *Characoids of the World*. USA: T.F.H. Publications, Inc. Ltd.

Gery, J. (1995). Description of new or poorly known Alestinae (Teleostei: Characiformes: Alestidae) from Africa, with a note on the generic concept in the Alestinae. *Journal of Ichthyology and Aquatic Biology, 1*(4), 37-64.

Gould, S. J. (1977). *Ontogeny and Phylogeny*. Cambridge, Massachusetts: Belknap Press.

Greenwood, P. H., Rosen, D. E., Weitzman, S. H., & Myers, G. S. (1966). Phyletic studies of teleostean fishes with a provisional classification of living forms. *Bulletin of the American Museum of Natural History, 131*(4), 339-455.

Hanken, J. (1983). Miniaturization and its effects on cranial morphology in plethodontid salamanders, genus *Thorius* (Amphibia, Plethodontidae). 2. The fate of the brain and sense-organs and their role in skull morphogenesis and evolution. *Journal of Morphology, 177*(3), 255-268.

Hanken, J., & Wake, D. B. (1993). Miniaturization of body-size - organismal consequences and evolutionary significance. *Annual Review of Ecology and Systematics, 24*, 501-519.

Hanssens, M., & Snoeks, J. (2006). *Petersius conserialis*. The IUCN Red List of Threatened Species. Retrieved from https://www.iucnredlist.org/species/60326/12350116

Helfman, G. S., Collette, B. B., Facey, D. E., & Bowen, B. W. (2009). *The Diversity of Fishes: Biology, Evolution, and Ecology*. Chichester, West Sussex: Wiley-Blackwell: John Wiley & Sons LTD.

Herre, A. W. (1936). A new cyprinid genus and species and a new characin from Portuguese East Africa. *Proceedings of the Biological Scoiety of Washington, 49*, 99-102.

Hilgendorf. (1894). Neue Characinidengattung, *Petersius*, aus dem Kinganiflusse. *Sitzungs-Berichte der Gesellschaft Naturforschender Freunde zu Berlin*, 172.

Hoedeman, J. J. (1951). Studies on African Characid Fishes. The tribe Alestidi. *Beaufortia, 3*, 1-8.

Howes, G. J. (1982). Review of the genus *Brycon* (Teleostei: Characoidei). *Bulletin of the British Museum of Natural History (Zoology), 43*(1), 1-47.

Hubert, N., Bonillo, C., & Paugy, D. (2005). Early divergence among the Alestidae (Teleostei, Ostariophyses, Characiformes): Mitochondrial evidences and congruence with morphological data. *Animal Biology and Pathology, 328*(5), 477-491.

International Union for Conservation of Nature (IUCN). 2020. *The IUCN Red List of Threatened Species*. Version 2019-3. Retrieved from www.iucnredlist.org

Johnson, G. D., & Brothers, E. B. (1993). *Schindleria*: A paedomorphic goby (Teleostei: Gobioidei). *Bulletin of Marine Science, 52*(1), 441-471.

Kassambar, A., & Mundt, F. (2017). factoextra: Extract and visualize the results of multivariate data analyses (Version R package version 1.0.5). Retrieved from https://CRAN.R-project.org/package=factoextra

Knouft, J. H., & Page, L. M. (2003). The evolution of body size in extant groups of North American freshwater fishes: Speciation, size distributions, and Cope's rule. *American Naturalist, 161*(3), 413-421.

Konings, A., Bills, R., Hanssens, M., Kazembe, J., & Tweddle, D. (2018). *Hemigrammopetersius barnardi*. The IUCN Red List of Threatened Species 2018:e. Retrieved from https://www.iucnredlist.org/species/63238/3124598

Lawson, R., & Manly, B. F. J. (1973). Tooth growth and replacement in *Ctenolucius hujeta*, a Neotropical characoid fish. *Journal of Morphology, 141*(4), 383-394.

Lazzarotto, H., Barros, T., Louvise, J., & Caramaschi, E. P. (2017). Morphological variation among populations of *Hemigrammus coeruleus* (Characiformes: Characidae) in a Negro River tributary, Brazilian Amazon. *Neotropical Ichthyology, 15*(1), 1-10.

Le, S., Josse, J., & Husson, F. (2008). FactoMineR: An R package for multivariate analysis. *Journal of Statistical Software, 15*(1), 1-18.

Lindsey, C. C. (1966). Body sizes of poikilotherm vertebrates at different latitudes. *Evolution, 20*(4), 456-465.

Liston, J. (2013). The plasticity of gill raker characteristics in suspension feeders: Implications for Pachycormiformes In Arratia, G., Schultze, H-P., & Wilson, M. V. H. (Eds.). *Mesozoic Fishes 5.0 Global Diversity and Evolution* (p. 121 - 143). Munchen, Germany.

Liu, C. H. (2001). Early osteological development of the yellow tail *Seriola dumerili* (Pisces: Carangidae). *Zoological Studies, 40*(4), 289-298.

Lunkayilakio, S. W., & Vreven, E. (2008). *Nannopetersius mutambuei* (Characiformes: Alestidae), a new species from the Inkisi River basin, Lower-Congo. *Ichthyological Exploration of Freshwaters, 19*(4), 367-376.

Mabee, P. M., Olmstead, K. L., & Cubbage, C. C. (2000). An experimental study of intraspecific variation, developmental timing, and heterochrony in fishes. *Evolution, 54*(6), 2091-2106.

Malabarba, L. R., & Weitzman, S. H. (2003). Description of a new genus with six new species from Southern Brazil, Uruguay and Argentina, with a discussion of a putative Characid clade (Teleostei: Characiformes: Characidae). *Comun. Mus. Ciene. Tecnol. PUCRS. Ser. Zool. Porto Alegre, 16*(1), 67-151.

Mamonekene, V., & Stiassny, M. L. J. (2012). A new *Bathyaethiops* (Characiformes: Alestidae) from the Lekoumou River (Kouilou-Niari Basin) in the Republic of Congo; first record of the genus in the Lower Guinean Icthyofaunal Province. *Copeia, 2012*(3), 478-483.

Marinho, M. M. F. (2017). Comparative development in *Moenkhausia pittieri* and *Paracheirodon innesi* (Ostariophysi: Characiformes) with comments on heterochrony and miniaturization in the Characidae. *Journal of Fish Biology, 91*(3), 851-865.

Masters, J. C., Genin, F., Silvestro, D., Lister, A. M., & DelPero, M. (2014). The red island and the seven dwarfs: body size reduction in Cheirogaleidae. *Journal of Biogeography, 41*(10), 1833-1847.

Mattox, G. M. T., Britz, R., & Toledo-Piza, M. (2014). Skeletal development and ossification sequence of the charciform *Salminus brasiliensis* (Ostariophysi: Characidae). *Ichthyological Exploration of Freshwaters, 25*(2), 103-158.

Mattox, G. M. T., Britz, R., & Toledo-Pize, M. (2016). Osteology of *Priocharax* and remarkable developmental truncation in a miniature Amazonian fish (Teleostei: Characiformes: Characidae). *Journal of Morphology, 277*(1), 65-86.

Meyer, D., Dimitriadou, E., Hornik, K., Weingessel, A., and Leisch, F. (2019). e1071: Misc Functions of the Department of Statistics, Probability Theory Group (Formerly:E1071), TU Wien. R package version 1.7-3. https://CRAN.R-project.org/package=e1071.

Miller, P. J. (1994). *Miniature Vertebrates: The Implications of Small Body Size.* Oxford: Clarendon Press.

Morioka, S., & Matsumoto, S. (2002). Otolith features and utility of lapillus for daily increment analysis in Malawian Characidae *Hemigrammopetersius barnardi* (Herre, 1939) (Pisces: Characidae) collected from Lake Malawi. *Aqua-Fish Technical Report*, *1*, 1-8.

Moritz, T., & Schliewan, U. K. (2016). Description of two new *Bathyaethiops* species (Teleostei: Alestidae) from the Congo basin. *Zoo Taxa, 4117*(4), 476-490.

Munene, J. J. M. M., & Stiassny, M. L. J. (2012). A new *Alestopetersius* (Characiformes: Alestidae) from the Kwilu River (Kasai basin) of central Africa; with a phylogeny for the genus and synonymy of *Duboisialestes*. *Zootaxa, 3166*, 59-68.

Murray, A. M. (2004). Osteology and morphology of the characiform fish *Alestes stuhlmannii* Pfeffer, 1896 (Alestidae) from the Rufiji River basin, East Africa. *Journal of Fish Biology, 65*(5), 1412-1430.

Murray, A. M., & Stewart, K. M. (2002). Phylogenetic relationships of the African genera *Alestes* and *Brycinus* (Teleostei, Characiformes, Alestidae). *Canadian Journal of Zoology-Revue Canadienne De Zoologie, 80*(11), 1887-1899.

Myers, G. S. (1929). Cranial differences in the African characin fishes of the genera *Alestes* and *Brycinus*, with notes on the arrangement of the genera. *American Museum Novitates, 342*, 1-7.

Myers, G. S. (1958). Trends in the evolution of teleostean fishes. *Standford Ichthyological Bulletin, 7*, 7-30.

Nelson, J. S. (2006). *Fishes of the World* (Fourth ed.) Hoboken, New Jersey: John Wiley & Sons, Inc.

Nelson, J. S., Grande, T., & Wilson, M. V. H. (2016). *Fishes of the World* (Fifth ed.). Hoboken, New Jersey: John Wiley & Sons.

Netto-Ferreira, A. L., Birindelli, J. L. O., de Sousa, L. M., Mariguela, T. C., & Oliveira, C. (2013). A new miniature characid (Ostariophysi: Characiformes: Characidae), with phylogenetic position inferred from morphological and molecular data. *Plos One, 8*(1), 1-7.

Novelli, B., Otero-Ferrer, F., Socorro, J. A., Caballero, M. J., Segade-Botella, A., & Dominguez, L. (2017). Development of short-snouted seahorse (*Hippocampus hippocampus*, L. 1758): osteolgocial and morphological aspects. *Fish Physiology and Biochemistry, 43*(3), 833-848.

Nzeyimana, F., & Amiet, J. (1992) Redescription, affinities et distribution au cameroun de *Brachypetersius altus* (Boulenger, 1899) (Characidae, Petersiini). *Cybium, 16*(1), 31-42.

Oliveira, C., Avelino, G. S., Abe, K. T., Mariguela, T. C., Benine, R. C., Orti, G., Vari, R. P., & Correa e Castro, R. M. (2011). Phylogenetic relationships within the speciose family Characidae (Teleostei: Ostariophysi: Characiformes) based on multilocus analysis and extensive ingroup sampling. *BMC Evolutionary Biology, 11*(275), 1-25.

Orti, G., & Meyer, A. (1997). The radiation of characiform fishes and the limits of resolution of mitochondrial ribosomal DNA sequences. *Systematic Biology, 46*(1), 75-100.

Orti, G., & Vari, R. P. (1997). Characiformes. Tetras, piranhas, hatchetfishes, headstanders, pencilfishes, and their relatives. *The Tree of Life Web Project*. Retrieved from http://tolweb.org/Characiformes/15062/1997.01.27

Pastana, M. N. L., Dagosta, F. C. P., & Esguicero, A. L. H. (2017). A new sexually dichromatic miniature *Hyphessobrycon* (Teleostei: Characiformes: Characidae) from the Rio Formiga, upper Rio Juruena basin, Mato Grosso, Brazil, with a review of sexual dichromatism in Characiformes. *Journal of Fish Biology, 91*(5), 1301-1318.

Paugy, D. (1990a). Characidae. In C. Leveque, D. Paugy, & G. G. Teugels (Eds.), *Faune des poissons d'eaux douces et saumatres de l'Afrique de l'Ouest* (Vol. 28, pp. 195 - 236). Musee Royal de l'Afrique Centrale, Tervuren et O.R.S.T.O.M., Paris: Tome I. Coll. Faune Tropicale n.

Paugy, D. (1990b). Note a propos des Petersiini (Teleostei: Characidae) d'Afrique occidentale. *Ichthyological Exploration of Freshwaters, 1*(1), 75-84.

Pellegrin, J. (1929). Mutanda ichthyologica: *Clupeocharax* Pellegrin. *Revue de Zoologie et de Botanique Africaines, 16*(1), 75-84.

Peters, R. H. (1992). Lessons from the size efficiency hypothesis II. The mire of complexity. *Hydrobiologia, 235/236*, 435-455.

Poll, M. (1945). Descriptions de Mormyridae et de Characidae nouveaux du Congo Belge avec une etude du genre *Stomatorhinus* et des genres de Characidae nains africains. *Revue de Zoologie et de Botanique Africaines, 39*(1), 37-77.

Poll, M. (1967). Revision des Characidae nains Africains. *Annales du Musee Royal de l'Afrique Centrale Tervurum serie in-8 Sciences Zoologiques, 162*, 1-158.

Prokofiev, A. M. (2001). A new genus of Neoscopelidae for *Eomyctophum gracile* Daniltshenko from the Middle Eocene of Georgia (Pisces: Osteichthyes: Myctopheiformes). *Zoosystematica Rossica, 10*(1), 215-218.

Purvis, A., & Harvey, P. H. (1996). Miniature mammals: life-history startegies and macroevolution. In P. J. Miller (Eds.), *Miniature Vertebrates: The Implications of Small Body Size* (Vol. 69). Oxford: Clarendon Press.

R Core Team. (2017). R: A language and environment for statistical computing (Version 3.4.3). Vienna, Austria. Retrieved from https://www.R-project.org/

Roberts, T. R. (1966). Description and osteology of *Lepidarchus adonis*, a remarkable new characid fish from West Africa. *Standford Ichthyological Bulletin, 8*, 209-227.

Roberts, T. R. (1967). Tooth formation and replacement in characoid fishes. *Standford Ichthyological Bulletin, 8*, 231-247.

Roberts, T. R. (1969). Osteology and relationships of characoid fishes, particularly the genera *Hepsetus*, *Salminus*, *Hoplias*, *Ctenolucius*, and *Acestrorhynchus*. *Proceedings of the California Academy of Sciences, 36*(15), 391-500.

Roberts, T. R. (1975). Geographical distribution of African freshwater fishes. *Zoological Journal of the Linnean Society, 57*(4), 249-319.

Rosen, D. E., & Greenwood, P. H. (1970). Origin of the Weberian Apparatus and the relationships of the Ostariophysan and Gonorynchiform fishes. *American Museum Novitates, 2428*, 1-26.

Ruber, L., Kottelat, M., Tan, H. H., Ng, P. K. L., & Britz, R. (2007). Evolution of miniaturization and the phylogenetic position of *Paedocypris*, comprising the world's smallest vertebrate. *BMC Evolutionary Biology, 7*(1), 1-10.

Saborido-Rey, F. & Junquera, S. (1998). Histological assessment of variations in sexual maturity of cod (*Gadus morhua* L.) at the Flemish Cap (north-west Atlantic). *ICES Journal of Marine Science, 55*, 515-521.

Schönhofen Longoni, L., Giora, J., & Bernhardt Fialho, C. (2018). Development of secondary sexual characters and their relationship to ontogeny and seasonal reproductive period in *Hyphessobrycon igneus* (Ostariophysi: Characiformes). *Journal of Fish Biology, 92*(1), 131-149.

Skelton, P. H. (1994). Diversity and distribution of freshwater fishes in East and Southern Africa. *Annales du Musee Royale de l'Afrique Centrale, Sciences Zoologiques, 275,* 95-131.

Steele, S. E., & Lopez-Fernandez, H. (2014). Body size diversity and frequency distributions of Neotropical cichlid fishes (Cicliformes: Cichlidae: Ciclinae). *Plos One, 9*(9), 1-11.

Stiassny, M. L. J., & Mamonekene, V. (2007). *Micralestes* (Characiformes, Alestidae) of the lower Congo River, with a description of a new species endemic to the lower Congo River rapids in the Demogratic Republic of Congo. *Zootaxa, 1614*, 17-29

Stiassny, M. L. J., & Schaefer, S. A. (2005). *Rhabdalestes aeratis*, new species (Characiformes: Alestidae): first occurence of the genus from the Middle Congo River basin. *Ichthyological Exploration of Freshwaters, 16*(3), 271-278.

Taylor, W. R., & Van Dyke, G. C. (1985). Revised procedure for staining and clearing small fishes and other vertebrates for bone and cartilage study. *Cybium, 9*(2)*,* 107-119.

Toledo-Piza, M., Mattox, G. M. T., & Britz, R. (2014). *Priocharax nanus*, a new miniature characid from the rio Negro, Amazon basin (Ostariophysi: Characiformes), with an updated list of miniature Neotropical freshwater fishes. *Neotropical Ichthyology, 12*(2), 229-246.

van der Laan, R., Fricke, R., & Eschmeyer, W. N. (Eds) (2020) Classification. Retrieved from http://www.calacademy.org/scientists/catalog-of-fishes-classification/

Vandewalle, P., Germeau, G., Besancenet, P., Parmentier, E., & Baras, E. (2005). Early development of the head skeleton in *Brycon moorei* (Pisces, Ostariophysi, Characidae). *Journal of Fish Biology, 66*(4), 996-1024.

Vari, R. P. (1995). The Neotropical fish family Ctenoluciidae (Teleostei: Ostariophysi: Characiformes): Supra and intrafamilial phylogenetic relationships, with a revisionary study. *Smithosonian Contributions to Zoology, 564,* 1-108.

Villalobos, H., &Rodriguez-Sanchez, R. (2002). Pattern of increase in gill raker number of the California sardine. *Journal of Fish Biology, 60*, 256-259.

Walter, B. E. (2013). Cranial skeletogenesis and osteology of the redeye tetra *Moenkhausia sanctaefilomenae. Journal of Fish Biology, 82*(1), 69-95.

Wei, T., & Simko, V. (2017). R package "corrplot": Visualization of a Correlation Matrix (Version 0.84). Retrieved from https://gitub.com/taiyun/corrplot

Weitzman, S. H., & Vari, R. P. (1988). Miniaturization in South American freshwater fishes; An overview and discussion. *Proceedings of the Biological Society of Washington, 101*(2), 444-465.

West, G. (1990). Methods of assessing ovarian development in fishes: a review. *Australian Journal of Marine and Freshwater Research, 41*, 199-222.

Yeh, J. (2002). The effect of miniaturized body size on skeletal morphology in frogs. *Evolution, 56*(3), 628-641.

Zamba, A. I., & Vreven, E. (2008). *Rhabdaletes yokai* (Characiformes: Alestidae), a new species from the Lefini and Sangha River basins (Congo River basin), Africa. *Ichthyological Exploration of Freshwaters, 19*(4), 377-384.

Zanata, A. M., & Vari, R. P. (2005). The family Alestidae (Ostariophysi, Characiformes): a phylogenetic analysis of a trans-Atlantic clade. *Zoological Journal of the Linnaean Society, 145*(1), 1-144.

Appendix A: Definitions for Body Size Terminology

Table B.1. Definitions for different body size terms. Definitions used for the following terms for the fish specimens throughout this thesis are identified in bold.

Term	Reference	Definition
Developmental Truncated	Britz and Conway (2009)	Adult small fishes resemble earlier developmental stages of larger relatives
Dwarf Characids	Poll (1967)	The presence of compressed multicuspid teeth in Petersiini
Miniature	**Weitzman and Vari (1988)**	**Fish that does not exceed 26 mm SL or that reaches sexual maturity by 20 mm SL**
	Purvis and Harvey (1996)	If no obvious dichotomy of body size may consider smallest quarter of species miniature
Proportioned Dwarfs	Gould (1977)	Miniaturized taxa that are identical copies of larger relatives
Small	Lindsey (1966)	Fish less than 100 mm TL
	Castro (1999)	**Fishes less than 150 mm SL**

Appendix B: Guide of Completed Measurements and Counts

Table B.1. Detailed description of collected measurements and counts. Measurements and counts are separated by the double solid line. Any measurements and counts collected according to Lunkayilakio and Vreven (2008) are indicated by an asterisk (*). Vertebral counts were conducted according to Brewster (1986) and are indicated by an obelisk (†).

Measurement	Description
Total Length*	Distance from tip of snout to the posterior edge of caudal fin
Standard Length*	Distance from tip of snout to caudal peduncle
Head Length*	Distance from tip of snout to posterior edge of operculum
Preanal Distance*	Distance from tip of snout to the level of the first anal-fin ray
Preadipose Distance*	Distance from tip of snout to the level of the insertion point of the adipose fin
Predorsal Distance	Distance from tip of snout to the level of the first dorsal-fin ray
Prepelvic Distance*	Distance from tip of snout to the level of the pelvic-fin insertion
Prepectoral Distance*	Distance from tip of snout to the level of the pectoral-fin insertion
Snout Length*	Distance from tip of snout to the anterior edge of the orbit
Postorbital Distance*	Distance from the posterior edge of the orbit to the posterior edge of the operculum
Eye Diameter*	Distance between anterior and posterior edge of the orbit
Interorbital Distance*	Minimal distance between orbits
Body Depth*	Maximum vertical body depth (just anterior to the dorsal fin)
Head Depth	Maximum vertical depth of the head (just posterior to the posterior edge of the orbit)
Caudal Peduncle Depth*	Minimum vertical depth of caudal peduncle
Caudal Peduncle Length*	Distance between the last anal-fin ray insertion to caudal fin articulation
Caudal Length	Distance from caudal peduncle to the posterior edge of the caudal fin
Pectoral Fin Length	Distance from first pectoral-fin ray to distal end of longest pectoral-fin ray
Dorsal Fin Length*	Distance from first dorsal-fin ray to distal end of longest dorsal-fin ray
Dorsal Fin Base*	Distance between first dorsal-fin ray insertion and last dorsal-fin ray insertion

Pelvic Fin Length	Distance from first pelvic-fin ray to distal end of longest pelvic-fin ray
Adipose Fin Base	Distance between most anterior and posterior point of adipose fin
Anal Fin Base*	Distance between first anal-fin ray insertion and last anal-fin ray insertion
Anal Fin Length	Distance from first anal-fin ray to distal end of longest anal-fin ray

Lateral Line Scales*	Number of pored scales on lateral line
Transverse Scales	Number of scales starting from the dorsal-fin origin
Gill Rakers	Number of gill rakers on first gill arch
Anal Fin Rays	Number of anal fin rays
Pelvic Fin Rays	Number of pelvic fin rays
Dorsal Fin Rays	Number of dorsal fin rays
Pectoral Fin Rays	Number of pectoral fin rays
Total Vertebrae	Total number of vertebrae
Caudal Vertebrae†	Number of caudal vertebrae (fully developed haemal arch and spine)
Abdominal Vertebrae†	Number of abdominal vertebrae (most support pleural ribs)
Transitional Vertebrae†	Number of transitional vertebrae (transitional development of haemal spine and arch, associated with fine pleural ribs)

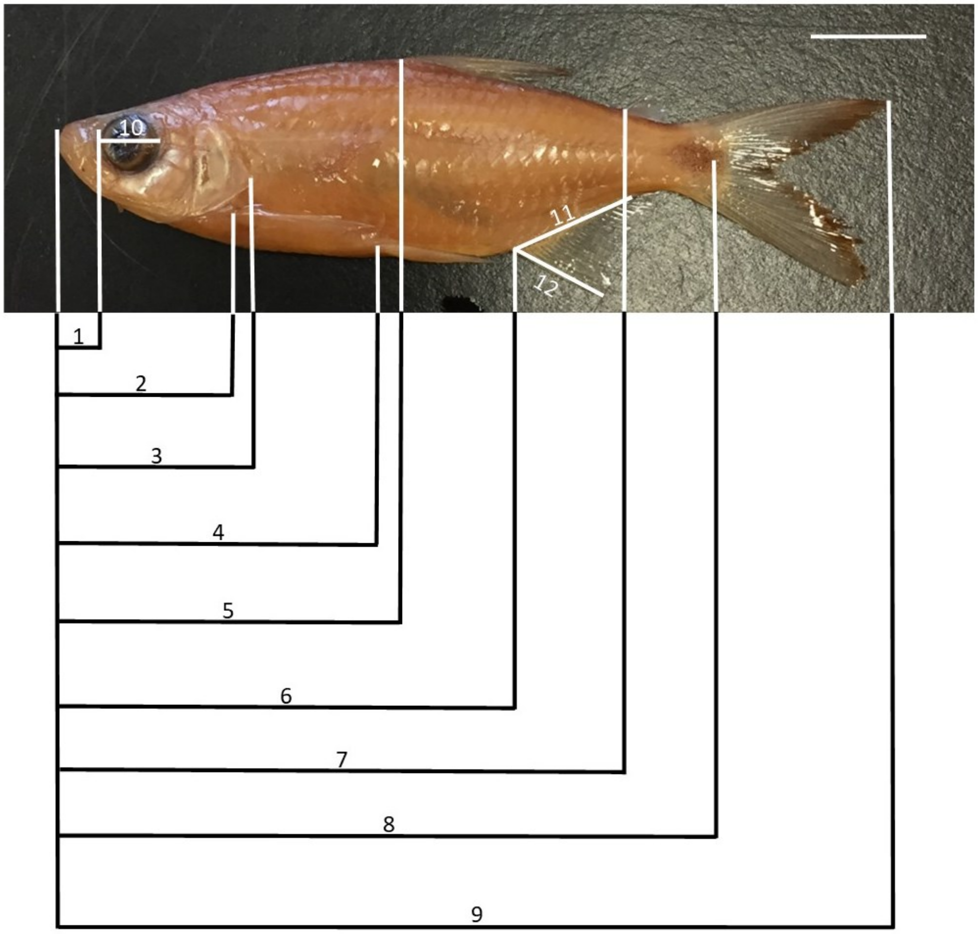

Figure B.1. Schematic of select measurements taken on specimens for this thesis. Photograph of a preserved specimen of *Petersius conserialis*, CMN F 81-0193, specimen number 106, SL = 91.0 mm, scale bar = 10 mm. (1) Snout length, (2) prepectoral distance, (3) head length, (4) prepelvic distance, (5) predorsal distance, (6) preanal distance, (7) preadipose distance, (8) standard length, (9) total length, (10) eye diameter, (11) anal fin base, (12) anal fin length.

Appendix C: Chapter 2 "Variation in the small African fish *Hemigrammopetersius barnardi* (Characiformes: Alestidae)"

C.1 Normality Test Results

Table C.1.Results of normal distribution tests for completed measurements. The skewness value represents the distortion of a bell-curve (a negative value represents a left-skewed curve, 0 represents a normal distribution, a positive value represents a right-skewed curve). The kurtosis value demonstrates if there are lots of outliers (higher values represent more outliers). The Shapiro-Wilk test was used to test the normal distribution of the data, with a null hypothesis that the data is from a normally distributed population.

Measurement	Skewness	Kurtosis	Shapiro-Wilk Test	p-value
Total Length	0.522	0.481	0.974	4.0×10^{-3}
Standard Length	0.882	0723	0.948	1.3×10^{-5}
Head Length SL^{-1}	0.165	0.302	0.994	0.81
Preanal Distance SL^{-1}	-0.280	-0.151	0.986	0.11
Preadipose Distance SL^{-1}	2.191	22.732	0.768	2.0×10^{-14}
Predorsal Distance SL^{-1}	0.019	0.360	0.994	0.78
Prepelvic Distance SL^{-1}	-0.178	0.248	0.993	0.64
Prepectoral Distance SL^{-1}	0.178	-0.209	0.992	0.52
Snout Length SL^{-1}	0.135	-0.526	0.990	0.37
Postorbital Distance SL^{-1}	0.361	0.101	0.983	0.05
Eye Diameter SL^{-1}	-0.204	0.333	0.991	0.45
Interorbital Distance SL^{-1}	0.438	-0.082	0.979	0.02
Body Depth SL^{-1}	0.598	0.508	0.969	1.4×10^{-3}
Head Depth SL^{-1}	1.412	5.816	0.888	1.4×10^{-9}
Caudal Peduncle Depth SL^{-1}	0.586	4.543	0.941	4.2×10^{-6}
Caudal Peduncle Length SL^{-1}	-0.076	1.566	0.974	5.0×10^{-3}
Anal Fin Length SL^{-1}	0.348	1.078	0.982	0.04
Anal Fin Base SL^{-1}	0.591	1.055	0.978	0.01
Adipose Fin Base SL^{-1}	0.636	0.009	0.962	2.8×10^{-4}
Dorsal Fin Length SL^{-1}	-0.129	-0.047	0.996	0.94
Dorsal Fin Base SL^{-1}	0.262	1.035	0.986	0.11
Pelvic Fin Length SL^{-1}	0.453	1.636	0.971	2.0×10^{-3}

Pectoral Fin Length SL^{-1}	-0.139	-0.450	0.993	0.59

C.2 Histograms of Measurements and Meristics

The following histograms represent the distribution for the completed measurements and meristics.

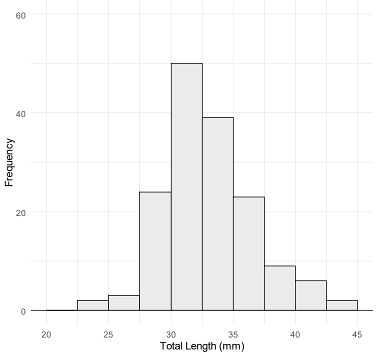

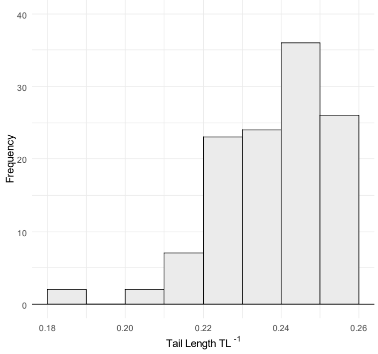

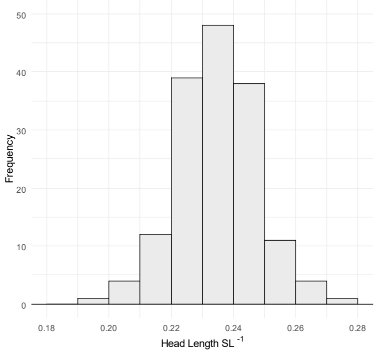

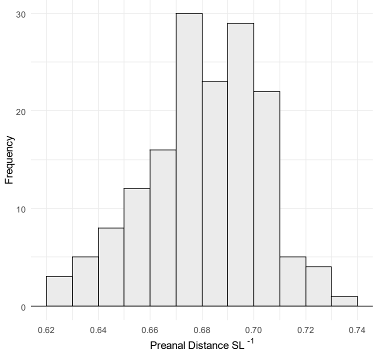

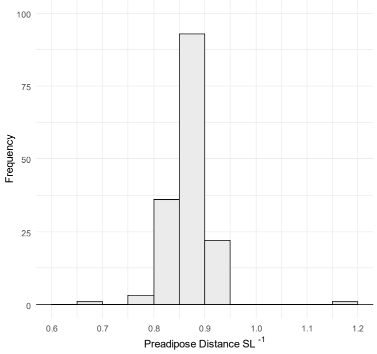

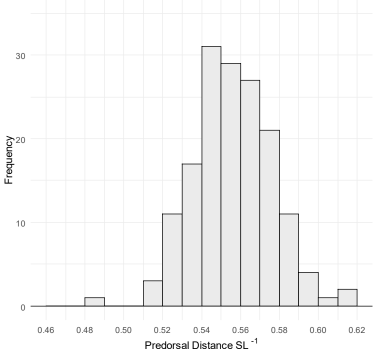

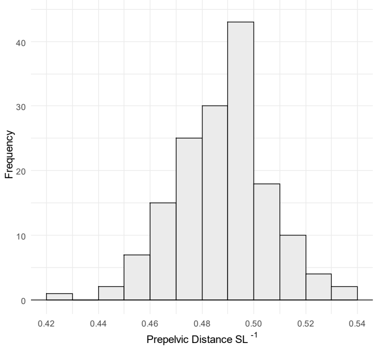

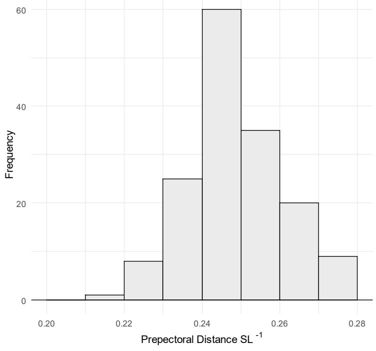

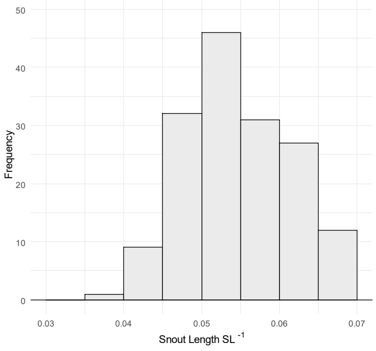

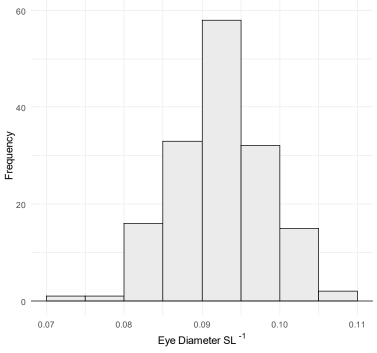
60
40
20
0
Frequency
0.07
0.08
0.09
0.10
0.11
Eye Diameter SL $^{-1}$

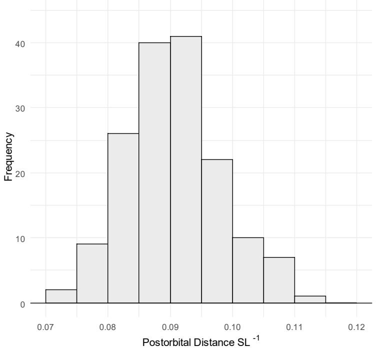
40
30
20
10
0
Frequency
0.07
0.08
0.09
0.10
0.11
0.12
Postorbital Distance SL $^{-1}$

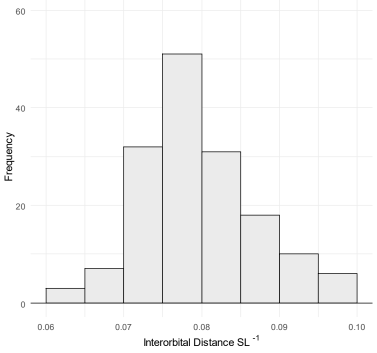
60
40
20
0
Frequency
0.06
0.07
0.08
0.09
0.10
Interorbital Distance SL $^{-1}$

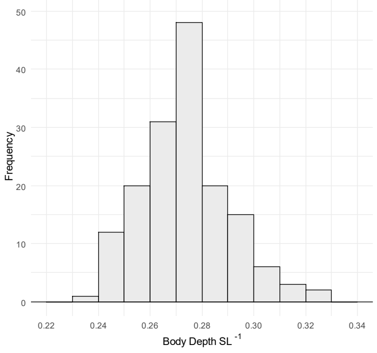
50
40
30
20
10
0
Frequency
0.22
0.24
0.26
0.28
0.30
0.32
0.34
Body Depth SL $^{-1}$

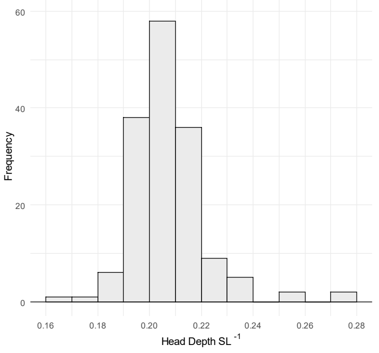
60
40
20
0
Frequency
0.16
0.18
0.20
0.22
0.24
0.26
0.28
Head Depth SL $^{-1}$

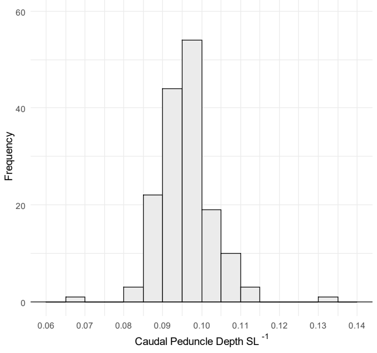
60
40
20
0
Frequency
0.06
0.07
0.08
0.09
0.10
0.11
0.12
0.13
0.14
Caudal Peduncle Depth SL $^{-1}$

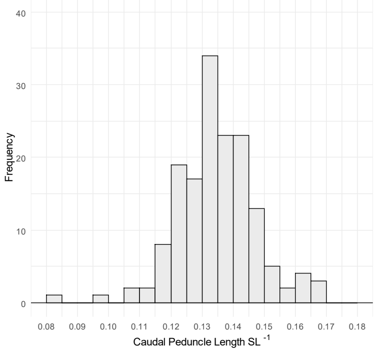
40
30
20
10
0
Frequency
0.08
0.09
0.10
0.11
0.12
0.13
0.14
0.15
0.16
0.17
0.18
Caudal Peduncle Length SL $^{-1}$

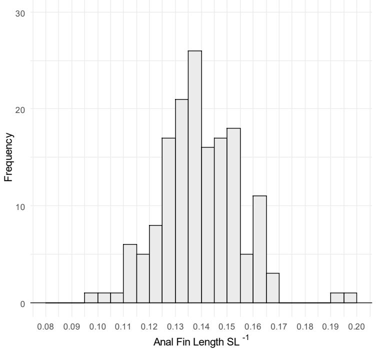
30
20
10
0
Frequency
0.08
0.09
0.10
0.11
0.12
0.13
0.14
0.15
0.16
0.17
0.18
0.19
0.20
Anal Fin Length SL $^{-1}$

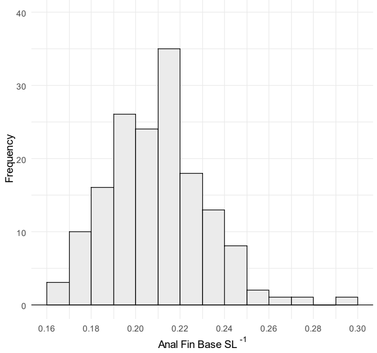
40
30
20
10
0
Frequency
0.16
0.18
0.20
0.22
0.24
0.26
0.28
0.30
Anal Fin Base SL $^{-1}$

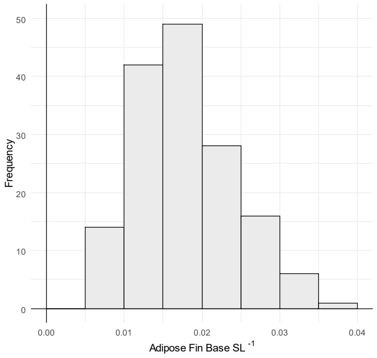
50
40
30
20
10
0
Frequency
0.00
0.01
0.02
0.03
0.04
Adipose Fin Base SL $^{-1}$

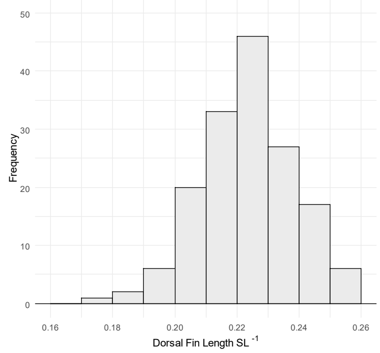
50
40
30
20
10
0
Frequency
0.16
0.18
0.20
0.22
0.24
0.26
Dorsal Fin Length SL $^{-1}$

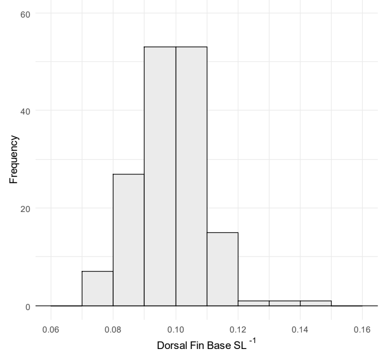
60
40
20
0
Frequency
0.06
0.08
0.10
0.12
0.14
0.16
Dorsal Fin Base SL $^{-1}$

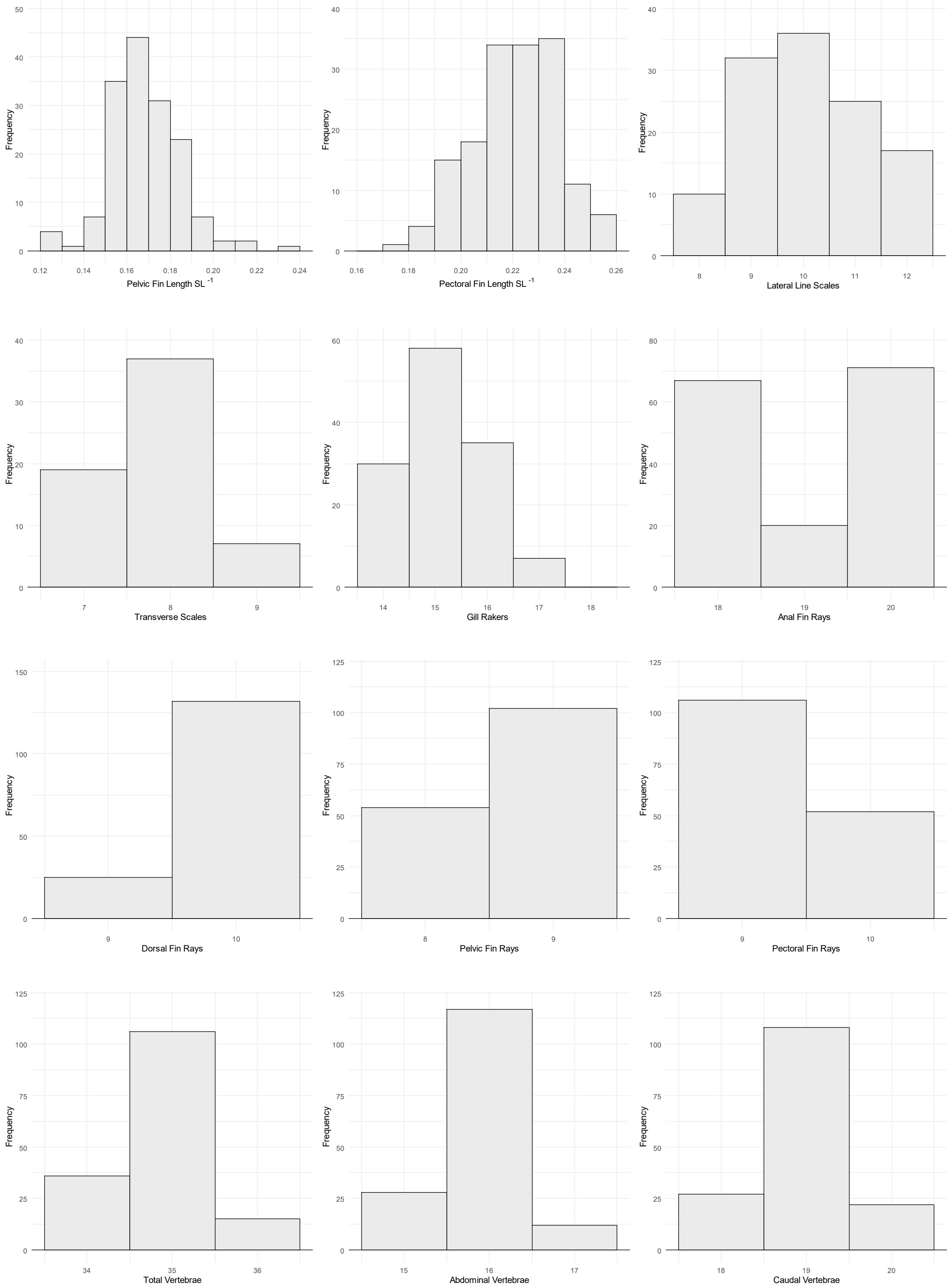
Frequency
0
10
20
30
40
50
0.12
0.14
0.16
0.18
0.20
0.22
0.24
Pelvic Fin Length SL -1
Frequency
0
10
20
30
40
0.16
0.18
0.20
0.22
0.24
0.26
Pectoral Fin Length SL -1
Frequency
0
10
20
30
40
8
9
10
11
12
Lateral Line Scales
Frequency
0
10
20
30
40
7
8
9
Transverse Scales
Frequency
0
20
40
60
14
15
16
17
18
Gill Rakers
Frequency
0
20
40
60
80
18
19
20
Anal Fin Rays
Frequency
0
50
100
150
9
10
Dorsal Fin Rays
Frequency
0
25
50
75
100
125
8
9
Pelvic Fin Rays
Frequency
0
25
50
75
100
125
9
10
Pectoral Fin Rays
Frequency
0
25
50
75
100
125
34
35
36
Total Vertebrae
Frequency
0
25
50
75
100
125
15
16
17
Abdominal Vertebrae
Frequency
0
25
50
75
100
125
18
19
20
Caudal Vertebrae

C.3 Scatterplots of Measurements and Meristics

C.3.1 Scatterplots of Measurements

Scatterplots of all measurements were completed using logarithmic data. The Pearson's correlation coefficient (r), p-value, and slope are represented in the top left corner. Scatterplots of measurements represent isometric growth (with a slope ≈ 1.0).

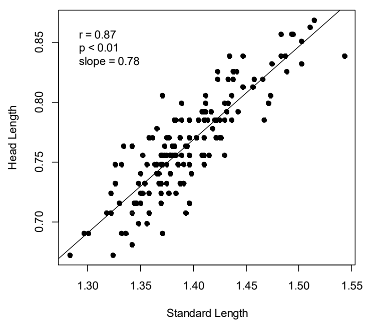

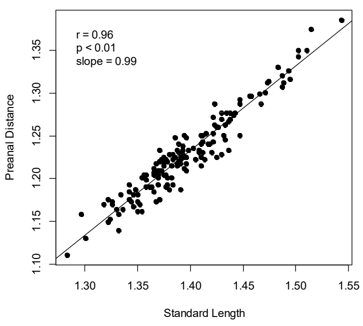

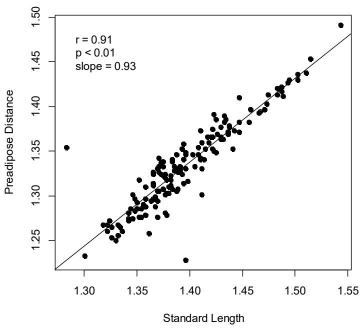

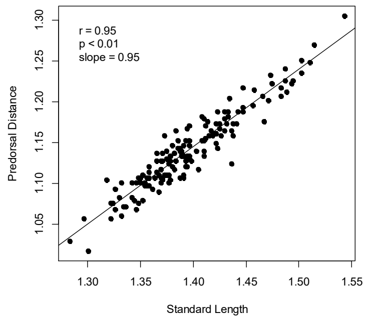

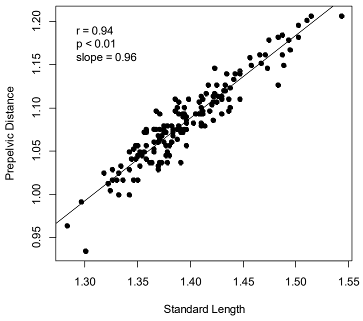

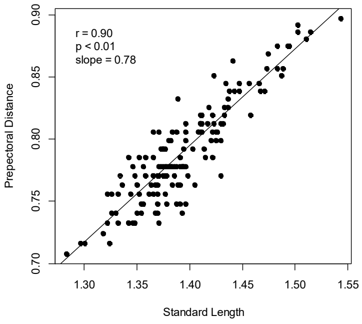

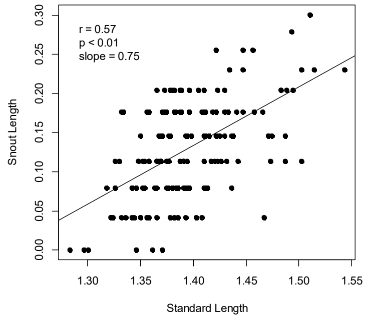

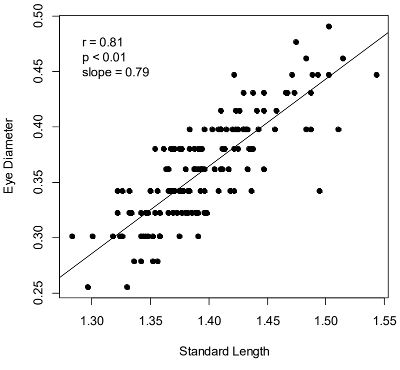

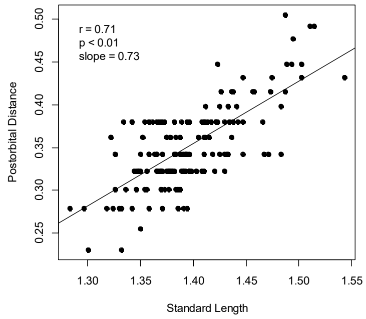

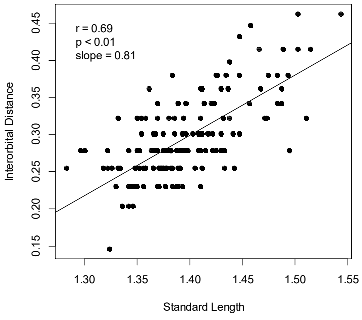
r = 0.69
p < 0.01
slope = 0.81
Interorbital Distance
0.15
0.20
0.25
0.30
0.35
0.40
0.45
1.30
1.35
1.40
1.45
1.50
1.55
Standard Length

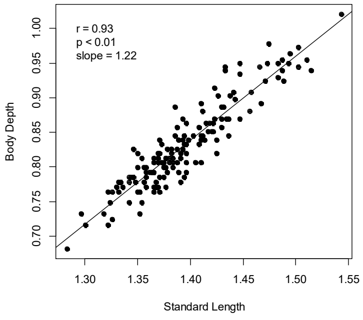
r = 0.93
p < 0.01
slope = 1.22
Body Depth
0.70
0.75
0.80
0.85
0.90
0.95
1.00
1.30
1.35
1.40
1.45
1.50
1.55
Standard Length

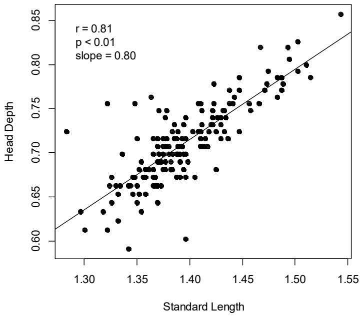
r = 0.81
p < 0.01
slope = 0.80
Head Depth
0.60
0.65
0.70
0.75
0.80
0.85
1.30
1.35
1.40
1.45
1.50
1.55
Standard Length

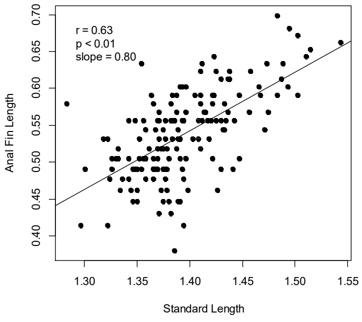
r = 0.63
p < 0.01
slope = 0.80
Anal Fin Length
0.40
0.45
0.50
0.55
0.60
0.65
0.70
1.30
1.35
1.40
1.45
1.50
1.55
Standard Length

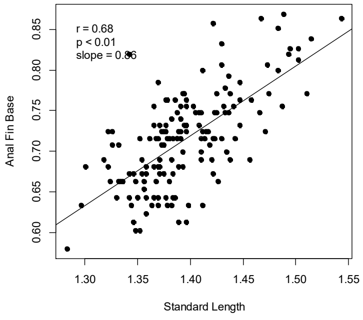
r = 0.68
p < 0.01
slope = 0.86
Anal Fin Base
0.60
0.65
0.70
0.75
0.80
0.85
1.30
1.35
1.40
1.45
1.50
1.55
Standard Length

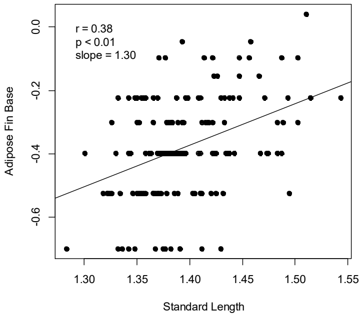
r = 0.38
p < 0.01
slope = 1.30
Adipose Fin Base
-0.6
-0.4
-0.2
0.0
1.30
1.35
1.40
1.45
1.50
1.55
Standard Length

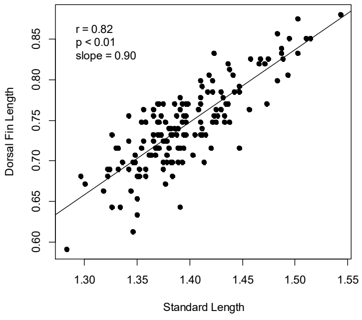
r = 0.82
p < 0.01
slope = 0.90
Dorsal Fin Length
0.60
0.65
0.70
0.75
0.80
0.85
1.30
1.35
1.40
1.45
1.50
1.55
Standard Length

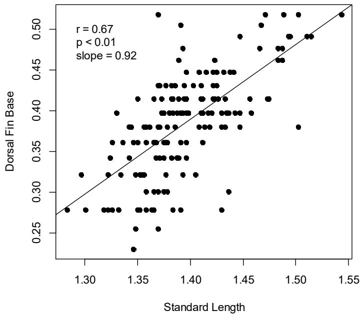
r = 0.67
p < 0.01
slope = 0.92
Dorsal Fin Base
0.25
0.30
0.35
0.40
0.45
0.50
1.30
1.35
1.40
1.45
1.50
1.55
Standard Length

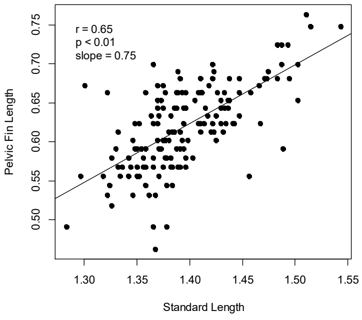
r = 0.65
p < 0.01
slope = 0.75
Pelvic Fin Length
0.50
0.55
0.60
0.65
0.70
0.75
1.30
1.35
1.40
1.45
1.50
1.55
Standard Length

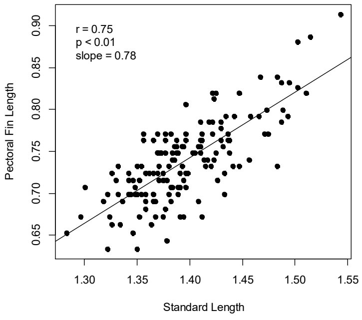
r = 0.75
p < 0.01
slope = 0.78
Pectoral Fin Length
0.65
0.70
0.75
0.80
0.85
0.90
1.30
1.35
1.40
1.45
1.50
1.55
Standard Length

C.3.2 Scatterplots of Meristics

Scatterplots of counts show no correlation with growth.

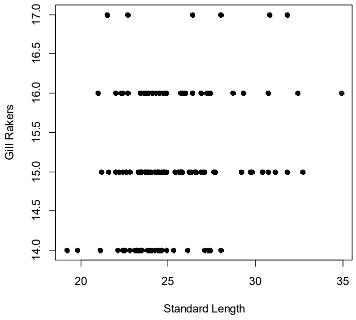

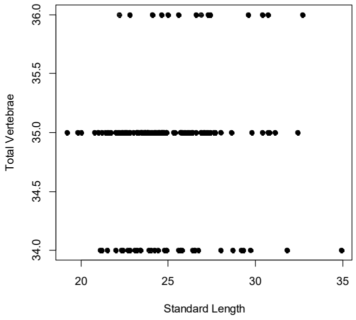

C.4 Principal Component Analysis

All measurements were turned into ratios in relation to standard length prior to principal component analysis (PCA). PCA results include (a) a scree plot of the first ten principal components (dimensions), (b) a correlation circle with each variable colored by its respective cos^2 (representation) value, (c) a contribution of variables table, and (d) a plot of the distribution of variables. The cos^2 value indicates which values are best represented by each component.

C.4.1 All Measurement Data

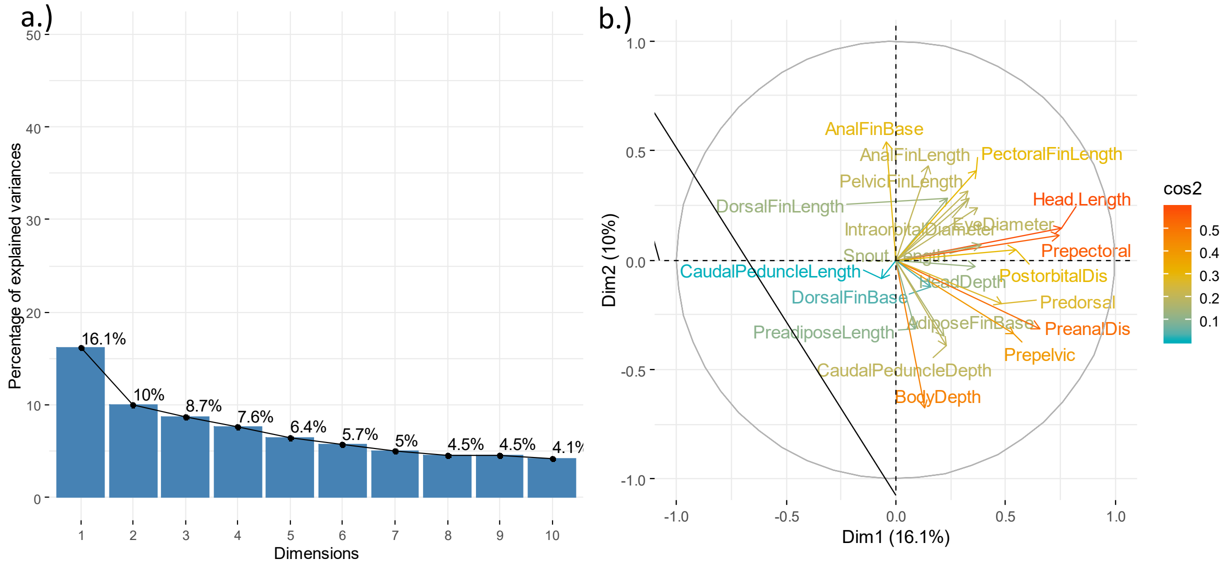

c.)

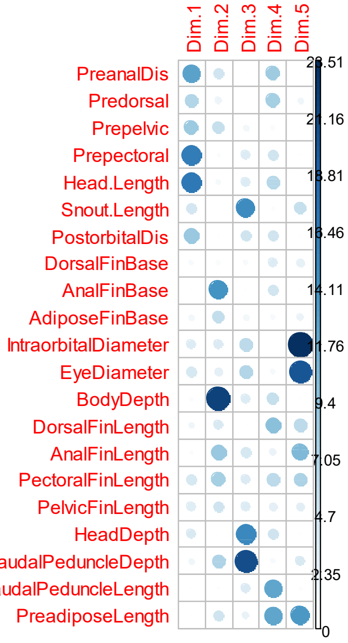

d.)

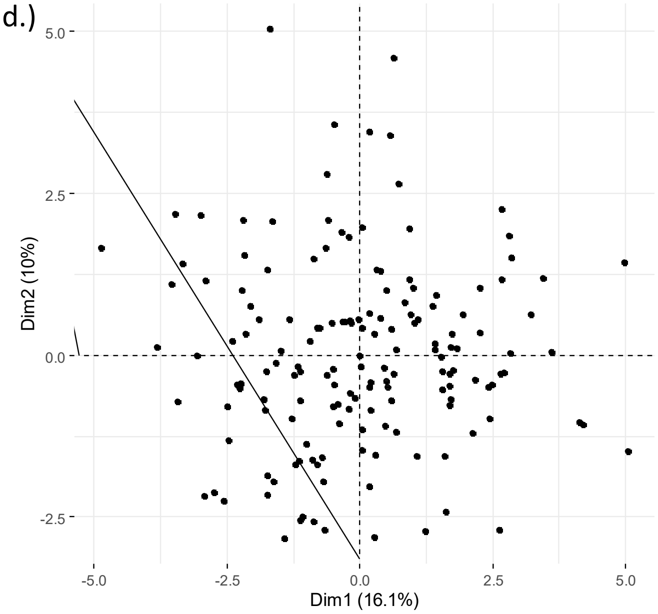

C.4.2 All Measurement and Meristic Data

a.)

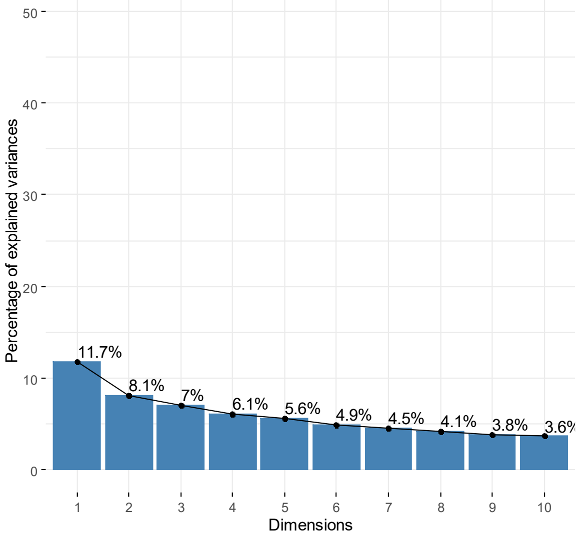

b.)

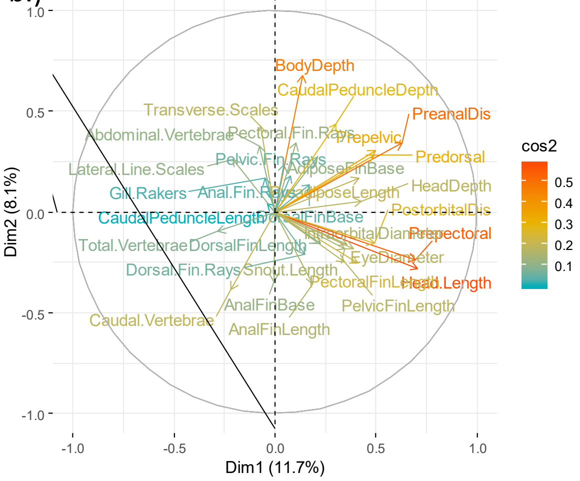

c.)

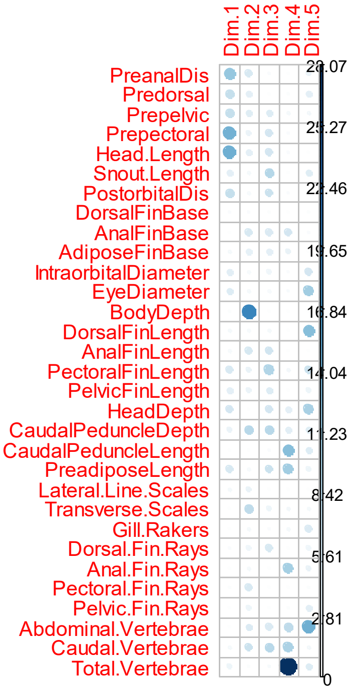

d.)

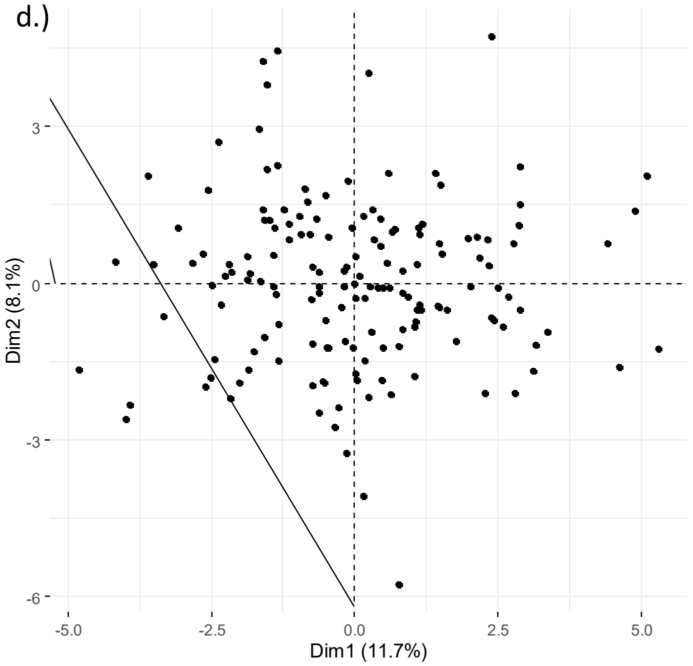

C.4.3 Select Measurements

Corresponding (a) scree plot and (b) contribution table to figure 4 presented in chapter 2.

a.)

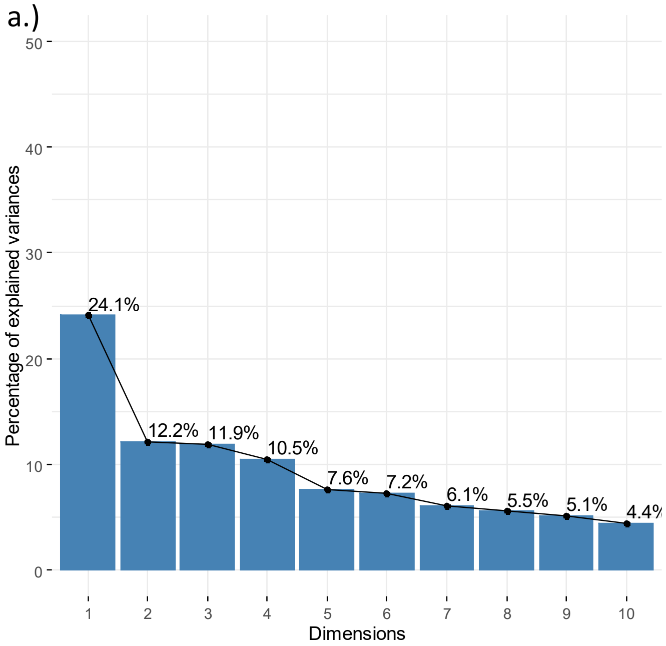

b.)

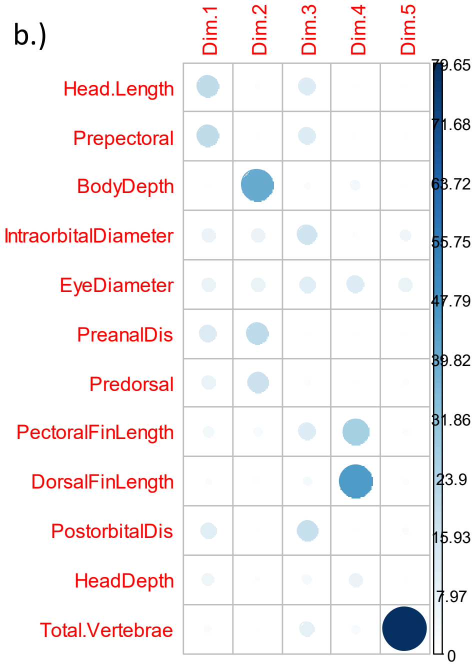

Appendix D: Chapter 3 "Size series of the small African fish *Petersius conserialis* (Characiformes: Alestidae)"

D.1 Normality Test Results

Table D.1.Results of normal distribution tests for completed measurements. The skewness value represents the distortion of a bell-curve (a negative value represents a left-skewed curve, 0 represents a normal distribution, a positive value represents a right-skewed curve). The kurtosis value demonstrates if there are lots of outliers (higher values represent more outliers). The Shapiro-Wilk test was used to test the normal distribution of the data, with a null hypothesis that the data is from a normally distributed population.

Measurement	Skewness	Kurtosis	Shapiro-Wilk Test	p-value
Total Length	1.323	0.622	0.779	2.8×10^{-3}
Standard Length	1.294	0.531	0.778	2.7×10^{-3}
Head Length SL^{-1}	0.240	-1.518	0.917	0.2
Preanal Distance SL^{-1}	-0.028	-1.401	0.959	0.71
Preadipose Distance SL^{-1}	0.876	0.511	0.916	0.20
Predorsal Distance SL^{-1}	0.002	-0.849	0.993	1.00
Prepelvic Distance SL^{-1}	0.590	-0.356	0.946	0.50
Prepectoral Distance SL^{-1}	0.485	-0.584	0.934	0.35
Snout Length SL^{-1}	-0.380	-1.506	0.901	0.12
Postorbital Distance SL^{-1}	-0.219	-1.273	0.931	0.32
Eye Diameter SL^{-1}	0.273	-1.268	0.954	0.62
Interorbital Distance SL^{-1}	-0.076	-0.451	0.964	0.78
Body Depth SL^{-1}	0.399	-1.219	0.948	0.53
Head Depth SL^{-1}	0.589	-0.574	0.903	0.12
Caudal Peduncle Depth SL^{-1}	0.037	-1.073	0.986	0.99
Caudal Peduncle Length SL^{-1}	-0.951	0.611	0.917	0.20
Anal Fin Length SL^{-1}	-0.496	0.250	0.930	0.31
Anal Fin Base SL^{-1}	-0.009	-1.360	0.959	0.71
Adipose Fin Base SL^{-1}	-0.506	-0.828	0.955	0.64
Dorsal Fin Length SL^{-1}	-0.418	-0.489	0.965	0.81
Dorsal Fin Base SL^{-1}	-0.216	-1.177	0.975	0.94

Pelvic Fin Length SL^{-1}	-1.886	3.444	0.752	$1.4\text{x}10^{-3}$
Pectoral Fin Length SL^{-1}	0.518	-0.381	0.961	0.74

D.2 Histograms of Measurements and Meristics

The following histograms represent a normal distribution for the completed measurements and meristics.

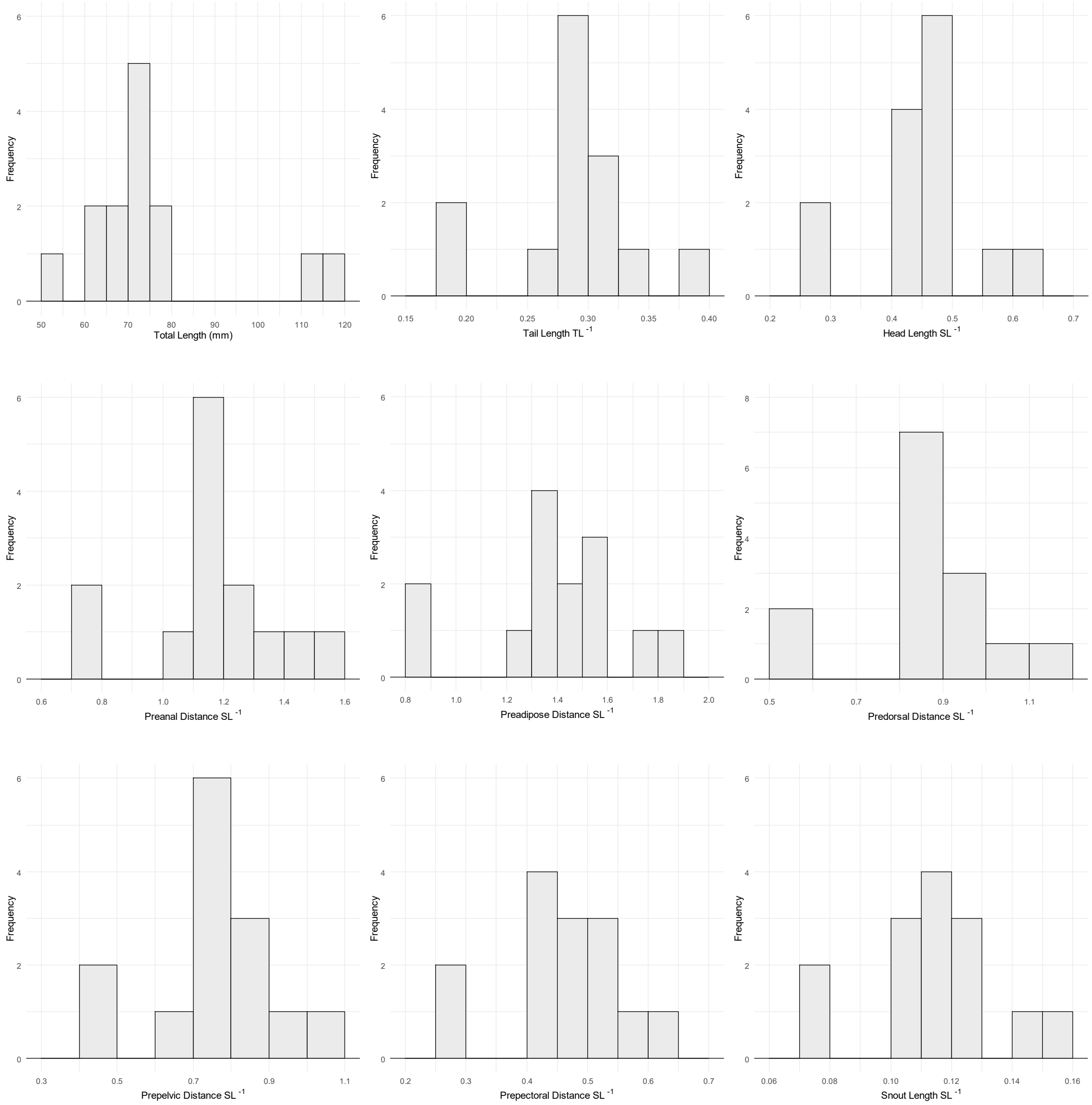

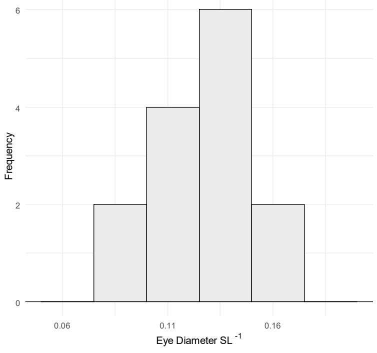
Frequency
0
2
4
6
0.06
0.11
0.16
Eye Diameter SL $^{-1}$

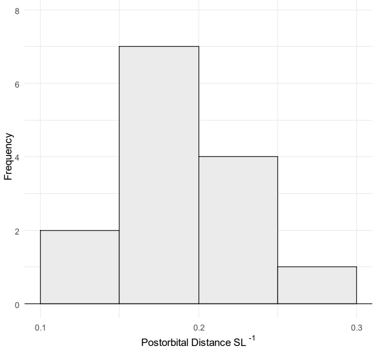
Frequency
0
2
4
6
8
0.1
0.2
0.3
Postorbital Distance SL $^{-1}$

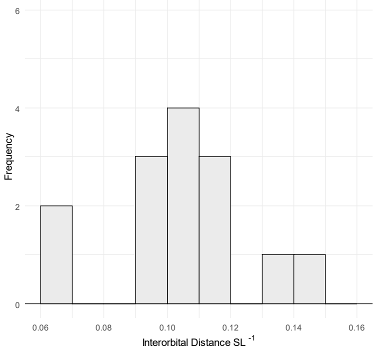
Frequency
0
2
4
6
0.06
0.08
0.10
0.12
0.14
0.16
Interorbital Distance SL $^{-1}$

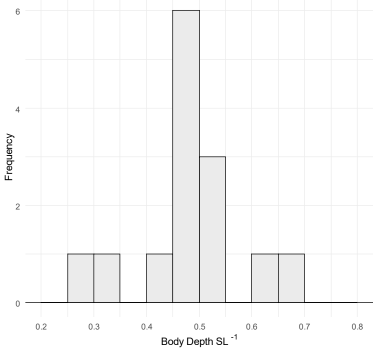
Frequency
0
2
4
6
0.2
0.3
0.4
0.5
0.6
0.7
0.8
Body Depth SL $^{-1}$

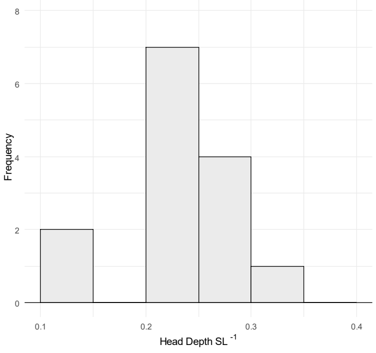
Frequency
0
2
4
6
8
0.1
0.2
0.3
0.4
Head Depth SL $^{-1}$

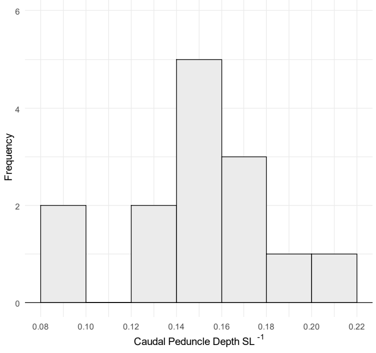
Frequency
0
2
4
6
0.08
0.10
0.12
0.14
0.16
0.18
0.20
0.22
Caudal Peduncle Depth SL $^{-1}$

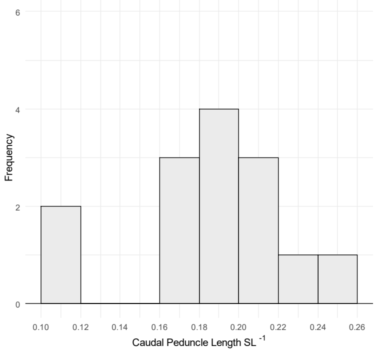
Frequency
0
2
4
6
0.10
0.12
0.14
0.16
0.18
0.20
0.22
0.24
0.26
Caudal Peduncle Length SL $^{-1}$

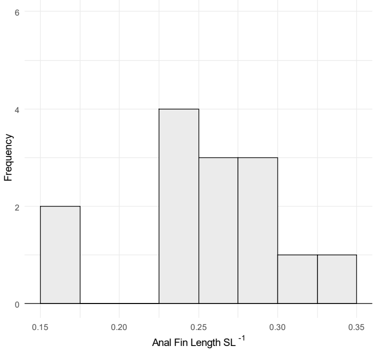
Frequency
0
2
4
6
0.15
0.20
0.25
0.30
0.35
Anal Fin Length SL $^{-1}$

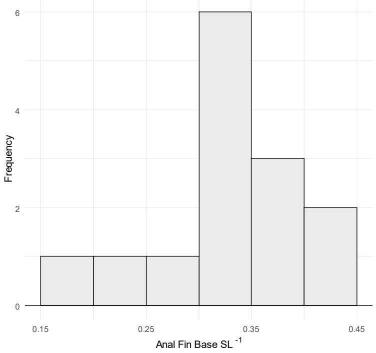
Frequency
0
2
4
6
0.15
0.25
0.35
0.45
Anal Fin Base SL $^{-1}$

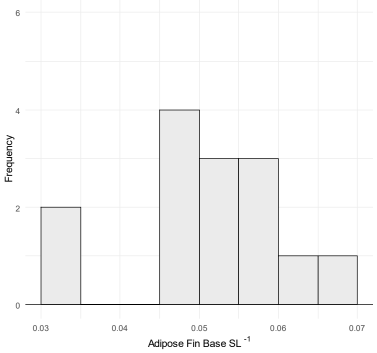
Frequency
0
2
4
6
0.03
0.04
0.05
0.06
0.07
Adipose Fin Base SL $^{-1}$

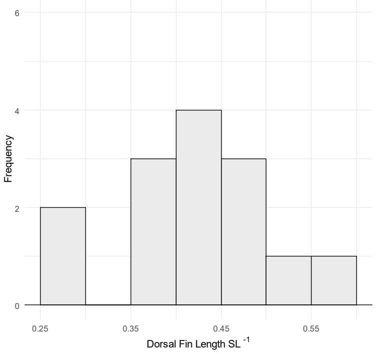
Frequency
0
2
4
6
0.25
0.35
0.45
0.55
Dorsal Fin Length SL $^{-1}$

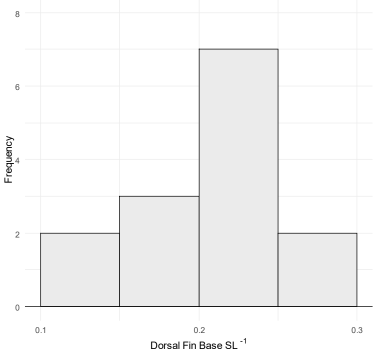
Frequency
0
2
4
6
8
0.1
0.2
0.3
Dorsal Fin Base SL $^{-1}$

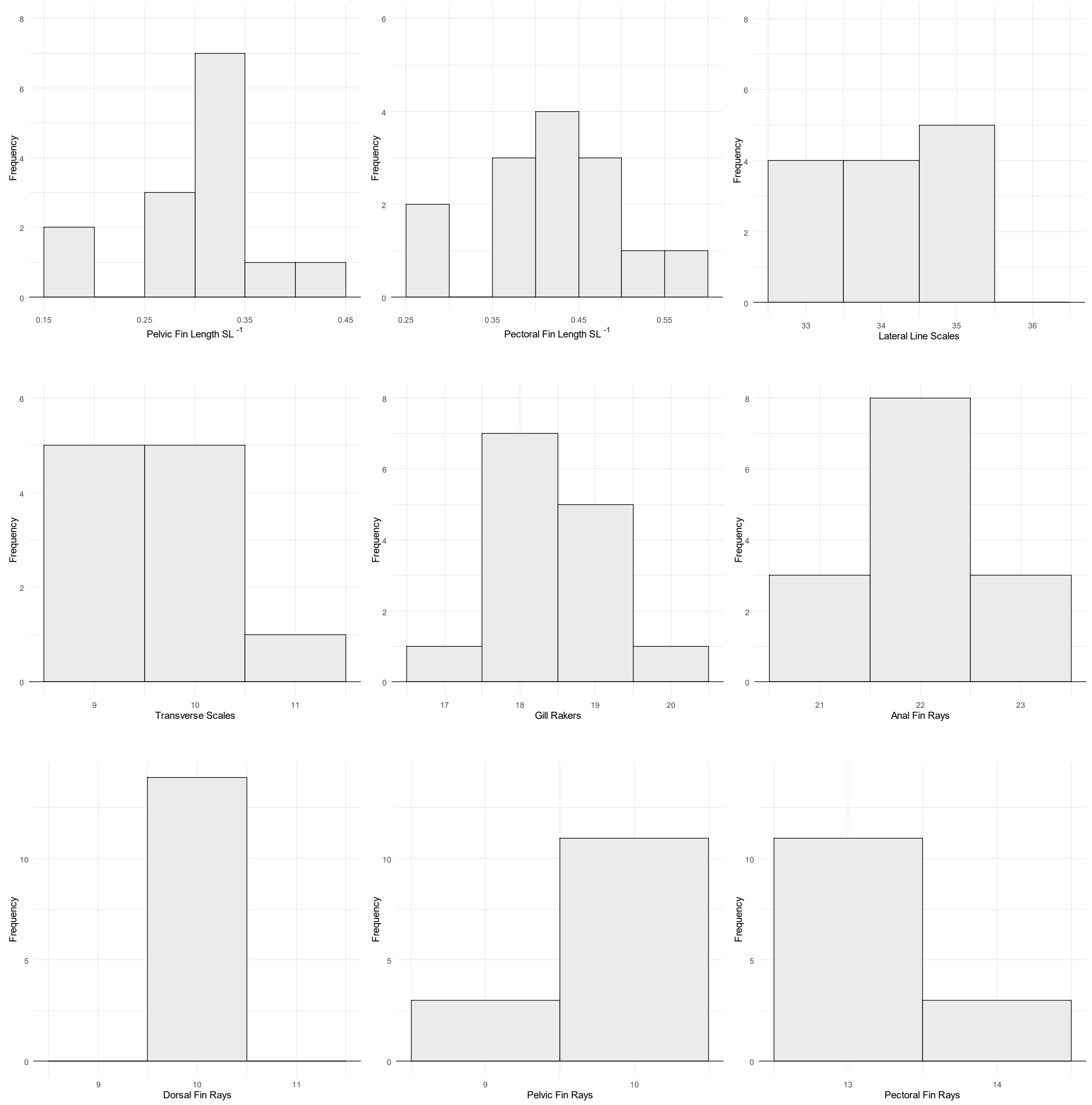
Frequency
0
2
4
6
8
0.15
0.25
0.35
0.45
Pelvic Fin Length SL $^{-1}$
Frequency
0
2
4
6
0.25
0.35
0.45
0.55
Pectoral Fin Length SL $^{-1}$
Frequency
0
2
4
6
8
33
34
35
36
Lateral Line Scales
Frequency
0
2
4
6
9
10
11
Transverse Scales
Frequency
0
2
4
6
8
17
18
19
20
Gill Rakers
Frequency
0
2
4
6
8
21
22
23
Anal Fin Rays
Frequency
0
5
10
9
10
11
Dorsal Fin Rays
Frequency
0
5
10
9
10
Pelvic Fin Rays
Frequency
0
5
10
13
14
Pectoral Fin Rays

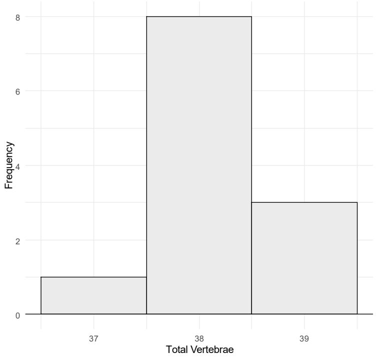

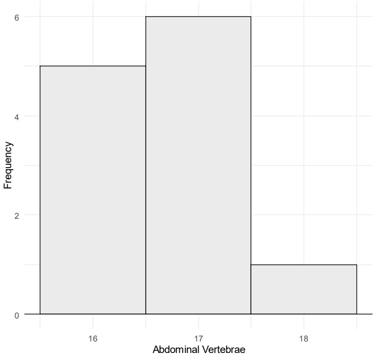

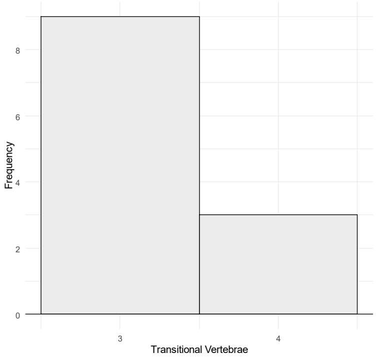

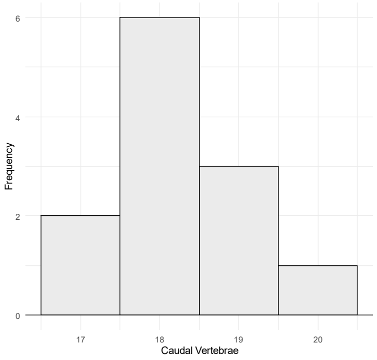

D.3 Scatterplots of Measurements and Meristics

D.3.1 Scatterplots of Measurements

Scatterplots of all measurements were completed using logarithmic data. The Pearson's correlation coefficient (r), p-value, and slope are represented in the top left corner. Scatterplots of measurements represent isometric growth (with a slope ≈ 1.0).

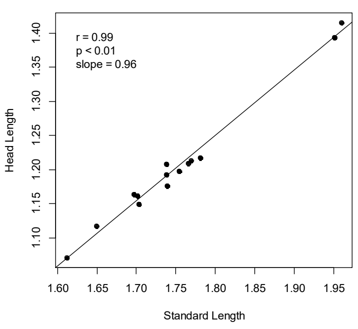
r = 0.99
p < 0.01
slope = 0.96
Head Length
1.10
1.15
1.20
1.25
1.30
1.35
1.40
1.60
1.65
1.70
1.75
1.80
1.85
1.90
1.95
Standard Length

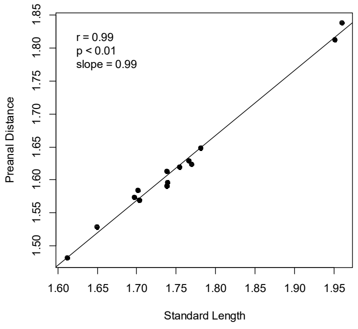
r = 0.99
p < 0.01
slope = 0.99
Preanal Distance
1.50
1.55
1.60
1.65
1.70
1.75
1.80
1.85
1.60
1.65
1.70
1.75
1.80
1.85
1.90
1.95
Standard Length

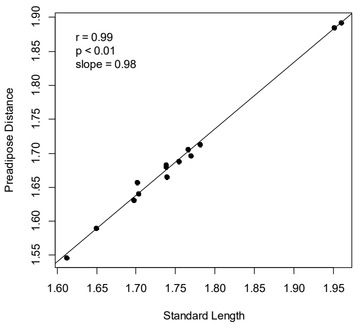
r = 0.99
p < 0.01
slope = 0.98
Preadipose Distance
1.55
1.60
1.65
1.70
1.75
1.80
1.85
1.90
1.60
1.65
1.70
1.75
1.80
1.85
1.90
1.95
Standard Length

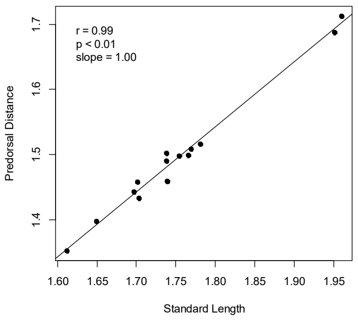
r = 0.99
p < 0.01
slope = 1.00
Predorsal Distance
1.4
1.5
1.6
1.7
1.60
1.65
1.70
1.75
1.80
1.85
1.90
1.95
Standard Length

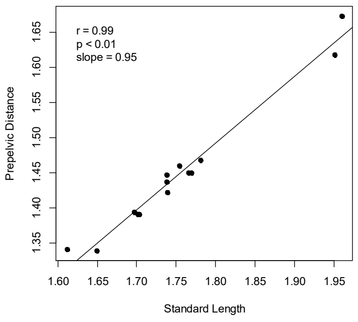
r = 0.99
p < 0.01
slope = 0.95
Prepelvic Distance
1.35
1.40
1.45
1.50
1.55
1.60
1.65
1.60
1.65
1.70
1.75
1.80
1.85
1.90
1.95
Standard Length

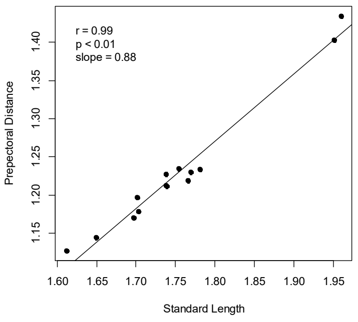
r = 0.99
p < 0.01
slope = 0.88
Prepectoral Distance
1.15
1.20
1.25
1.30
1.35
1.40
1.60
1.65
1.70
1.75
1.80
1.85
1.90
1.95
Standard Length

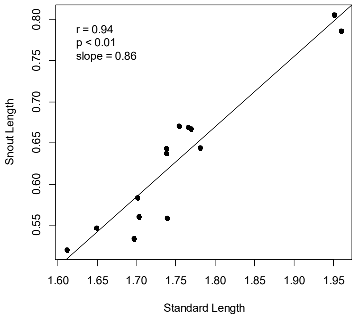
r = 0.94
p < 0.01
slope = 0.86
Snout Length
0.55
0.60
0.65
0.70
0.75
0.80
1.60
1.65
1.70
1.75
1.80
1.85
1.90
1.95
Standard Length

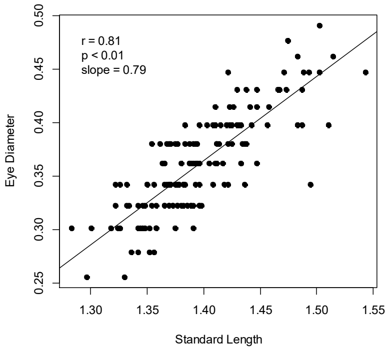
r = 0.81
p < 0.01
slope = 0.79
Eye Diameter
0.25
0.30
0.35
0.40
0.45
0.50
1.30
1.35
1.40
1.45
1.50
1.55
Standard Length

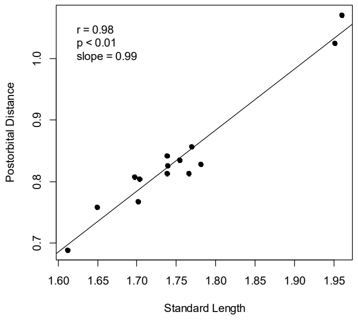
r = 0.98
p < 0.01
slope = 0.99
Postorbital Distance
0.7
0.8
0.9
1.0
1.60
1.65
1.70
1.75
1.80
1.85
1.90
1.95
Standard Length

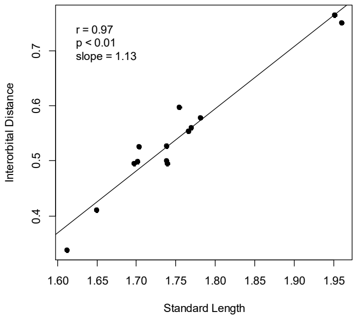
r = 0.97
p < 0.01
slope = 1.13
Interorbital Distance
0.4
0.5
0.6
0.7
1.60
1.65
1.70
1.75
1.80
1.85
1.90
1.95
Standard Length

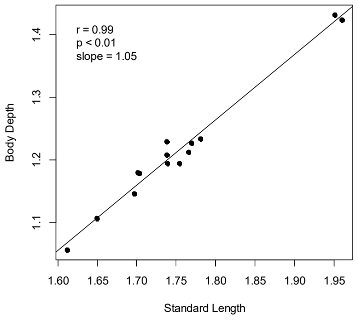
r = 0.99
p < 0.01
slope = 1.05
Body Depth
1.1
1.2
1.3
1.4
1.60
1.65
1.70
1.75
1.80
1.85
1.90
1.95
Standard Length

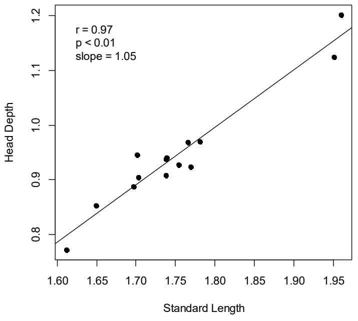
r = 0.97
p < 0.01
slope = 1.05
Head Depth
0.8
0.9
1.0
1.1
1.2
1.60
1.65
1.70
1.75
1.80
1.85
1.90
1.95
Standard Length

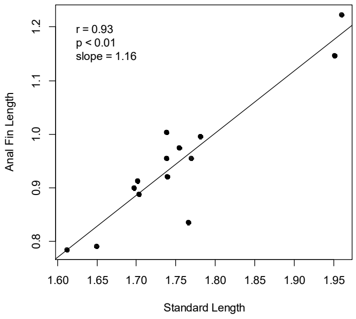

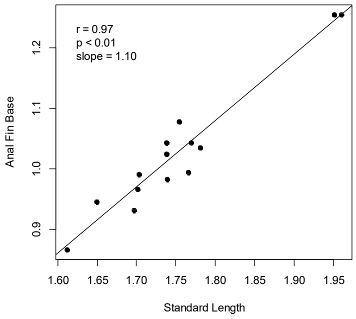

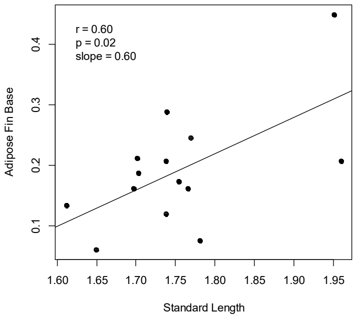

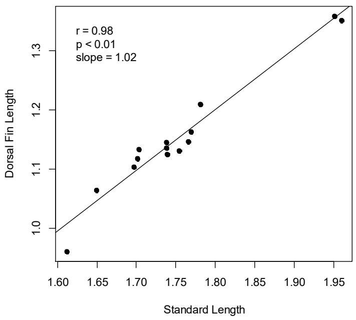

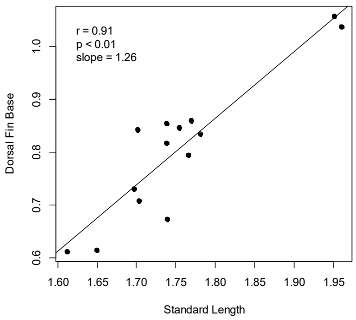

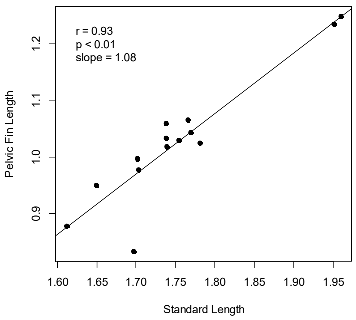

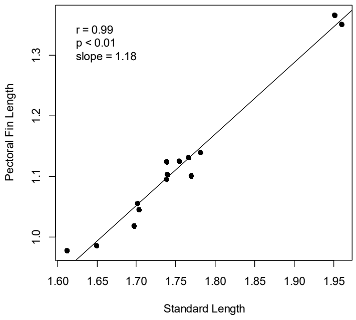

D.3.2 Scatterplots of Meristics

Scatterplots of counts show no correlation with size.

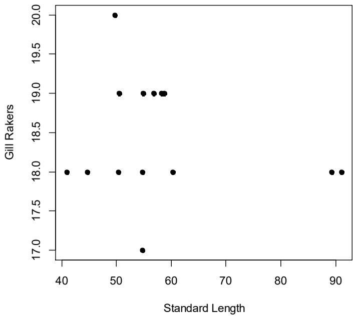

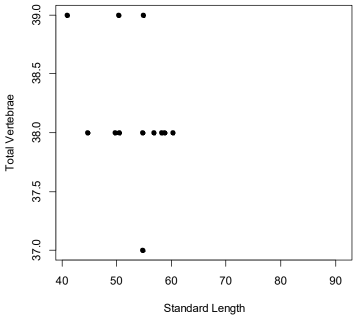

D.4 Principal Component Analysis

All measurements were turned into ratios in relation to standard length prior to PCA. PCA results include (a) a scree plot of the first ten principal components (dimensions), (b) a correlation circle with each variable colored by its respective cos^2 (representation) value, (c) a contribution of variables table, and (d) a plot of the distribution of variables. The cos^2 value indicates which values are best represented by each component.

D.4.1 All Measurement Data

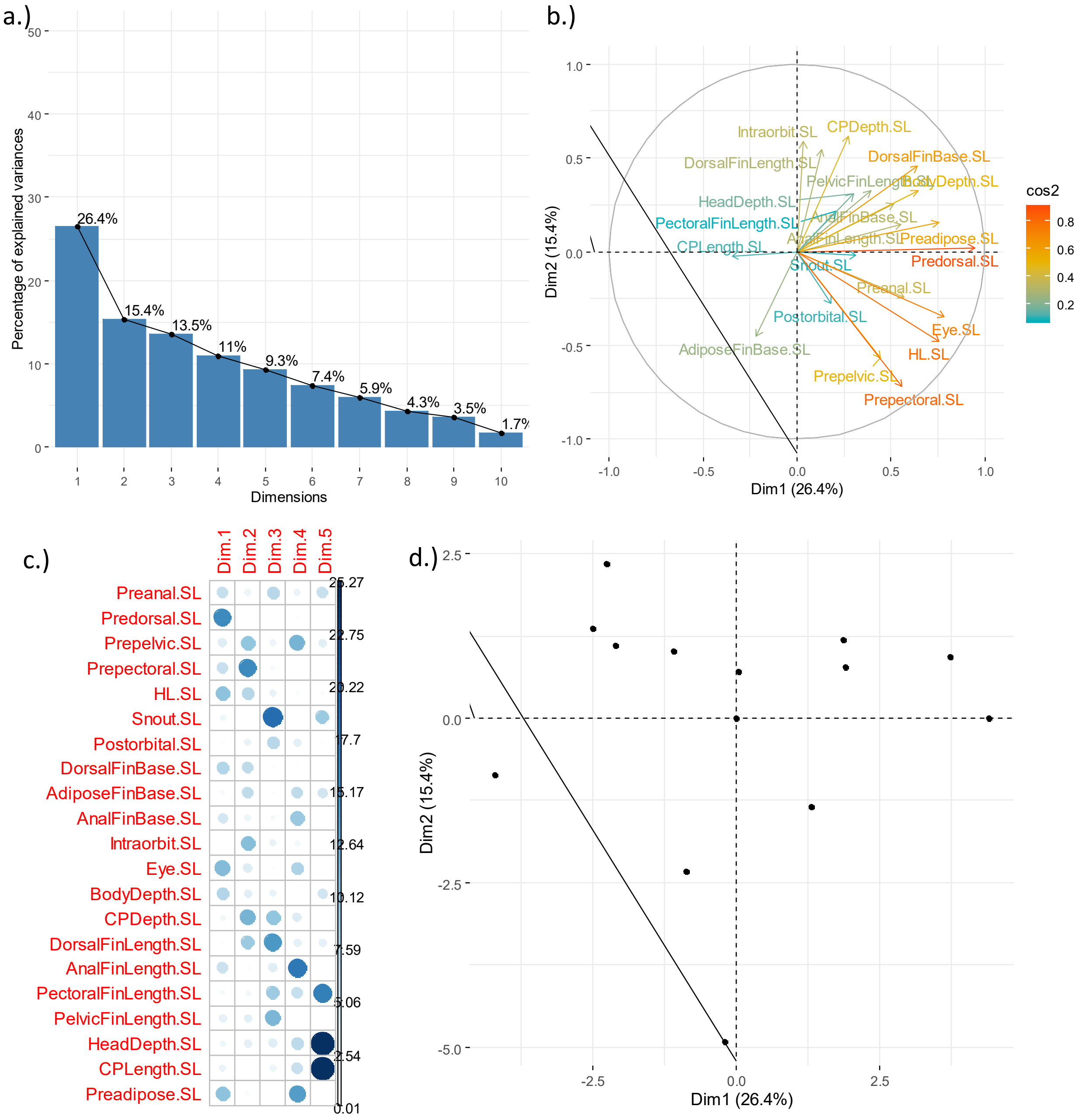

D.4.2 All Measurement and Meristic Data

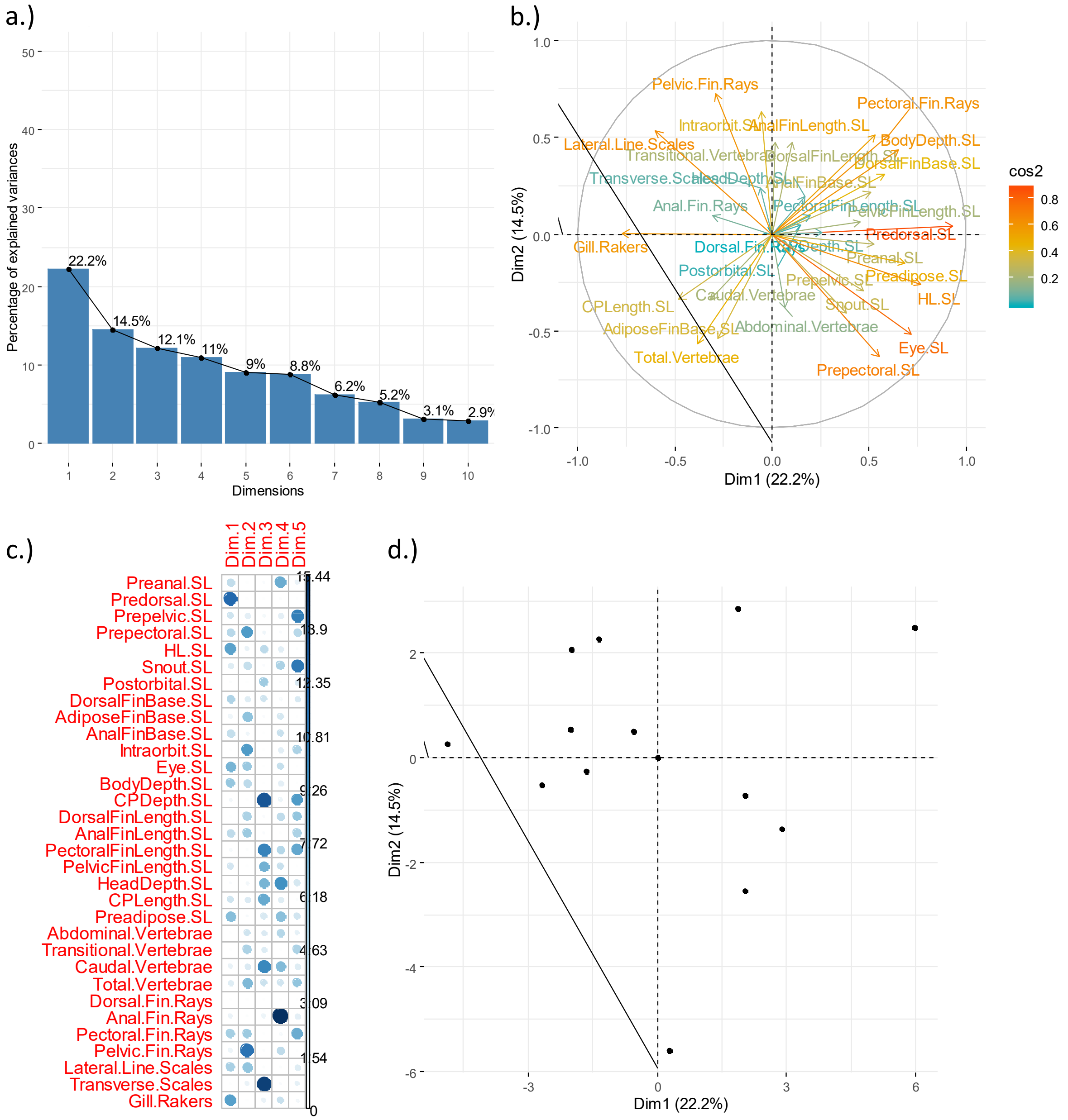

Appendix E: Chapter 4 “Miniaturization of African alestids: A comparison of miniature species to juveniles of mid-sized species”

Table E.1. Presence (+) or absence (-) of cartilage in 39 endochondral bones for juvenile specimens of *Alestes dentex* (Linnaeus), and adult specimens of *Hemigrammopetersius barnardi* (Herre) and *Petersius conserialis* Hilgendorf. Shaded squares represent instances when the presence of cartilage could not be confidently determined due to articulation of cleared and stained material.

	Alestes dentex			*Hemigrammopetersius barnardi*				*Petersius conserialis*		
Specimen Number	4	5	6	3	106	4	2	12	15	2
SL (mm)	43.2	55.8	62.7	26.2	31.2	32.7	38.6	40.9	60.9	70.4
Skull										
Supraoccipital	+	+	+	-	+	-	-	+	-	-
Lateral Ethmoid	-	-	-	-	-	-	-	-	-	-
Orbitosphenoid	+	-	+	-	+	-	-	-	-	-
Pterosphenoid	+	-	+	-	+	-	-	-	-	-
Sphenotic	-	-	-	-	-	-	-	-	-	-
Prootic	+	-	▨	▨	+	-	▨	▨	▨	▨
Pterotic	+	+	+	-	+	+	-	+	-	-
Epioccipital	+	+	+	+	+	+	-	+	-	-
Exoccipital	+	-	▨	-	+	-	-	▨	▨	▨
Basioccipital	▨	-	▨	-	+	-	-	▨	▨	▨
Suspensorium										
Hyomandibula	+	+	+	+	+	+	+	+	+	+
Symplectic	+	+	+	+	+	+	-	+	+	-
Metapterygoid	+	+	+	+	+	+	+	+	-	+
Quadrate	+	-	+	+	+	+	+	+	-	+
Branchial Arches and Pharyngeal Region										
Basihyal	▨	+	▨	+	+	+	+	+	▨	-
Basibranchials	+	-	▨	+	+	+	+	+	▨	-
Hypobranchials	+	-	+	+	+	+	+	+	▨	+
Ceratobranchials	+	+	+	+	+	+	+	+	+	+
Pharyngobranchials	+	+	+	+	+	+	+	+	+	+
Endobranchials	+	+	+	+	+	+	+	+	+	+
Interhyal	+	+	+	+	+	+	+	+	▨	+
Posterior Ceratohyal	+	+	+	+	+	+	+	+	+	+
Anterior Ceratohyal	+	+	+	+	+	+	+	+	▨	+
Dorsal Hypohyal	+	+	+	+	+	+	+	+	+	+
Ventral Hypohyal	+	+	+	+	+	+	+	+	+	+
Pectoral and Pelvic Girdle										

Coracoid	-	-	-	-	-	-	-	-	-	-
Mesocoracoid	+	+	+	-	-	-	-	-	-	-
Scapula	+	+	+	-	-	-	-	-	+	+
Pelvic Girdle	+	+	+	-	-	-	-	+	+	+
Weberian Apparatus										
Neural Crest	-	-	+	+	+	-	-		-	-
Claustrum	-	-	-	-	-	-	-		-	-
Scaphium	-	-	-	-	-	-	-		-	-
Intercalarum	-	-	-	-	-	-	-		+	-
Tripus	-	-	-	-	+	-	-		+	-
Caudal Skeleton										
Epurals	+	+	+	+	+	+	+	+	-	-
Uroneural	+	-	-	-	-	-	-	-	-	-
Urostyle	-	-	-	-	-	-	-	-	-	-
Parhypural	+	+	+	+	+	+	+	+	+	+
Hypurals	+	+	+	+	+	+	+	+	+	+